Construction of potential drug delivery systems based on polysaccharides

ATIGA EMHEMED ABODINAR

B.Sc. (CHEMISTRY); M.Sc. (ANALYTICAL CHEMISTRY)

A THESIS SUBMITTED TO THE UNIVERSITY OF HUDDERSFIELD IN PARTIAL FULFILMENT OF THE DEGREE OF THE REQUIRMENT FOR THE DEGREE OF DOCTOR OF PHILOSOPHY
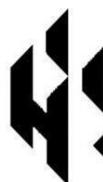
University of HUDDERSFIELD

November 2016

COPYRIGHT STATEMENT

ABSTRACT

Enhancement of the drug efficacy and elimination of the side effects resulting from drug overdoses are an essential aspect in drug therapy. To achieve these demands two general guidelines have been used; producing new drugs with higher selectivity and therefore less side effects and improving controlled/sustained drug delivery agents based on polymers. Thus, the relationship between the active pharmaceutical ingredient and the polymeric system is important in the development of a drug delivery system and several considerations need to be taken in to account, for example the polymer should be biocompatible, biodegradable, and non-toxic and physiochemical properties. Because mucus is the first barrier with which food and drugs can interact with and diffuse through to be absorbed and enter the circulatory system, characterisation of mucin is an essential step towards establishing suitable pharmaceutical excipients. Therefore, the aim of the present study was to investigate the potential to construct and study drug delivery systems based on polysaccharides

The physicochemical characterisation of extensively degraded pig gastric mucin was studied and revealed that this type of mucin contains: protein, carbohydrate (Fuc, Gal, GalN, GlcN) and sialic acid, which provides the negative charges that becomes progressively stronger with increasing pH. The measurements of viscosity vs. shear rate showed that mucin has a shear thinning behaviour and a relatively low viscosity which is consistent with a high critical overlap concentration (c*), small hydrodynamic size and hence compact structure. The insight in to the compositional, hydrodynamic and viscoelastic properties support the understanding of mucin interactions with polysaccharide based drug delivery systems.

Several polysaccharides including chitosan (Cs), two grade of alginates; high guluronate alginate (HGA) and low guluronate alginate (LGA) (which differ in structural conformation) and two kinds of pectin; high methoxyl pectin (HMP) and low methoxyl pectin (LMP) (with different degrees of esterification) have been characterised. The structure of these polysaccharides as powder have been studied; Fourier transform infrared spectroscopy) findings indicate the structure and the function group for each polysaccharide whereas powder X-ray diffraction measurements displays that all the polysaccharide which were analysed are amorphous in nature except LMP which has a number of sharp crystalline peaks. In addition, solution properties of these polysaccharides such as zeta potential and intrinsic viscosity were investigated at several ionic strengths and pH. Furthermore the molecular weights were evaluated based on intrinsic viscosity and the Smidsrød-Haug stiffness parameter (B) and intrinsic persistence length (L_p) were estimated using the novel ionic strength dependency of zeta potential method and intrinsic viscosity (traditional method).

The interaction between polysaccharides and pig gastric mucin were evaluated based on relative viscosity. It has been suggested that polysaccharide–mucin interactions are not only driven by electrostatic forces, but also by the molecular weight, conformation and flexibility of the polymer also played significant roles. As the mucin-HGA system displayed exceptionally high viscosity, the viscoelastic properties of this system were extensively studied. The mechanical spectra of the mucin-HGA blends indicate that with the exception of the system involving only HGA (0 % mucin) and 60 % mucin, all mixtures including mucin itself displayed typical 'weak gel' rheological behaviour and the gel became stronger with decreasing HGA content in the system. Moreover 80 % of mucin was successfully encapsulated within phospholipids bilayer using liposomal encapsulation technology. The liposomal vesicles with encapsulated mucin display larger sizes than the control vesicles (prepared in DI water)

3

this may be due to the electrostatic interaction between mucin molecules and phospholipid which is the main component the vesicles.

In the final part of the thesis the hydrogel containing chitosan and naturally occurring polyanions and its potential for drug release were studied. Chitosan - polyanion (HGA, LGA, HMP and LMP) hydrogels complexes were successfully prepared (in acetate buffer 0.05M, 4.3 pH) at various ratios (10 %, 30 %, 50 %, 70 % 90 % of Cs) using the ionotropic gelation method. The freeze dried hydrogels were characterized by FT-IR and XRD and the results confirmed the electrostatic interactions between chitosan and polyanions at all ratios and percentage yield of hydrogel ζ and η_{sp} results of the supernatant was determined and it was found that the optimum ratios 3:7 and 1:1 of chitosan-pectins and chitosan-alginates respectively. The hydrogels of ideal ratios were studied by determining zeta potential, particles size, water uptake, morphology by scanning electron microscopy for freeze dried hydrogels and optical microscopy analysis for homogenous suspension. In addition, dynamic small deformation oscillatory measurements and adhesion property were studied. Finally, ibuprofen was successfully encapsulated by the chitosan-polyanion hydrogel complexes and the encapsulation efficiency of the formulations was calculated. Finally the drug release behaviour of the formulations was *in vitro* assessed over the time. The findings demonstrated that HMP and LGA hydrogels displayed the highest percentage of retained ibuprofen followed by HGA and LMP. This could be attributed to the fibrous appearance small size of pores which may impedes movements of entrapped molecules.

ACKNOWLEDGEMENT

This thesis is dedicated to

My Dear Husband; Mr Muftah Elhdad

My Daughters; Rzan & Rwan & Ryan

My Sons; Ali & Mohammed

I will always Love you......

LIST OF ABBREVIATIONS

Cs	Chitosan
DDA	Degree of Deacetylation
HGA	High Guluronate Alginate
LGA	Low Guluronate Alginate
HMP	High Methoxyl Pectin
LMP	Low Methoxyl Pectin
FTIR	Fourier transform infrared spectroscopy
IS	Ionic strength
P- XRD	Powder X-Ray diffraction
PECs	Polyelectrolyte complexes
LET	Liposomal Encapsulation Technology
Z	Zeta potential
LEM	Liposome encapsulating mucin
SEM	Scanning electron microscopy
IS	Ionic strength
η_{rel}	Relative viscosity
η_{sp}	Specific viscosity
$[\eta]$	Intrinsic viscosity
B	Smidsrød-Haug stiffness parameter
EE	Encapsulation efficiency

NTA	Nanoparticle tracking analysis
HPAEC–PAD	High-Performance Anion-Exchange Chromatography with Pulsed Ampe rometric Detection
SEC–MALLS	Size - Exclusion Chromatography coupled to Multi-Angle Laser Light Scattering
c*	Critical coil overlap
WU	Water uptake
G"	Loss modulus
G′	Storage modulus
LGLVA	Low guluronate low viscosity alginate
GIT	Gastrointestinal tract
API	Active pharmaceutical ingredient

CONTENTS

LIST OF FIGURES

16

LIST OF TABLES

Chapter 1

General Introduction

1. GENERAL INTRODUCTION

1.1. Why Polysaccharides/polyelectrolyte complexes are important in drug delivery systems

Enhancement of the drug efficacy and elimination of the side effects resulting from drug overdoses are an essential aspect in drug therapy (Popa *et al.*, 2011). To achieve these demands two general guidelines have been used; producing new drugs with higher selectivity and therefore less side effects and improving controlled/sustained drug delivery agents based on polymers (Popa *et al.*, 2011). The latter case (polymer-based drug delivery systems) is utilised using three different mechanisms to achieve the desired effect (Popa *et al.*, 2011)

i. Diffusion the drug through hydrogels (*e.g.* films or micro/nanoparticles)
ii. Erosion polymer matrix comprising the drug (*e.g.* micro/nanoparticles)
iii. Hydrolysis of the chemical links that associate the drug with polymer (drug-polymer conjugates).

Clearly, the relationship between the active pharmaceutical ingredient (API) and the polymeric system is important in the development of a drug delivery system and several considerations need to be taken in to account, for example the polymer should be biocompatible, biodegradable, non-toxic and provide high reactivity towards the treatment under specific conditions (*e.g.* temperature, and pH) (Popa *et al.*, 2011). Several polysaccharides including chitosan, alginates, pectins, cellulose, starch, dextran, agar, *etc* (Pillai and Panchagnula, 2001) have been widely utilised in drug delivery systems.

1.1.1. Common polysaccharides used in drug delivery

1.1.1.1. Chitosan

Chitosan (Cs) is the only naturally occurring positively charged polysaccharide which composed of β-D-glucosamine and β-D-*N*-acetyl-glucosamine residues linked $(1 \rightarrow 4)$ (Kujawa *et al.*, 2007, Laurienzo, 2010) of molecular weights in the range of $\sim 5 \times 10^4$ - 2×10^6 g/mol (Li *et al.*, 2008) and is obtained via the deacetylation of chitin (Kujawa *et al.*, 2007, Laurienzo, 2010) **(Figure 1.1)** (Mukoma *et al.*, 2004). Chitin is present in several fungi, the shells of insects and crustaceans (Li, 2012) and as the second most abundant polymer on the

planet its potential as a sustainable resource of biomaterial has been underutilised (Matlack, 2010, Yan and Chen, 2015). Chitosan's history dates back to the 90th century, when Rouget studied the deacetylated form of chitin in 1859 (Dodane and Vilivalam, 1998).
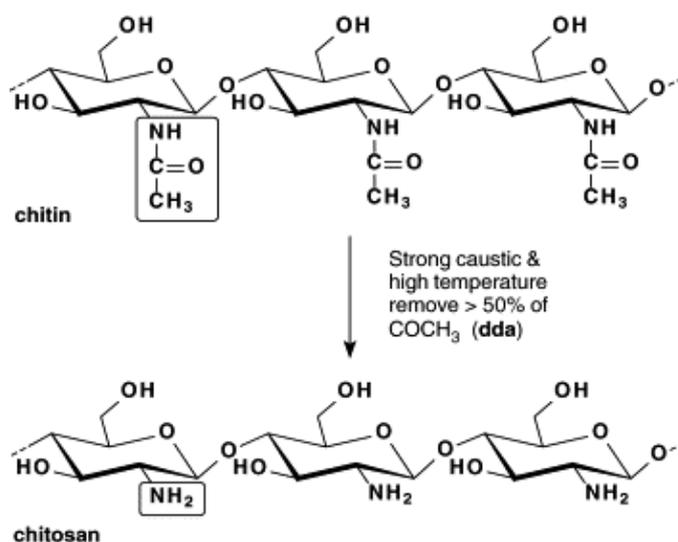
Figure 1.1: Production of Cs from chitin using concentrated NaOH at high temperature (DDA is degree of deacetylation)
(Mukoma *et al.*, 2004)

There are certain factors that affect the solubility of Cs including: pH, ionic strength and the degree of deacetylation (DDA). The presence of the amino groups on Cs chain means that pH considerably influences the charged state and therefore the physico-chemical properties of the polymer **(Figure 1.2)**. At pH < 6 Cs is soluble due to the protonation the amino groups and it becomes a cationic polyelectrolyte which can therefore undertake electrostatic interactions with negatively charged molecules and polymers for example mucin, pectin or alginate. However, at pH higher than 6.5 Cs solutions show phase separation due to deprotonation of the amino groups (Mireles-DeWitt, 1994) and can potentially interact due to hydrophobic interactions with several substrates such as fatty acids (Il Dueik and Morris, 2013) and cholesterol (Wydro *et al.*, 2007). Cs molecules at pH between 6.0 and 6.5 become less protonated thereby positive charge and hydrophilicity along the Cs chain decreases. The pH is also has very important influence on the conformation of the Cs polymer as it is extended (less flexible) at low pH. So, Cs pH-dependent properties have impact on its potential biomedical and pharmaceutical applications (Kumirska *et al.*, 2011).
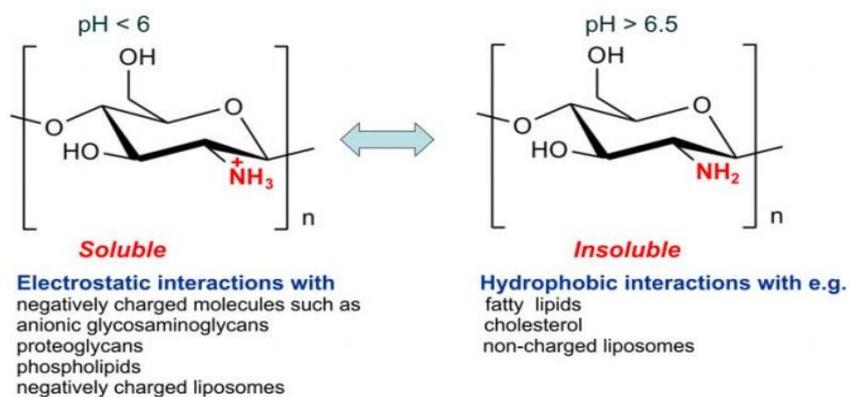
Figure 1.2 Diagrammatic illustration of chitosan's versatility with pH
(Kumirska *et al.*, 2011)

Similarly to pH, ionic strength has an essential influence the physicochemical properties of Cs solutions which can also powerfully influence their biological activity. (Rinaudo *et al.*, 1993) studied the effect of ionic strength on Cs chain expansion and found that the ionic environment influences on the electrostatic properties of the polymer due to the presence of charged amino groups in acid conditions. Lower ionic strength associated with higher solubility (Guo, 2007). One of the other important factors which affect the solubility of Cs is DDA which is the percentage of glucosamine in the Cs molecule; the copolymer is normally known as Cs when the DDA is greater than 50 % (Cho *et al.*, 2006). The Cs solubility is affected by DDA because it is responsible for the charge distribution on the polymer chains (Pillai *et al.*, 2009).

In addition to the ability for both electrostatic and hydrophobic interactions chitosan's other important properties include: non-toxicity, biodegradability and biocompatibility which together with its positive charge explains why Cs is a unique polymer in medical and pharmaceutical areas. Cs has been widely utilised in the delivery of pharmaceutical ingredients through nasal, ocular, oral, parenteral and transdermal routes (Krauland *et al.*, 2006, de Campos *et al.*, 2004, Bowman and Leong, 2006, Chen *et al.*, 2012). Because Cs protonates at acidic pH and can adhere to the mucus (Gåserød *et al.*, 1998), it has become an important excipient in drug delivery (Anal and Stevens, 2005, Önal and Zihniğlu, 2002, Sarmento *et al.*, 2007, Macleod *et al.*, 1999, Oliveira *et al.*, 2010). Moreover, Cs due to its ability to alter the rate of diffusion of the encapsulated drug, can be applied as a coating agent to alginate beads (Anal and Stevens, 2005) and it may also modify the alginate bead structure (Gotoh *et al.*, 2004, Lin *et al.*, 2005).

1.1.2.1. Alginates

Alginate is a family of unbranched binary copolymers of (1-4) linked β-D-mannuronic acid (M) and α-L-guluronic acid (G) residues (**Figure 1.3 (a) and (b)**) (Phillips and Williams, 2000). "Alginate" is the term used for the salts of alginic acid, and their derivatives (McHugh, 2003). The first description of these polysaccharides was by the British chemist E. C. C. Stanford in 1881 (Phillips and Williams, 2000). Although alginate can be produced by microbial fermentation (*e.g.* soil bacteria), commercially, brown algae *(e.g. Laminaria hyperborea, Macrocystis pyrifera, Laminaria digitata, Ecklonia maxima and Ascophylum nodosum)* are the main sources of alginate (Norton, 2010). Alginates have three structural forms and can be separated into three fractions using partial acidic hydrolysis and fractionation. The three idealised forms of alginate are homopolymeric molecules of guluronic acid (G-block) and homopolymeric molecules of mannuronic acid (M-block) and the third fraction contains nearly equal proportions of both monomers (MG-block) (**Figure 1.3 (c)** (Phillips and Williams, 2000, Stokke *et al.*, 1991, Haug, 1964). The physical properties of these polymers in an aqueous medium depend on the M/G ratio and the distribution of G and M units along the chain. The GG blocks that have an axial–axial linkage which is more rigid than the di-equatorially links found in MM blocks; consequently, the composition (M/G ratio) and distribution of M and G units in the chains strongly affects the stiffness of the alginate chains and their complex formation (Rinaudo, 2008). In addition, the viscosity of alginate is affected by the fraction present; studies have indicated that the viscosity increases in the order: MG-blocks < MM-blocks < GG-blocks. This is because G-rich samples entangles in solution more than the M-rich sample(Sartori, 1997). Therefore, sodium alginate could be classified according to viscosity including high, medium and low viscosity and also based on proportions of monomers high G alginate or low G alginate. In this research low guluronate low viscosity alginate, (LGLVA), low guluronate high viscosity alginate, (LGHVA) and high guluronate alginate (HGA) have been used.

a

COO⁻

β-ᴅ-mannuronate (M)   α-ʟ-guluronate (G)

b

G   G   M   M   G

c

M M M M GM GGGGGM GM GGGGGGGGGM M GM GM GGM

M-block   G-block   G-block   MG-block
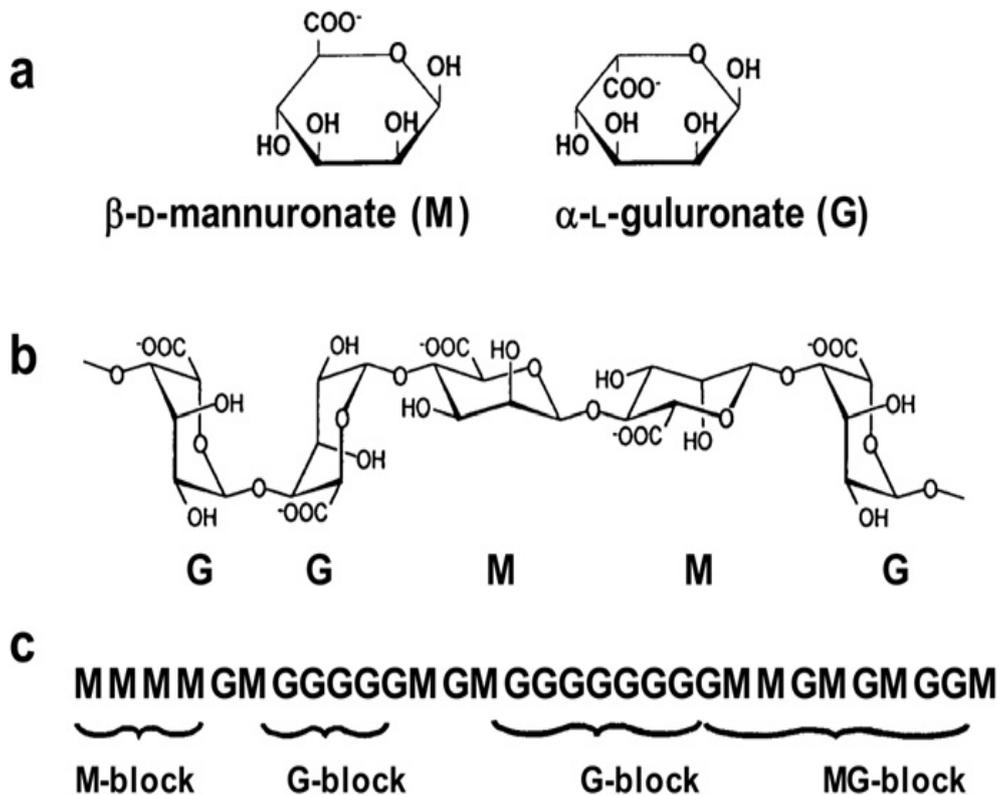
Figure 1.3 Structural characteristics of alginates: (a) alginate monomers, (b) chain conformation, (c) block distribution,
Adapted from (Draget and Taylor, 2011)

The solubility of alginates in water is influenced by three factors:

- pH of the solvent; the pH value of the solvent is essential as it defines the electrostatic charge of uronic acid residues (Draget *et al.*, 2005); alginate can dissolve at pH value below the pk_a of mannuronate (3.38) and guluronate (3.65) monomer (Wilson and Crowley, 2011).

- Ionic strength; changing the ionic strength of the medium influence solution features for instance polymer conformation, thickness, chain extension, and thus solubility.

- Presence of gelling agent in the solvent for example divalent cations (*e.g.* Ca^{+2}, Sr^{+2} and Ba^{+2}) in the system can lead to lack of alginate dissolution (Pawar and Edgar, 2012). Alginates with high G contents can produce stronger gels than MG blocks because gel formation is driven by the interactions between G-blocks and divalent cations (Rinaudo, 2008).

Alginates have many valuable properties that enable them to be frequently applied in research applications such as electrostatic complex formations with a cationic polymers (*e.g.* Cs acidic conditions), homogeneous gels formation by ionic crosslinking in the presence of multivalent cations (*e.g.* Ca^{2+}) (Phillips and Williams, 2000). Among of these applications are pharmaceutical, biomedical, nutritional and industrial. For example they are useful for tissue engineering, delivery vehicles for drugs as capsules, beads, fibres or films that are marketed as haemostatic substances or as wound dressings (Rinaudo, 2008). (Gåserød *et al.*, 1998, Lee and Min, 1995) have studied the application polyelectrolyte complexes of Cs and alginate. Microparticles and beads of Cs and alginate have been proposed for controlled drug release (Sezer, 1999). Moreover, alginates are also used as additives to modify, improve, and stabilise the texture of several foods (Stephen *et al.*, 2006).

1.1.2.1. Pectin

Pectin is negatively charged, hydrophilic, nontoxic biopolymer (Tsai *et al.*, 2014) which is extracted from middle lamella and primary cell walls of plant tissues (Rinaudo, 2008). Pectin is primarily comprised of 1, 4-linked α-D-galacturonic acid (GalpA) residues **(Figure 1.4)** (Rajpurohit *et al.*, 2010).

Pectin easily dissolves in pure water (Sriamornsak, 2003) and its solubility is influenced by their degree of methylation (DM) and degree polymerisation (DP) and the distribution of methoxyl groups on the chain. In general, the molecule dissolves more easily with lower molecular weight and higher in degree of esterification, although pH temperature, and the nature and concentration of pectin have an influence on solubility (Thakur *et al.*, 1997).

Based on degree of methylation, pectin is classified into two types: high methoxyl (HM) pectin (DM > 50%), and low methoxyl (LM) pectin DM < 50%). DEs values for HM-pectins and LM-pectins usually range from 60-75 % and 20-40 % respectively (Sriamornsak, 2003). Based on their molecular structure, pectins classified to three types: homogalacturonan (HG), rhamnogalacturonan-I (RG-I) and rhamnogalacturonan II (RG-II). HG is a linear chain of 1, 4- linked α-D-galactopyranosyluronic acid (GalpA) residues of which certain percentage of the carboxyl groups are methyl esterified. (RG-I) is a family of pectic polysaccharides that have a backbone of the repeating disaccharide units [→4)-α-D-GalpA-(1→2)-α-l-Rhap-(1→]. (RG-II) domains have lower molecular weights and more complex in structures than HG (Fukuda, 2014).
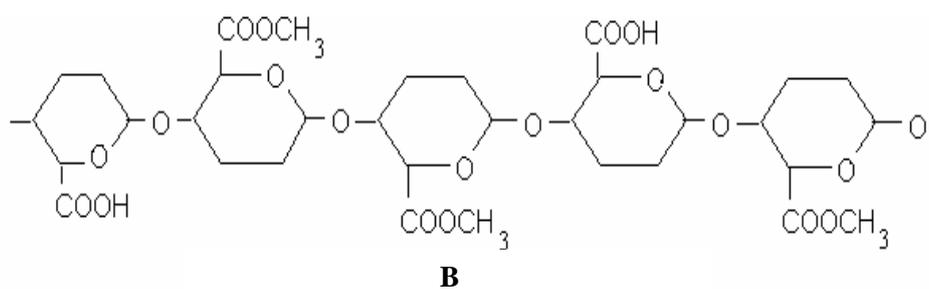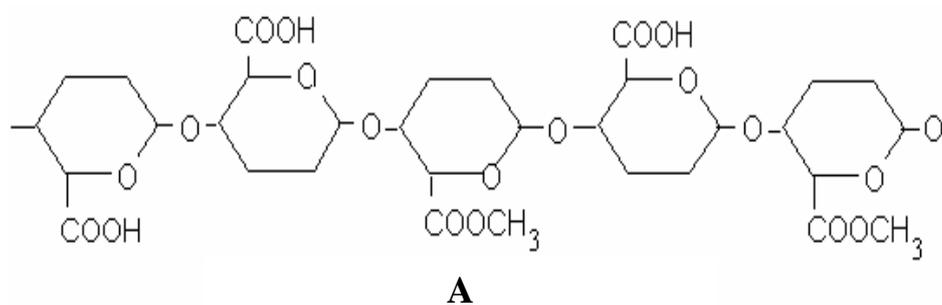
Figure 1.4 Structure of (A) low methoxyl pectin and (B) high methoxyl pectin
(Ghanbarzadeh and Almasi, 2013)

Pectins have many pharmaceutical applications as hydrogels, films, tablets, pellets and beads (Ghaffari *et al.*, 2007, Ghaffari *et al.*, 2006) and have been applied specially for colonic drug delivery systems (Bigucci *et al.*, 2009, Fernández-Hervás and Fell, 1998, Li *et al.*, 2015, Macleod *et al.*, 1999, Bigucci *et al.*, 2008) and the most important application of pectin is based on its ability form hydrogels. In addition, because pectin has many positive influences on human health such as lowering cholesterol and serum glucose levels, limiting cancer and immune system stimulation, it is also applied as a gelling and stabilizing agent in nutritional and cosmetic products. Furthermore, pectin is used to produce an assortment of special products such as edible and biodegradable films, glues, paper alternatives, foams and plasticizers and surface modifiers for medical tools (Mohnen, 2008).

1.2. Mucin

Mucins are the main macromolecular components of the mucus secretions that cover the oral cavity, respiratory, gastrointestinal and urogenital tracts of animals. Moreover, they provide protection for the delicate exposed epithelial surfaces and are responsible for the viscoelastic properties of the mucosal secretions (Adikwu, 2006).

The polymeric structure of the component mucins are directly correlated with the protective properties of the mucus gel (Sellers *et al.*, 1988). Mucins are large, extracellular, abundant, filamentous molecules (Dekker *et al.*, 2002) with the molecular weight range from 5×10^5 up to 2×10^7 g/mol (Yu *et al.*, 2014). Mucin structures are stabilized by inter-chain disulphide bonds (Carlstedt *et al.*, 1985, Ichikawa and Ishihara, 2011). The mucin protein core contains highly glycosylated regions comprising of 80 % carbohydrates primarily of N-acetylgalactosamine (GalNac), N-acetylglucosamine (GlcNac),galactose (Gal), fucose (Fuc) and sialic acid (N-acetylneuraminic acid, Neu5Ac) and traces of sulfate (SO_4^{2-})and mannose (Man) **(Figure 1.5)** (Bansil and Turner, 2006) which makes these regions therefore highly resistant to proteolysis, whereas the sections which are sparsely glycosylated or non-glycosylated are subsequently much more susceptible to proteolysis (Carlstedt *et al.*, 1985, Donald, 1973, Scawen and Allen, 1977). Mucin is negatively charged due to the presence of sulfate esters and sialic acid. The oligosaccharide chains consisting of 5–15 units show moderate branching and are attached to the protein core by O-glycosidic linkages to the hydroxyl side chains of serine and threonines and arranged in a "bottle brush" shape about the protein core (Bansil and Turner, 2006, Harding *et al.*, 2015). Colonic mucin in either its polymeric, reduced (with mercaptoethanol) or digested (with papain) forms have been described to adopt random coil conformations (Jumel *et al.*, 1997, Gillis *et al.*, 2013) as was proposed by the general model (Harding *et al.*, 1989, Sheehan, 1989). In addition, highly purified porcine gastric "Orthana" mucin (which is pharmaceutical grade porcine gastric mucin is used in a saliva substitute formulation "Saliva Orthana") was characterised and the experimental data indicated that the total carbohydrate content was in the range of 71-76% which mainly includes fucose, galactose, *N*-acetylglucosamine, and *N*-acetylgalactosamine residues and trace amount of Sialic acid and 6-7% of all of the amino acid residues includes shistidine, arginine, and lysine .The molecular conformation of "Orthana" mucin also analysed and the result shown the comb subunits has daisy-chain configuration. The daisy beads has sphere-shaped and are isolated by flexible chains. This configuration are likely attributable to

intramolecular assemblies of various hydrophobic domains that are enclosed by hydrophilic parts of the molecule (Yakubov *et al.*, 2007). Furthermore, porcine stomach mucin studied using small-angle X-ray scattering the results stated that this type of mucin consist of a double-globular comb structure. Investigation of the amino acid sequence of the protein core shows that the two-globule dumbbell model is defined by both the hydrophobic association and the charge of the amino acids and the present of the hydrophilic carbohydrate side chains (Di Cola *et al.*, 2008).
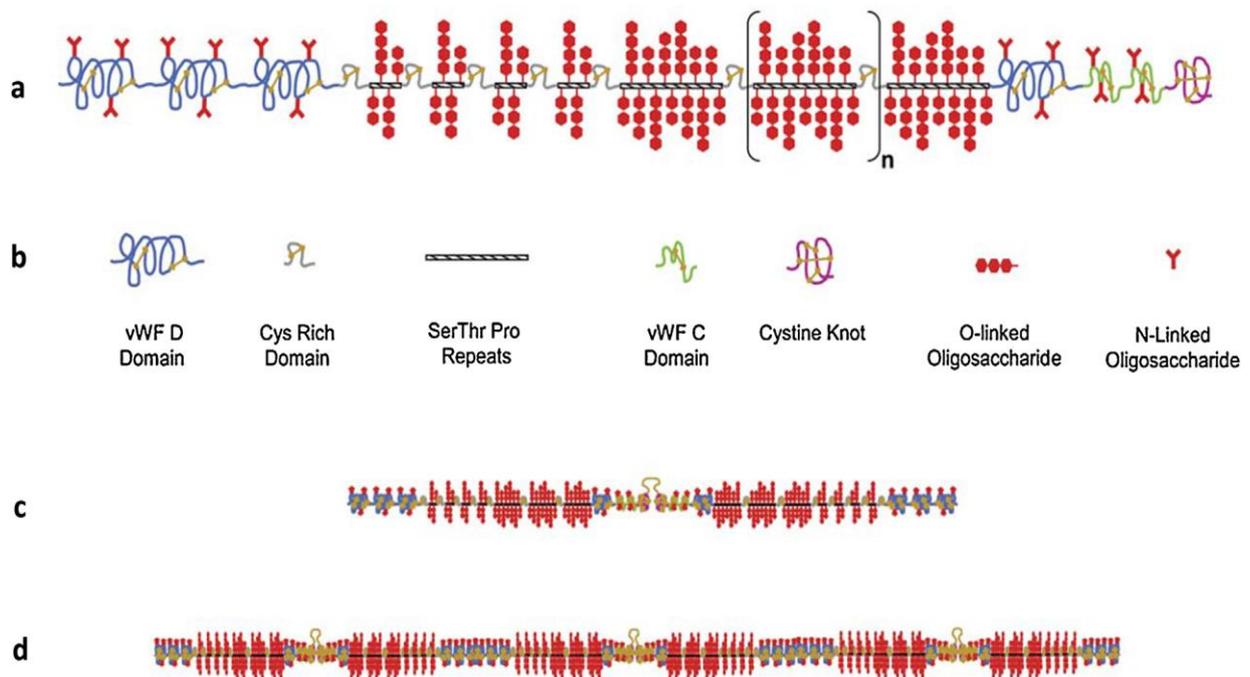
Figure 1.5 Structural conformations of mucin

a) schematic drawing of the pig gastric mucin monomer consisting of glycosylated regions flanked by regions with relatively little glycosylation. (b) The symbols indicate the different domains in the sketch in (a). (This representation is based in part on Figs. 1 and 2 in (Dekker et al., 2002)). The cysteine rich regions contain domains that are similar tovon Will brand factor (vWF) C and D domains, and C-terminal cysteine knot domains which have been shown to be involved dimerization and subsequent polymerisation to form larger multimers. The bottom of the figure shows (c) a dimer formed by two monomeric subunits linked via disulfide bonds in the non-glycosylated regions and in (d) dimers that are further disulfide linked to form higher multimers. This gives rise to the high molecular weight and polydispersity of secretory mucins. Polymers of greater than 16-mers have been described in MUC5AC from human airway secretions by. (The bottom part of the figure is adapted from Fig. 8 in (Sheehan *et al.*, 2004) . Figure reprinted with permission from (Bansil and Turner, 2006)

Based on amino acid sequences and the presence of certain domains mucins are classified into three different groups: secreted gel-forming mucins (*e.g* MUC2, MUC5AC, MUC5B, MUC6, MUC19) secreted non-gel-forming mucins (*e.g.* MUC7, MUC8) and membrane bound (structural) members (*e.g* MUC1, MUC3A, MUC3B, MUC4, MUC12, MUC13, MUC15, MUC16, MUC17, MUC20 and MUC21) (Junker, 2008, Niv and Boltin, 2012).

All these types have one or more of mucin-like domain that hold the typical mucin O-glycosylation. This domain was made from a different of tandem repeats rich in threonine, serine and proline residues. Secreted gel-forming mucins oligomerise when the disulphide bridges form between cysteine residues otherwise the other types are not undergo any oligomerization (Niv and Boltin, 2012). Non-gel forming mucins are present in salivary glands, respiratory tract and middle ear epithelium (Linden *et al.*, 2008) whereas membrane-bound mucins are found on the apical membrane of epithelial cells. Secreted gel forming mucins are found in many parts of the body including: eyes, middle ear epithelia, small intestines, colon, respiratory tract, stomach, cervix, salivary glands, gallbladder, seminal fluid, duodenum, pancreas and submandibular gland (Linden *et al.*, 2008).

1.2.1. Why the characterisation of mucin is important for drug delivery system

An insight in to the basic structure, viscoelastic characteristics and interactions of mucin glycoproteins has increased due to the essential protective role that these materials play in gastric physiology and mucus is the first barrier with which food and drugs can interact with and diffuse through to be absorbed and enter the circulatory system. In addition to being a protective barrier, mucus is also involved in many diseases; mucus hypersecretion is a main signal of many lung diseases (*e.g.* chronic bronchitis, cystic fibrosis and asthma) (Basbaum *et al.*, 1989) and cancers (*e.g.* cancers of the pancreas, lung, breast, ovary and colon) (Singh *et al.*, 2007) also it has been found that there is an association between decreasing mucin levels in tear film and eye dryness disease (Javadi and Feizi, 2011) So, by understanding the behaviour of mucins as polymers or complexes construction (hydrophilic, hydrophobic and electrostatic interaction with other polymers) we can optimise the conditions used in delivering nutrients and drugs and perhaps also diagnosis of the health status epithelium (Bansil and Turner, 2006, Kim, 2011).

1.3. Nanotechnology

Nanotechnology is one of the most interesting areas in study of biopolymers which has led to new exciting developments and applications in drug delivery systems, food technology and cosmetics. Polysaccharide nano/micro-particles can be prepared by stimulating self-association or aggregation of single (Patel *et al.*, 2007, Heinze *et al.*, 2011) or by creating phase separation in mixed biopolymer systems (Phillips and Williams, 2000). Over time, many polysaccharides have been used in the preparation of nanoparticles which significantly enriches the diversity of nanoparticle carriers in terms of type and function. With respect to structural features, polysaccharide nanoparticles are prepared by different mechanisms (Phillips and Williams, 2000, Vauthier and Ponchel, 2017, Sharma *et al.*, 2011, Yang *et al.*, 2015, Pinto Reis *et al.*, 2006):

- ionic crosslinking (Bodmeier *et al.*, 1989)
- covalent crosslinking (Barthelmes *et al.*, 2011)
- self-assembly of hydrophobically modified polysaccharides (Akiyoshi *et al.*, 2000)
- polyelectrolyte complexation(Mi *et al.*, 1999)
- nanoprecipitation method (Barichello *et al.*, 1999)
- emulsion method (Tewes *et al.*, 2007)
- supercritical fluids (Byrappa *et al.*, 2008)
- anti-solvent evaporation (Wang *et al.*, 2004)

1.3.1. Polyelectrolyte complexes (PECs)

Upon mixing two biopolymers together, one of three possibilities can occur (Tolstoguzov, 1991, Harding, 1997a):

- nothing,
- covalent or non-covalent interaction between biopolymers in either a reversible or non-reversible manner: *e.g.* molecules" sticking together" which correspond to possibilities 1 and 2 in Figure 1.6.
- Phase separation (due to thermodynamic incompatibility) *e.g.* molecules "pushing apart" which correspond to possibilities 3 and 4 in Figure 1.6.

Therefore, although many mixtures of biopolymers are thermodynamically incompatible and "phase separate"; other mixtures however indicate ability for interaction to give soluble complexes in the suitable pH, ionic strength and temperature conditions. The situation can be more complicated because attractive interactions "sticking together" can produce phase separation, particularly if the complex results in minor net charge furthermore, at low concentration, even thermodynamically incompatible systems can remain as a one phase system **Figure 1.6** indicates the four possibilities (1-4).
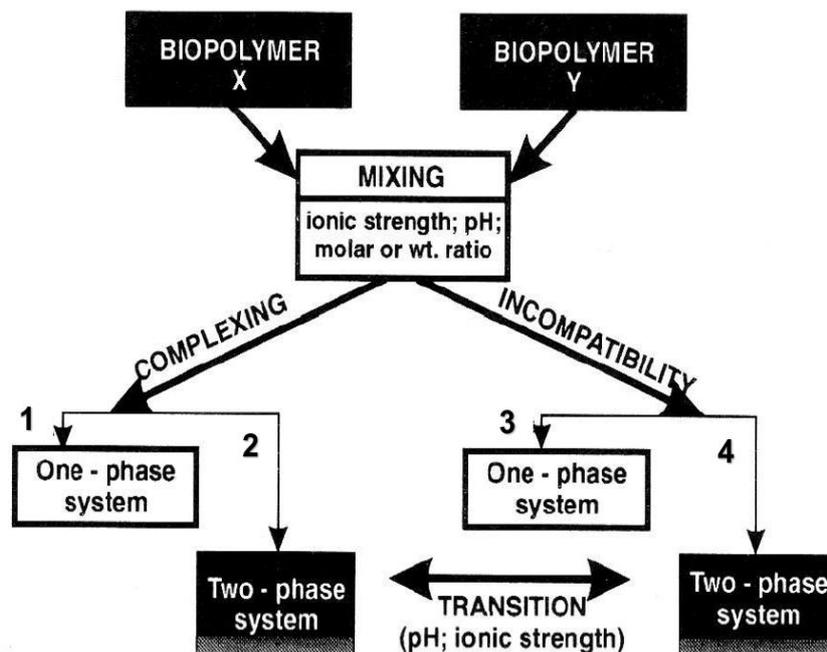
Figure 1.6 Tolstoguzov diagram representing the four possibilities resulted from mixing two soluble biopolymers together in an aqueous environment.
For example mucin (anion) mixed with the Cs (cation) under slightly acidic conditions seems to correspond to possibilities 1 and 2 (Adapted from Tolstoguzov, 1991)

Macromolecules in which a considerable portion of the structural units have ionic, ionisable groups or both are termed polyelectrolyte (Hess *et al.*, 2006), which when dissolved in an appropriate polar solvent (usually water), spontaneously obtain or can be made to obtain a large amount of fundamental charge spread along the macromolecular chain (Hess *et al.*, 2006) and their solubility is attributed to the electrostatic interactions between their charged monomer and water molecules (Lankalapalli, 2009). The polyelectrolytes are classified into

different types. Based on their origin; natural polyelectrolytes, synthetic polyelectrolytes and chemically reformed biopolymers. Based on composition they are copolymers and homo-polymers. Based on molecular architecture they are classified into linear, branched and cross linked. Finally, depending on electrochemistry they are categorized as polyacids/polyanions, polybases/polycations and polyampholytes (Lankalapalli, 2009). The association between oppositely charged particles can form polyelectrolyte complexes (PECs) such as polymer/polymer, polymer/drug and polymer/drug/polymer complexes (Lankalapalli, 2009). These are formed due to electrostatic interactions between oppositely charged polyions (Hess *et al.*, 2006). The formation of polyelectrolyte complexes involves three main steps as shown in **Figure 1.7**. Firstly, the primary complex is formed by Coulomb forces (very fast). The next step is the formation process within intra-complexes which includes creation of new bonds and/or the reformation of the distortions of the polymer chains. Finally, inter-complex compilation process take place which includes the aggregation of secondary complexes mainly by hydrophobic interactions (Dakhara and Anajwala, 2010). The properties of polyelectrolyte complexes are influenced not only by the chemical structure of the polymers such as the molecular weight, stereo-chemical fitting and charge densities, but also by experimental conditions such as the concentrations of the polyelectrolytes prior to mixing, the mixing ratio, ionic strength, pH of the solution and temperature (Dakhara and Anajwala, 2010).
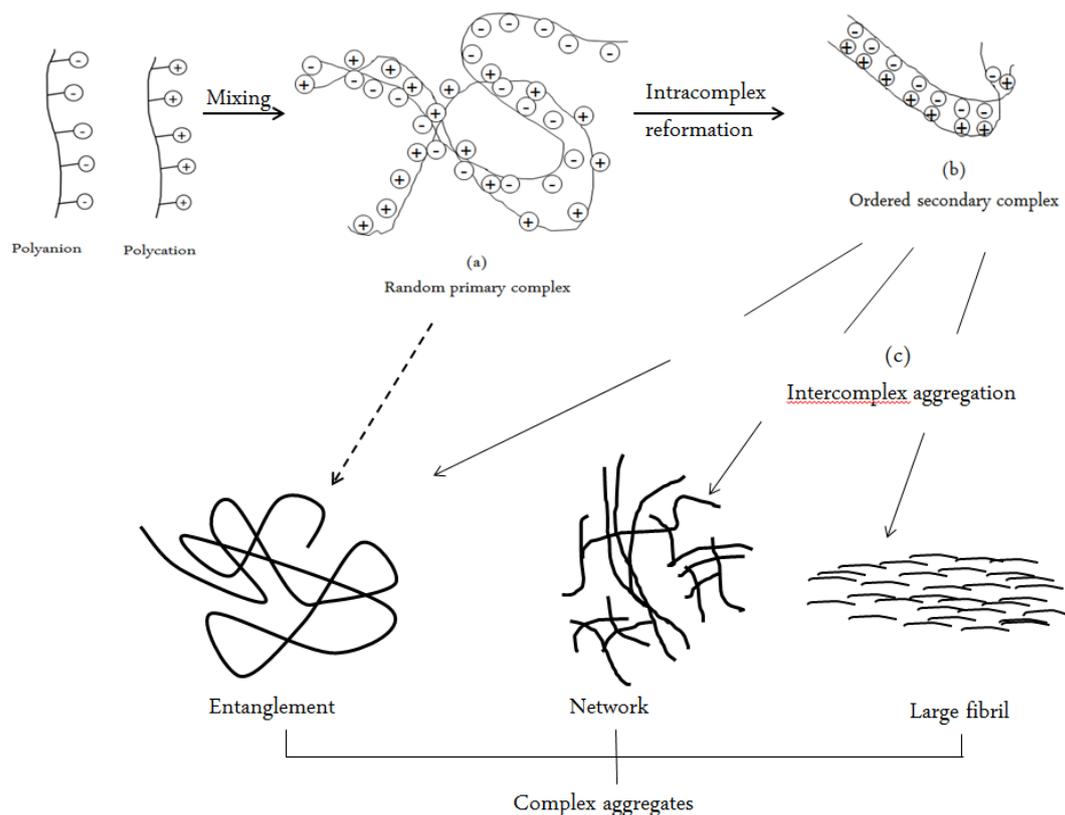
Figure 1.7 Diagram representation of the formation and aggregation of PECs (a) Primary complex formation (b) Formation process within intracomplexes (c) Inter complex aggregation process (Dakhara and Anajwala, 2010)

The different structures a PEC can be classified into three different subtypes: soluble, colloidally stable, and coacervate complexes depending on many factors such as pH, salt and polymer concentration (Ankerfors, 2008). According to the nature of polyelectrolyte the PECs can be classified into five types (Dakhara and Anajwala, 2010, Gubbala, 2012).

i. Polyelectrolyte complex between natural polymers such as Cs with numerous natural polyanions (*e.g.* carboxymethyl cellulose, alginic acid, pectin, dextran sulfate, carboxymethyl dextran, heparin, carrageenan and xanthan).

ii. Polyelectrolyte complex between a natural and a synthetic polymer such as that which forms a polymeric protein with synthetic polyelectrolytes.

iii. Polyelectrolyte complex between synthetic polymers for instance poly (sodium styrene sulfonate) and a series of synthetic polycations such as quarternized poly (4-vinyl pyridine).

iv. Complex formation between polyions and surfactants *e.g.* poly (stryenesulfonate) and different alkyltrimethylammonium derivatives.

v.   Polyelectrolyte complex between polymers and oppositely charged drugs such as polyelectrolyte complexes that form between ionic drugs and the polyelectrolytes.

1.3.2. Liposomal encapsulation technology (LET)

Liposomes are defined as spherical artificial vesicles consisting of aqueous solution core enclosed by one or more phospholipid bilayers (Akbarzadeh *et al.*, 2013). The term "liposome" is derived from two Greek words which has two words: *lipo* ("fat") and *soma* ("body"); it is named because phospholipid is the essential part of its structure (Dua *et al.*, 2012). Liposomes were discovered by British hematologist Dr Bangham in the early of sixties. When Bangham was testing new laboratory tools, he observed that phospholipids were able to form multilayer vesicles spontaneously in aqueous solution (Laouini *et al.*, 2012).

The main ingredients of liposomes are synthetic and/or natural phospholipids which include phosphatidylserine, phosphatidylglycerol, phosphatidylinositol, phosphatidylcholline (lecithin) and phosphatidylethanolamine. The last two constitute the most widespread structural components of most biological membranes. Moreover, cholesterol has been widely utilized in liposome preparation to improve the lipid bilayer properties of the liposomes such as decreasing the flexibility of the surrounding lipid chains, improving stability and decreases the permeability of water soluble substances cross the bilayer (Laouini *et al.*, 2012).

Structurally, liposomes are small vesicles **(Figure 1.8)**, in which an aqueous volume is completely surrounded by phospholipids bilayer. A phospholipid molecule consists of two parts: a hydrophilic head group (polar region) and a hydrophobic tail group (hydrocarbon chains) which are naturally found as stable membranous bilayer. However, in the aqueous medium, the hydrophilic regions are attached to water molecules and line up to compose a surface attracting aqueous solution. The hydrophobic region is repelled by water and line up to compose a surface far from the water (Dua *et al.*, 2012).
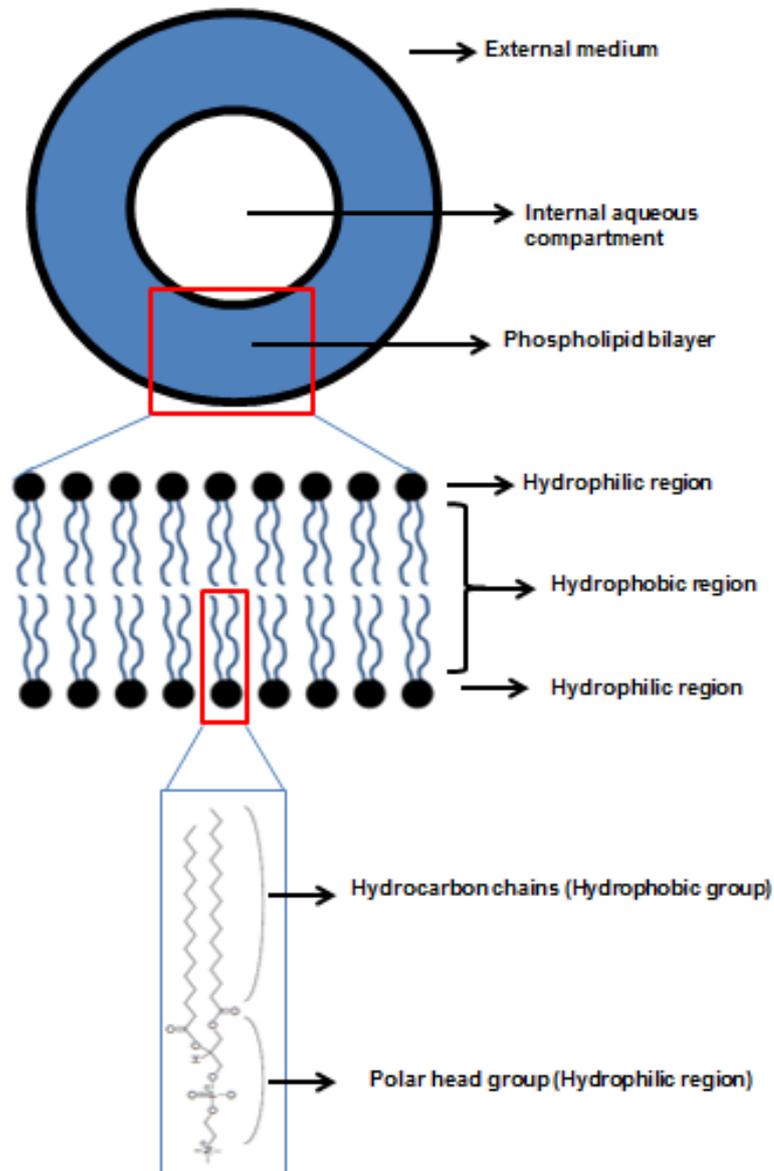
Figure 1.8 Schematic diagram of structure and composition of liposome
(De Araújo Lopes et al., 2013).

The physical characterisation of liposomes plays a prominent rule in identifying their appropriateness for a specific objective from a range of applications and gives good understanding of actual biological membranes. Based on their structure and preparation method, liposomes display wide diversity in their physical and chemical features. For example: particle size, size-distribution, morphology, stability, membrane lamellarity, surface charge, permeability and the encapsulation efficiency (Yitbarek, 2010).

1.3.2.1. Classification of liposomes

Liposomes can be classified in terms of their structural parameters, preparation method and functionality. As vesicle size and the number of bilayers are essential parameters in studying encapsulation efficiency and stability of liposomes **(Figure 1.9)**, the classical classification of liposomes was made according to their structural properties which are: small unilamellar vesicles (SUV), large unilamellar vesicles (LUV), multilamellar vesicles (MLV), oligolamellar vesicle (OLV), giant unilamellar vesicles (GUV) and multivesicular vesicles (MVV) (Laouini *et al.*, 2012). Based on their composition and delivery systems and they can also classified as conventional liposomes, charged liposomes, long-circulating (stealth) liposomes, and active liposome (pH-sensitive liposomes, temperature sensitive liposomes and immune-liposomes) (Gomez-Hens and Fernandez-Romero, 2006). They also can be classified according to the method of preparation for example: lipid hydration followed by vortex or manually mixing (MLV), reverse-phase evaporation (MLV, LUV), organic solvent injection to prepare (MLV, LUV, SUV) freeze-thawing (MLV, LUV), pH gradient (LUV, SUV), dehydration-rehydration (MLV) and detergent dialysis (MLV, LUV) in their preparation protocols (De Araújo Lopes *et al.*, 2013).
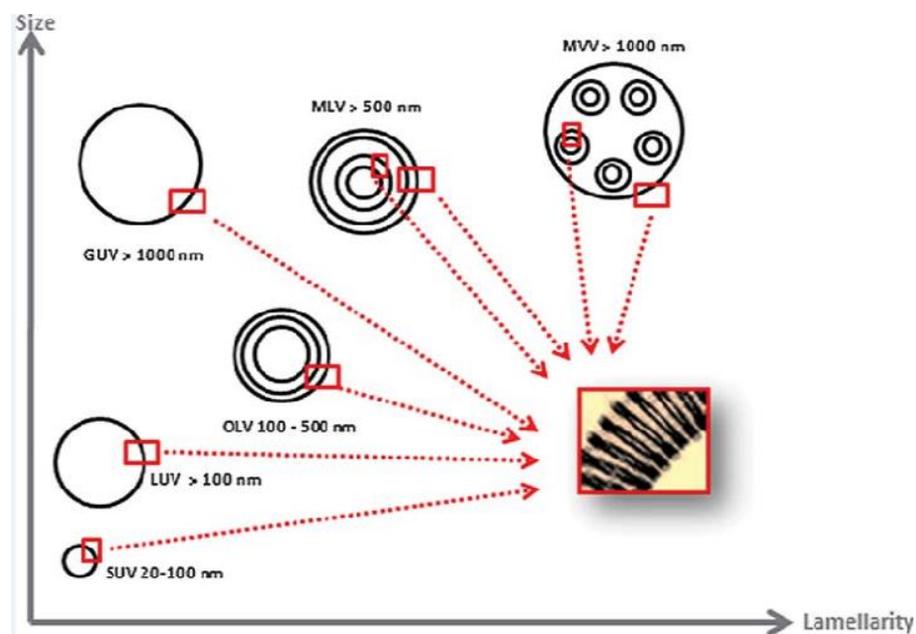
Figure 1.9 Classification of liposomal vesicles based on size and lamellarity
(Laouini et al., 2012)

1.3.2.2. Methods for the preparation of liposomes

There are several methods to prepare liposomes. In selecting the most convenient method there are several factors which must be taken into account *e.g.* structural parameters, stability, cost, toxicity, the quantity of the loaded material, reproducibility, applicability, type of dispersion media and further processes which may be undertaken during the application of liposomes. These methods can be classified to classic and new (Bozzuto and Molinari, 2015).

1.3.2.2.1. Classic methods:

These methods are different in terms of the technique that is used to dry down lipids from organic solvent.

- Hydration of a Thin Lipid Film (Bangham Method)

This method is the most common technique for liposomes manufacture. In brief, it involves three stages: dissolving the phospholipid and cholesterol in an organic solvent, removing the organic solvent by rotary evaporation and finally dispersing the dry lipid layer in aqueous solution under agitation at temperature above the phospholipid transition temperature (Laouini *et al.*, 2012). The encapsulation of substances can be achieved by the addition of a hydrophilic substance to the aqueous media and lipophilic material to the lipid film (Gomez-Hens and Fernandez-Romero, 2006). The main feature of the resultant liposomes are that they are heterogeneous in size and shape (100 - 500 nm diameter) (Laouini *et al.*, 2012). Thus sonication or extrusion is required to produce homogeneous small unilamellar vesicles (Gomez-Hens and Fernandez-Romero, 2006).

- Reverse-Phase Evaporation (REV) Method

The procedure of this method based on the redispersion of the lipid film in a second organic phase (diethyl ether and/or isopropyl ether) under nitrogen. When the aqueous solution is introduced to the mixture, LUVs, OLVs are formed then the organic solvent is removed (Laouini *et al.*, 2012). Although this method is influenced by the solubility of lipids in the organic solvent and the removal of the solvent from the products, it provides higher encapsulation efficiency than previous method (Bozzuto and Molinari, 2015).

- Solvent (Ether or Ethanol) Injection Technique

These methods depend on dissolving the lipid into an organic solvent (ethanol or ether) followed by injecting the lipid solution into aqueous media, subsequently, the liposomal product formed will be heterogeneous (Laouini *et al.*, 2012).

- Detergent Dialysis

In this method, the lipid film is hydrated with a detergent solution then the detergent is eliminated by controlled dialysis and the liposome formed (Laouini *et al.*, 2012). Although the liposomal products are homogeneous unilamellar vesicles and can encapsulate large volumes (Laouini *et al.*, 2012), this method is rarely utilized due to the longer times required for preparation (Bozzuto and Molinari, 2015).

1.3.2.2.2. New Large-Scale Liposome Technique

With the widespread need for liposome applications in the field of industry, the number and the range liposome-preparation techniques have increased dramatically (Wagner and Vorauer-Uhl, 2010). Novel methods such as heating, spray-drying, freeze-drying and supercritical reverse-phase evaporation are now available.

- Heating Method

In this method the liposome components are hydrated in an aqueous medium then heated up to 120 °C in the presence of glycerol (3 % v/v). Glycerol is used due to its solubility in water, acceptable physiological properties, to improve the stability of lipid bilayers and it does not need to be eliminated from the final product. Heating provides appropriate energy for the production of stable liposomes (Laouini *et al.*, 2012).

- Spray-Drying

This method is one the most adopted techniques in the industry because it is simple and fast. Briefly, the vesicles are prepared by dissolving lecithin and mannitol in chloroform and sonicating the mixture then spray drying, finally, the obtained product is hydrated. The size of liposome varies depending on the volume of aqueous solution used for hydration of the dried product (Laouini *et al.*, 2012).

- Freeze-drying

This is one of the industrial techniques used in liposome preparation which is based on removing the aqueous solution from a sample in the frozen phase by sublimation and desorption through vacuum (De Araújo Lopes *et al.*, 2013). The produced liposome is usually homogenous and its size is influenced by lipid/carrier ratio of the liposome preparation (Laouini *et al.*, 2012).

- Super Critical Reverse Phase Evaporation (SCRPE)

SCRPE is single-step technique for liposome preparation which is based on the introduction of aqueous solution into a homogeneous mixture of supercritical carbon dioxide/lipid/ethanol under adequate stirring and following pressure reduction. The main features of this method it yields large unilamellar vesicles with diameters of 100-120 nm with a high encapsulating efficiency for water soluble solutes and does not requires the usage of toxic solvents (Imura *et al.*, 2003).

1.3.2.3. Applications of Liposome:

1.3.2.3.1. Medicinal and pharmaceutical applications

Due to the wide range of properties including the ability to encapsulate both hydrophobic molecules and hydrophilic molecules, liposome are widely used in medicine and pharmacology (Dua *et al.*, 2012). The medicinal and pharmaceutical applications could be either in the diagnostic and therapeutic fields; as a model, a tool, or reagent in cellular interaction studies, assessment processes and the activities of specific materials (Akbarzadeh *et al.*, 2013).

Regrettably, several drugs have very narrow therapeutic index because the toxic concentration is not much higher than the therapeutic one. In these cases, an appropriate drug carrier can be used to reduce the toxicity or enhance the efficacy by altering the temporal and locative delivery of the drug (Bozzuto and Molinari, 2015). Many pre-clinical and clinical studies indicate that antitumor drugs encapsulated in liposomes reduced toxicities (Gabizon *et al.*, 1994, Lasic, 1997), while retaining enhanced efficacy (Akbarzadeh *et al.*, 2013). Development in the design of liposomes leads to new product technologies for drug delivery systems for instance oligonucleotide drugs, reproduced genes, and recombinant proteins. Recent advances containing liposomal formulations of all-*trans*-retinoic acid and daunorubicin

have been accepted by Food and Drug Administration (FDA) as a first-line therapy of acquired immune deficiency syndrome (AIDS) such as vincristine, doxorubicin, and amphotericin B (Akbarzadeh *et al.*, 2013).

1.3.2.3.2. Cosmetic applications

Recently, liposomes have become essential ingredient in cosmetic products due to their vast array of properties; they can be utilized in skin care to reduce the transdermal water loss, treat dry skin diseases, reduce the aging and they can also supply and replenish fatty acids including linolenic acid to the skin. In cosmetics, liposomes have been widely used to treat hair loss such as minoxidil and vasodilator products. "Capture" anti-ageing cream is considered to be the first liposomal product and was marketed by Christian Dior in 1986 (Laouini *et al.*, 2012). Several liposome products from egg and soya phospholipid formulations were studied *in vivo* for skincare applications. Since 1987, various cosmetics have become commercially available; for example: Efect du Soleil (L'Oréal), Future Perfect skin gel (Estée Lauder), Aqua Some LA (Nikko Chemical Co), Eye Perfector (Avon) and Flawless Finish (Elisabeth Arden) (Laouini *et al.*, 2012).

1.3.2.3.3. Food industry applications

Although the nanotechnology has only recently been applied in food industry, considerable developments have been observed in this sector. The key applications, up to now, have been targeted to improving the texture of food constituents, encapsulating nutritional components or food additives, developing the savours and sensations, modifying the release of flavours, and enhancing the bioavailability of nutritional constituents (Reza *et al.*, 2008). Although biopolymer matrices formed of sugars, starches, gums, proteins, dextrins, and alginates are the most common encapsulation techniques employed in the food industry, nano-liposome technologies have recently begun to increase in significance because of their aforementioned properties (Reza *et al.*, 2008). Following on from the successful results achieved by liposome technology in the medical and pharmaceutical fields (drug delivery, gene targeting and cancer therapy), food and nutrition scientists have become interested in this technology to control delivery of food constituents *e.g.* proteins, vitamins and flavours in numerous food applications. Among these applications are improved dairy products, stabilization of food constituents versus degradation and delivery and improved efficiency of antimicrobial peptides (Taylor *et al.*, 2005b).

1.3.2.3.4. Agricultural applications

Liposomal technology is also now being applied in agricultural systems (both for plants and animals). The primary use of liposomes in this sector is in developing some drug and reagent delivery systems and to generate model or controlled membrane systems; to investigate the carriage of solutes through cellular membranes, illustrate the uptake mechanism of toxic substances and antimicrobial activity, study the mechanism of pesticides and transport therapeutics materials to farm animals (Taylor *et al.*, 2005b).

1.4. Mucoadhesion

For four decades, the concept of mucoadhesion has occupied an essential place in the field of pharmaceutical technology. Bioadhesion term is referred to the attachment of synthetic or natural macromolecules to a biological by interfacial forces of period time (Mortazavi and Smart, 1994, Peppas and Buri, 1985, Park and Robinson, 1984). When bioadhesive interactions occur mainly with mucus or a mucous membrane, the state is defined as mucoadhesion (Smart, 2005). The American Society of Testing and Materials has described mucoadhesion as the state of association of two surfaces together through interfacial forces (*i.e.* valence forces, interlocking action or both) (Boddupalli *et al.*, 2010). The hydrophilic macromolecules that have ability to establish hydrogen bonds with mucus are known as mucoadhesive materials (Mortazavi and Smart, 1994, Smart, 2005) some examples such as Cs and Carbopol® have been used as mucoadhesive (Lehr *et al.*, 1992b) and adhesion properties of some formulations to porcine stomach was studied (Gåserød *et al.*, 1998). The mucoadhesion process between a formulation and mucus basically involves three regions **(Figure 1.10)**: the mucoadhesive formulation surface, the mucosal surface and an interfacial region (Mortazavi and Smart, 1993) and is based on two steps: contact stage and consolidation stage **(Figure 1.11)**. The first step is the attachment between the mucoadhesive and the mucosal surface, followed by spreading and swelling of the formulation into the mucus layer (Smart, 2005, Carvalho *et al.*, 2010, Peppas and Buri, 1985).
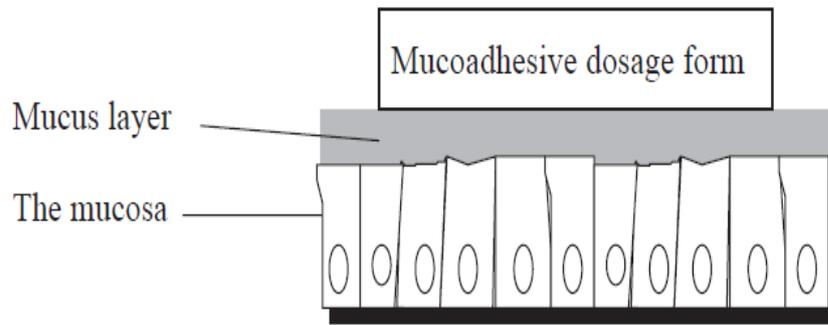
Figure 1.10 The three regions where the mucoadhesive bond joint
(Smart, 2005)

In the consolidation stage, moisture is required to activate the mucoadhesive materials in order to plasticise the system, allowing the mucoadhesive molecules to break free and establish weak van der Waals and hydrogen bonds (Smart, 2005). This stage can be described by two theories: diffusion theory and the dehydration theory. Based on diffusion theory, the mucoadhesive materials and mucin mutually interact via the interpenetration of their chains to establish secondary bonds (Carvalho *et al.*, 2010). So, for mucoadhesion to occur there are several features promoting both chemical and mechanical interactions which support its spread throughout the mucus layer. For instance, molecules building hydrogen bonds, charged surfaces, high molecular weight molecules with flexible chains (Carvalho *et al.*, 2010). According to dehydration theory, substances that readily can became gelatinous in an aqueous medium, become dehydrated when attached to the mucus layer due to the difference of osmotic pressure. This difference leads water being drawn into the formulation until the osmotic equilibrium is reached thus increasing contact time between the mucous and the formulation. However, this theory is not appropriate for the solid or highly hydrated formulation (Smart, 2005, Carvalho *et al.*, 2010).
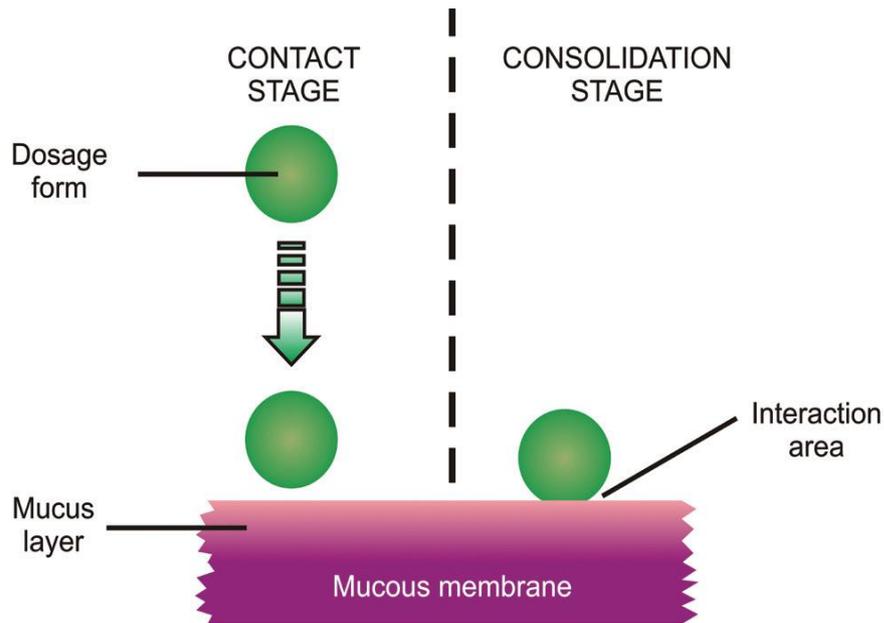
Figure 1.11 The two stages of the mucoadhesion process
(Carvalho et al., 2010)

Because the mucosal layer exists negative charge, positively charged polymers can have a rule in the mucoadhesion process. This phenomenon involves many forces; the primary stage of this process is driven by electrostatic force, followed by entanglements of the polymers chains, van der Waals force, hydrogen bonds and other forces (Lehr *et al.*, 1993). The mucoadhesion is slightly complicated so its mechanism has been proposed through various theories as summarised in **Table 1.1**:

1.4.1. Mucoadhesion theories

1.4.2.1. Wetting theory

This theory is mainly applied to fluid systems and depends on surfaces and interfacial energies. It based on the ability of a wet formulation to spread spontaneously onto a surface as a prerequisite to improve the adhesion to mucus (Lehr *et al.*, 1993, Lehr *et al.*, 1992a). Wetting theory depends on evaluation of the affinity of a liquid for a surface. This affinity can be determined by using contact angle goniometry technique which measures the contact angle of the liquid on the surface, where generally a lower contact angle the greater the affinity of the liquid to the surface (Smart, 2005, Carvalho *et al.*, 2010, Lehr *et al.*, 1993). The relationship between contact angle and mucous membrane is shown in **Figure 1.12**.
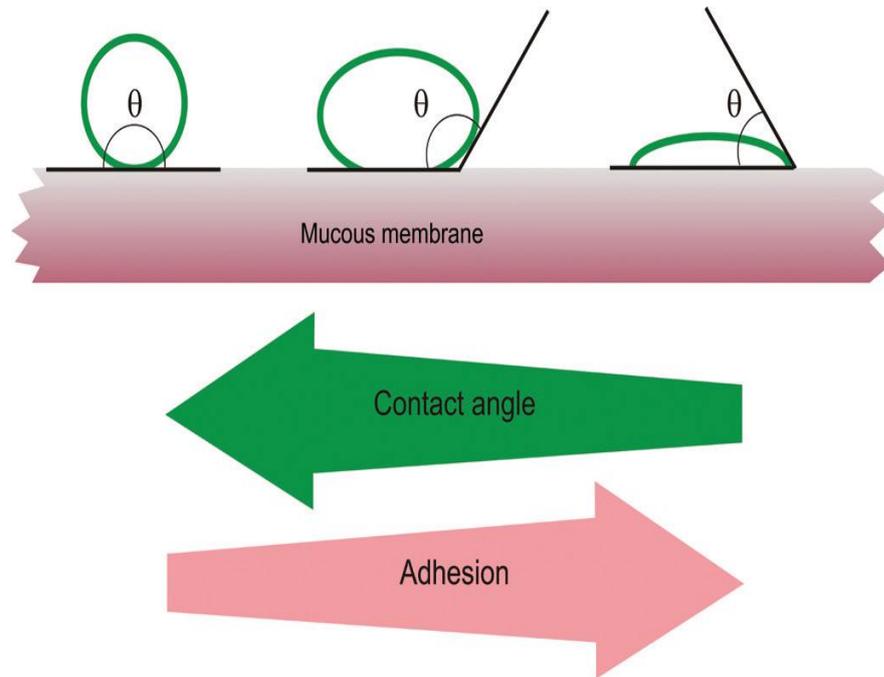
Figure 1.12 Schematic diagram showing relationship between contact angle and mucous membrane (Carvalho et al., 2010)

The spreading coefficient (S_{AB}) can be calculated from the surface tensions of the solid and fluid using the following equation:

$$S_{AB} = \gamma_B - \gamma_A - \gamma_{AB} \tag{1.1}$$

Where γ_A is the surface energy (tension) of the liquid A, γ_B is the surface energy of the solid B and γ_{AB} is the interfacial energy between the solid and liquid. The contact angle should be equal or close to zero to offer sufficient spread ability. The contact angle measurements can be experimentally evaluated from interfacial tension (γ) using the Young equation:

$$\gamma SG = \gamma SL + \gamma LG \cos \theta \tag{1.2}$$

Where γSG is the interfacial tension between solid and gas; γSL is the interfacial tension between solid and liquid; γLG is the interfacial tension; and θ is the contact angle between solid and liquid interface **(Figure 1.13)**

The relationship between interfacial tension and with contact angle displays the level of wetting; when $\theta = 0°$, wetting is complete and the formulation completely spread through the surface. On the other hand, a contact angle of 180° indicates no wettability. If contact angle ranges between 0° and 180° that means Moistening between the liquid (formulation) and the surface of material (e.g., mucosal surface) occurs (das Neves and Sarmento, 2014).
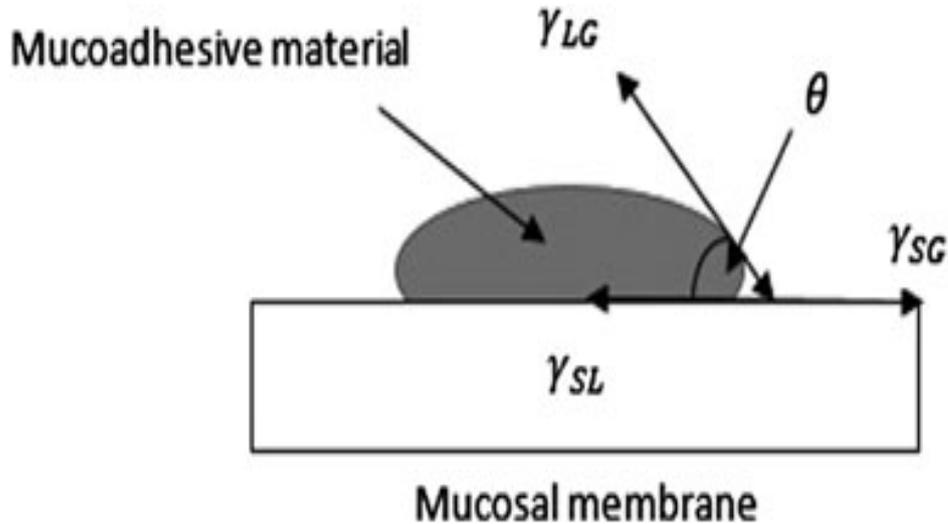
Figure 1.13 Contact angle measurement between a droplet and solid surface
(das Neves and Sarmento, 2014)

1.4.2.1. Diffusion theory

This theory describes the interpenetration of mucoadhesive polymers chains across mucus surface to an adequate depth to make a semi-permanent adhesive bond (**Figure 1.14**) (Leung and Robinson, 1990, Park and Robinson, 1985). The adhesion strength of a polymer to mucus surface in is depends on degree of penetration of the polymer chains and penetration rate affected by of the polymer construction (*i.e.* the flexibility and length chains), the diffusion coefficient, mobility and contact time (Smart, 2005, Carvalho *et al.*, 2010, Vinod *et al.*, 2012a).
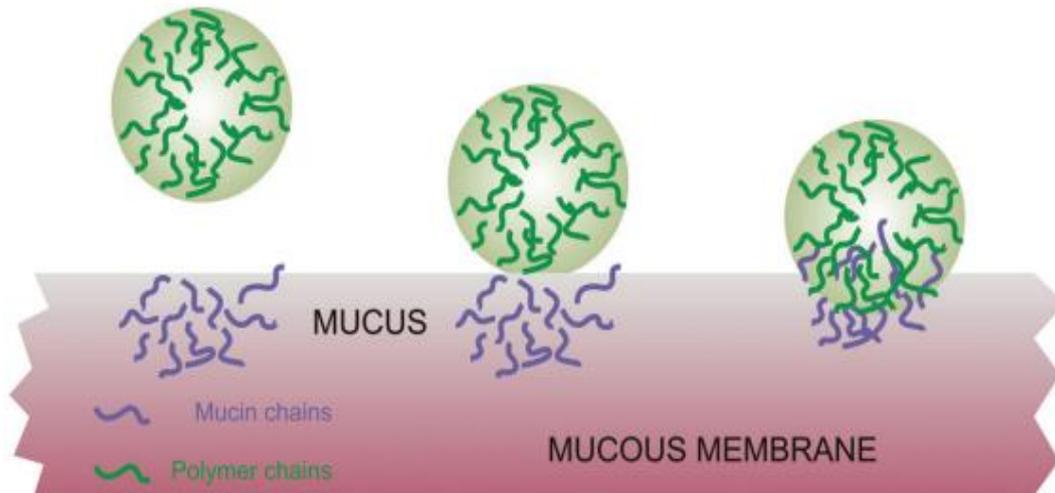
Figure 1.14 Schematic illustration of inter-diffusion between bioadhesive device (polymer chains)
and of mucus
(Carvalho et al., 2010)

- Electronic theory

Electronic theory is based on both mucoadhesive polymer and biological materials displaying opposing electrical charges. Consequently, when the polymer attach with mucus surface a double electronic layer is formed at the interface due to electron transfer. So, the mucoadhesive strength can be determined by the evaluation of interaction forces within this electronic double layer (Derjaguin *et al.*, 1977, Derjaguin *et al.*, 1994, Carvalho *et al.*, 2010).

1.4.2.1. Adsorption theory

The adsorption theory depends on secondary chemical interactions between the mucoadhesive polymers and the mucus including van der Waals and hydrogen bonds, electrostatic attraction or hydrophobic interactions. For instance, in the case mucoadhesion of polymers containing carboxyl groups the interfacial forces is mainly driven by hydrogen bonds. Although these forces are individually weak, they have been considered essential in the adhesive interaction phenomenon because a large number of interactions can establish a strong intense adhesion (Kinloch, 1980, Chickering *et al.*, 1999, Smart, 2005, Vinod *et al.*, 2012b).

1.4.2.1. Fracture theory

The fracture theory is different from the other theories in terms of that it examines the force required to separate two surfaces after adhesion (Kinloch, 1980). This force, S_m, is

normally calculated in tests of resistance to rupture by the ratio of the maximal detachment force, F_m, and the total surface area, A_0, of the adhesive interaction (equation 1.3) (Vinod *et al.*, 2012a).

$$S_m = F_m/A_0 \qquad\qquad (1.3)$$

Fracture theory is the most applied theory to evaluate the mechanical measurement of mucoadhesion (Carvalho *et al.*, 2010). As this theory works only with the energy needed to separate the portions (**Figure 1.15**), it does not take into consideration the penetration or diffusion of polymer chains (Carvalho *et al.*, 2010).
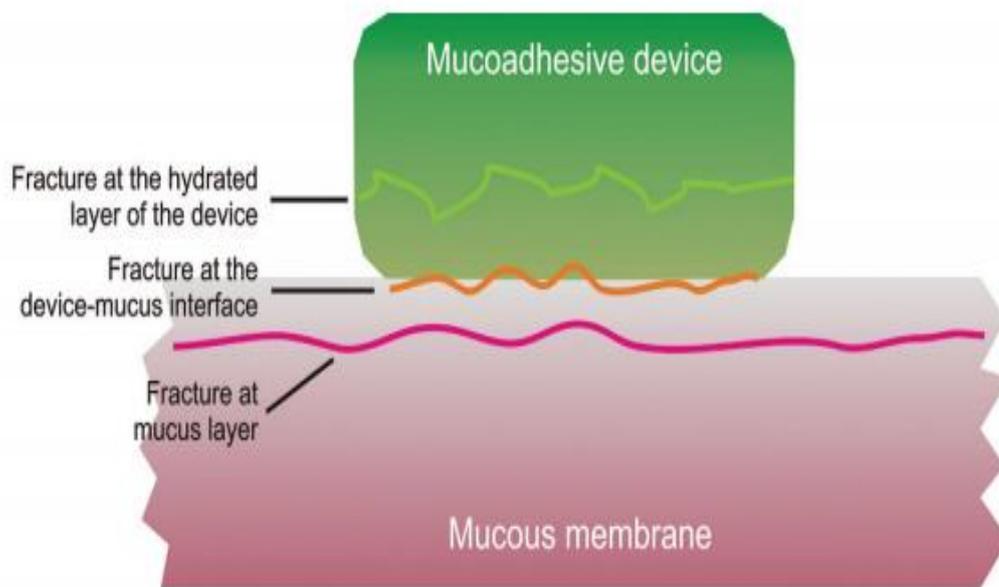
Figure 1.15 Areas where the mucoadhesive bond separation can take place
(Carvalho et al., 2010)

1.4.2.1. Mechanical theory

According to mechanical theory, the adhesive liquid interlocks into irregularities on a rough surface and fills them. Moreover, such roughness provides more interfacial area for interactions to take place thus assisting dissipating energy with enhancing viscoelastic and

plastic properties at the point of interaction which are essential for mucoadhesion phenomenon (Smart, 2005, Carvalho *et al.*, 2010).

Because the chances and degree of polymer/mucus interaction can be influenced by many factors and occur under effect of many forces, this give opportunity for designing and construction of mucoadhesive delivery systems by variation or control of such polymer features (Ponchel *et al.*, 1987). The mucoadhesion process does not occur by a single mechanism but all the above mechanisms are relevant to identify the essential process variables. Numerous factors have been identified as influencing the strength of the mucoadhesion.

Table 1.1 Theories of mucoadhesion.
Adapted from(Vasir *et al.*, 2003)

Theory	Mechanism of adhesion	Comments
Electronic theory	There are attractive electrostatic forces between the glycoprotein mucin network and the bioadhesive material	Electron transfer occurs between the mucin and the bioadhesive material forming a double layer of electric charge at the interface(Derjaguin *et al.*, 1977, Derjaguin *et al.*, 1994)
Adsorption theory	There are surface forces resulting in chemical bonding	The surface forces include strong primary forces which are covalent bonds and weak secondary forces, which include ionic bonds, hydrogen bonds and van der Waal‟s forces (Kinloch, 1980, Chickering *et al.*, 1999)
Wetting theory	The ability of bioadhesive polymers to spread and develop intimate contact with the mucus membranes	Spreading coefficients of polymers must be positive. Contact angle between polymer and cells must be near to zero(Lehr *et al.*, 1992a, Lehr *et al.*, 1993)
Diffusion theory	Physical entanglement of mucin strands and the flexible polymer chains	For maximum diffusion and best bioadhesive strength; solubility parameters (δ) of the bioadhesive polymer and the mucus glycoproteins must be similar interpenetration of mucin strands into the porous structure of the polymer substrate(Leung and Robinson, 1990, Park and Robinson, 1985)
Fracture theory	Analyses the maximum tensile stress developed during detachment of the bioadhesive drug delivery system from mucosal surfaces	Does not require physical entanglement of bioadhesive polymer chains and mucin strands, hence appropriate to study the bioadhesion of hard polymers which lack flexible chains (Kinloch, 1980)

1.4.2. Factors affecting mucoadhesion

These factors can be classified to three sections: polymer related factors, environment related factors and physiological factors.

1.4.2.1. Polymer related factors

1.4.2.1.1. Polymer molecular weight

As defined by Gurny et al., 1984, it shown that there are an optimum molecular weight to achieve strong mucoadhesion; the mucoadhesive force becomes higher with increasing molecular weight of the polymer up to one hundred thousand, and larger than this size there is not much influence. Another studies indicated that molecular weight of polymer ranging from $\sim 1 \times 10^4$ to $\sim 4 \times 10^6$ g/mol can Perform strong mucoadhesion while the polymers with larger size will not hydrate easily to allow the binding groups to connect with mucus layer but polymers with lower molecular weight will form weak gels and easily dissolve (Smart, 2005).

1.4.2.1.2. Degree of cross-linking

Another factor which influences mucoadhesive strength is the degree of cross-linking within a polymer system. It is obvious that, the internal cross-linking density of polymer molecules significantly affects chain mobility and resistance to dissolution (Sudhakar *et al.*, 2006). In the presence of water, cross-linked hydrophilic polymers are swellable whilst retaining their structure, whereas linear hydrophilic polymers (with similar molecular weight) can swell and disperse more readily. Swelling property is not only important in the control the drug release, but it also provides a greater surface area for polymer/mucus interpenetration. So, with increasing cross-link density the chain mobility and the effective chain length will decrease thereby less penetration for the mucoadhesive polymer into the mucus layer occurred and mucoadhesive strength will reduce (Andrews *et al.*, 2009). That mean the structure of the polymer chain has a significant effect; mucoadhesion increases with linear polymers but not with nonlinear polymers because linear polymers provide better interpenetration and entanglement which is important for bioadhesiveness (Lee *et al.*, 2000).

1.4.2.1.3. Flexibility and length of polymer chains

Chain flexibility is critical to join formulation with mucus layer by entangling and interpenetrating (Smart, 2005, Carvalho *et al.*, 2010). Menchicchi et al., 2015 and Huang et al., 2000 have suggested that higher chain flexibility improves mucin- polymer interactions; flexible chain assists to maximise the formation of heterotypic contact sits between the polymer and mucin molecule, therefore, enhancing interpenetration and entanglement. Moreover, In case of water-soluble cross-linked polymers, flexibility and movement of single polymer chains are limited as result penetration of chain into the mucus layer will be reduced resulting in a reduction in the strength of mucoadhesion (Lee *et al.*, 2000). In addition ,appropriate length chain polymer molecule is important to allow interpenetration with mucus (Gurny *et al.*, 1984). Moreover, the size and configuration of the polymer molecule must be taken in consideration. For instance, adhesive force of polyethylene oxide, which are well known highly linear configuration molecules, increases even up to molecular weights of 1×10^6 because it support the interpenetration (Okano, 1998). In contrast, dextran molecules which have molecular weight higher 19.5×10^6 do not display stronger mucoadhesive force than molecules with a molecular weight of 2×10^6 (Gu *et al.*, 1987). Generally, there are association between flexibility and mobility of polymers and their viscosities and diffusion coefficients; polymer with higher flexibility can diffuse deeper into the mucus layer (Gu *et al.*, 1987)

1.4.2.1.4. Concentration

There is an optimal level for the concentration of mucoadhesive polymer to achieve maximum bioadhesion. In systems that have high concentration (higher than the optimum level), the adhesive strength decreases considerably due to separation of the coiled polymer molecules from mucus surface and consequently the degree of interpenetration becomes limited (Lee *et al.*, 2000). In concentrated solutions, the molecules become poorly soluble and the site for interpenetration on the chain of mucin are not adequate (Gurny *et al.*, 1984). (Ponchel *et al.*, 1987) indicated that the higher polymer concentration exhibits stronger mucoadhesion for solid dosage forms *e.g.* tablets.

1.4.2.1.5. Functional group contribution

Mucoadhesive polymers attach and link with the mucus layer mainly by interpenetration followed by secondary non-covalent bonding between the mucoadhesive

formulation and the mucus. This secondary bonding is due to hydrogen bonds and therefore hydrophilic polymers which have functional groups such as carboxyl (COOH), hydroxyl (OH), amide (NH$_2$) and sulphate (SO$_4$H) groups should have greater potential in formulation of mucoadhesive drug delivery system (Andrews *et al.*, 2009). Interaction between Polymers that rich of hydrogen bond and mucin glycoproteins is stronger because hydrogen bonds alow for physical entanglements which contribute to form a strengthened network (Madsen *et al.*, 1998).

1.4.2.2.   Environment related factors

1.4.2.2.1.   pH and polymer charge

One of these factors is pH and polymer charge; the pH value of the system has an important role in mucoadhesion mechanism because it impacts on the formal charge of both mucin and (ionisable) bioadhesive polymers (Lee et al., 2000). Charge density of mucin will differ depending on pH due to differences in dissociation of functional groups on the constituent of mucin (Lee et al., 2000) in other words, at pH≥4 mucin exhibits a random coil conformation structure and this conformation changes to an anisotropic, extended structure at pH < 4. This means gastric mucin displays a pH dependent sol–gel transition when pH is reduced to < pH 4 as indicated (Celli et al., 2007, Cao et al., 1999). Studies have shown that the mucoadhesive properties of ionisable polymers are influenced by the pH of the system. For instance, mucoadhesion of poly (acrylic acid) is adequate when the degree of ionization of carboxylate groups are lower, which happens at pH below the pKa (Smart, 2005, Carvalho *et al.*, 2010). On the other hand, the systems in which involve bioadhesive polymers with intensive ionisable groups such as carbomers and chitosans, the local pH within or at the surface of a formulation will be significantly different from the surrounding environment (Smart, 2005, Carvalho *et al.*, 2010). Moreover, some studies have shown that the pH level of the system is important for the swelling. For example, cross-linked polyacrylic acid displays a high degree of hydration from pH 4 to pH 7, and then a drop due to the alkalinity and the uncharged (rather than ionized) carboxyl groups react with mucin molecules the chains are completely extended because of electrostatic repulsion (rather than numerous hydrogen bonds) of the carboxylate anions (Lee *et al.*, 2000). So, there is an optimum pH for polymer adhesion due to the charge density and degree of hydration depends to a great extent on the pH hence mucoadhesivity is also dependent on pH (Mortazavi and Smart, 1994).

1.4.2.2.2. Initial contact time

The other influence is initial contact time, it has been found that the mucoadhesion increases with the longer initial contact time between the bioadhesive and mucus layer (Lee *et al.*, 2000) and with the consolidation force applied to the joint (Vinod *et al.*, 2012a) because this provides better swelling and interpenetration of the formulation (Lee *et al.*, 2000). In addition, initial contact time is affected by the presence of metal ions in the formulation which can interact with charged polymers hence can affect the adhesion strength (Vinod *et al.*, 2012a).

1.4.2.2.3. Degree of hydration and swelling

The degree of hydration and swelling has also an effect on mucoadhesion phenomenon. In *vitro* there is an optimum degree of hydration corresponding to the best mucoadhesion and over the optimum level the hydration this leads to the formation of moist slippery mucilage without adhesion (Lee *et al.*, 2000). Swelling depends on several issues including the concentration of polymer, ionic strength of medium and the quantity water present of in the system (Lee *et al.*, 2000).

1.4.2.3. Physiological factors

There are certain physiological variables have influence the mucoadhesion for example mucin physico-chemical properties, turnover, and disease states, concomitant diseases and rate of renewal mucoadhesive cell (Alexander *et al.*, 2011), one of the disadvantage related with such mucoadhion systems is that the mucus layer that cover the stomach is continually being renewed, so making mucoadhesion of the formulation changeable (Chun *et al.*, 2005).

1.4.3. Advantages of mucoadhesive delivery systems

Mucoadhesion is one of the widely advocated means of achieving site-specific drug delivery. When mucoadhesive hydrophilic polymers are joined with pharmaceutical formulations the active pharmaceutical ingredient (API) are able to interact with mucus layer hence API gets released close to the site of action with resulting enhanced bioavailability. Moreover, during systemic uptake mucoadhesive polymers will not inhibit the wide distribution of the API (Andrews *et al.*, 2009). Mucoadhesive drug delivery systems provide several of advantages:

- Due to adhesion, intimate contact, residence time of the formulation at the site of action will increase hence improving the bioavailability by lower concentrations of API.

- The formulation remaining longer at the delivery site in conjunction with controlled release of the drug can lead to reduced administration frequency and thereby improve patient compliance.

- First-pass metabolism of API can be avoided.

- Using specific bioadhesive molecules offer opportunity of target specific delivery of API. So, site specific deliveries to the GIT tract have become a possible (Woodley, 2012).

- Mucoadhesive drug delivery systems (includes oral (Jiménez-Castellanos *et al.*, 1994) , nasal (Farraj *et al.*, 1990) ,ocular (Zimmer and Kreuter, 1995), vaginal (Knuth *et al.*, 1993), rectal, cervical and gastrointestinal (Lehr, 1994) mucoadhesive drug delivery systems) considerably contribute to reduce cost of medications by reducing the potential dosage, and dose related side effects by locating API at the site of action (Andrews *et al.*, 2009).

1.5.   Research aims and objectives

The main purpose of this research was to highlight the potential to construct and study drug delivery systems based on polysaccharides. To achieve this aim the following objectives will be followed:

1. Full characterisation of extensively degraded pig gastric mucin with the respect to compositional and hydrodynamic properties to underpin the understanding of mucin interactions with polysaccharide based drug delivery systems because any information about this material could open up opportunities for novel application areas of digested mucins.
2. Physicochemical characterisation of Cs, alginates and pectins.
3. Study the biophysical molecular interactions between mucin (as free molecule and as encapsulated molecule within liposome) and several of polysaccharides characterised previously.
4. Preparation and characterisation of polyelectrolyte complexes containing Cs and naturally occurring polyanions and study the potential polyelectrolyte complex hydrogel for drug release.

1.6.   Thesis structure

This thesis covers the construction and characteristics of new drug delivery systems based on polysaccharides. Chapter 1 offers basic information about the structural and physiochemical properties of applied materials and their importance in drug delivery systems. Chapter 2 (general experimental) provides background information about the main techniques and methodology that applied in all the results chapters (chapters 3-6):

Chapter 3 discusses the results obtained from characterisation of extensively degraded pig gastric mucin with the respect to compositional and hydrodynamic properties to support the understanding of mucin interactions with polysaccharide based drug delivery systems. Part of this chapter is reported in the following peer-reviewed article: Abodinar, A., Tømmeraas, K., Ronander, E., Smith, A. M. and Morris, G. A. (2016) 'The physicochemical characterisation of pepsin degraded pig gastric mucin' *International Journal of Biological Macromolecules*, 87, 281-286.

55

Chapter 4 presents the results obtained from physicochemical characterisation the polysaccharides that used in this study which include Cs, two types of alginates (which differ in structural conformation) and two kinds of pectin (with different degrees of esterification). Part of this chapter is reported in the following peer-reviewed article: Abodinar, A., Smith, A. M. and Morris, G. A. (2014) 'A novel method to estimate the stiffness of carbohydrate polyelectrolyte polymers based on the ionic strength dependence of zeta potential' *Carbohydrate Polymers*, 112, 6-9.

Chapter 5 studies the biophysical molecular interactions between mucin (as free molecule and as encapsulated molecule within liposome) and the polysaccharides that characterised in chapter 4.

The final results chapter (Chapter 6) discusses the characteristics of hydrogel containing Cs and naturally occurring polyanions and the potential for drug release.

Finally, Chapter 7 summarizes the results obtained in this thesis together with recommendations for future work.

1.7.   Publications resulting from this PhD programme

Abodinar, A., Smith, A. M. and Morris, G. A. (2014) 'A novel method to estimate the stiffness of carbohydrate polyelectrolyte polymers based on the ionic strength dependence of zeta potential' *Carbohydrate Polymers* , **112**, 6-9. ISSN 0144-8617

Abodinar, A., Tømmeraas, K., Ronander, E., Smith, A. M. and Morris, G. A. (2016) 'The physicochemical characterisation of pepsin degraded pig gastric mucin' *International Journal of Biological Macromolecules* , **87**, 281-286. ISSN 0141-8130

Chapter 2

General Experimental

2. GENERAL EXPERIMENTAL

2.1. Chapter review

This chapter (Chapter 2) briefly gives overview of the general materials, methods and techniques that are commonly used in this thesis. Any materials and methods that are specific to an individual chapter are presented in the specific chapter and section.

2.2. Materials

Each chapter includes a section of the used materials. Here, the materials that frequently used in the most of chapters are indicated.

Glacial acetic acid, sodium acetate trihydrate and sodium chloride were all obtained from Sigma–Aldrich (Gillingham, UK). Specifications of Cs, pectins, and sodium alginates are presented in details in **Table 2.1**.

Table 2.1 specifications the polysaccharides used in this study

Polysaccharide	Specification [a]
Chitosan	It was obtained from Sigma-Aldrich (Gillingham, UK) and reported with medium molecular weight and an average degree of deacetylation (DD) of ~ 75 - 85 %.
High G sodium alginate	It was obtained from FMC Biopolymer (Drammen, Norway) and reported to have M: G ratios of 1:2 (high G, Mv~25 000 g/mol) and viscosity is 300 – 700 (10%) (mPas).
Low G high viscosity sodium alginate	It was obtained from Sigma–Aldrich (Gillingham, UK) reported to have M: G ratios of 1:0.6 (low G, Mv~290,000 g/mol) and viscosity ≥2,000 cP, 2 %(25 °C) (lit.).
Low G low viscosity sodium alginate	It was obtained from Sigma–Aldrich (Gillingham, UK) reported to have M: G ratios of 1:0.6 (low G, Mv between 120,000 and 190,000 g/mol) and medium viscosity (15-20 cP, 1 % in H_2O (lit.).
High methyl pectin (GENU®)	It was obtained from CP Kelco (Leatherhead, UK) were reported to have an average degree of methyl esterification (DM) of 70.5 %.
Low methoxy pectin (GENU®)	It was obtained from CP Kelco (Leatherhead, UK) and reported to have an average degree of methyl esterification (DM) of 35.5 %.
Extensively degraded mucin	Mucin was kindly gifted from Biofac A/S (Kastrup, Denmark) and was prepared as a by-product from large scalepreparation of pharmaceutical quality pepsin at Orthana KemiskeFabrik A/SA. Approximately 1000 kg of frozen linings were minced in a large meat mincer (screen 18 mm).The minced raw material was transferred into a stirred tank before adding 100 kg of reverse osmosis water. Then, the pH was adjusted to 2.0 using concentrated HCl before heating to 38°C. After 4.5 h, the pH was adjusted to 2.8 using concentrated NaOH. The process liquid was transferred to a precipitation tank and cooled down to −5°C. The crude mucin was then precipitated with 97% acetone added slowly until 61% w/w. The precipitation liquid was held at −5°C and mixed using mild agitation for 30 min. The process liquid was then separated on a Flotweg decanter (1500 rpm inner speed, 6000 rpm outer speed) into liquid and solid phases where the latter contained fat and mucins. The precipitate was solubilized by adding approx. 5volumes of water. Remnants of acetone were evaporated off at 40°Cunder vacuum. Subsequently, the liquid was left to sediment for 3 days before pumping the top phase (clear liquid) out. The crude mucin was then filtered on a Seitz Orion plate and frame filter press three times using cellulose and filter aid based filter plates (firstT2600, T1000 and finally K250, all from Seitz, Pall Corporation, New York, USA) coated with filter aid (Hyflo Super Cel). The mucin was then concentrated to 5% solid content and washed with 3 volumes of reverse osmosis water before pH adjustment to 3–4 and subsequently frozen at −18°C and lyophilized (Abodinar *et al.*, 2016).

[a] Data obtained from the manufacturers.

2.3. Methods

2.3.1. Preparation of sodium acetate buffers

De-ionized (DI) water was used to prepare sodium acetate buffer solutions with different IS (pH 4.3) and different pH (IS 0.05 M) using sodium acetate tri-hydrate salts ($NaC_2H_3O_2.3H_2O$, M_w is 134.08 g/mol) and acetic acid (CH_3COOH, M_w is 60 g/mol, pK_a= 4.75). **Table 2.2** shows the amount of acetic acid and sodium acetate tri-hydrate needed to prepare the different ionic strengths (pH = 4.3) by applying Equation 2.1.

$$pH_{buffer} = pK_a + \log([salt_{(aq)}] / [acid_{(aq)}]) \tag{2.1}$$

Table 2.2 Weight of acetic acid and sodium acetate trihydrate weight needed to prepare the different ionic strengths (pH= 4.3).

Ionic strength (M)	Acetic acid weight (g)	Sodium acetate tri-hydrate weight (g)
0.05	2.22	1.78
0.1	4.41	3.55
0.15	6.65	5.36
0.2	8.86	7.13
0.3	13.3	10.69
0.5	22.16	17.82
0.8	35.46	28.52

2.3.2. Preparation sodium chloride solutions with different ionic strengths

Certain ionic strengths of sodium chloride (NaCl, Mw is 58.44 g/ mol) was prepared as shown in **Table 2.3** using equations 2.2 and 2.3.

$$Molarity = moles\ of\ solute\ /\ 1liter\ of\ solution \tag{2.2}$$

Moles = mass / molar mass   (2.3)

Table 2.3 Weight of sodium chloride needed to prepare the different ionic strengths

Ionic strength (M)	NaCl weight (g) /1L
0.05	2.92
0.1	5.84
0.15	8.77
0.2	11.7
0.3	16.9
0.5	29.22
0.8	46.75

2.4. Statistical analysis

All the findings that obtained from all experiments are expressed as the mean value $\pm$ standard deviations of at least three readings.

2.5. Theoretical discussion of techniques commonly used in this research

2.5.1. Zetasizer

The zetasizer is a technique used to measure the zeta potential (ζ) of hydrocolloids by determining the electrophoretic mobility. In colloidal systems, particles are electrostatically charged by positive or negative charges. Under the influence of an electric field, the particles migrate in the direction which has the opposite charge (Hunter, 1981). After reaching equilibrium between the opposing forces, the particles travel at a constant speed. The direction and speed (electrophoretic mobility) of the particles in applied field depends on (Streng, 2012):

- The strength of the applied electric field
- Solvent dielectric constant
- Solvent viscosity
- Zeta potential

The distribution of ions surrounding the particle is influenced by the movement of the particle which leads to an increase in the concentration of counter-ions (the opposite charged ions to that of the particle charge) near the surface. This lead to the formation of an electrical double layer which surrounds each particle which is separated in to two regions Stern layer and diffuse layer as they shown in **Figure 2.1** (Kumar and Kumbhat, 2016):

- Stern layer (inner region): where the ions are strongly attached
- Diffuse layer (outer region): where the ions are less firmly associated.
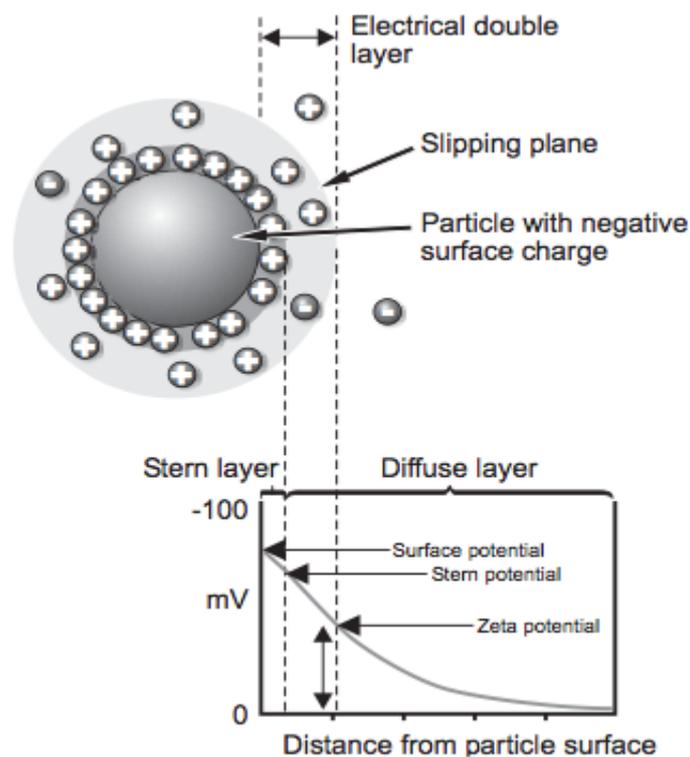
Figure 2.1 Schematic illustration for electric double layer around a charged particle in solution (Kumar and Kumbhat, 2016)

Notionally, there is boundary within the diffuse layer where the ions and particles establish a stable entity and ions do not move with the particle. This boundary is known as slipping plane or the surface of hydrodynamic shear. The potential that exists at this boundary is described as the zeta potential. The relationship between zeta potential and the

electrophoretic mobility described in the Henry equation (Eq. 2.4) (Kumar and Kumbhat, 2016):

$$UE = \frac{2\varepsilon\zeta f(ka)}{3\eta}$$ (2.4)

where UE is electrophoretic mobility, ζ is zeta potential, ε is dielectric constant, η is viscosity and f(κa) is Henry's function.

The unit of κ, refers to reciprocal length and κ^{-1} usually describes the thickness of the electrical double layer. The parameter 'a' states the particle radius consequently κa is the ratio of the particle radius to thickness of electrical double layer (**Figure 2.2**). Because the common way to determine zeta potential prepares the particles in aqueous media, F (κa) in this case is 1.5, which is the Smoluchowski approximation (Kumar and Kumbhat, 2016).
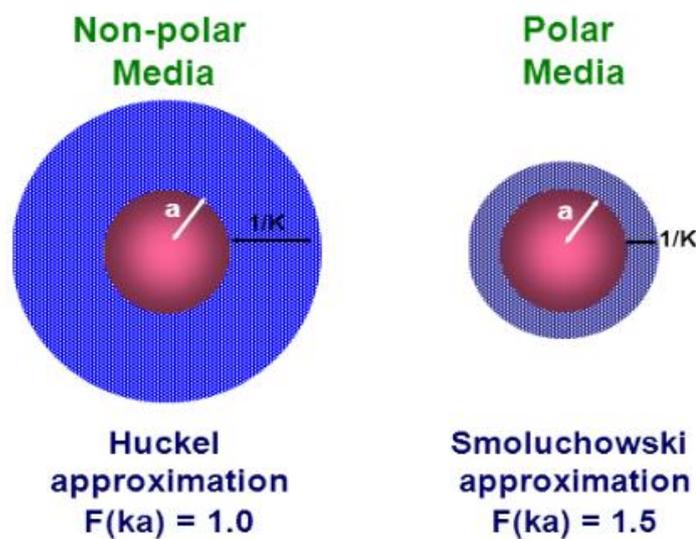
Figure 2.2 Huckel and Smoluchowski's approximations
(Kishen, 2015)

The measurements of zeta potential allow the dispersion stability of the particles can be evaluated; many particles in suspension exhibit good dispersibility due to the repulsion force becoming stronger. On the other hand, when the zeta potential is close to zero, the particles start to aggregate thus become unstable (Xu, 2006) as is shown in **Figure 2.3**. Normally, +30 mV or -30 mV is the boundary between stable and unstable suspensions; particles with zeta potentials less positive than +30 mV or less negative than -30 mV are generally considered unstable (Schmidt *et al.*, 2012).
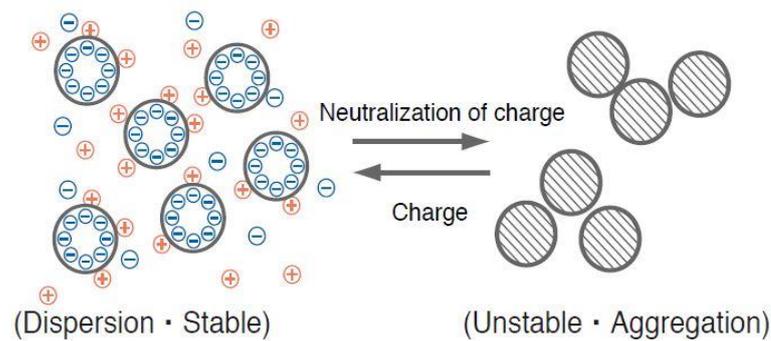
Figure 2.3 Schematic illustration indicates how zeta potential value influences particle stability in solution

2.5.2. Viscometry

Capillary viscometers are very commonly used in the physico-chemical characterisation of polysaccharides (and other biopolymers) as they are experimentally simple and relatively low priced and accurate when used correctly (Harding, 1997b) **(Figure 2.4).**
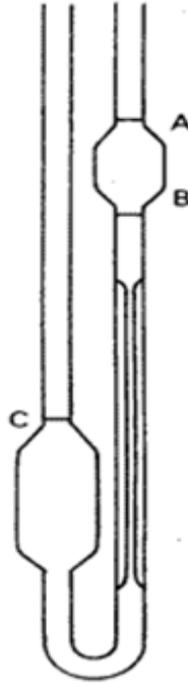
Figure 2.4 Ostwald viscometer
(Rahman et al., 2012)

The principle of this technique is as follow the relative, η_{rel} and specific viscosities, η_{sp} were calculated as described in equations 2.5 and 2.6, respectively:

$$\eta_{rel} = \left(\frac{t}{t_0}\right)\left(\frac{\rho}{\rho_0}\right) \tag{2.5}$$

$$\eta_{sp} = \eta_{rel} - 1 \tag{2.6}$$

Where t is the average flow time of the solutions at each concentration, t_o is the flow time for the appropriate buffer and because of the low concentrations used (ρ/ρ_o) is usually taken to be one (Harding, 1997b).

Measurements were made at different concentrations and extrapolated to infinite dilution using both equation 2.7 (Huggins, 1942) and equation 2.8 (Kraemer, 1938):

$$\frac{\eta_{sp}}{c} = [\eta](1 + K_H[\eta]c) \tag{2.7}$$

$$\frac{\ln(\eta_{rel})}{c} = [\eta](1 - K_K[\eta]c) \tag{2.8}$$

Where the intrinsic viscosity $[\eta]$ is taken as the mean of the intercepts from equations (3) and (4) and K_H and K_K are the Huggins and Kraemer constants respectively (**Figure 2.5**).
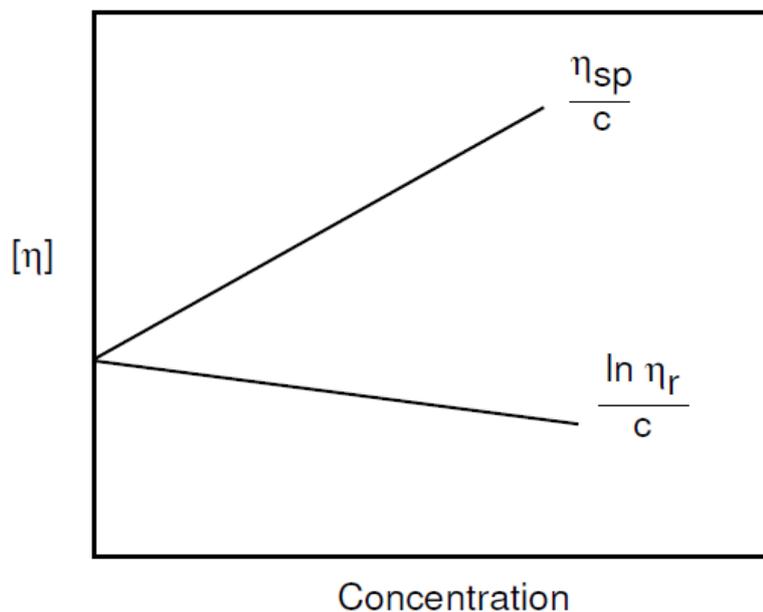
Figure 2.5 Typical plots of ηsp/c and ln ηrel/c or (ηr/c) as a function of concentration. The curves extrapolate to the same $[\eta]$ at zero concentration
(Harding, 1997b)

Because the flow of sample through the capillary is derived by pressure, the velocity is unequal through the capillary; the velocity gradient (shear rate γ) is zero at the centre and a

66

maximum at the wall. For that reason, the flow is not homogeneous and the functions of capillary viscometers are restricted to determining steady shear (steady shear stress - shear rate systems) (Chhabra and Richardson, 2008). To avoid these limitations the rheometer can be used to cover wide functions.

2.5.3. Rheometry

Rheometry is the technological system determining the rheological data which consist of measuring system, instruments and test and analysis methods (**Figure 2.6**) (Mezger, 2006). Rheology is the science that studies the flow and deformation of materials and it is a section of physical chemistry science. The 'rheology' term originates from the Greek words; "*rheo*" means flowing and "*logos*" means science (Martin *et al.*, 2011) and was invented by Bingham and Reiner in (Gallegos, 2010, Partal and Franco, 2010).
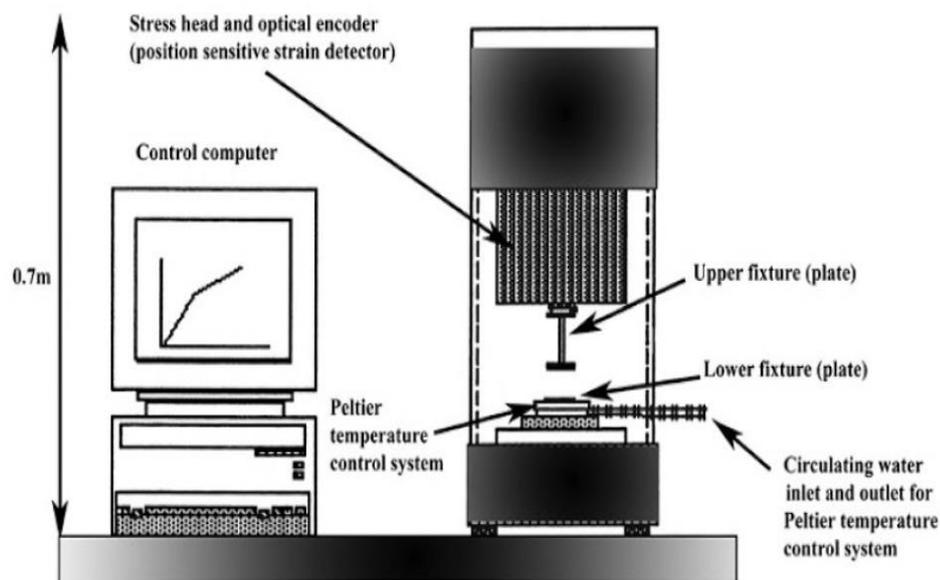
Figure 2.6 Diagram representation of a modern controlled strain rheometer
(Kasapis *et al*., 2009)

According to physical behaviour (deformation and flow) of substances, they are classified to two categories **(Figure 2.7)**: viscous liquid (according to Newton's law) or elastic solid (according to Hooke's law). The materials that have both elasticity and viscosity are referred to viscoelastic materials (Mezger, 2006). Therefore, rheology determines the relationship between viscoelastic properties and the structure of material (Murata, 2012).
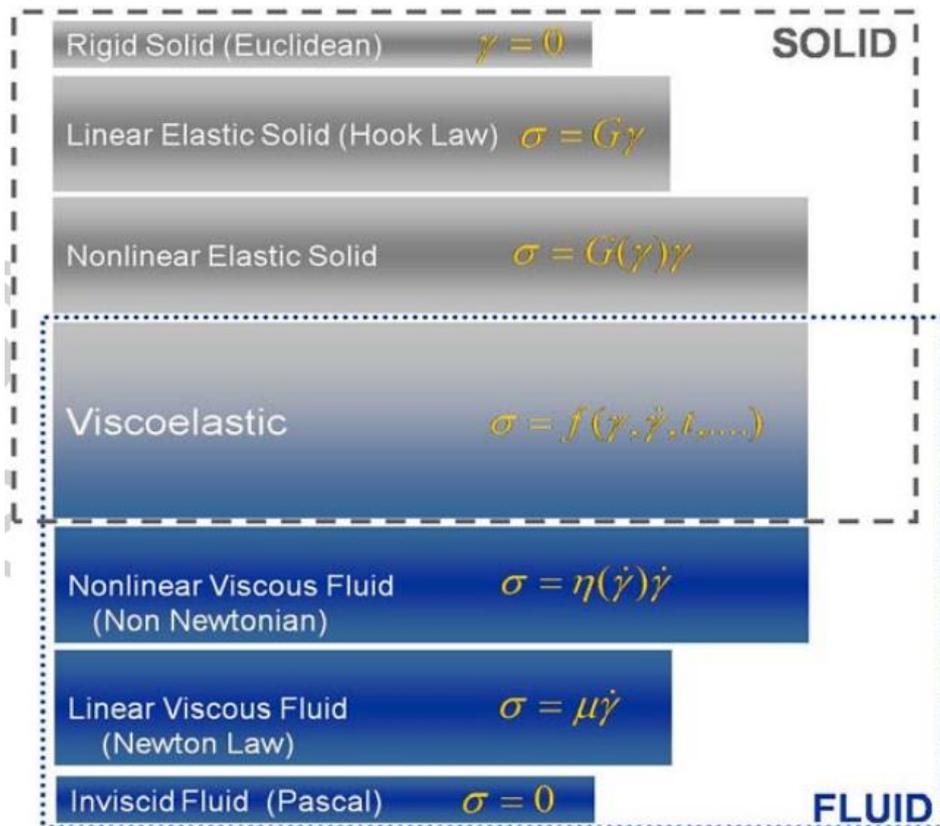
Figure 2.7 Classifications of materials in sample shear
(Partal and Franco, 2010)

Stress and strain are essential parameters in studying rheological properties of hydrocolloid systems; "stress" term refers to the force (F) per unit area (A) on or within matter as expressed in Eq.2.9 and is measured by pressure unit which is Pascal (Pa):

$$Stress = F/A \tag{2.9}$$

The fractal deformation resulting from the applied stress is called "strain". Because strain is dimensionless ratio, it has no units. As is given by Equation 2.10.

$$\text{Strain} = \Delta l / l \qquad\qquad\qquad (2.10)$$

Where Δl is the change in the length of sample and l is the original length of the sample.

The change in strain over the time is also an essential parameter and is defined as the shear rate or strain rate (γ) and its unit the reciprocal of seconds (1/s) (Rao, 2010, Mezger, 2006).

The relationship between stress and strain gives the parameter termed the modulus which can be used to identify the mechanical properties of matter (Mezger, 2006).

2.5.3.1. Types of fluid flow behaviours

The first description of viscosity was by Isaac Newton who was firstly recognised that there are direct proportional relationships between flows of some liquids and the applied stress. This relationship is defined to Newton's Law as shown in the following equation (Eq.2.11) (Ibarz and Barbosa-Canovas, 2014):

$$\text{Viscosity } (\eta) = \text{Stress } (\sigma)/\text{rate of shear } (\gamma) \qquad\qquad (2.11)$$

Depending on viscous behaviour of fluids as a function of shear rate, stress, fluids are categorized to Newtonian or non-Newtonian systems (Martin *et al.*, 2011). With a constant temperature in the Newtonian fluid system the relationship between the shear stress and shear rate is linear and there is no change in viscosity when shear are applied, for example: water, oils, alcohol (Chhabra and Richardson, 2008). In contrast, in non-Newtonian fluids the relation between shear stress and shear rate are non-linear and the viscosity changes when shear is applied. When non-Newtonian systems were studied by rotational viscometry three types of flows were recognized: dilatant, pseudo-plastics and Bingham plastic (Chhabra and Richardson, 2008, Martin *et al.*, 2011, Rao, 2010) as shown in **Figure 2.8**:

69

- Dilatant behaviour (shear thickening fluids) is displayed when the viscosity of the fluid increases as the rate of shear increases, common example of dilatant behaviour is a mixture of corn starch and water.

- Pseudoplastic behaviour (shear thinning fluids) is displayed when the viscosity of the fluid decreases as the rate of shear increases such as, paints and blood.

- Bingham plastic fluids exhibit a linear relation between shear stress and shear rate after particular point of shear stress (yield value) has been reached such as mayonnaise.
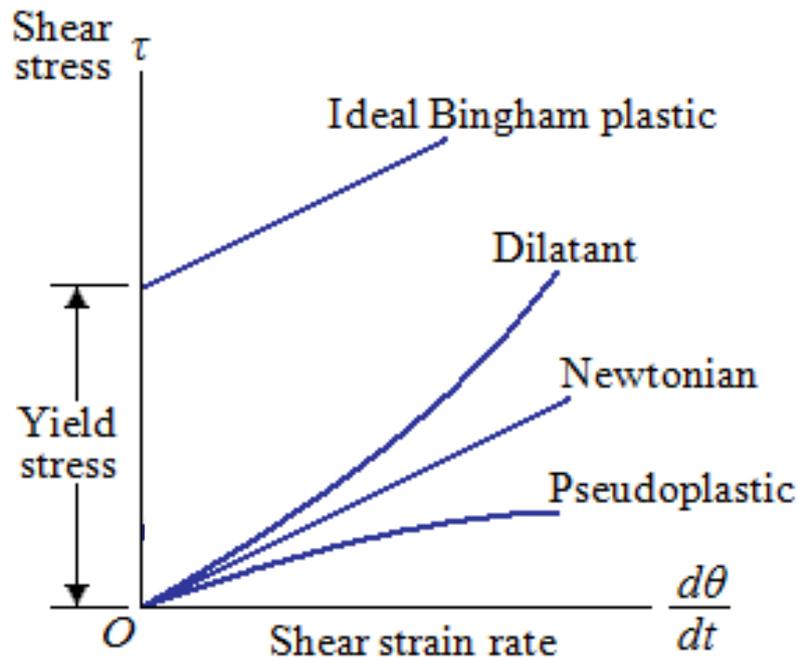
Figure 2.8 Flow curves (shear stress ageist shear rate) for Newtonian and non-Newtonian systems (Adapted from Gallegos, 2010b)

Generally, hydrated polysaccharides exhibit shear thinning behaviour (Martin *et al.*, 2011, Dumitriu, 2004) and the degree of this behaviour is affected by many factors *e.g.* conformation, molecular weight and net of charge distribution on the chain which will therefore be important when we are considering mucoadhesive potential. Also the concentration of solution, temperature and pH of medium can have influence on flow properties (Dumitriu, 2004). This behaviour occurs when at high shear rates the structure of chain start to breakdown and hence reduce entanglement density which leads in to decrease the viscosity (Rao, 2010). Many pharmaceutical formulations including liquid dispersions of natural or synthetic gums

display this kind of behaviour which is very advantageous for suspending and stabilising formulations (Martin *et al.*, 2011).

2.5.3.2. Oscillator rheology and Viscoelasticity

Oscillatory measurements are commonly used in the determination of the viscoelastic behaviour of soft matters *e.g.* emulsions, colloidal suspensions and polymer systems. Studying the mechanical behaviour of these materials is really important when evaluating their potential to be employed an appropriate application such as industrial products and formulations (Weitz *et al.*, 2007).

The principle of oscillation studies basically depends on inducing a sinusoidal shear deformation in the material and measuring the response of subsequent stress as a function of time, frequency of oscillation ω or amplitude of oscillation. In other words, if a sample was subjected to a sinusoidal strain wave with a stationary low amplitude and frequency, the sinusoidal strain can be represented as the following formula (Eq.2.12).

$$\gamma = \gamma_0 \sin \omega t \tag{2.12}$$

where γ is the instantaneous strain, γ_0 is the strain amplitude and ω the angular frequency.

The resultant shear stress also will be a sine wave but the amplitude and phase will be different and can be represent as Equation 2.13.

$$\sigma = \sigma_0 \sin (\omega t + \delta) \tag{2.13}$$

where δ is the phase angle between the strain and stress waves.

The resultant stress wave from the applied strain reveals the main differences between materials, as presented schematically in **Figure 2.9**.

If the stress is proportional to strain and the stress and strain waves would be completely in phase (phase angle, $\delta = 0°$), then the material will be perfect elastic solid (Hookean solid). In contrast, if the stress in the sample is proportional to the rate of strain deformation, the material is perfect fluid (Newtonian fluid) ($\delta = \pi/2 = 90°$). If the phase angle, δ are between $0°$ and $90°$ that means the material behaves as both liquid-like and solid-like (viscoelastic materials).
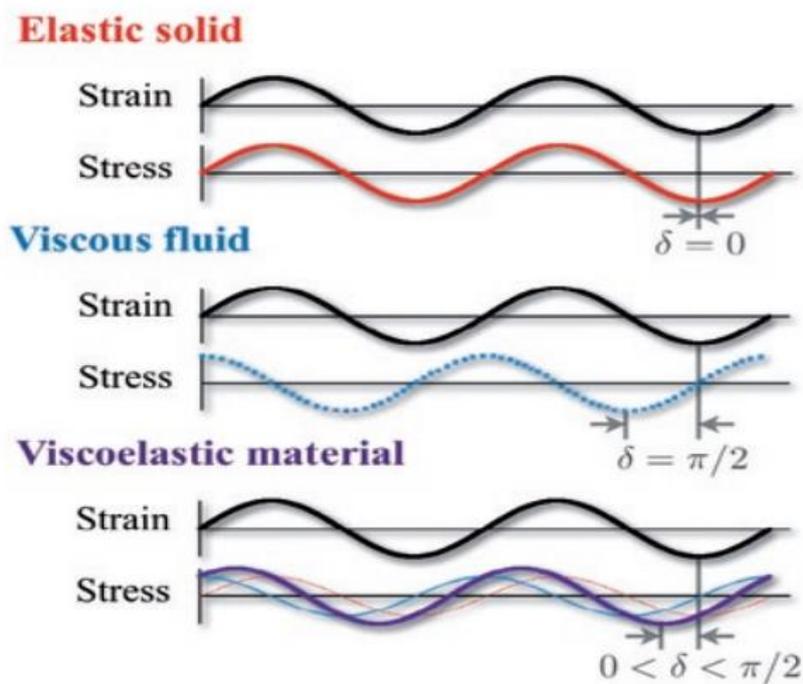
Figure 2.9 Representative stress response to oscillatory strain deformation for elastic (red curve), viscous (blue curve) and viscoelastic material (purple line)
(Weitz et al., 2007)

The viscoelastic properties of the material can be studied by determining the storage modulus G' which characterises the solid-like behaviour and the loss modulus G'' which characterises liquid-like behaviour. The storage modulus (G′) is represents the ratio between phase stress and strain (eq 2.14). This means that G' measures the storage of elastic energy in the material (Larson, 1999).

$$G' = (\sigma_0 / \gamma_0) \cos \delta \qquad\qquad (2.14)$$

The loss modulus G" is described as the ratio between out of phase stress and strain as shown in Equation 2.15. In other words, G" represents the energy stored in the material the viscous dissipation of that energy (Larson, 1999).

$$G'' = (\sigma_0 / \gamma_0) \sin \qquad\qquad (2.15)$$

The ratio G"/ G' is defined as the loss tangent (tan δ) which is an essential parameter which provides useful information about the materials studied; it is high (>> 1) for materials that have fluid-like behaviour and is low (<< 1) for materials that have solid-like behaviour (Larson, 1999). Moreover, linear viscoelastic region (LVR) is a critical parameter must be taken in consideration in oscillation measurements. LVR can be practically identified by applying gradual increase in amplitude of strain or stress on the sample and the region will be where the stress is linearly related to the response (Larson, 1999). The linear viscoelastic region can be influenced by the properties of the sample *e.g.* molecular structure and it gives indication for structural stability of systems (Schuster, 1996).

2.5.3.3. Mechanical properties of polysaccharide solutions and gels

Studying mechanical properties of polymers can offer essential information about its structural characteristics. The mechanical spectra of a material can be obtained by plotting G', G" and η* versus a range of oscillation frequencies and identify the mechanical responses of the system. **Figure 2.10** indicates the mechanical spectra for four typical behaviours of polysaccharide systems which are dilute solutions, entangled solution (concentrated solutions), weak gels and strong gels (true gels):
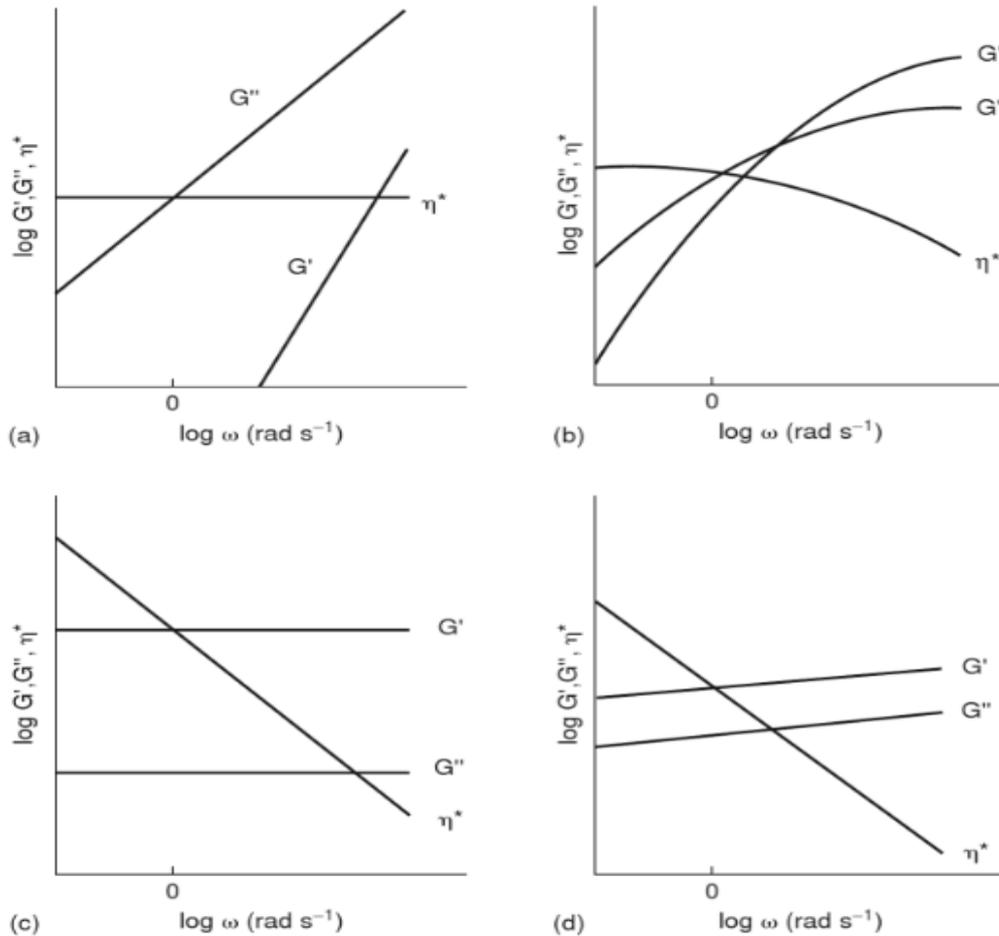
Figure 2.10 The four main categories of mechanical spectra for biopolymer systems: (a) dilute solution, (b) concentrated polymer solution, (c) strong gel and (d) weak gel
(Hui and Sherkat, 2005)

- **Dilute solutions**: This behaviour is observed at concentrations lower that critical overlap concentration (c*) and its spectrum exhibit liquid-like behaviour where G" > G' at all the frequency ranges (Hui and Sherkat, 2005). Both moduli G" and G' increase with increasing the frequency while the complex dynamic viscosity (η*) is independent of frequency (ω) (McCleary and Prosky, 2008, Hui and Sherkat, 2005).

- **Concentrated (entangled) solutions**: which is a concentrated solution where coil overlap occurs(c*). At low frequencies it indicates a viscous liquid behaviour where G" > G' while at higher frequencies the system exhibits an elastic response due to increasing entanglement of the chains thus G' and G" cross over then G' becoming greater than G" (Garrec, 2013, Hui and Sherkat, 2005).

- **Weak gels**: the mechanical spectra of this system is identified by G' is greater than G" at all frequencies and show linear inverse relationship between the complex dynamic viscosity (η*) and frequency. Weak gel behaviour is provided due to weak associations between single coils. Moreover, it disentangles under shear thus have free flowing solution behaviour but with very small deformations it is display elastic response. (Garrec, 2013, Hui and Sherkat, 2005).

- **Strong gel (true gel):** The mechanical spectra of strong gel show G′ is considerably greater than G" in comparing with and both moduli are less dependent on frequency (Garrec, 2013).

2.5.3.4. Adhesion properties of polymer gels

When a soft polymeric material comes in to contact with the surface of another material (substrate) at a temperature above the glass transition temperature, an adhesive link of assessable strength is established in most cases (Zosel, 1985). The adhesion phenomena is investigated by measuring the adhesive failure energy (or fracture energy) *w* using an appropriate apparatus. The bond contact between molecular dimensions and the geometric contact area (A) increases in the number and size with increasing contact time by deformation, wetting and flow processes also the applied pressure, temperature and rate of separation has effect on this phenomena (Zosel, 1985).

The strength of the adhesive joint can be determined by acting detachment per unit area of interface as given in following equation (Zosel, 1985):

$$w = \frac{1}{A} . \int F . v dt \qquad (2.16)$$

where *F* the tensile force during the unbonding process *v* is the separation rate.

Adhesive separation of soft polymer is normally evaluated by a fibril forming ability during the separation process (Zosel, 1989). The formation of fibrillar structures is highly effected by the molecular conditions including the viscoelasticity of the polymer; a slight degree of crosslinking and branching can support the stability of the

fibrils. The excessive crosslinking however can cause a precocious failure of the fibrils, thus considerably reducing the adhesion energy (Lakrout *et al.*, 1999). The microscopic mechanisms of adhesive separation are normally divided into 4 stages as shown in **Figure 2.11.**
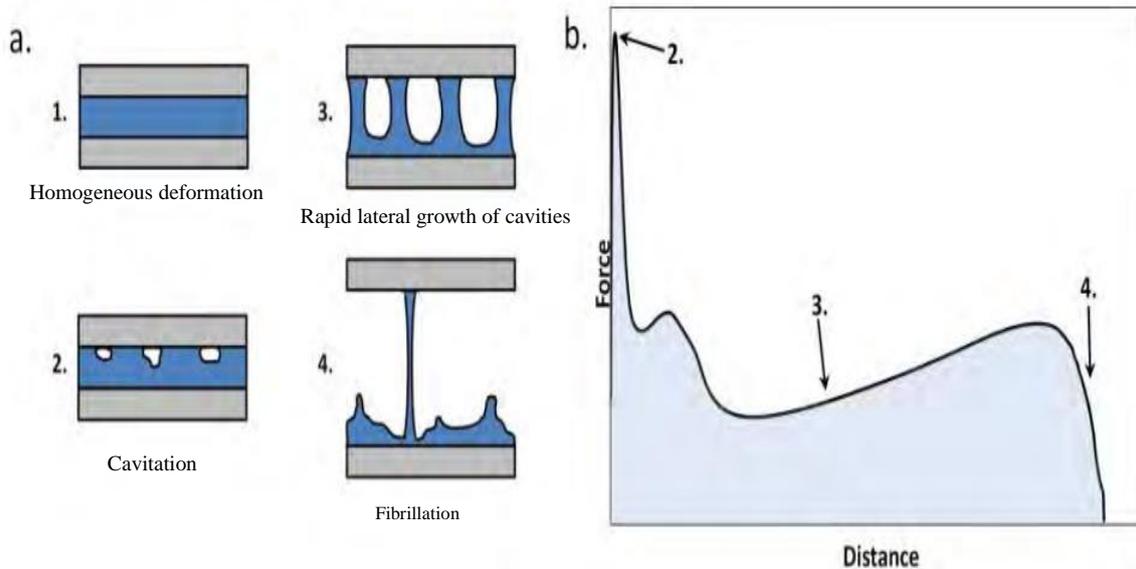
Figure 2.11 (a) Schematic representation of the microscopic mechanisms of adhesive separation (b) a curve of force against distance for adhesive polymer
(Grillet et al., 2012)

Adhesive force between polymer and a substrate is usually identified by one of those methods: 1) peel testing, 2) probe (tack) testing (Grillet *et al.*, 2012):

The first method basically depends on casting and/or curing a polymeric material on a substrate. When the material is cured, one edge of the cured material is controlled by a pulling tool and following by peeling from the substrate at a regular speed and peel angle (normally 90°). This test involves recording the force necessary to peel the polymeric material from the substrate.

Measuring the tack adhesion by probe test involves carrying a probe into contact with the surface of the tested substance under a specified force. Afterwards, the probe is raised at a constant rate of speed and the required force is measured. Therefore, beneficial information about the adhesion characteristic of the matter can be provided from the curve of the force against distance.

2.6. Summary

This chapter highlighted the main techniques that applied in this thesis including: zetasizer, viscometry and rheometer. The first one evaluates zeta potential and surface charge, which is an important factor in the characterisation of many materials such as PEC. Viscometry and rheology can provide useful information about mechanical properties of a material, which in turn is essential in physical characterisation. Moreover, the material and buffers that frequently used in the most of chapters were illustrated.

Chapter 3

The physicochemical characterisation of pepsin degraded pig gastric mucin

3. THE PHYSICOCHEMICAL CHARACTERISATION OF PEPSIN DEGRADED PIG GASTRIC MUCIN

3.1. Chapter overview

Mucins are gaining more interest by many researchers due to their being the key component of mucous which is the first biopolymer with which food and drugs interact and diffuse through prior to being absorbed in the circulatory system, furthermore it acts a physical protective barrier (Kim, 2011). Characterisation of mucin can give us insight into mucin-polymer interpenetration character (Adikwu, 2006) and enables the potential to optimize the adhesion of food and drugs which help to improve nutrition diffusion and more importantly, to control drug delivery. The gel-forming ability of mucin enhances the great potential of many drug delivery methods; amongst these are mucoadhesive drug delivery systems which have a great potential in the pharmaceutical field due to their therapeutic benefits in controlling the amount of the released drug (Kim, 2011). The aim of this work is to fully characterise extensively degraded pig gastric mucin with the respect to compositional and hydrodynamic properties to underpin the understanding of mucin interactions with polysaccharide based drug delivery systems (see Chapter 5). Furthermore, any information about this material could open up opportunities for novel application areas of digested mucins.

3.2. Materials

Glucose, sodium tetraborate (borax), sodium acetate, 3-phenyl phenol, glacial acetic acid, sodium acetate trihydrate, trifluoacetic acid, sialic acid, periodic acid, sodium arsenite, bovine serum abumin (BSA), Bradford reagent, n-butanol, hydrochloric acid, sodium hydroxide, sulphuric acid, thiobarbituric acid and sodium chloride were all obtained from Sigma–Aldrich (Gilling-ham, UK). Extensively degraded pig gastric mucin was kindly gifted from Biofac A/S (Kastrup, Denmark). All materials were used without any further purification.

3.3. Experimental

3.3.1. Chemical characterisation of gastric mucin

3.3.1.1. Determination of total carbohydrate using a phenol sulphuric acid assay

The phenol-sulfuric acid method is a colorimetric assay that determines the total carbohydrates in a sample. This method detects almost all the forms of carbohydrates (mono-, di-, oligo-, and polysaccharides). Phenol sulphuric acid assay is based on the fact that the concentrated sulphuric acid breaks down any polysaccharides, oligosaccharides, and disaccharides to monosaccharaides. After that pentoses and hexoses are dehydrated to furfural and hydroxymethyl furfural respectively, which than reacts with phenol to produce a yellow-gold colour .Glucose is most common monosaccharide used to create the standard curve and the absorption is measured between 480 to 490 nm (Dubois *et al.*, 1956).

Total carbohydrates in the mucin sample were calorimetrically determined by *m*-hydroxydiphenyl method (Dubois *et al.*, 1956). Firstly, a stock solution of glucose (200 mg/L) was prepared and from this stock solution, standard solutions with concentrations of 0 - 100 mg/L were prepared, then the total carbohydrate assay was performed by taking 400 µL from the standard solutions. 2 mL of 0.5 % borax in concentrated sulphuric acid was added and the solutions were incubated at 100 °C in water bath for 5 minutes, finally 40 µL of 0.15 % 3-phenylphenol (in 1 M sodium hydroxide) was added and the mixtures were incubated for a further 5 minutes. The absorbance for each standard and the sample was measured at 520 nm using Shimadzu UV-160AUV-Vis spectrophotometer. The blank for the sample was prepared by taking 400 µL of the sample, 2 mL of deionised water and 40 µL of 0.15 % 3-phenylphenol while the blank for the standard was prepared by taking 400 µL of deionised water, 2 mL of 0.5 % boraxin concentrated sulfuric acid and 40 µL of 0.15 % 3-phenylphenol. A typical calibration curve for glucose dissolved in DI water is shown in **Figure 3.1.**
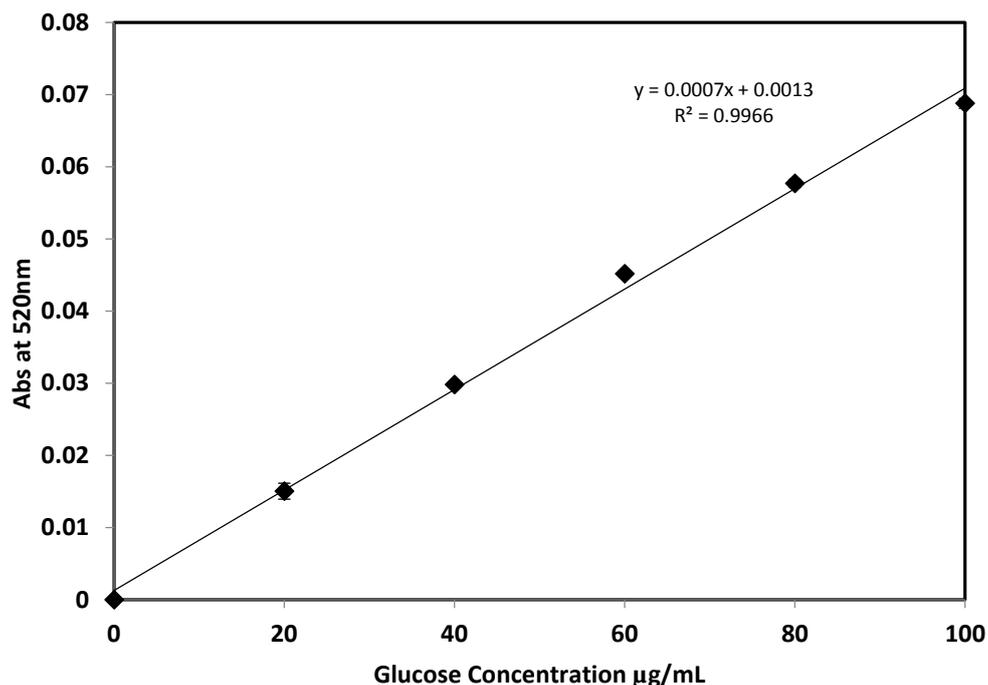
Figure 3.1 Calibration curve of glucose at 520 nm using Shimadzu UV-160AUV–vis spectrophotometer. Values represent mean ± SD (n=3)

3.3.1.2. Determination of total protein using Bradford assay

The Bradford assay is a colorimetric protein assay that is based on the binding of Brilliant Blue G-250 dye to the protein and the dye has three forms: cationic (red), neutral (green), and anionic (blue).Because the assay is performed at acid pH, the dye is in protonated form but when the dye binds to protein (forms dye- protein complex) it is converted to a stable unprotonated blue form and the absorbance maximum of the dye-protein complex is detected at 595 nm. So the quantity of the complex existing in solution is a value for the protein concentration and can be estimated by using a spectrophotometer or microplate reader (Kruger, 1994). Total protein in the mucin sample were calorimetrically determined using a previous method (He, 2011). Five dilutions of BSA standards with a concentration range of 5–100 mg/L were prepared. 30 µL of each mucin solution (250 mg/L) and the standard solutions were added to separate test tubes. The blank was prepared using 30 µL of ultrapure water instead of standard solution or mucin sample. Bradford reagent (1.5 mL) was added to each tube and mixed well. The samples were incubated at room temperature for 10 min. The absorbance measurements of the mucin samples were recorded at 595 nm using Shimadzu UV-160 AUV–Vis spectrophotometer and the concentration of protein was calculated from a standard curve and expressed as a percentage

by weight of mucin. A typical calibration curve for BSA dissolved in DI water is shown in **Figure 3.2.**
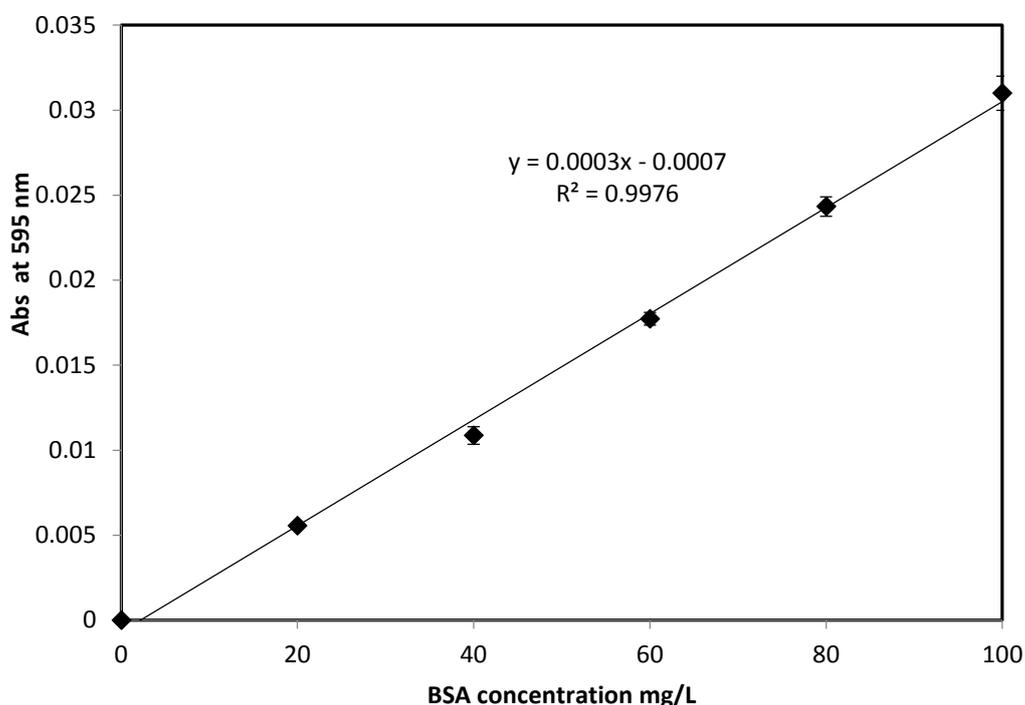
Figure 3.2 Calibration curve of bovine serum albumin at 595 nm using Shimadzu UV-160AUV–Vis spectrophotometer. Values represent mean ± SD (n=3)

3.3.1.3. Determination of the constituent sugars by high-performance anion-exchange chromatography with pulsedamperometric detection (HPAEC–PAD)

Mucin (2.0 mg in duplicate) was dissolved in 2 mL of DI water in separate pressure tubes. Concentrated trifluoroacetic acid (0.85 mL) was then added to each sample solution using a micropipette. The pressure tubes were then placed in a heating block for 2 h at 120 °C. After 2 h the samples were evaporated to dryness under a stream of nitrogen gas at 65 °C for 1 h. The dried samples were reconstituted with 2 mL of deionized water and the sample diluted 10 times prior to HPAEC–PAD analysis. Neutral sugars, amino sugars and sialic acid composition were analysed using a Dionex ICS-5000HPAEC-PAD system (Thermo Fisher, Loughborough, UK). A 0.5 mL/min flow rate was used the first 12 min at a concentration of 10 mM NaOH this was then followed by a 0.05 min step to change from 0 to 17 % 1 M sodium acetate in 150 mM NaOH and the remainder of the run was continued at 17 % 1 M sodium acetate in 150 mM NaOH to elute any uronic acids present. A pre-run equilibration step of 10

min using 200 mM NaOH followed by 20 min of 10 mM NaOH was used to regenerate the column prior to each injection.

3.3.1.4. Determination of sialic acid using sialic acid assay

Sialic acid determination was achieved by using the method of (Hoang *et al.*, 2010). 10 mg of mucin was hydrolysed in 2 mL 100 mM H_2SO_4 at 80 $^{\circ}$C for 1 h to release sialic acids (in triplicate), then neutralised with 1 M NaOH (45 µL). The samples were incubated with 250 µL periodic acid solution (25 mM in 62.5 mM H_2SO_4) at 37 $^{\circ}$C for 30 min. The reaction was concluded by adding 0.2 mL sodium arsenite (2 % in 0.5 M HCl), left for 3 min before adding 2 mL thiobarbituric acid (0.1 M, pH 9.0). The solutions were heated in a boiling water bath for 7.5 min then cooled in ice water and mixed with 5 mL of n-butanol/concentrated HCl solution (95:5, v/v), shaken and the absorbance of the butanol layer was measured at 550 nm. The concentration of sialic acids was calculated from a standard curve (**Figure 3.3**) constructed with *N*-acetyl neuraminic acid (1–100 µg/mL) and expressed as a percentage by weight of mucin.
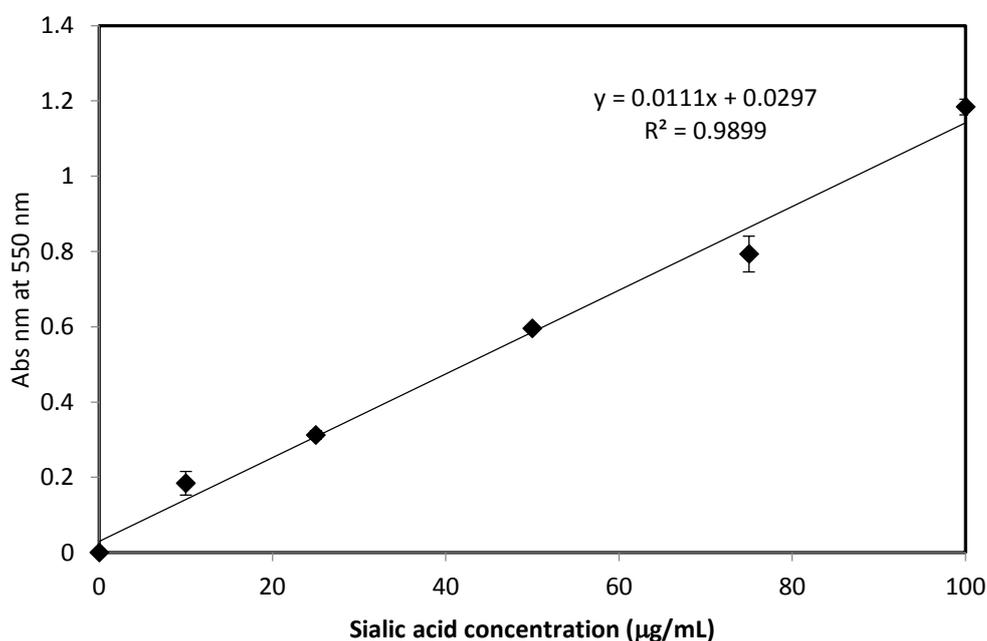
Figure 3.3 Calibration curve of sialic acid (NANA) at 550 nm using Shimadzu UV-160AUV–Vis spectrophotometer. Values represent mean ± SD (n=3)

3.3.2. Physical characterisation of gastric mucin

3.3.2.1. Determination of weight-average molecular weight by size-exclusion chromatography coupled to multi-angle laser light scattering (SEC–MALLS)

A 0.5 % w/v of solution of mucin in DI water was analysed by size exclusion chromatography which was carried out at ambient room temperature on a PL Aquagel guard column (Polymer Labs, Amherst, U.S.A.) which was linked in series with PL Aquagel-OH 60, PL Aquagel-OH 50and PL Aquagel-OH 40 (Polymer Labs, Amherst, U.S.A.) and was eluted with distilled water at a flow rate of 0.7 mL/min. The eluent was then detected online firstly by a DAWN EOS light scattering detector scattering detector (Wyatt Technology, Santa Barbara, U.S.A.) and a REX differential refracto-meter (Wyatt Technology, Santa Barbara, U.S.A.). The refractive index increment, *dn/dc* was taken to be 0.150 mL/g.

3.3.2.2. Determination of intrinsic viscosity

Appropriate concentrations of mucin were prepared (0.025 - 0.2 % w/v) at pH 1.2, 4.4 and 7.4. The flow time of the solutions at each concentration was measured by using a Cannon capillary viscometer size 50 at 37 $^{\circ}$C. The relative (η_{rel}) and specific (η_{sp}) intrinsic [η] viscosities were calculated as described in Chapter 2 section 2.1.1.

3.3.2.3. Determination of the critical coil overlap (c*)

A stock solution mucin (40 w/v %) was prepared by dissolving 40 g of mucin in 100 mL of deionized water. Once fully dissolved, the stock solution was diluted to appropriate range of concentrations (1 - 40 %). Mucin solutions of the same concentrations were also prepared at pH 1.2 and 7.4 pH by adjusting the pH with 0.1 M HCl and 0.1 M NaOH respectively. The viscosities at 130 s^{-1} were measured using cone plate 55 mm geometry on a Bohlin Gemini HR Nano Rheometer at 37 $^{\circ}$C.

3.3.2.4. Determination zeta potential

A solution of mucin (0.5 % w/v at pH 1.2, 4.4 and 7.4) was prepared by dissolving 0.5 g of mucin in 100 mL of deionized water and the pH was adjusted accordingly with 0.1 M HCl or 0.1 M NaOH. The zeta potential of the three samples was determined using Malvern Zetasizer NANO-Z (Malvern Instruments Limited, Malvern, UK). Measurements in triplicate

were performed by using a folded capillary cell at 25.0 ± 0.1 ºC and refractive index was set to 1.450.

3.3.2.5. Rheological study

Measurements of viscosity *vs.* shear rate were performed at 37 ºC on 7 % and 15 % w/v mucin samples prepared at pH 1.2, 4.4 and 7.4 across shear rates ranging from 1 s^{-1} to 1000 s^{-1} using cone and Plate 55 mm geometry fitted to a Bohlin Gemini Rheometer (Malvern Instruments, UK). Small deformation oscillatory measurements were also performed on these solutions (7 % and 15 % at pH 1.2, 4.4, and 7.4) to monitor the viscoelastic behaviour of the mucin using the same rheometer as in the viscosity measurements but using a double gap geometry to minimise signal to noise ratio. Measurements of storage modulus (G') and loss modulus (G'') were taken at frequencies from 0.1 rad/s to 10 rad/s to ascertain mechanical spectra of the gels at an isothermal temperature of 37 °C and at a fixed strain of 2 %. Measurements were performed in triplicate and mean values plotted.

3.4. Results and discussion

3.4.1. Chemical characterisation of gastric mucin

Total carbohydrate of the mucin samples was determined using phenol sulphuric acid assay relative to glucose standards and the total protein using the Bradford assay relative to BSA. The total carbohydrate and protein contents of mucin sample were 55 % (as glucose equivalents) and 15 % (using bovine serum albumin as a standard) respectively (**Table 3.1**). as it can be seen the recovery for total protein and total carbohydrate does not equate to 100 % this may be because the use of glucose as standards, as the response to the assay varies with different monosaccharaides (Dubois *et al.*, 1956, Bath, 1958). The mucin also contains ∼10 % moisture. Constituent sugar analysis using HPAEC shown the presence of Fuc, Gal, GalN and GlcN (**Table 3.1**) which are consistent with previous results (Ohara *et al.*, 1993). Sialic acid could not be detected using this method however it has been determined by an alternative method (sialic acid assay Section 3.3.1.4) to be 1.7 %.

3.4.2. Molecular weight

The weight-average molecular weight as measured by size-exclusion chromatography coupled to multi-angle laser light scattering (SEC–MALLS) was found to be 1.04×10^6 g/mol

which is in general agreement with previous estimates (Jumel *et al.*, 1997) and demonstrates that the enzymatic digestion has resulted in a large reduction in molecular weight as typically non-degraded pig gastric mucin has a weight-average molecular weight of 5–9×10^6 g/mol (Jumel *et al.*, 1997, Deacon *et al.*, 1998, Gillis *et al.*, 2013). MALLS can also give an approximation of the radius of gyration ($r_{g, z}$), which was estimated to be 31 nm. This is indicative of compact structure and is of the size of typical T-domains (Sheehan and Carlstedt, 1984).

Table 3.1 Some physicochemical properties of extensively degraded pig gastric mucin (Abodinar et al., 2016) (Used with permission)

Property	Measurement
Total carbohydrate, % (as glucose equivalents)	55 ± 1
Fucose, mol%	4 ± 1
Galactose, mol%	9 ± 1
N-acetylgalactosamine, mol%	55 ± 1
N-acetylglucosamine, mol%	33 ± 1
Sialic acid, %	1.7 ± 0.1
Total protein, % (relative to BSA standards)	15 ± 1
M_w, 10^6 g/mol	1.04 ± 0.05
M_w/M_n	5.5 ± 0.5
$r_{g,z}$, nm	31 ± 6

3.4.3. Zeta potential

Zeta potential as an indirect measurement of surface charge of mucin samples at pH 1.2, 4.4 and 7.4 was measured using Malvern Zetasizer NANO-Z (Malvern Instruments Limited, Malvern, UK). **Figure 3.4** shows that mucin is negatively charged for all the samples tested with a progressive negative charge increase with increasing pH. This may be attributed to the presence of the carboxylic acid group in sialic acid. Previous studies on native pig gastric mucin have shown an isoelectric point at $\sim$ pH 2 - 2.5 and sialic acid has a pKa of 2.6 (Hurd, 1970).
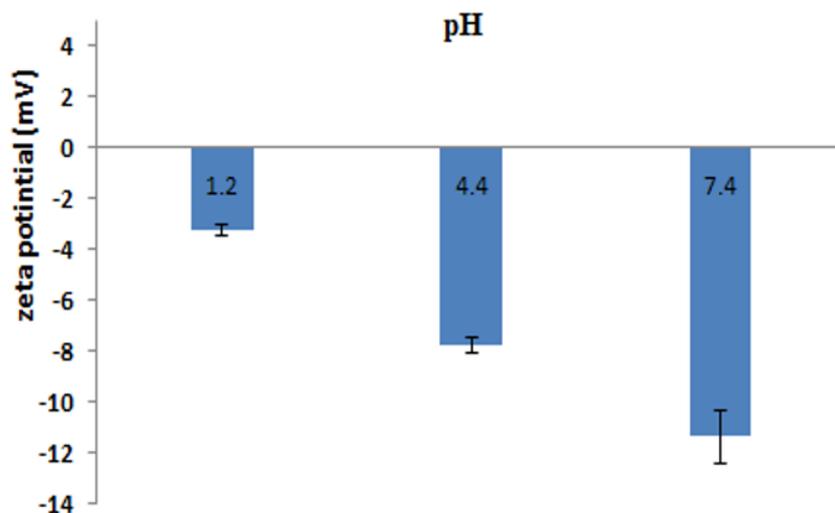
Figure 3.4 Zeta potential of samples of gastric mucin (0.5 % w/v) prepared in deionised water and pH adjusted to pH 1.2, 4.4 and 7.4. Values represent mean ± SD (n=3) (Abodinar *et al.,* 2016) (Used with permission)

3.4.4. Intrinsic viscosity

The weight-average intrinsic viscosity, [η] w was found to be 0.42–0.44 dL/g which is in general agreement with previous estimates (Fogg *et al.*, 1996) and is also consistent with the reduction in molecular weight. A weight-average intrinsic viscosity of 0.42–0.44 dL/g coupled with a weight-average molecular weight of 1.04×10^6 g/mol suggests a compact conformation (Harding *et al.*, 2011, Morris *et al.*, 2014).

Table 3.2 The effect of pH on several physical properties of digested porcine gastric mucin (Abodinar et al., 2016) (Used with permission)

Property	pH		
	pH 1.2	**pH 4.4**	**pH 7.4**
[η], dL/g	0.416 ± 0.003	0.426 ± 0.004	0.443 ±0.012
c*, g/dL (%)	11.0 ± 0.1	11.1 ± 0.1	10.3 ± 0.3
ζ-Potential, mV	−3.4 ± 0.2	−7.8 ± 0.3	−11.4 ±1

3.4.5. Critical overlap concentration (c*)

In a dilute solution, random coils of polymer are spaced from each other. With increasing the concentration of polymer solution, the distance between the coils become

smaller and coils starts to overlap and entangle. The concentration at which the individual polymer coils starts to overlap and entangle is termed overlap concentration (c*) (Tanaka, 2011). Above c*, viscosity increases rapidly with increasing concentration (Svensson, 2008) as the chains of polymer interpenetrate with each other. This leads to difficulty in studying the characteristics of individual chains in solution as shown in **Figure 3.5** (Tanaka, 2011). Entanglement characteristics are affected by the concentration of the solution and the hydrodynamic radius of the polymer, which for polyelectrolytes is dependent on pH and ionic strength (Tømmeraas and Wahlund, 2009). As the entanglement of polymer coils depend on their molecular size (hydrodynamic volume), chain stiffness and excluded volume effects (Tømmeraas and Wahlund, 2009). Where the latter is probably very important for branched mucins, therefore a decrease in molecular weight would be expected to have high impact on the viscoelastic properties of degraded mucin solutions (Svensson, 2008).

dilute region   overlap concentration   semiconcentrated region
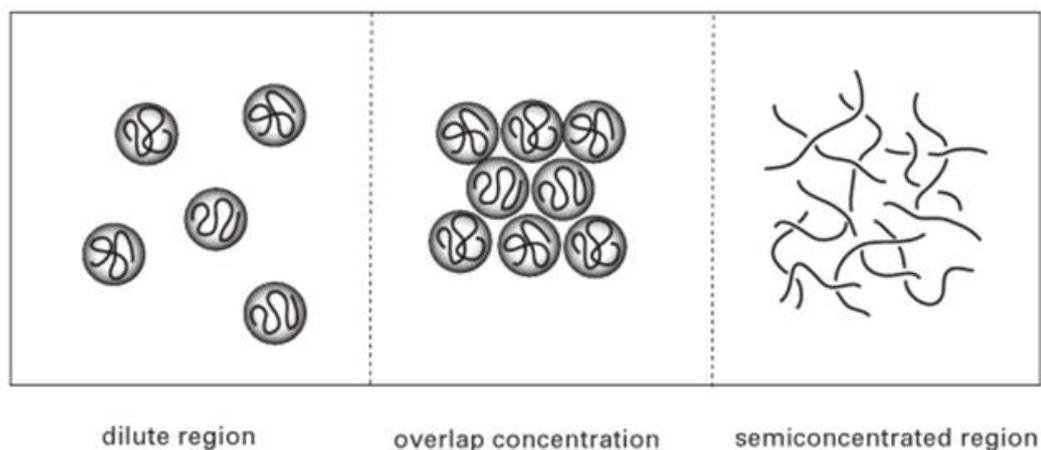
Figure 3.5 Concentration regimes in polymer solutions
(Tanaka, 2011)

It has been found that, at a mucin concentration of ~11 % (w/v) the mucin chains start to overlap (**Figure 3.6**) which agrees with the generalised theory where log c*[η] ~ 0.6 and log η_{sp} ~ 1 (Morris *et al.*, 1981). The relatively high c* is consistent with the molecular weight of the mucin being relatively low (compared with native mucins) and in this case adopting a compact conformation (**Table 3.2**) for example pullulan (a random coil type polysaccharide) of the same molar mass would be expected to have an intrinsic viscosity of ~2 dL/g (Kasaai, 2006) under similar conditions and a polyanion like pectin (semi-flexible coil) would be expected to be ~20 dL/g (Morris *et al.*, 2002). There is little influence of the pH change on

either intrinsic viscosity or c*, probably due to excluded volume effects between the different branches on each mucin molecule forcing the chains into an expanded conformation giving less possibility for relaxation of the chain stiffness even when electrostatic repulsion along the chains decreases with lower pH due to fewer of the carboxylic acid moieties of sialic acid being deprotonated (Tømmeraas and Wahlund, 2009).
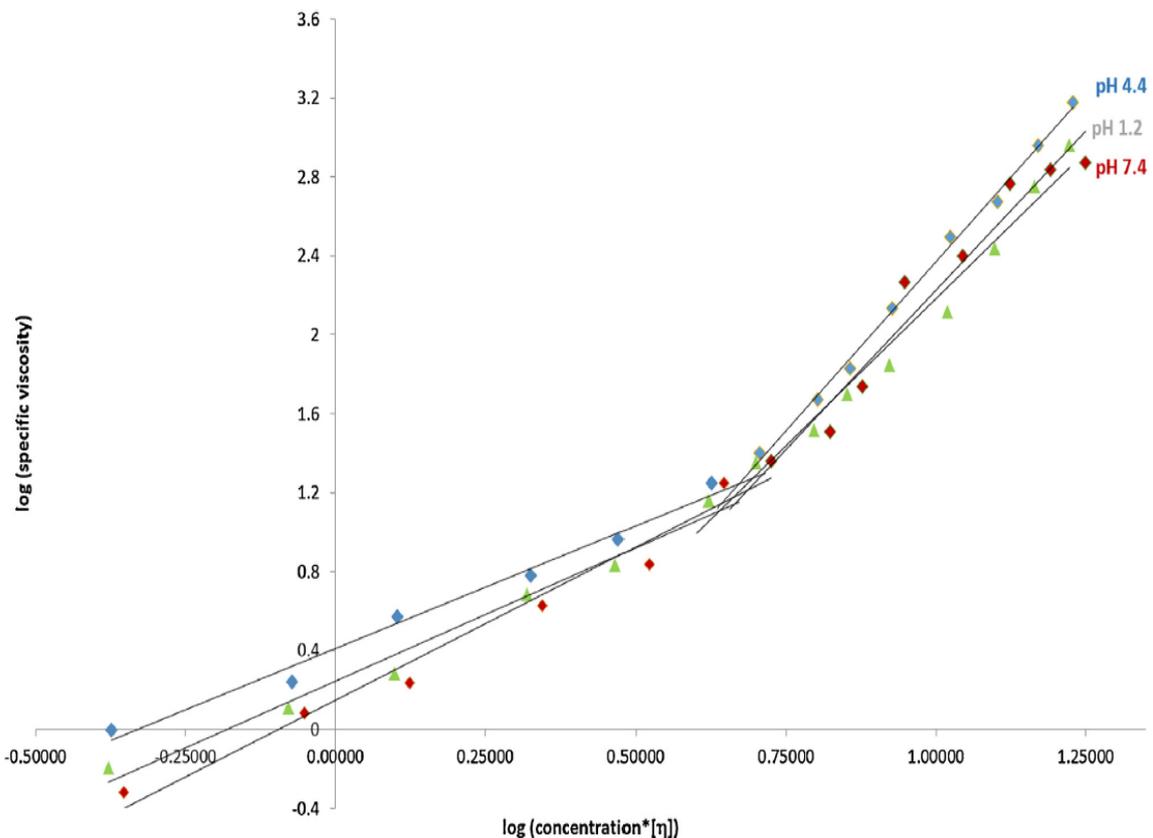
Figure 3.6 Intersection of two curves of log concentration* [η] versus log specific viscosity. The means of the slopes of the plots are 1.4 and 3.2 for the dilute and concentrated regimes, respectively (Abodinar *et al.*, 2016) (Used with permission)

3.4.6. Rheological study

3.4.6.1. Viscosity measurements

All mucin samples showed typical shear-thinning behaviour with viscosity decreasing with increasing shear rate (**Figure 3.7**). The 7 % w/v sample (below c*) at pH 7.4 showed a distinctly higher viscosity compared with the samples at acidic pH. This can be explained by

the mucin molecules becoming more extended at a higher pH causing an increase in entanglement and hence viscosity. Zeta potential measurements showed that the charge increased with increasing pH which would likely be the cause of a more extended conformation due to an increased intra-molecular repulsion which is consistent with increased viscosity. This difference is not apparent at 15 % w/v (above c*) due to the increase in polymer concentration, the inter-molecular entanglements increase and dominate the viscosity effect of intra-molecular repulsion. The relatively low viscosity suggests that the hydrodynamic size of the mucins is likely to be relatively small due to compact structure and/or branching.
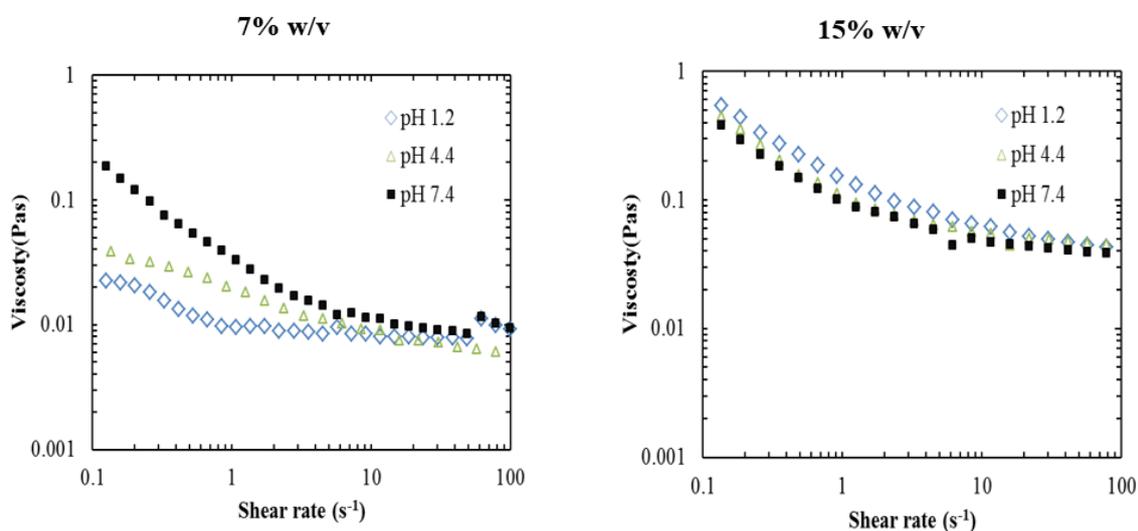
Figure 3.7 Viscosity against shear rate of 7 % (w/v) and 15 % (w/v) mucin samples at varying pH measured at 37 ∘C
(Abodinar *et al.,* 2016) (Used with permission)

3.4.6.2.Dynamic mechanical measurements

Small deformation oscillatory measurements of elastic (G') and viscous modulus (G'') were undertaken to monitor the viscoelastic behaviour of the mucin using a Bohlin Gemini rheometer fitted with a double gap geometry. Amplitude sweeps were performed to ascertain the linear viscoelastic region of the samples. To reveal the mechanical spectra of the mucin, measurements were taken over a frequency range of 0.1–10 rad/s at 2 % strain at 37 ℃. **Figure 3.8** highlights the difference in mechanical spectra of 7 % w/v mucin at pH 1.2, 4.4 and 7.4.
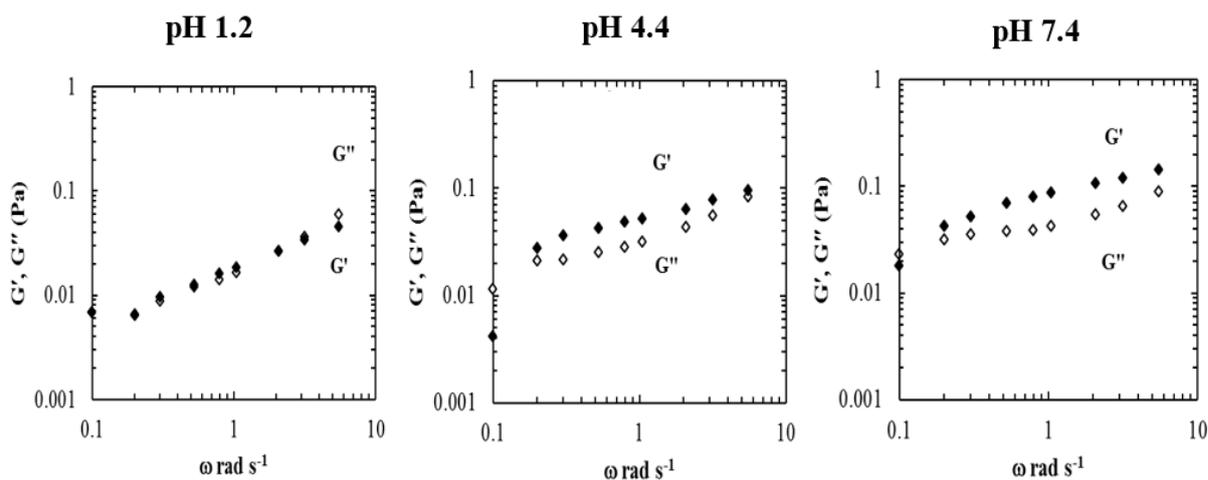
Figure 3.8 Mechanical spectra of 7 % (w/v) mucin samples at varying pH measured at 37 ºC
(Abodinar *et al*., 2016) (Used with permission)

These results show a slight increase in moduli at pH 4.4 and 7.4 compared with the values obtained at pH 1.2. Interestingly this contradicts the results on native pig gastric mucin which exhibits a pH dependent sol–gel transition when pH is reduced to ≤ pH 4 (Celli *et al.*, 2007), although this would also be expected to be concentration dependent (Georgiades *et al.*, 2014). Again this is attributed to the polymer extending as the pH increases allowing a higher degree of polymer entanglement.

3.5. Summary

In this chapter, the physicochemical properties of extensively degraded mucin were studied and revealed that this type of mucin contains: protein, carbohydrate (Fuc, Gal, GalN, GlcN) and sialic acid, which provides the negative charges that becomes progressively stronger with increasing pH. The measurements of viscosity vs. shear rate showed that mucin has a shear thinning behaviour and a relatively low viscosity which is consistent with a high critical overlap concentration (c*), small hydrodynamic size and hence compact structure (high molecular weight coupled with low intrinsic viscosity). This is further supported by the weak pH dependency of the mechanical spectra. Knowledge of the physicochemical properties of this low molecular weight, degraded mucin could lead to new applications of this material, and in addition, is fundamental to understanding interactions of mucins with other macromolecules as it can be seen in Chapter 5.

Chapter 4

Characterisation Cs (polycation), LMP, HMP, HGA and LGA (polyanions)

4. CHARACTERISATION CS (POLYCATION), LMP, HMP, HGA AND LGA (POLYANIONS)

4.1. Chapter review

Polysaccharides and their derivatives have received a great deal of attention from, for example, the food, cosmetic and pharmaceutical industries. The physiochemical characterisation of polysaccharides is important in these applications. Therefore, knowledge of polysaccharide conformation and understanding its behaviour as solute can give us insight into the complexation mechanisms and help for predicting optimum conditions to form PECs (as it can be seen in Chapter 6).

The conformation (flexibility/ stiffness) of polysaccharide systems have been characterised using a variety of hydrodynamic techniques including sedimentation velocity, sedimentation equilibrium, size exclusion chromatography multi-angle light scattering (SEC-MALLS), zetasizer and viscometry (Wyatt, 1993, Harding, 1997b, Morris *et al.*, 2008, Morris *et al.*, 2014). Results have shown that polysaccharides span a wide range of sizes and conformational flexibilities with large hydrated volumes; these properties are important in relation to polysaccharide structure - function relationships.

This study aims were to investigate several characteristics including intrinsic viscosity, molecular weight and zeta potential of Cs, HM-pectin, LM-pectin, HG-alginate and LG alginate. Also Smidsrød-Haug stiffness parameter (B) has been estimated using the ionic strength dependency of both zeta potential and intrinsic viscosity. Also the effect of varying of pH value on intrinsic viscosity and zeta potential was studied. Moreover, structure and morphology of these polysaccharides were characterised using FTIR and XRD techniques respectively.

4.2. Materials

All the materials that used in this chapter were sourced in Chapter 2 Section 2.2.

4.3. Experimental

4.3.1. Sample preparation

4.3.1.1. Preparation of Cs samples at different ionic strengths

A stock solution of Cs (5×10^{-3} g / mL) was prepared by dissolving 500 mg of Cs in 100 mL of the appropriate pH 4.3 sodium acetate buffer which contains glacial acetic acid, sodium acetate trihydrate (0.05, 0.1, 0.15, 0.2, 0.3, 0.5 and 0.8 M). After complete dissolution, stock solutions were diluted to appropriate range of concentrations for intrinsic viscosity and zeta potential measurements (2.5×10^{-4} g/mL – 2×10^{-3} g / mL).

4.3.1.2. Preparation of HMP, LMP, HGA and LGA samples at different ionic strengths

A stock solution of each polyanion (LMP, HMP, HGA and LGA) (5×10^{-3} g / mL) were prepared by dissolving 500 mg of each type of pectin in 100 mL of the appropriate sodium chloride buffer (0.05, 0.1, 0.15, 0.2, 0.3, 0.5 and 0.8 M). Complete dissolution was achieved after 4 h of mild stirring at room temperature. Stock solutions were diluted to appropriate range of concentrations for intrinsic viscosity and zeta potential measurements (2.5×10^{-4} g / mL – 2×10^{-3} g / mL).

4.3.1.3. Preparation of Cs, HMP, LMP, HGA and LGA samples with different pH

A stock solution of each polymer (Cs, HMP, LMP, HGA and LGA) (5×10^{-3} g / mL) was prepared by dissolving 500 mg of the polymer in 100 mL of an appropriate pH (3.3, 3.8, 4.3, 4.8 and 5.3 pH) (ionic strength: 0.3 M) of sodium acetate buffer (contains glacial acetic acid, sodium acetate trihydrate). After completed dissolution, stock solutions were diluted to appropriate range of concentrations (2.5×10^{-4} g/mL – 2×10^{-3} g / mL) for intrinsic viscosity and zeta potential measurements. HGA did not dissolve in 3.3 and 3.8 pH solutions.

4.3.2. Fourier transform infrared (FTIR) spectroscopy

Samples of Cs, HMP, LMP, HGA and LGA (as powders) were analysed by to FTIR (Thermo electron corporation) within a frequency range of $\lambda = 400 – 4000$ cm^{-1} the absorption for each sample was run triplicate.

4.3.3. Powder X-Ray diffraction (P- XRD) study

The crystallinity of Cs, HMP, LMP, HGA and LGA was investigated using the following procedure: a dry sample of each polysaccharide was analysis using a Bruker AXS diffractometer (D2 phasher). The data was recorded at 2θ range of 5° to 100° at a scanning rate of 4°/min.

4.3.4. Determination of intrinsic viscosities

The prepared solutions and reference solvents were analysed using a 15 mL Oswald viscometer (Rheotek, Burnham-on-Crouch, UK) under precise temperature control (25.0 ± 0.1 ℃). The flow time (*t*) average (of 3 replicates) of the solutions at each concentration, and the flow time for the appropriate buffer was taken. The intrinsic viscosity was calculated as described in Section 2.5.2.

4.3.5. Determination of zeta potential, ζ

Zeta potential for all samples was determined using Malvern Zetasizer NANO-Z (Malvern Instruments Limited, Malvern, UK). Measurements were performed by using folded capillary cell at 25.0 ± 0.1 ℃. Each data value is an average of three measurements. For consistency zeta potential was measured at each concentration, however no concentration dependency of zeta potential was observed over the series of concentrations studied.

4.4. Results and discussion

4.4.1. Structural Characteristics

4.4.1.1. FT-IR analysis

FT-IR spectra of Cs, HMP, LMP, HGA and LGA are shown in **Figure 4.1**. Characteristic bands of Cs were at 3322 cm^{-1} representing the O-H group, 1650 cm^{-1} and 1560 cm^{-1} indicate C=O stretching in amide I vibration group (CONH$_2$) and N-H deformation in amide II group vibration (NH$_2$) respectively and 1151 cm^{-1} representing the asymmetric bridge oxygen (C-O-C) (Wang and Liu, 2014). HMP and LMP have two bands at 1750 cm^{-1} and 1607cm^{-1} which represent the ester carbonyl (C=O) groups and carboxylate ion stretching band (COO^{-}) respectively. It was observed that intensity and band area of the ester carbonyl groups increased as the increase of methylation (Gnanasambandam and Proctor, 2000). The most

important characteristics of HGA and LGA spectrum indicate that the asymmetric stretching band of the carboxylate ion group at 1590 cm^{-1} and the symmetric stretching band of the COO^{-} group at 1410 cm^{-1} (COO^{-}) (van Hoogmoed *et al.*, 2003).
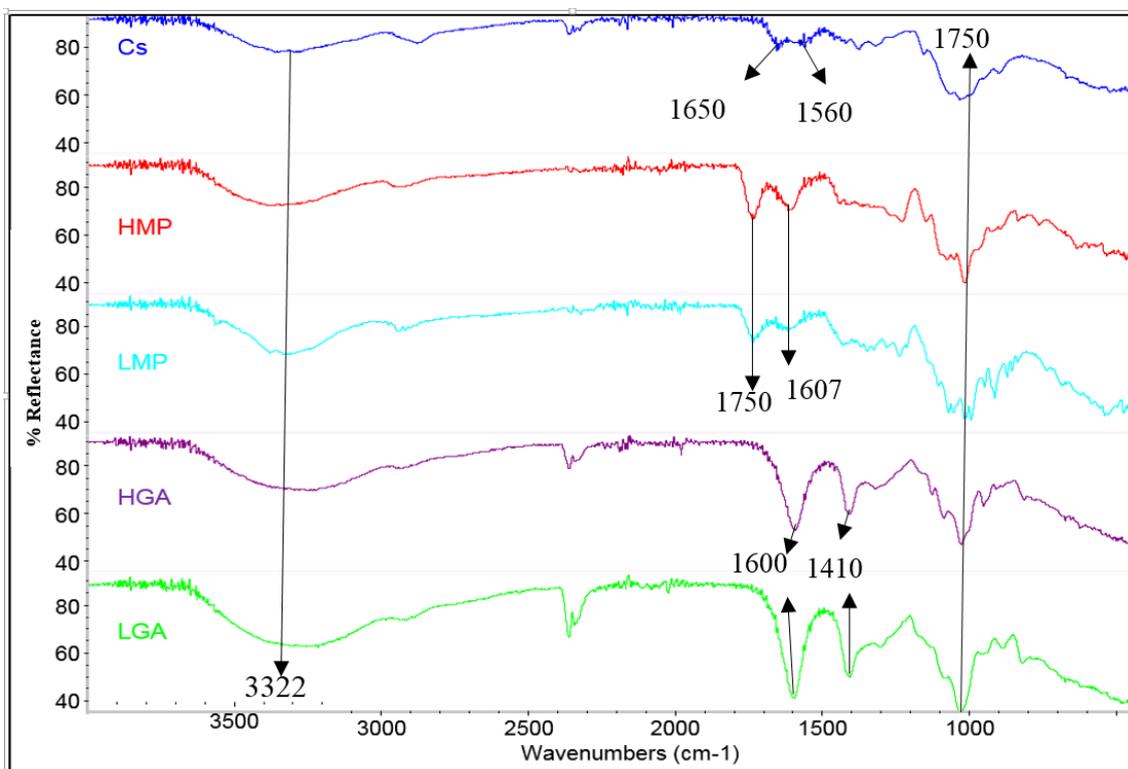
Figure 4.1 FTIR spectrum of CS, HMP, LMP, HGA and LGA with a frequency range of 400 – 4000 cm^{-1}

4.4.1.2. P-XRD analysis

P –XRD measurements were used to study the crystalline or amorphous nature of the polysaccharides. The XRD pattern of Cs, HMP, LMP, LGA and HGA are depicted in **Figure 4.2**. The diffractogram of LMP displays sharp crystalline peaks at 2θ equals 9°, 12°, 12.70°, 15.4°, 16°, 19°, 19.97°, 22.5°, 24.98°, 25.30°, 38.04°, 38.74°, and 40° this may be attributed to the high degree of polymerization (DP), however in contrast HMP has an amorphous structure as shows by two wide peaks at 2θ equals 14° and 21°. Moreover, the other polysaccharides have an amorphous nature; Cs exhibits two broad peaks at 2θ = 10° θ and 20° θ which is in agreement with (Isa *et al.*, 2012), LGA show a broad peak in 12.5° and HGA displays two broad peaks at 2θ = 10° and 20.1°.
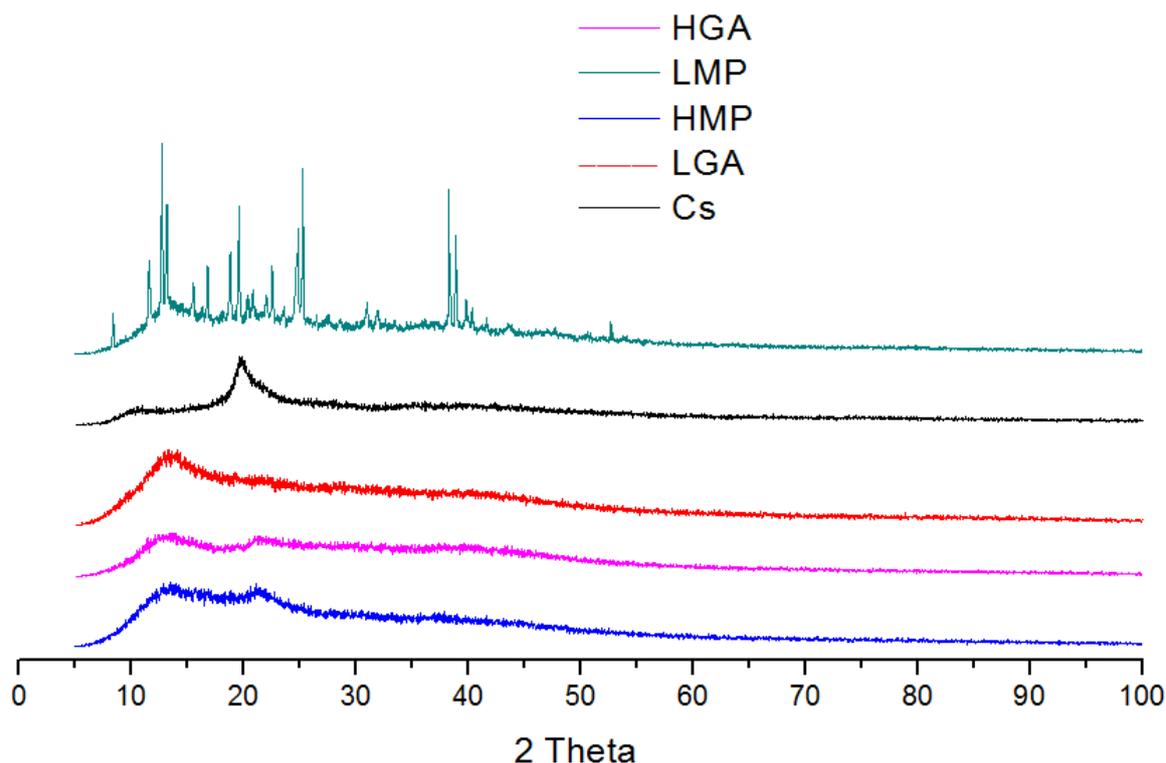
Figure 4.2 X-ray diffraction pattern of CS, HMP, LMP, HGA and LGA at 2θ range of 5° to 100° at a scanning rate of 4°/min

4.4.2. Intrinsic viscosity and zeta potential

The findings of intrinsic viscosity for Cs, HMP, LMP, HGA and LGA at different IS (**Figure 4.3**) revealed a linear reduction of [η] with increasing salt concentrations due to influence of the salt ions on polymer charges (Halabalova *et al.*, 2011); the degree of ionization (α) significantly increases with a decrease of ionic strength which led to high intrinsic viscosity (Walstra, 2002). Likewise, the measurements of zeta potential are shown in **Figure 4.4**, pectin samples (LMP & HMP) and alginates (LGA & HGA) have negative ζ which decreases (closer to zero) with increasing ionic strength. However, in the case of Cs there is positive ζ which also decreased at higher salt concentration. These behaviours would be expected for polycations and polyanions which might be attributed to the reduction of the repulsive potential that results in the interaction between the charged amino groups NH_3^+ with the anions CH_3COO^- in Cs and between COO^- with cations Na^+ in pectin and alginate (Carneiro-da-Cunha, Cerqueira et al. 2011).
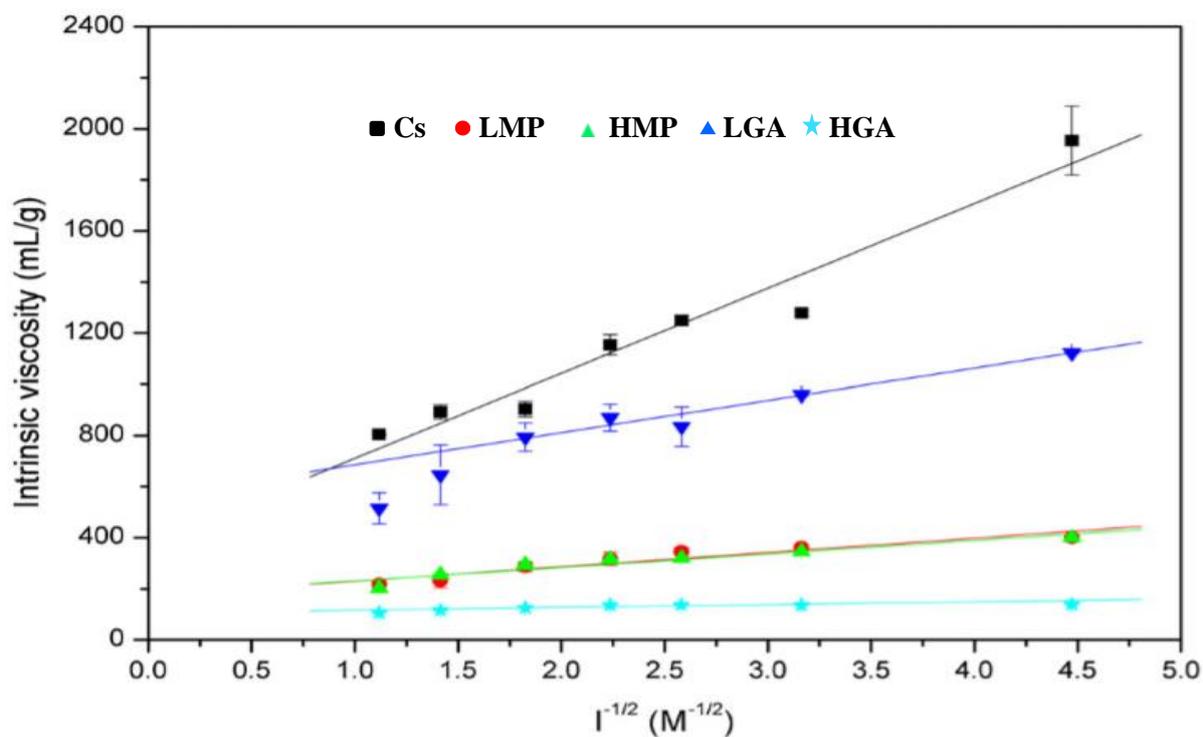
Figure 4.3 Observed behaviour for intrinsic viscosity of Cs, LMP, HMP, LGA and HGA as function of inverse square-root of ionic strength
(Abodinar *et al.*, 2014) (Used with permission)
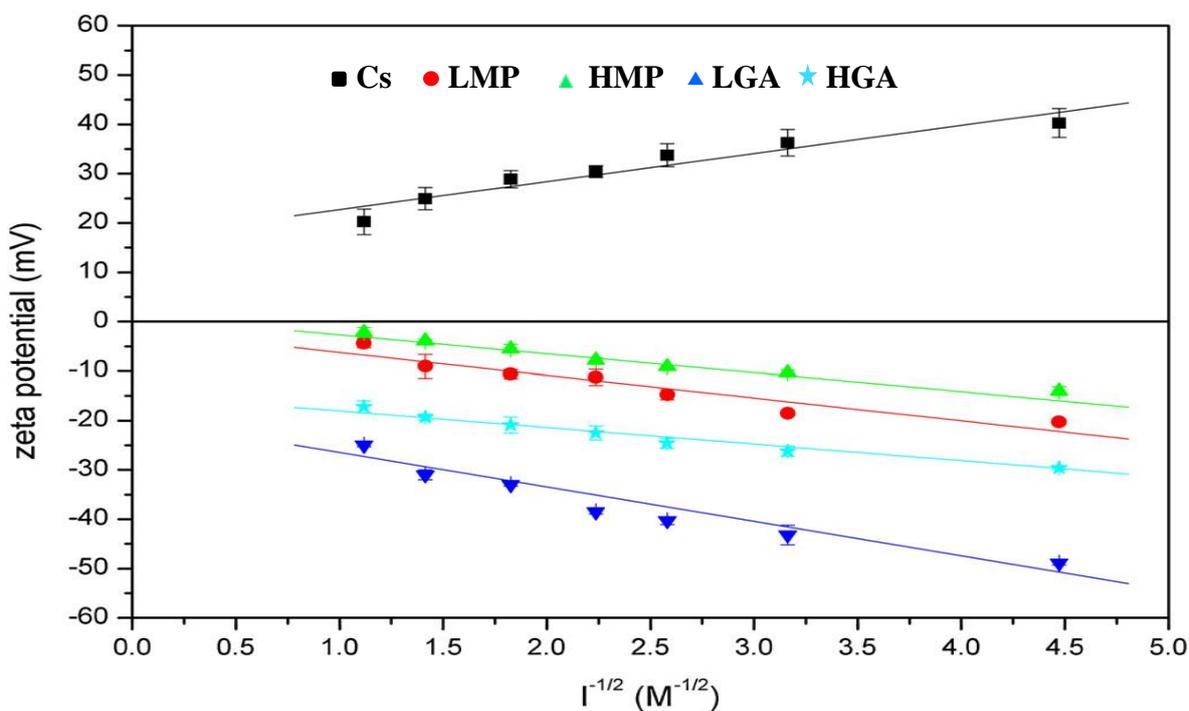
Figure 4.4 Observed behaviour for zeta potential of Cs, LMP, HMP, LGA and HGA as function of inverse square-root of ionic strength
(Abodinar *et al.*, 2014) (used with permission)

4.4.3. Average molecular weight calculation

Intrinsic viscosity can be used to calculate the average molecular weight by applying the classical Mark-Houwink equation (eq.4.1) (Harding, 1997b):

$$[\eta] = K\,(Mw)^{a} \tag{4.1}$$

where $[\eta]$ is the intrinsic viscosity of polymer. In this study we use intrinsic viscosity at 0.2 M for Cs and 0.1 M for pectins and alginate, K and a are constants for given solute–solvent system and temperature. For Cs: $K = 7.4 \times 10^{-3}$, $\alpha = 0.95$, for pectin: $K = 0.0174$, $\alpha = 0.84$ and for alginate: $K = 4.85 \times 10^{-3}$, $\alpha = 0.97$ were reported (Morris *et al.*, 2009, Morris *et al.*, 2010, Davidovich-Pinhas and Bianco-Peled, 2010) respectively. The viscosity-average molecular weight of Cs, pectins and alginate were therefore calculated as in **Table 4.1.**

4.4.4. Estimation Smidsrød-Haug stiffness parameter (B) using the traditional intrinsic viscosity ([η]) and the novel zeta potential (ζ) methods

Perhaps the simplest parameter available to estimate the dilute solution conformation of polysaccharides is the Smidsrød-Haug stiffness parameter (B). This is a very simple conformational parameter based on the intrinsic viscosity; however it is only applicable for polyelectrolytes. In brief the stiffness of polyelectrolytes can be estimated by measuring the intrinsic viscosity at a number of different ionic strengths and then extrapolation to infinite ionic strength as shown in equation 4.2 (Pals and Hermans, 1952).

$$[\eta] = [\eta]_{\infty} + (SI^{\frac{1}{2}}) \tag{4.2}$$

S refers to stiffness parameter which is calculated from is the intrinsic viscosity $[\eta]_\infty$ at infinite ionic strength (I). This parameter can be applied to estimate the conformation of many polyelectrolytes but with the limitation that they be of the identical molar mass at solvent has identical conditions. In 1971, Smidsrød and Haug proposed a novel parameter (B), which eliminate these constraints by comparing $[\eta]$ at a constant ionic strength (typically 0.1 M). The Smidsrød-Haug stiffness parameter, B is calculated as the following (eq.4.3) (Smidsrød and Haug, 1971):

$$S = B([\eta]_{0.1M})^\nu \tag{4.3}$$

Where ν has been shown experimentally to be approximately 1.3 ± 0.1, therefore B can be estimated from a plot of $[\eta]$ versus $I^{-1/2}$.

Therefore in addition to assessing the screening of charges on a polyelectrolyte by measuring intrinsic viscosity at a number of different ionic strengths, it is also possible to measure the zeta potential of polyelectrolyte under the same conditions.

The slopes of the plots in **Figure 4.3** can be used to calculate the Smidsrød-Haug stiffness parameter (B) from equation 4.2 and an alternative version where the intrinsic viscosity was substituted for zeta potential (equation 4.4) can be used to estimate B from the slopes of the plots in **Figure 4.4.**

$$S=B\ (\zeta_{0.1M})^\nu \tag{4.4}$$

The corresponding values of B from both the traditional intrinsic viscosity and novel zeta potential estimation are shown in **Table 4.1**. Although the absolute values from all estimations are different and considerably so in the case of low-methoxyl pectin they are in good agreement with those previously found in the literature.

4.4.5. Estimation persistence length, L_p

Smidsrød-Haug stiffness parameter, B of Cs has been related to the persistence length, L_p (Lárez Velásquez *et al.*, 2008) via the following relationship (eq.4.5):

$$Lp \approx \frac{1.04}{B}$$ (4.5)

Therefore we can estimate the persistence length of Cs to be 35 nm from the traditional intrinsic viscosity measurement and 21 nm from the new procedure. Both of these estimates are in general agreement with the current literature, although the value from intrinsic viscosity is close to the upper limit (Brugnerotto *et al.*, 2001, Lamarque *et al.*, 2005, Mazeau and Rinaudo, 2004, Morris *et al.*, 2009, Terbojevich *et al.*, 1991, Lárez Velásquez *et al.*, 2008, Vold, 2004).

The intrinsic viscosity was replaced for zeta potential as shown in Equation 4.4 which can be used to estimate B from the slopes of the scheme in **Figure 4.4**. The estimation of corresponding values of B from both the traditional method [η] and novel method ζ are presented in **Table 4.1**. Although the absolute values from both estimations are significantly different, the case of both HMP and LMP are generally in good agreement with those previously indicated in the literature. In addition, it is found that there are relationship between the Smidsrød–Haug stiffness parameter, B and the intrinsic persistence length, Lp (Smidsrød &Christensen, 1991) via the following equation:

$$L_p \approx 0.18 \ B^{-1.11}$$ (4.6)

The estimations from both techniques are typical of random or semi-flexible coils and are in general agreement with the current study. The L_p calculated from the stiffness parameter B of approximately 6 - 14 nm (Cs), ~ 6 nm (alginate) and 2 - 14 nm (pectin) although the values estimated from intrinsic viscosity are in all cases higher (**Table 4.1**).

Table 4.1 Estimates for the Smidsrød-Haug stiffness parameter (B) for Cs, LMP, HMP, LGA and HGA using both the tradition intrinsic viscosity ($[\eta]$) and the novel zeta potential (ζ) methods and their comparison with the previous literature (Abodinar *et al.,* 2014) (used with permission).

Polysaccharide	M_w (g/mol)	Smidsrød-Haug stiffness parameter	Intrinsic persistence length, Lp (nm)	Reference
Cs	≈ 295000	$B_{[\eta]} = 0.03 \pm 0.01$	6-14	This study
		$B_\zeta = 0.05 \pm 0.01$	4-6	This study
		$B_{[\eta]} = 0.07$	3	(Jiang and Han, 1998)
		$B_{[\eta]} = 0.11$	2	(Curti and Campana-Filho, 2006)
		$B_{[\eta]} = 0.04 - 0.09$	3-6	(Christensen et al., 2008)
		$B_{[\eta]} = 0.11 - 0.15$	1-2	(Tsaih and Chen, 1997)
		$B_{[\eta]} = 0.10$	2	(Trzciński et al., 2002)
		$B_{[\eta]} = 0.02 - 0.10$	2-14	(Anthonsen et al., 1993)
		$B_{[\eta]} = 0.06 - 0.12$	2-4	(Gartner and López, 2010)
		$B_{[\eta]} = 0.06$	4	(Morariu et al., 2012)
		$B_{[\eta]} = 0.02 - 0.15$	1-14	(Kasaai, 2007)
		$B_{[\eta]} = 0.08 - 0.11$	2-3	(Lárez Velásquez et al., 2008)
LMP	≈ 119000	$B_{[\eta]} = 0.03 \pm 0.01$	6-14	This study
		$B_\zeta = 0.10 \pm 0.02$	2-3	This study
		$B_{[\eta]} = 0.03 - 0.04$	6-9	(McConaughy et al., 2008)
		$B_{[\eta]} = 0.02 - 0.07$	3-14	(Axelos and Thibault, 1991)
HMP	≈ 114000	$B_{[\eta]} = 0.03 \pm 0.01$	6-14	This study
		$B_\zeta = 0.16 \pm 0.04$	1-2	This study
HGA	≈ 39000	$B_{[\eta]} = 0.031$	9	(Dentini et al., 2005)
		$B_{[\eta]} = 0.020 \pm 0.001$	13-15	This study
		$B_\zeta = 0.05 \pm 0.002$	6	This study
LGA	≈ 290000	$B_{[\eta]} = 0.04$	6	(Smidsrød and Christensen, 1991),Dentini et al., 2005)
		$B_{[\eta]} = 0.022 \pm 0.001$	12–13	This study
		$B_\zeta = 0.050 \pm 0.003$	5–6	This study

Different methods (intrinsic viscosity and zeta potential) that have been proved to be used in the estimation of the Smidsrød-Haug stiffness parameter can lead to a bias in the results (**Table 4.1**) and therefore it is more appropriate to characterise macromolecules using more than one technique. This has been demonstrated previously in the estimation of persistence lengths of for example, konjac glucomannan (Kök, Abdelhameed, Ang, Morris and Harding, 2009). The estimation of conformation is very sensitive to the choice of model and it is therefore important that when trying to estimate solution conformation of polysaccharides (or any other flexible macromolecule) the quality of the estimate is determined by the amount of experimental data available.

4.4.6. Influence of pH on intrinsic viscosity and zeta potential

Because the charge of molecules has influence on their solution properties, the findings of intrinsic viscosity for Cs, HGA, LGA, HMP and LMP are closely correlated with zeta potential results in all cases. **Figure 4.5** clearly shows that the positive charge of Cs is reduced as pH increases due the suppression of surface ionisation by increasing negative charges in the media for that reason the molecule becomes less extended and hence the viscosity reduced.

The influence of pH on intrinsic viscosities and negative charges of polyanions samples (pectins and alginates) is shown in Figures 4.6, 4.7, 4.8 and 4.9. In general, HMP has affected with varying pH of media; the highest negative charge and the lowest [η] have been seen at 3.8 pH. Whilst the effect in case of LMP, LGA and HGA (which is insoluble at pH 3.3 and 3.5 which is lower than the pKa of glucuronic acid (Rehm, 2009)) is slight and negligible. Although these experiments have been repeated several times, the results still look odd as findings were consistent with Cs, alginates and LMP while HMP indicates a considerable change at pH 3.8; increasing in negative charge and decreasing in [η]and this behaveur is illogical because normally increasing the net charge of molecules leads to increase the viscosity This is probably due to the hydrophobic nature of the methyl groups as it is very pronounced in HMP and is much less pronounced in LMP and not seen in alginates.
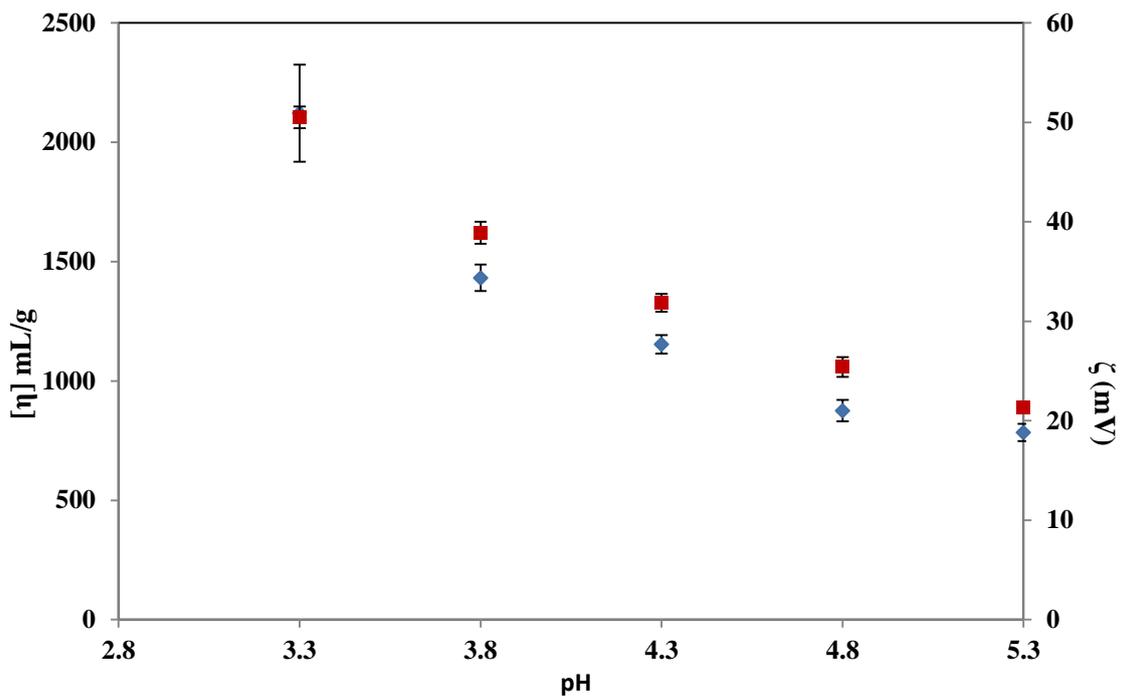
Figure 4.5 Observed behaviour for intrinsic viscosity (blue square) and zeta potential (red square) of Cs as function of pH at 25 ºC
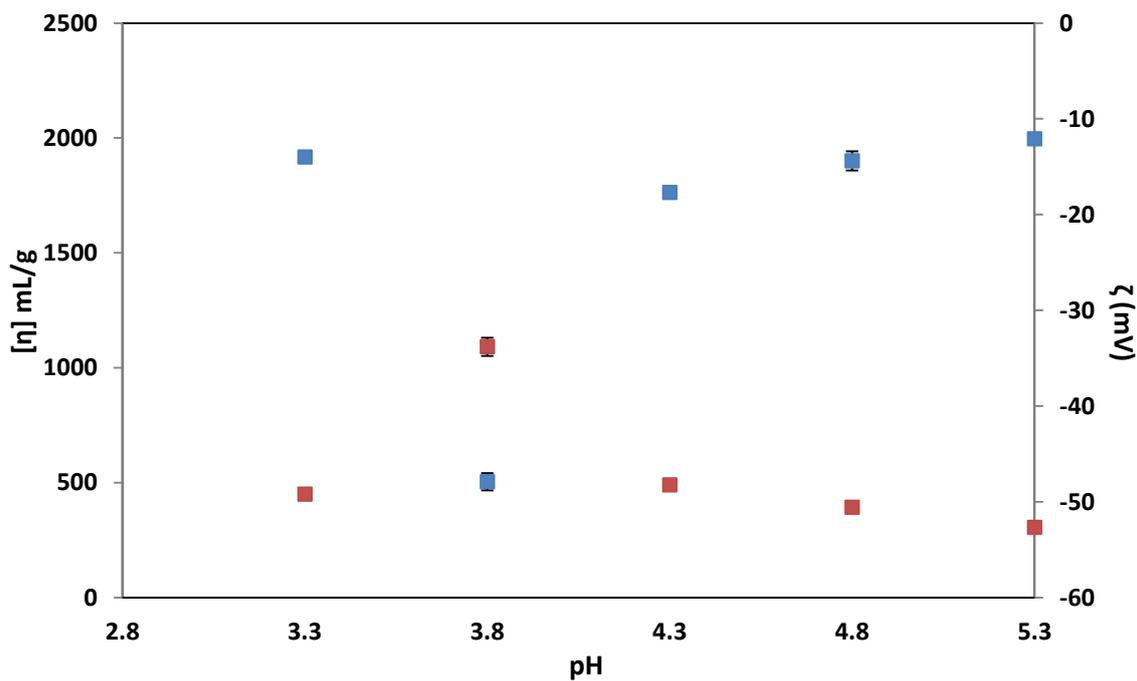
Figure 4.6 Observed behaviour for intrinsic viscosity (blue square) and zeta potential (red square) of HMP as function of pH at 25 ºC
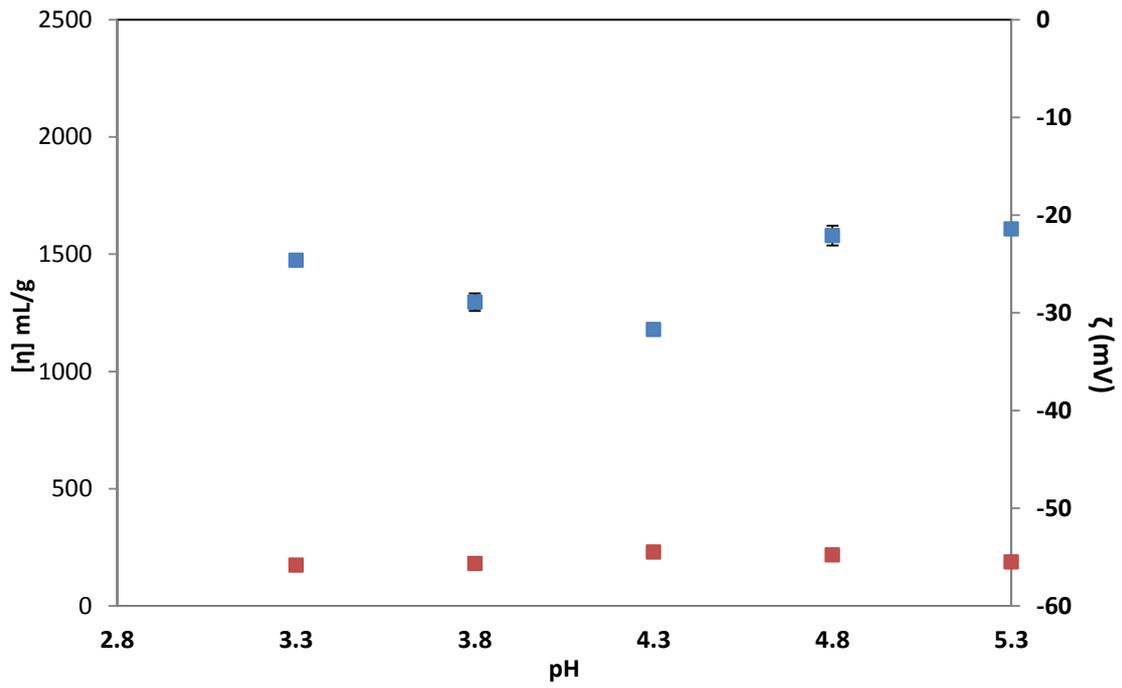
Figure 4.7 Observed behaviour for intrinsic viscosity (blue square) and zeta potential (red square) of LMP as function of pH at 25 ºC
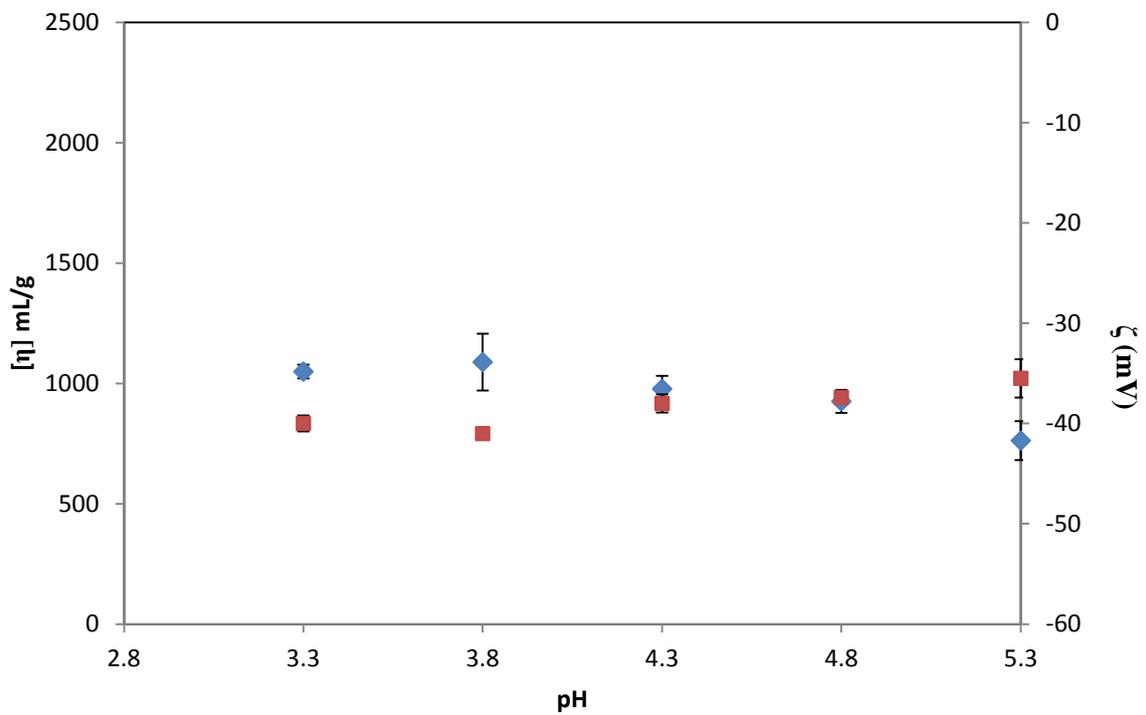
Figure 4.8 Observed behaviour for intrinsic viscosity (blue square) and zeta potential (red square) of LGA as function of pH at 25 ºC
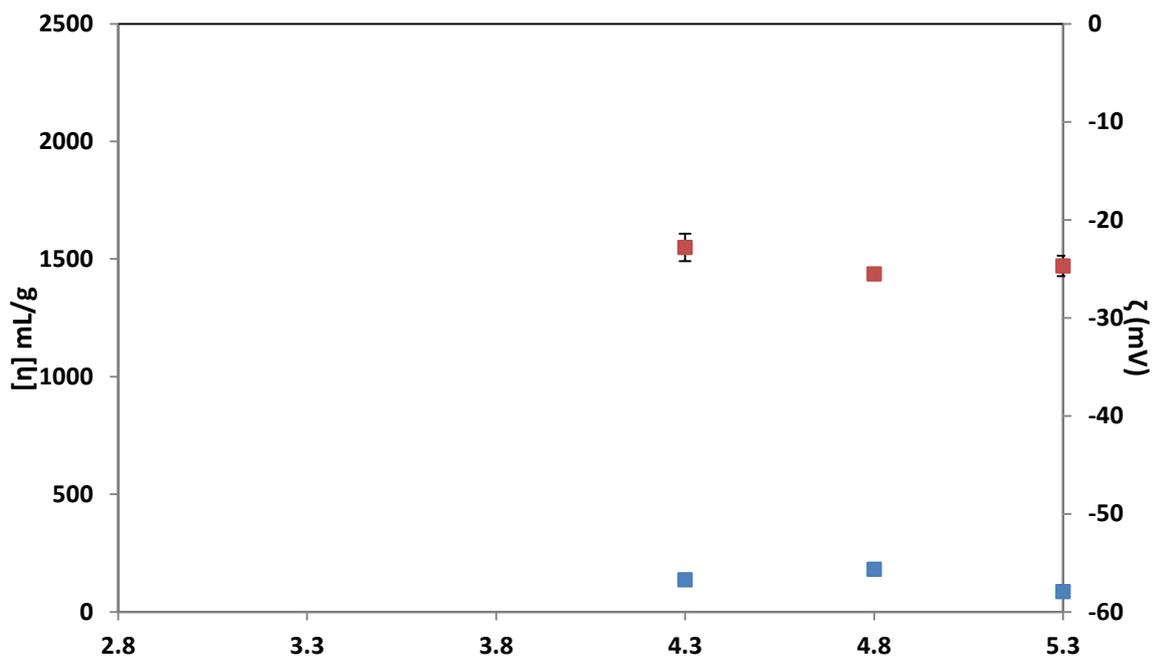
Figure 4.9 Observed behaviour for intrinsic viscosity (blue square) and zeta potential (red square) of HGA as function of pH at 25 ℃. N.B. HGA is insoluble at pH 3.8 and 3.3

4.5.   Summary

In order to study the interaction between mucin and polysaccharides and identify the appropriate conditions for Cs -polyanions polyelectrolyte complex formulation, we needed to first characterize our starting polyelectrolytes, Cs, alginates and pectins. In this chapter the structure of Cs, HMP, LMP, LGA and HGA as powder have been studied; FTIR findings indicate the structure and the functional group for each polysaccharide whereas powder X-ray (XRD) diffraction measurements displays that all the polysaccharide which were analysed are amorphous in nature except LMP which has a number of sharp crystalline peaks which is likely to be due to the low degree of esterification which enables the molecules have long-range thereby high degree of polymerization (DP).

Moreover, solution properties of these polysaccharides were investigated and it was found that there are inverse relationship between ionic strength and intrinsic viscosity with all the samples. The measurements of zeta potential for pectins and alginates (featuring negative ζ values) show a liner decrease (closer to zero) as ionic strength increase. However, in the case of Cs increasing salt concentration leads to decrease in positive charge. This behaviour would

be expected for polycations and polyanions. The Smidsrød-Haug stiffness parameter was estimated using two methods: the ionic strength dependency of zeta potential (novel method) and intrinsic viscosity (traditional method). The results from this new approach are consistent with previous estimates in the literature. We have demonstrated that different approaches (*e.g.* intrinsic viscosity and zeta potential) used in the estimation of the Smidsrød-Haug stiffness parameter can lead to a bias in the results (**Table 4.1**) and therefore it is more appropriate to characterise macromolecules using more than one technique. This has been demonstrated previously in the estimation of persistence lengths of for example, konjac glucomannan (Kök, Abdelhameed, Ang, Morris and Harding, 2009). The estimation of conformation is very sensitive to the choice of model and it is therefore important that when trying to estimate solution conformation of polysaccharides (or any other flexible macromolecule) the quality of the estimate is determined by the amount of experimental data available. The ionic strength indicates a great effect on intrinsic viscosity and zeta potential on the polymers, therefore; it can be used to improve the polyelectrolyte behaviour of the polysaccharides. The influence of pH on intrinsic viscosity and zeta potential also were studied and it was found that the positive charge of Cs reduced as increase the pH due to the suppression of the surface ionisation by increasing negative charges in the media that make the molecule less extended and hence the viscosity is reduced. Whereas in case of polyanions, HMP has shown difference with varying pH of media; the highest negative charge and the lowest [η] have been seen at 3.8 pH. Whilst in case of LMP, LGA and HGA the effect is slight and negligible. This is probably due to the hydrophobic nature of the methyl groups as it is very pronounced in HMP and is much less pronounced in LMP and not seen in alginates.

Chapter 5

Biophysical study of the direct and indirect molecular interactions between mucin and several polysaccharides

5. BIOPHYSICAL STUDY OF DIRECT AND INDIRECT MOLECULAR INTERACTIONS BETWEEN MUCIN AND SEVERAL POLYSACCHARIDES

5.1. Chapter review

5.1.1. Mucin polysaccharide interactions

Mucins play an important role in the pharmaceutical industries as drug delivery agents. Due to abundance of mucin in many human tissues and their negative charge, this make them a suitable candidate for drug delivery interactions as they can interact with positively charged molecules which is important in targeted or controlled delivery. Moreover, the characteristics of biomaterials can be modified by using cationic polymers such as Cs; cationic polymers assist in the stabilization of mucin as it can be easily degraded.

Adhesive properties of mucin and mucoadhesive biopolymers has been of interest in many of pharmaceutical applications especially in drug delivery area due to its importance in increasing residence time and providing high efficiency of drug absorption (Yang *et al.*, 2012, Carvalho *et al.*, 2010, Grillet *et al.*, 2012). Mucin is main constituent of mucous and the viscoelastic and adhesive features of mucous are attributed to presence of mucin. Mucin is able to electrostatically interact with positively charged biopolymers due to prevalence sialic acid on oligosaccharides chains (Harding, 1997a). In addition, the region that does not contain oligosaccharide chains can offer scope for hydrophobic interactions and due to the large size of mucin macromolecules there is the probability of physical entanglements (Ebnesajjad, 2012).

Mucoadhesive systems are influenced by several factors including factors relating to the biopolymer, environmental factors and physiological factors. Biopolymer related factors include molecular weight, chain length, spatial arrangement, flexibility, hydration of polymer, functional groups, hydrogen bonding, charge and degree of ionization of polymer and polymer concentration. With higher molecular weights and longer chain lengths it has been suggested that bioadhesion increases. Polymers with flexible chains can provide deep penetration and entanglement in mucosal layer thereby providing better bioadhesiveness. The conformation of polymer molecules, functional groups and net charges of polymer influence the strengths of

hydrogen bonding and electrostatic interactions thereby having an effect on mucoadhesion. Additionally mucoadhesion may be affected by the pH of medium, contact time, swelling degree and texture and thickness of mucosa (Mythri *et al.*, 2011).

Cs has significant role in drug delivery systems especially in target delivery sites due to its mucoadhesive features which are based on electrostatic interactions between positively charged (NH_3^+) of Cs and negatively charged group (COO^-) of mucin. The interaction is stronger in acidic media because the net charge on Cs is greater (depending on DDA) (Ebnesajjad, 2012).

Negatively charged polysaccharides (*e.g.* alginates, pectins) also have mucoadhesive characterises, indicating that it is not only the electrostatic interactions that are responsible, but also hydrogen bonding between sialic acids and carboxylate and hydrophobic interactions with amino acids have an effective role in formation a complex macromolecular network between the polymer and mucin thereby offering better mucoadhesive strength (Nordgard and Draget, 2011).

5.1.2. Liposomal encapsulation technology (LET)

LET is an exciting modern process that have achieved remarkable development in the pharmaceutical industry due to their unique characteristics such as ability to encapsulate hydrophilic and hydrophobic drugs, good biocompatibility, safety, and targeted delivery of bioactive substances to the site of action (Dua *et al.*, 2012).

Because mucus is the first barrier where food and drugs interact with and diffuse through to be absorbed and access to the blood circulation, efforts are underway to optimize mucoadhesive interactions for improved drug transfer. Mucin can be used in treating dry eye syndrome as additive to improve the mucoadhesion of artificial tear drops also there is great interest in developing nanoparticles for mucosal DNA vaccines and gene therapy (Bansil and Turner, 2006). Moreover, many molecular interactions have been used to enhance mucoadhesion systems, for example, electrostatic interactions (chitosans/ poly-acrylic acid), hydrogen bonds (hydrogels) (Harding *et al.*, 1999) and disulphide linking (thiomers) (Leitner *et al.*, 2003).

The present set of experiments has multiple aims. Firstly, to investigate biophysical molecular interactions between pig gastric mucin (see Chapter 3 for more details) and several polysaccharides (see Chapter 4 for more details) differing in main structure, type and density of charge, molecular weight and conformation. As the mucin-HGA system displays the highest viscosity, the viscoelastic property of this system was taken as the best candidate to be extensively studies. The second challenge was to entrap a hydrophilic molecule (mucin) into phospholipids bilayer using liposomal encapsulation technology and study the potential of interaction between the encapsulated mucin and the polysaccharides using a rheological approach at temperature over the 20 - 60 °C.

5.2. Materials

Egg lecithin mixtures (egg lecithin: cholesterol (42:12) micromoles) obtained from Nutfield Nurseries (Surrey, UK). The other materials used in this study were as described in Section 2.2.

5.3. Study direct interaction between mucin and polysaccharides (Cs, alginates and pectins) at matched viscosity (Menchicchi et al., 2015)

5.3.1. Preparation of polysaccharide-mucin mixtures

Stock solutions of mucin and polysaccharides were prepared using acetate buffer (0.05M, 4.3 pH) at different concentrations (mucin = 5 % (at c < c*), Cs = 0.2, LMP = 1 %, HMP = 0.5 %, HGA = 1.5 %, LGLVA = 1.5 % and LGHVA = 0.175 % as shown in **Figure 5.2 A**) to be closely matched in terms of relative viscosity (η_{rel} ~5). Each solution was well mixed under gentle stirring overnight was filtered under vacuum with a Buchner funnel through filter paper (Whatman No.1). Finally, mucin was mixed with each polysaccharide using various ratios to obtain (25 % v/v, 50 % v/v and 75 % v/v mucin).

5.3.2. Determination of relative viscosity of polysaccharide-mucin solutions

The flow time (t) average (of 3 replicates) of dilute polysaccharide solutions, polysaccharide-mucin solutions and the buffer (t_0) was taken using a 15 mL Oswald viscometer (Rheotek, Burnham-on-Crouch, UK) at 37 °C. The relative viscosity (η_{rel}) was calculated as described in equation (5.1). Then, the relative viscosity deviation between the blends was defined as described in (Menchicchi *et al.*, 2015). A theoretical additive line (line of no

interaction) was calculated by summing each individual contribution to the overall viscosity value, according to the following equation:

$$\eta_{rel} = t/t_0 \tag{5.1}$$

$$\eta_{t\ (f)} = V_{p\ (f)}\ \eta_p + V_{m(f)}\ \eta_m \tag{5.2}$$

Where, $\eta_{t\ (f)}$: the additive theoretical value of relative viscosity at a given fraction (f) mass ratio, $V_{p\ (f)}$: the relative volumes of polysaccharide in the mixture given value of f, $V_{m\ (f)}$: the relative volumes of mucin in the mixture given value of f, η_p: the relative viscosity of polysaccharide stock solution, η_m: the relative viscosity of the stock solution of mucin. Percentage deviation from the theoretical additive line was calculated from the difference between the experimental values (η_{exp}) of the blends and the corresponding theoretical values as the following equation:

$$\%\ deviation\ _{(f)} = (\eta_{t\ (f)} - \eta_{\ (exp)\ (f)})\ /\ \eta_{t\ (f)} \times 100\ \% \tag{5.3}$$

The total area under the curve (AUC) at different values of mucin fraction was calculated from summing of the trapezoids described by the experimental percentage deviation and the theoretical additive line values using Origin v 6.1 (Origin Lab Corp., Northampton, USA).

5.3.3. Preparation mucin - HGA mixture

Mucin HGA blend was prepared by gentle mixing of the mucin and HGA solutions (prepared in Section 5.3.1) in different ratios to achieve 50 (v/v) %, 60 (v/v) %, 70 (v/v) %, 80 (v/v) % and 90 (v/v) % of mucin, whilst making sure that the agitation of the samples was not

too strong in order to allow spontaneously gel formation and to avoid making bubbles in the mixture.

5.3.4.   Rheological measurements of mucin - HGA gels

5.3.4.1. Viscosity measurements

Viscosity measurements of prepared mucin-HGA gels were taken over shear stress range of 0.1 pas to 10 pas at 37 °C using Kinexus Pro$^+$ rheometer (Malvern Instruments, Worcestershire, UK) with CP4/40 SR 2567 plate geometry.

5.3.4.2. Frequency sweep measurement

Frequency sweeps for the prepared mucin-HGA gels were carried out over a frequency range of 0.1 to 10 rad/s at 2 % strain at 37 °C. The moduli G′ and G″ of the gels were determined within the linear viscoelastic regime and plotted as a function of increasing frequency.

5.3.4.3. Evaluation the mucoadhesive properties for polysaccharide-mucin mixtures

The adhesive forces of the highest viscosity blends of polysaccharide- mucin mixture: 25 % HGA, 25 % LMP, 50 % Cs, 50 % HMP, 50 % LGLVA and 75 % LGHVA were assessed using mucoadhesion profile on the rheometer fitted with a CP4/40 SR 2567SS upper plate and PLS 6152174 SS lower plate. The experiment involve putting 1 g of the sample in the centre of the lower plate (with making sure no pressure was applied) at gap 0.1mm and 37 °C then the gap was moved from 1 mm to 10 mm and the normal force was recorded as function of time. Negative peaks and negative areas were calculated by Origin v 6.1 (Origin Lab Corp., Northampton, USA). The values of negative areas and negative peaks are associated with the work of adhesion to the probe and the maximum adhesive force respectively (Tamburic and Craig, 1997).

5.4.   Encapsulation mucin by LET

5.4.1.   Liposome preparation

Liposomal vesicles were prepared (as shown in **Figure 5.1**) using Bangham Method (Gad, 2008) which involves hydration of a thin lipid film by drying 1 mL of the egg lecithin mixtures in a round-bottom flask under vacuum using rotary evaporation at 60 °C for 15-20

min to get a thin film. The film hydrated by adding 1 mL of 2 % mucin (or DI water for the control) then completely mixed using vortex mixer for 5 minutes at 60 °C (above the transition temperature of lecithin 55 °C) to yield a milky-white lipid suspension. The suspension was centrifuged at room temperature and separated to supernatant and precipitate. The latter was washed and centrifuged and suspended again in deionised water. Particle image, particle size and zeta potential for the liposomal product were determined.
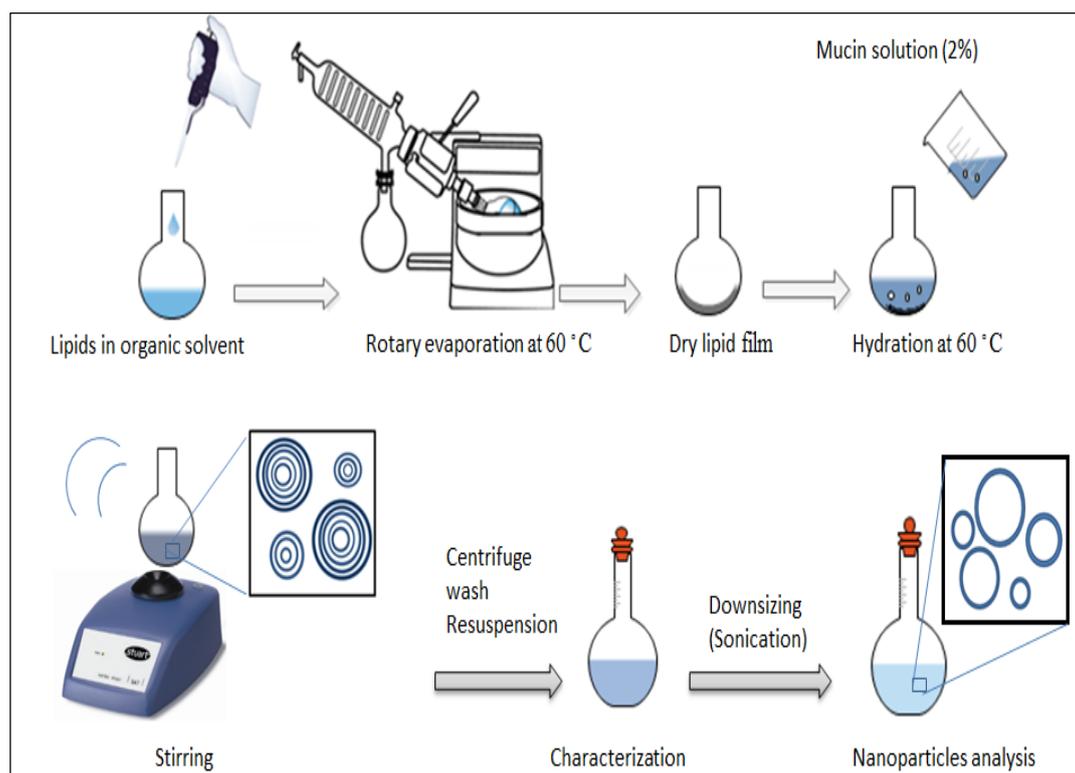
Figure 5.1 Diagram of liposome production by lipid hydration followed by vortex mixing and downsizing

5.4.2. Liposome nano-sizing

The obtained liposomes were diluted 10 times and sonicated by SONICS Uibra Cell using microprobe at room temperature, 10 seconds on, 5 seconds off, at 50 % amplitude for 1 min. Finally, the nanoparticles were measured by using Nanoparticle Tracking Analysis (NTA) version 2.3 build 0033 (Nanosight, UK).

5.4.3. Liposome characterisation

5.4.3.1. Zeta potential

Zeta potential of liposome suspension that dispersed in distilled water (0.5 % w/v) was determined using Malvern Zetasizer NANO-Z (Malvern Instruments Limited, Malvern, UK). Measurements in triplicate were performed by using a folded capillary cell at 25.0 ± 0.1 °C and refractive index was set at 1.450.

5.4.3.2. Particle size

The particle size distribution of the liposome samples were measured by a Mie scattering using a Malvern Mastersizer 2000 (Malvern Instruments Ltd., Malvern, UK). The dispersion concentration was around 0.1 g/L. The suspension was prepared by dispersing the liposome pellet in distilled water. Refractive index of particles and dispersion medium (DI water) were set to 1.45 and 1.33 respectively.

5.4.3.3. Microscopy method

Liposome samples were imaged using an optical microscope (KEYENCE VHX Digital Microscope RZ $\times$ 250 $\times$ 1500 real zoom lens, Milton Keynes, UK). The samples were prepared for imaging by applying a drop of each sample on microscope slide and covered by slip slide then scanned under the microscope.

5.4.3.4. Mucin detection using HPAEC-PAD

2 mL (in triplicate) of the suspended vesicles and the supernatant were placed in separate pressure tubes. Concentrated trifluoroacetic acid (0.85 mL) was then added to each sample using a micropipette. The pressure tubes were then placed in a heating block for 120 minutes at 120 °C. After 2 hours, the samples were evaporated to dryness under a stream of nitrogen gas at 65 °C for 1 hour. The dried samples were reconstituted with 2 mL of deionized water prior to HPAEC-PAD analysis. Neutral sugars, amino sugars and sialic acid composition were analysed using a Dionex ICS-5000 HPAEC-PAD system (Thermo Fisher, Loughborough, UK). A 0.5 mL/min flow rate was used the first 12 minutes at 10 mM NaOH followed by a 0.05 minute step from 0 -17 % 1 M sodium acetate in 150 mM NaOH and the remainder of the run at the upper limit of this gradient to elute any uronic acids present. A pre-run equilibration

step of 10 minutes using 200 mM NaOH followed by 20 minutes of 10 mM NaOH was used to regenerate the column prior to each injection.

5.4.3.5. Evaluation encapsulation efficiency (EE)

Encapsulation efficiency evaluates quantity and rate of entrapment of water soluble material in aqueous compartment of liposome. EE was calculated according to a method that reported (Nii and Ishii, 2005):

$$\text{Encapsulation efficiency (\%)} = ((C_{total} - C_{out})/C_{total}) * 100\,\% \qquad (5.4)$$

Where C_{total} is the total concentration of mucin added, C_{out} is the amount of mucin detected only in the supernatant.

The concentrations of the mucin (C_{out}, C_{total}) were quantitatively analysed using sulphuric acid–UV method (Albalasmeh *et al.*, 2013). The method was applied without modification; in a test tube (in triplicate) 1 mL of the supernatants obtained from liposome suspensions (prepared in Section 5.2.2.1) were rapidly mixed with 3 mL of concentrated sulphuric acid using vortex mixer for 30 s. after which the solution was cooled in ice for 2 min to bring it to room temperature. Finally, UV light absorption at 315 nm was read using UV spectrophotometer (Agilent Technologies Cary 60 UV-Vis). Calibration curve was prepared using glucose as standard at concentrations range from 10 - 100 µg/mL. The spectrophotometer was zeroed using the blank (1 mL DDI water and 3 mL of concentrated sulphuric acid).

5.4.3.6. Nanoparticle tracking analysis (NTA)

Nanoparticle tracking analysis (NTA) is a technique for studying and examining particles in solutions that associates Brownian motion movement to particle size. This method is used to the determinate a size distribution of small particles with a diameter of ≈10-1000 nm in suspension. The system is coupled with an ultramicroscope and a laser illumination unit that together allow to envisage the movement of the small suspended particles under Brownian motion. Also it equipped with a charge-coupled device (CCD) or electron multiplying charge-

coupled device (EMCCD) camera that captured the light scattered by the particles (Filipe *et al.*, 2010)

A sonicated sample was subjected to nanoparticle tracking analysis (NTA) using NanoSight NS300 equipment and NTA 2.3 build 0033 software to obtain the diameter of liposomal particles as follows: the sonicated sample was diluted about 50 times using ultra-pure water. After washing NanoSight sample chamber by ultra-pure water, an aliquot of the sample was injected using a plastic syringe and allowed to flow through the sample chamber (about 1 mL, 4 times) to make sure there are no bubbles and no particles stuck to the chamber. The focus and camera parameters were adjusted until the best possible vision of the particles was obtained then the measurements were recorded.

5.5. Study the indirect interaction between mucin (encapsulated in liposome) and polysaccharides

5.5.1. Sample preparation

Polysaccharide-LEM (Liposome encapsulating mucin) samples were prepared by mixing each sample prepared in section 5.2.1.1 with LEM using the ratios that gave the highest viscosity of each polymer (25 % HGA, 25 % LMP, 50 % Cs, 50 % HMP, 50 % LGLVA and 75 % LGHVA) with taking into account the fraction of mucin encapsulated in liposome. The aqueous prepared liposome was used as control.

5.5.2. Frequency sweep measurement for polysaccharide-LEM samples

Small deformation measurements of polysaccharide-LEM samples were carried out using Kinexus Pro$^+$ rheometer (Malvern Instruments, Worcestershire, UK) with cp2/50 SR 1683SS geometry to determine storage modulus (G') and the loss modulus (G") with increasing temperature. The samples were placed on the flat plate followed by coming down the geometry and covering the edges with a thin layer of paraffin oil to prevent water evaporation during measurement. The measurements were achieved by create sequences using rSpace software at frequency 10 red/s, strain 2 %, start temperature 20 °C and final temperature 60 °C.

5.6. Results and discussion

5.6.1. Study the direct interaction between mucin and polysaccharides (Cs, alginates and pectins) at matched relative viscosity

Samples of polysaccharides (Cs, HGA, LGHVA, LGLVA, LMP and HMP) and mucin were prepared at matched relative viscosity ($\eta_{rel} \sim 5$) using acetate buffer (0.05M, 4.3 pH). Mucin was mixed with each polysaccharide at various ratios (25 (v/v) %, 50 (v/v) % and 75 (v/v) % and the degree of interaction the polysaccharide and mucin was evaluated by determining relative viscosity.

5.6.1.1. Evaluation of Polysaccharide -mucin interactions by relative viscosity (Synergism)

Figure 5.2.B shows the percentage deviation of relative viscosity of the mucin-polysaccharides mixture from an additive line as a function of fraction of mucin (eqs 5.1 and 5.2). In this experiment, synergies (either synergism, antagonism or no interaction) between mucin and polysaccharides molecules were studied. The findings indicate that when mucin mixed with negatively charged molecules, the produced blends generally exhibits a positive synergy (an increase in relative viscosity) while in case of mucin-polycation (Cs), reduction in the viscosity occurred (negative synergy). These are driven mainly by electrostatic interactions between positive charges groups on Cs and negative charges on mucin which supported by hydrogen bonds and hydrophobic forces. Thereby the molecular mass, degree of acetylation conformation and flexibility of Cs also played an important role in this interaction (Menchicchi *et al.*, 2014). Significant deviations from the additive line were observed in all cases except HMP case which revealed no appreciable deviation resulting from lower negative charge due to high degree of methylation.
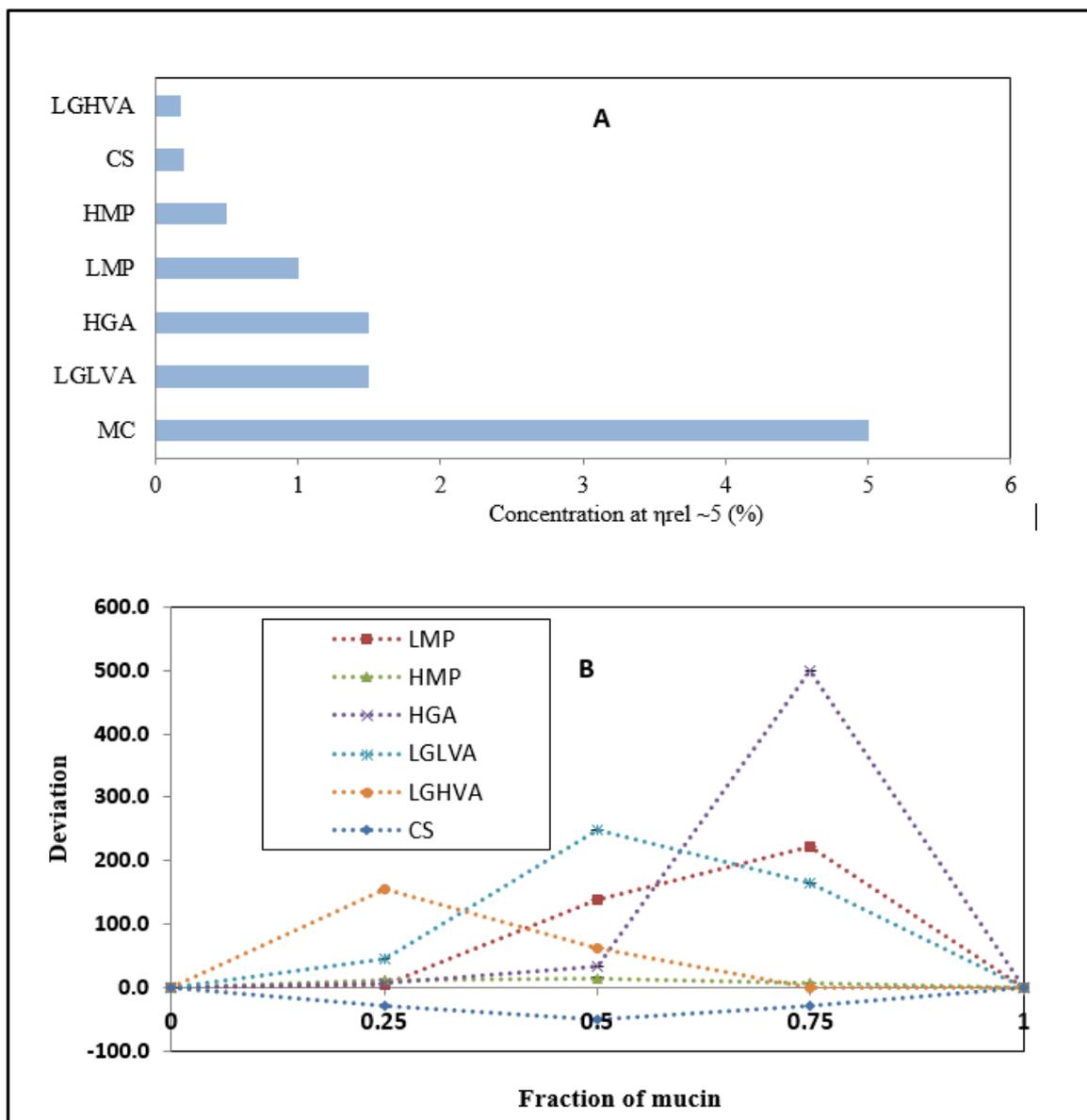
Figure 5.2 (A) Concentration of stock solutions to achieve relative viscosity of ~5.0 in acetate buffer (pH 4.3, IS 0.05 M) at 37 °C. (B) Percentage of deviation of relative viscosity for mucin-polysaccharide mixture in acetate buffer (IS= 0.05 M, pH 4.5) at 37 °C

Regarding to alginate molecules, the three types of alginates showed an increase in viscosity (positive synergy) with mucin which attributed to the electrostatic repulsive between alginate and mucin. Mixture of mucin and HGA exhibited the greatest positive synergy (up to~ 498 %) with a maximum at f = 0.75. Whereas, the maximum positive synergy appeared less in cases of mucin-LGLV alginate (up to ~248 %) and LGHV alginate (up to 154 %) at f = 0.50 and 0.25 respectively. This suggests that the guluronic acid (G-block) content of alginate

has an effect on interaction degree; increasing the G content of alginate led to increase viscosity therefore higher area under the curve **(Figure 5.3)**. The explanation is that mucin-alginate system is derived by two forces homopolymeric mucin-mucin interactions (hydrogen bonds) and heteropolymeric mucin-alginate interactions (electrostatic repulsion) (Taylor *et al.*, 2005a). The presence G-blocks (in small amounts) in the system leads to increase mucin-alginate interactions by promoting mucin-mucin interactions. However, low G-block (*i.e.* abundance of M-blocks) in the system may lead to the inhibition of homopolymeric mucin-mucin interactions caused by structural composition of M-block thereby the mixture displays less viscosity. Likewise, pectin shows positive synergy; LM pectin substantial deviation from the additive line synergy (up to $\sim$220 %) with a maximum at f = 0.75, whereas HM pectin displays no appreciable deviation resulting from the lack of the negative charge and the high degree of methylation.

Therefore, it suggests that to achieve specific features of a mixture of two biopolymers (*e.g.* polysaccharide and mucin), it is not only the concentration but also the net charge density and subunit composition of the polysaccharide which are fundamental components of the interaction which must be taking into consideration. Since mucin - HGA blend exhibits the highest viscosity its viscoelastic properties were studied further.
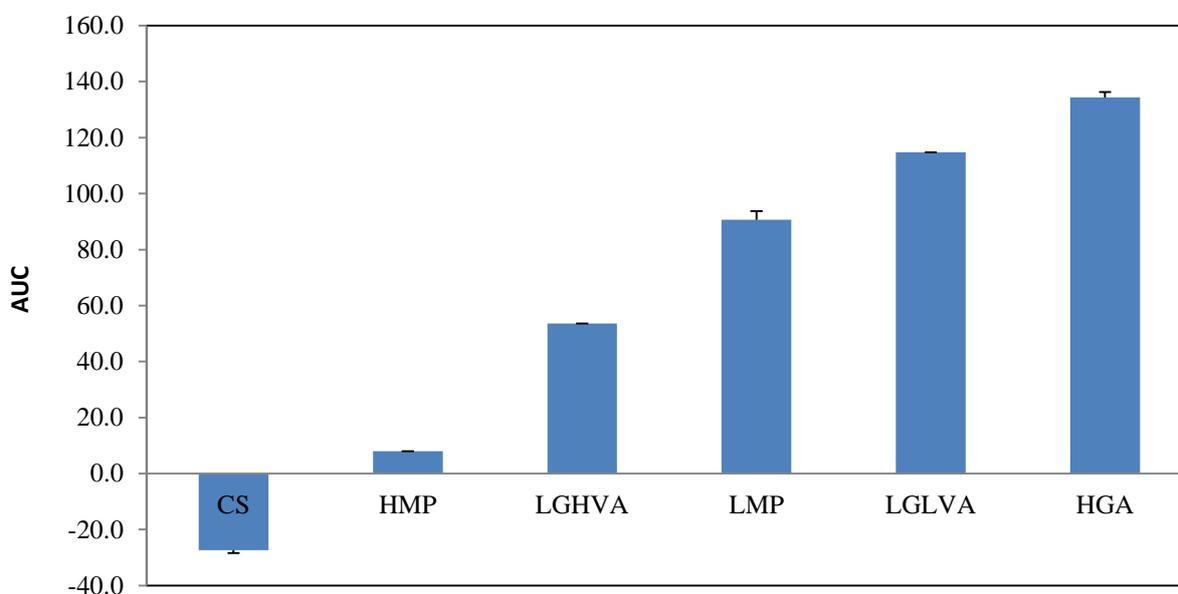
Figure 5.3 The area under the curve (AUC) of mucin - polysaccharides interaction representing the percentage deviation in the viscosity values of mixed solutions with respect to the additive line on Figure 5.2 B.

5.6.1.2. Rheological study of mucin- HGA mixtures

5.6.1.2.1. Viscosity measurements

The viscosity results (**Figure 5.4**) of mucin-HGA mixtures as a function of shear stress indicated that at low shear stress the increase in viscosity started at 70 % mucin, whereas no clear increase in viscosity was observed for 60 % and 50 % mucin (0.01 Pas) which was similar to mucin and alginate themselves (0.01 Pas). The viscosity of blend containing 90 % mucin (100 Pas) was significantly higher than the viscosity of its ingredients. Moreover, the system showed that the blend of 90 % mucin was able to resist greater stress compared with 70 % and 80 % (0.7 Pas, 0.2 Pas and 0.17 Pas) otherwise 0 %, 50 %, 60 % and 100 % mucin did not show any resistance. These findings can be interpreted as that mucin-HGA system is derived by two forces homopolymeric mucin-mucin interaction (hydrogen bond) and heteropolymeric mucin-alginate interaction (electrostatic repulsion) (Taylor *et al.*, 2005a). With high content of HGA in the system, intermolecular cross-link density of mucin molecules will lack inhibiting hydrogen binding sites of mucin by alginate reducing repulsion forces between mucin and alginate. On the other hand, less HGA in the system leads to greatly increase mucin-alginate interactions while maintaining the intermolecular interactions. This means the viscosity of the mucin - HGA blend is inversely proportional with mass of HGA (with respect to the total mass).
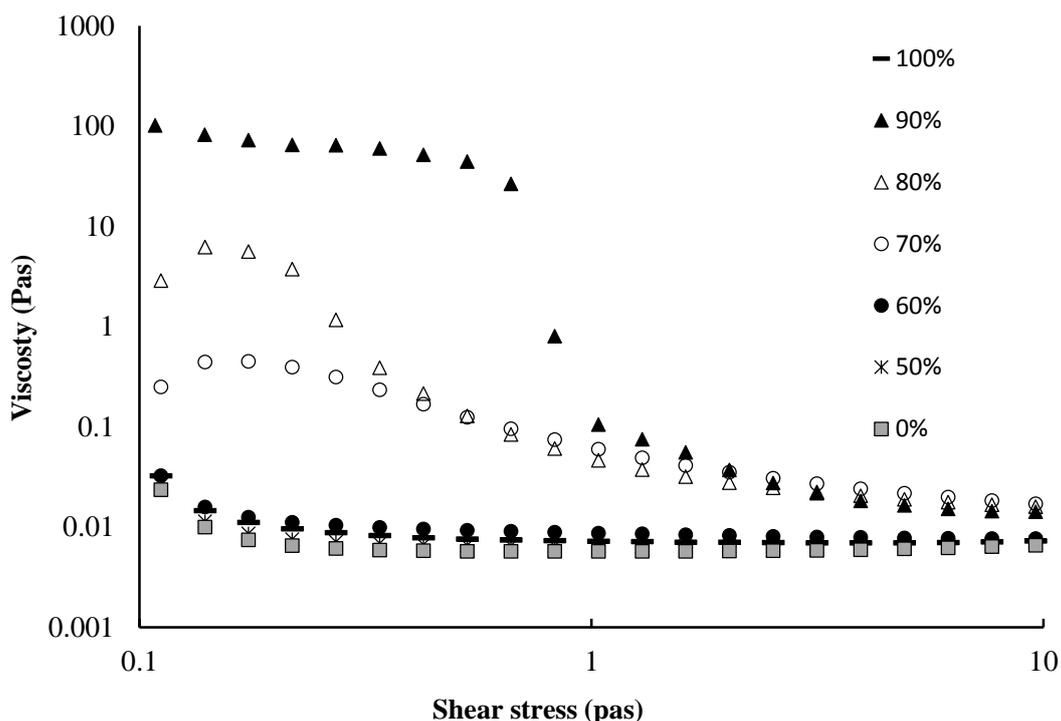
Figure 5.4 Viscosity *vs*. shear stress for different ratios of mucin – HGA mixture at 37 °C

5.6.1.2.2. Dynamic mechanical measurements

Similarly, the mechanical spectra (**Figure 5.5**) of the mucin - HGA blends indicate that with the exception of the system involving only HGA (0 % mucin) and 60 % mucin, all mixtures including mucin itself displayed typical 'weak gel' rheological behaviour as shown G˙ is greater than G" and they gradually increase with increasing frequency. The blend produced from 90 % w/w mucin exhibits the greatest G' (~10 Pa). Interestingly, reducing the content of HGA in the blend resulted in strengthening of the gel as seen by increasing G' and G" which means addition of excess alginate led to non-gelling blends which agree with (Taylor *et al.*, 2005a) because (as previously mentioned) large amounts of HGA tends to limit mucin-mucin interaction. At 60 % mucin the mixture goes from liquid like to gel like (sol-gel transition) where G" and G˙ crossover. In this process the subunits of material in the system physically join together and form network (Jones, 2002). So reducing the HGA content in the system leads to the promotion of homopolymeric and heteropolymeric interactions by activating bond sites of the subunits thereby the gel properties start to appear. Consequently, in addition to composition, variation in size of G-rich alginate molecules have effective influence on gel strength (**Figure 5.6**) (Taylor *et al.*, 2005a) (Reehorst, 2014); although HGA

and LGLVA have same concentration, HGA indicates higher viscosity and stronger gel than LGLVA with mucin.
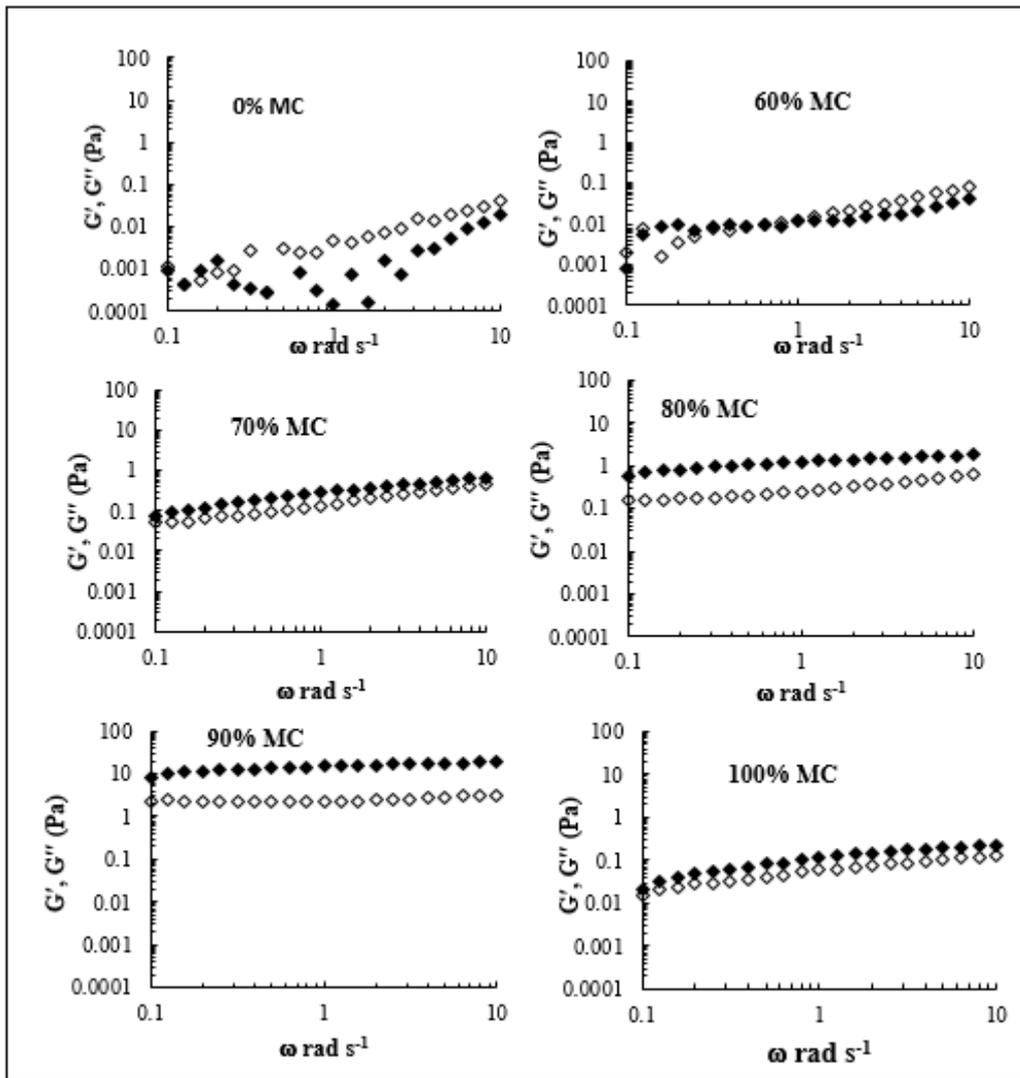
Figure 5.5 Mechanical spectrum of mucin - HGA gel at different ratios indicating variation of G′ (filled squares), G″ (open squares) at 2% strain; 37 °C.
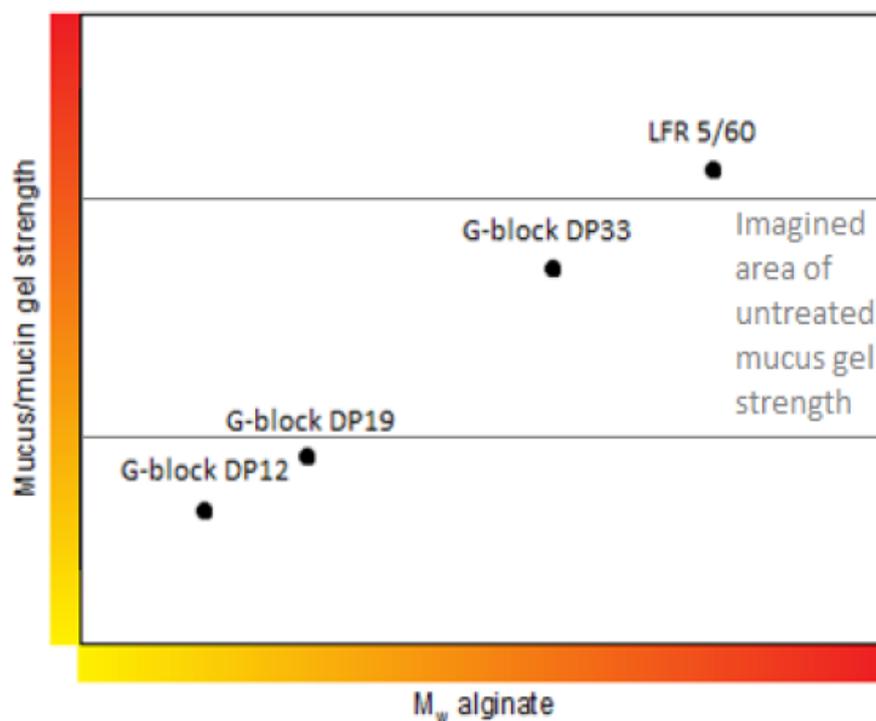
Figure 5.6 The influence of different size of G-rich alginate molecules on the strength of mucus/mucin gel
(Reehorst, 2014)

5.6.1.2.3. Mucoadhesion evaluation

Table 5.1 indicates the evaluation of mucoadhesiveness (stickiness) of polysaccharides-mucin interaction based on the work of adhesion (negative area) and maximum adhesiveness or stickiness (negative peak) obtained from mucoadhesion profile (**Figure 5.7**). The findings show that work of adhesion of LVLGA and HGA was greater than work of adhesion of LGA this may be because of the better thickness features. The work of adhesion of HMP was not significantly greater than LMP but not less than Cs. The maximum adhesive force (negative peak) of the mixtures (**Table 5.1**) shows the rank order of mucoadhesion to be LGLVA > HGA > LMP > LGHVA > Cs > HMP which seems to be a correlation with concentration of the polymer as shown in **Figure 5.2.A**.

Mucoadhesion studies highlight the greater mucoadhesiveness of LVLGA and HGA in comparison with the other mixtures (**Table 5.1**). This is possibly due to the better rheological gel features. Generally systems with higher elastic component exhibit a greater mucoadhesion as reported in previous works (Tamburic and Craig, 1995, Tamburic and Craig, 1997).

According to (Bernkop-Schnürch, 2000), the key factor effecting mucoadhesion process is chain flexibility. Flexible polymer chains able to deeply interpenetrate between the chains and mucus and form a strong adhesive links. Therefore, the author suggested that the cross-linking or the covalent interaction of large sized ligands may result in reducing in flexibility of chain thus strongly decreasing in mucoadhesion. This may explain the low values for work of adhesion and maximum mucoadhesiveness of Cs.
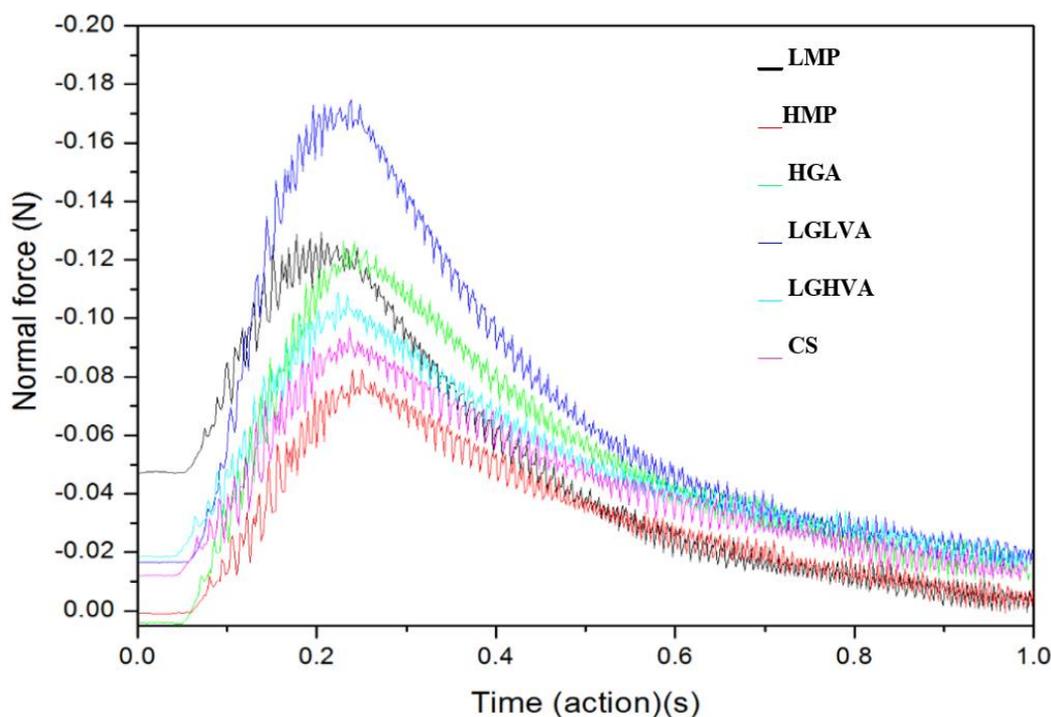
Figure 5.7 Mucoadhesion profiles obtained by rheometry instrument for polysaccharide-mucin mixtures

Table 5.1 The corresponding values for the work of adhesion (negative area) and maximum adhesiveness or stickiness (negative peak) of polysaccharides/mucin mixtures (n=3, mean ±SD)

Sample (polysaccharides/mucin)	- Peak area (N.s) Polysaccharide-mucin mixture	- Peak height (N) polysaccharide-mucin mixture
LMP	-0.024 ± 0.003	-0.093 ± 0.002
HMP	-0.028 ± 0.001	-0.083 ± 0.007
HGA	-0.046 ± 0.001	-0.128 ± 0.001
LGLVA	-0.048 ± 0.002	-0.156 ± 0.004
LGHVA	-0.031 ± 0.001	-0.089 ± 0.003
Cs	-0.030 ± 0.007	-0.085 ± 0.009

5.6.2. Liposome characterisation

5.6.2.1. Mucin detection

In this study mucin molecules were trapped in lipid bilayers by using liposomal encapsulation technology and were detected by using HPAEC-PAD as it shown in **Figure 5.8** Comparing LEM with the control it clearly indicates that LEM has four peaks in contrast the control sample were no peak appeared. When the chromatogram of LEM was compared with the mucin chromatogram, both results were almost identical; this means that the constituent mono saccharides of mucin are the same as those found in liposome indicating some degree of encapsulation. The four sugars were determined by running standard for each sugar, which were fucose, galactose, galactosamine and glucosamine (see **Table 3.1**).
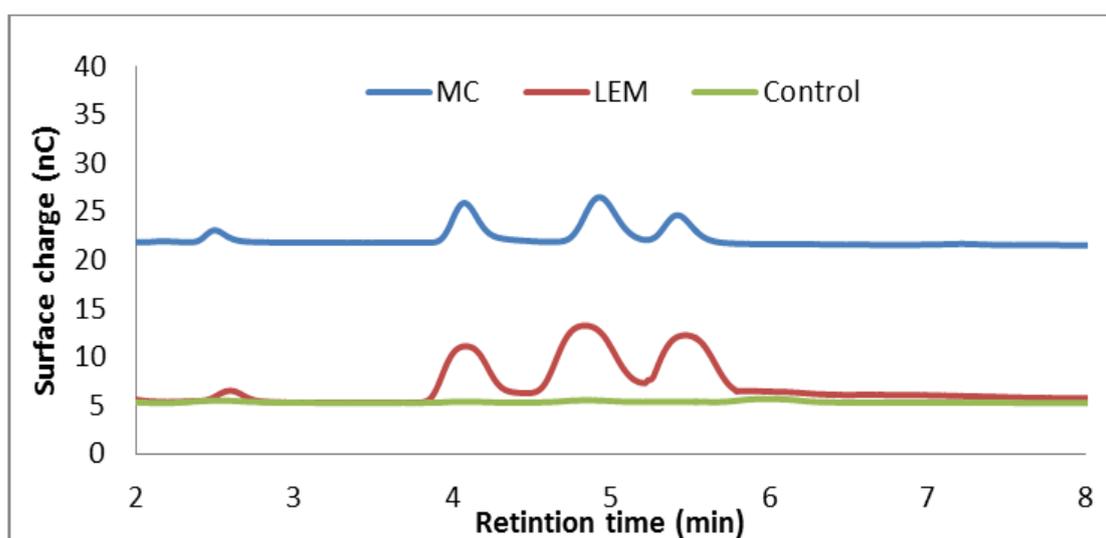
Figure 5.8 HPAEC-Pad data for mucin (MC), LEM and control at 25 °C

5.6.2.2. Zeta potential morphology size distribution of liposome

Although there were no noticeable changes in zeta potential values of the control and LEM (-36.8 ± 0.4 and -35.4 ± 1.0 respectively) (**Figure 5.9**), morphology and particles size distribution dramatically vary; the particles size of the control about 3 - 50 µm whereas LEM were arranged from 100 to 500 µm (**Figure 5.10**). As both liposomal products which were prepared in this study were essentially comprised of phospholipids and non-charged cholesterol, the net negative charge exhibited on the liposomes could be due to the

126

conformational influences of phospholipids in the assembly. In other words, the orientation of phospholipid's dipole head-group has the responsibility for imparting the negative charge on the liposome; the positive side dipole was pulled to the inside of the bilayer because of forming hydrogen-bond with the carboxylic group of cholesterol while the net negative charge of the dipole sticks out of the surface of the liposome as clarified in the schematic in (**Figure 5.11**) as proposed by (Makino *et al.*, 1991).
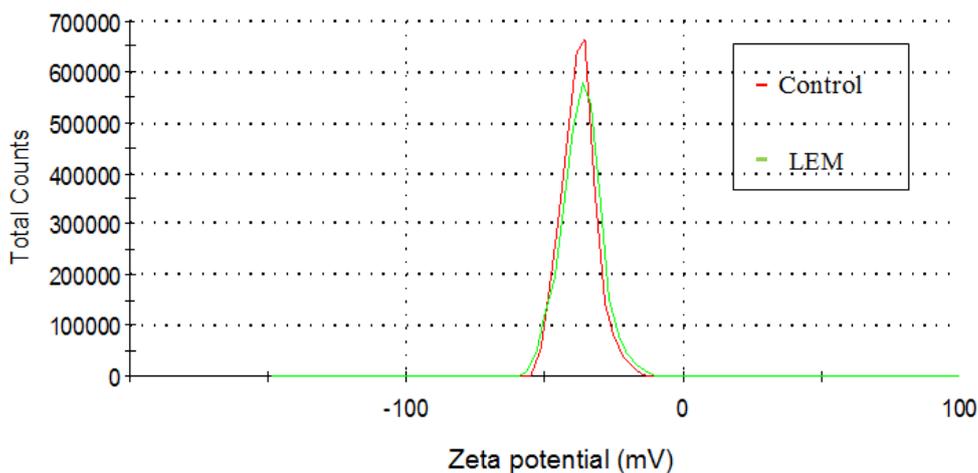
Figure 5.9 Zeta potential of LME sample and control suspended in in deionised water at 25 °C
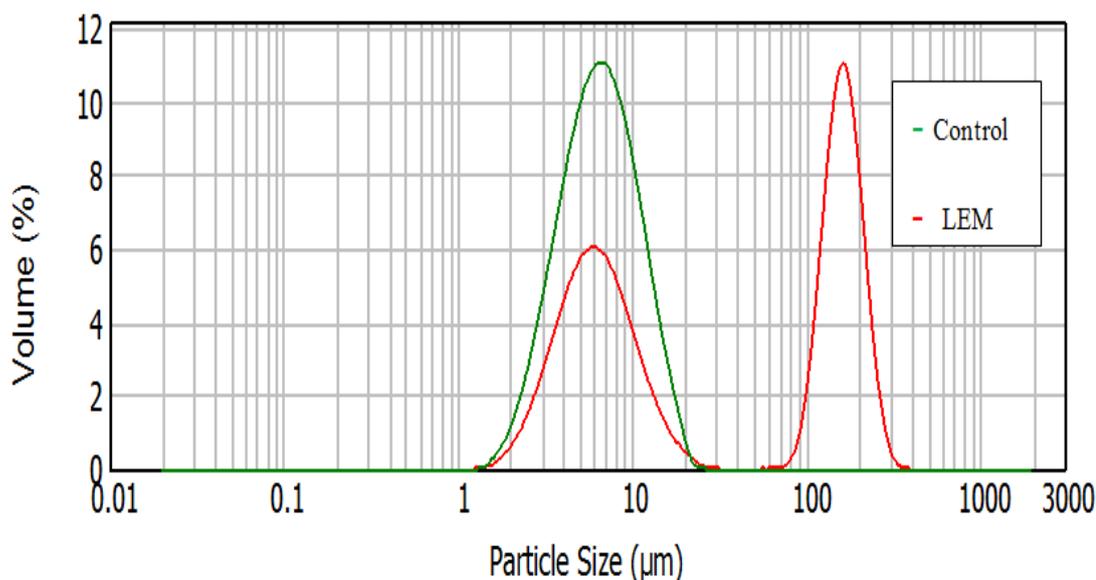
Figure 5.10 Size distribution of liposome encapsulating mucin (LEM) and liposomes prepared in DI water (as control) dispersing distilled water at 25 °C.
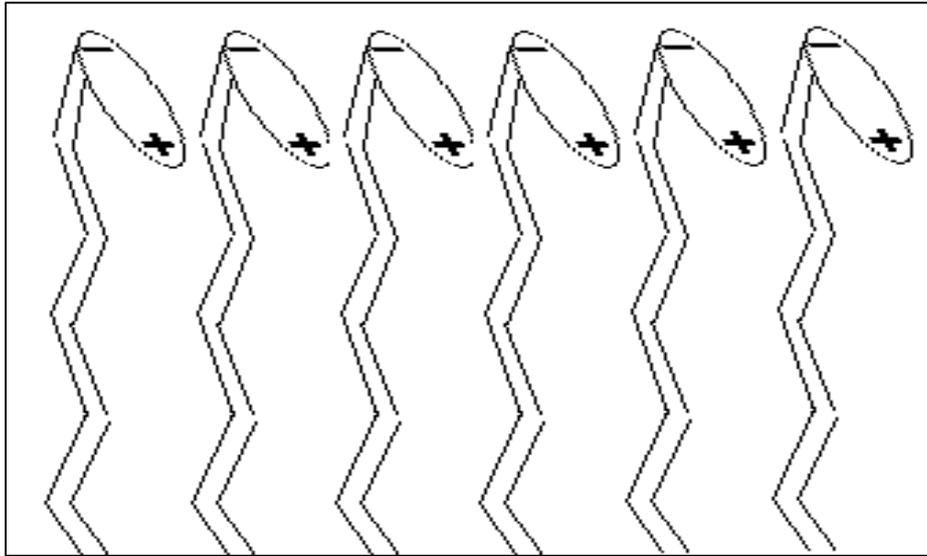
Figure 5.11 Schematic representation of the conformation of lipid head groups in the liposome (Hupfeld, 2009, Makino et al., 1991)

These results indicate that the nature of encapsulated material has significantly influenced liposome size. Size distribution of liposomes prepared in mucin (range of 100 to 250 µm) bigger than those prepared in deionized water (control) which range of 2 to 40 µm. This variation might be attributed to electrostatic interactions between the mucin molecules and the polar head group of phospholipids and the large size of mucin molecules compared with aqueous molecules. Accordingly, the association the molecule within the membrane bilayers provide bigger size of liposome.

Predictably, the microscopy images results of liposome morphology (**Figure 5.12**) indicate that the particles of LEM had lager size distribution (where in the region of 100 - 500 µm) than the control which range from 10 to 20 µm and the particles generally were spherical in shape. This proves particle sizes of liposomes are highly dependent on the nature of encapsulated substance. Hence, entrapped volume is a critical parameter that governs the morphology of liposomes.
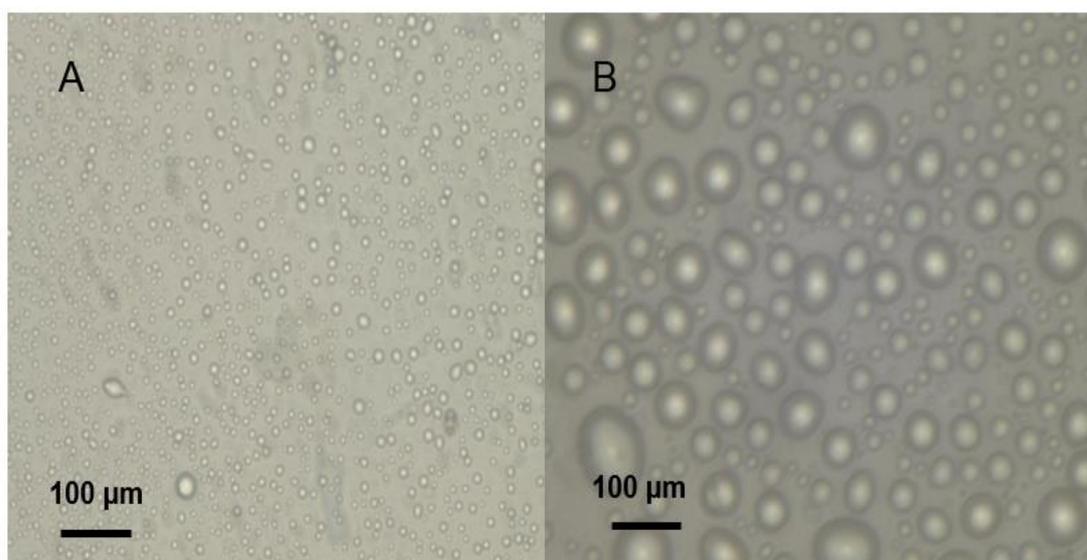
Figure 5.12 Light microscopy images of (A) liposomal vesicles prepared in DI water (as control) and (B) liposome encapsulating mucin (LEM)

5.6.2.3. Encapsulation efficiency:

The mucin entrapped in liposome was evaluated using carbohydrate assay (sulphuric acid UV method) and encapsulation efficiency of liposome was calculated based on equation (5.4).EE was defined as the ratio of total concentration of mucin added and the amount of mucin detected only in the supernatant. Up to 80 % of mucin was encapsulated which in agreement with (Xu *et al.*, 2012). Encapsulation efficiency in liposomes can be influenced by several factors including: method preparation, cholesterol percentage, lipid concentration and composition (Xu *et al.*, 2012) and the natural of encapsulated substance (Eloy *et al.*, 2014). Because LEM and control were prepared under identical conditions and based on morphology and size distribution results (**Figures 5.13 and 5.14**), it can be confirmed that the high EE is attributed to molecular interaction between the mucin and the lipid bilayer.

5.6.2.4. Nanosized liposomes study

Since size is one of the essential characteristics that govern the applications of liposomes in drug delivery systems, the produced liposomes were nanosized by sonication technology and in order to perform Nanoparticle Tracking Analysis to evaluate the mean diameter and size distribution of liposomes. The results reveal that for both cases the size distribution appeared within the range of nanoparticles. Again, the sonicated vesicles formed

with mucin (LEM) (**Figure 5. 13B**) were greater in size than those from on DI water (control) (**Figure 5. 13A**) which gave diameters of 175±26 nm and 84±9 nm respectively this can be attributed to the reasons that previously mentioned which is electrostatic interactions between the mucin molecules and the polar head group of phospholipids. Moreover, according to these results it can be predicted that the produced vesicles are multilamellar.
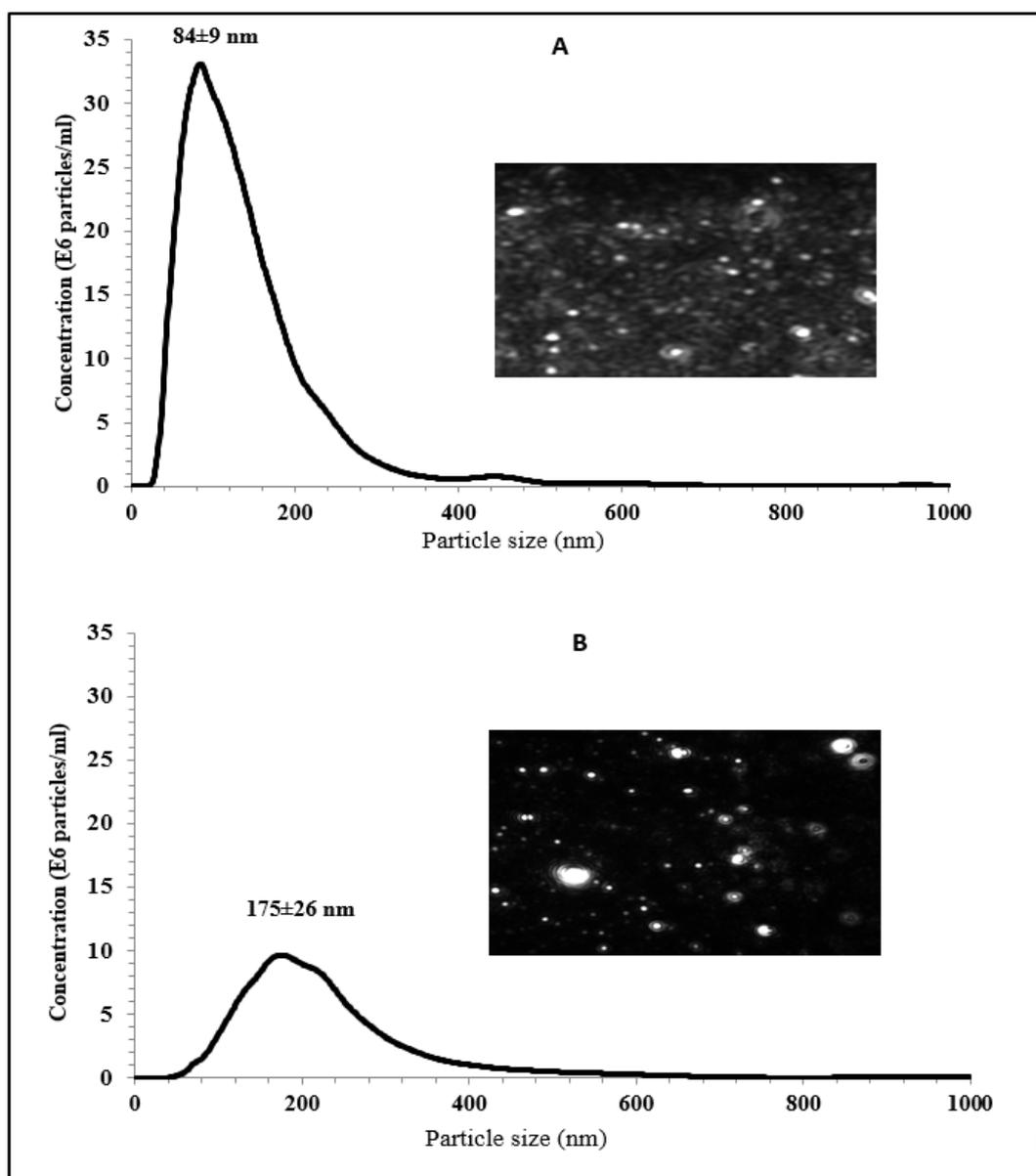
Figure 5.13 : Size-distribution of nanosized liposomes was measured by nanoparticle tracking analysis (NTA) for (A) control and (B) LEM. Insets show screen shots from NTA videos of the control and LEM

5.6.3. Analysis the indirect interaction between mucin (encapsulated in liposome) and polysaccharides based to rheological methods

The findings in **Figures 5.14, 5.15 and 5.16** indicate that in all cases there are no noticeable changes when compared with the control which generally exhibit a greater G". G" is going invariably increases up to 25 °C then gradually decreases until 60 °C where it became closer to G'. This means that upon increasing the temperature construction of liposome starts to be broken until it reaches ≈ 55 °C which is transition temperature for lecithin; at this temperature the phospholipid chains become free to move thereby the encapsulated mucin releases. Control sample of Cs shows viscoelastic characteristics this is because of the presence of lipid within supernatant which was difficult to separate due to its small size (as shown in **Figures 5.12 and 5.13**) therefore Cs can interact with the lipid and make complexes due electrostatic interactions and hydrogen bonding between them (Wydro *et al.*, 2007).

Collectively, there is no evidence indicating the encapsulated mucin can interact with polysaccharides. This is probably due to one of two reasons the concentration of mucin, which was encapsulated in liposome is not sufficient to create interactions with the polysaccharides, which could be detected rheologically or (which more likely) mucin molecules are electrostatically interacting with the phospholipid which is the main component of liposomal vesicles.
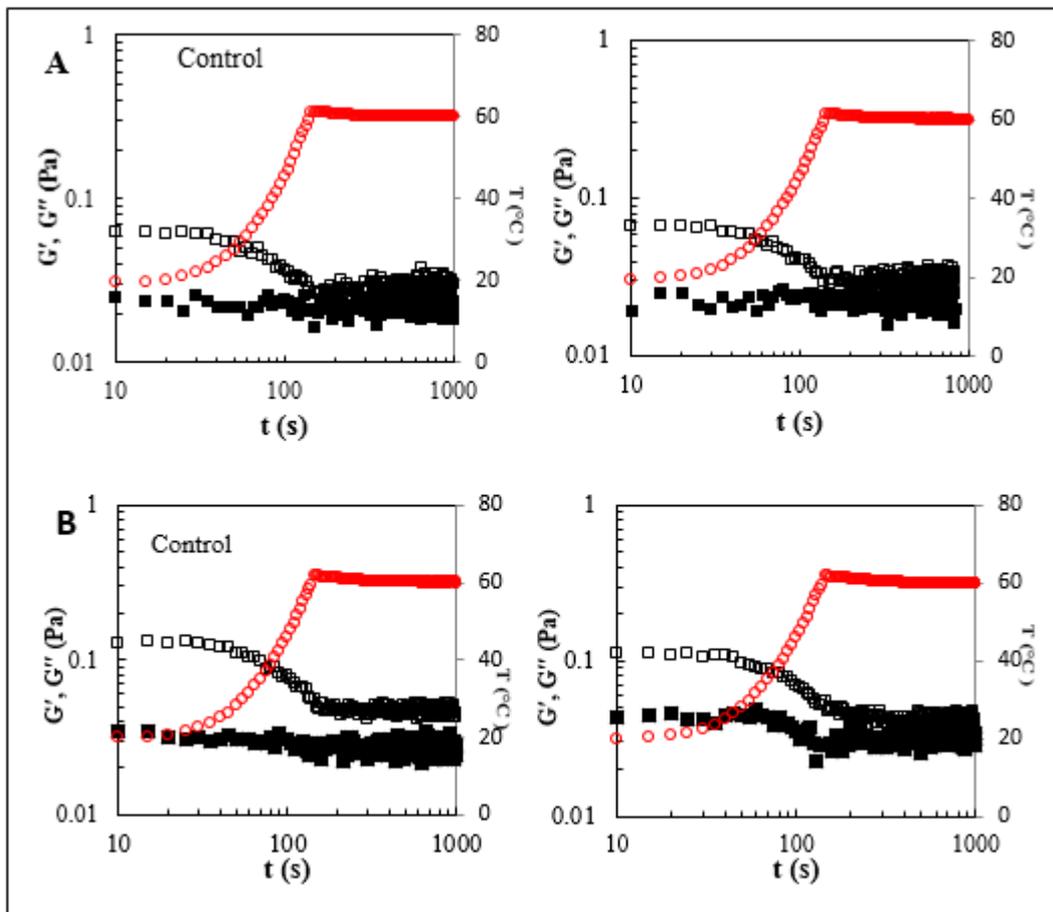
Figure 5.14 The effect of increasing temperature on rheological measurements for (A) HMP-LEM and (B) LMP-LEM. The mechanical spectrum at frequency 10 rad/s, strain 2 %, start temperature 20
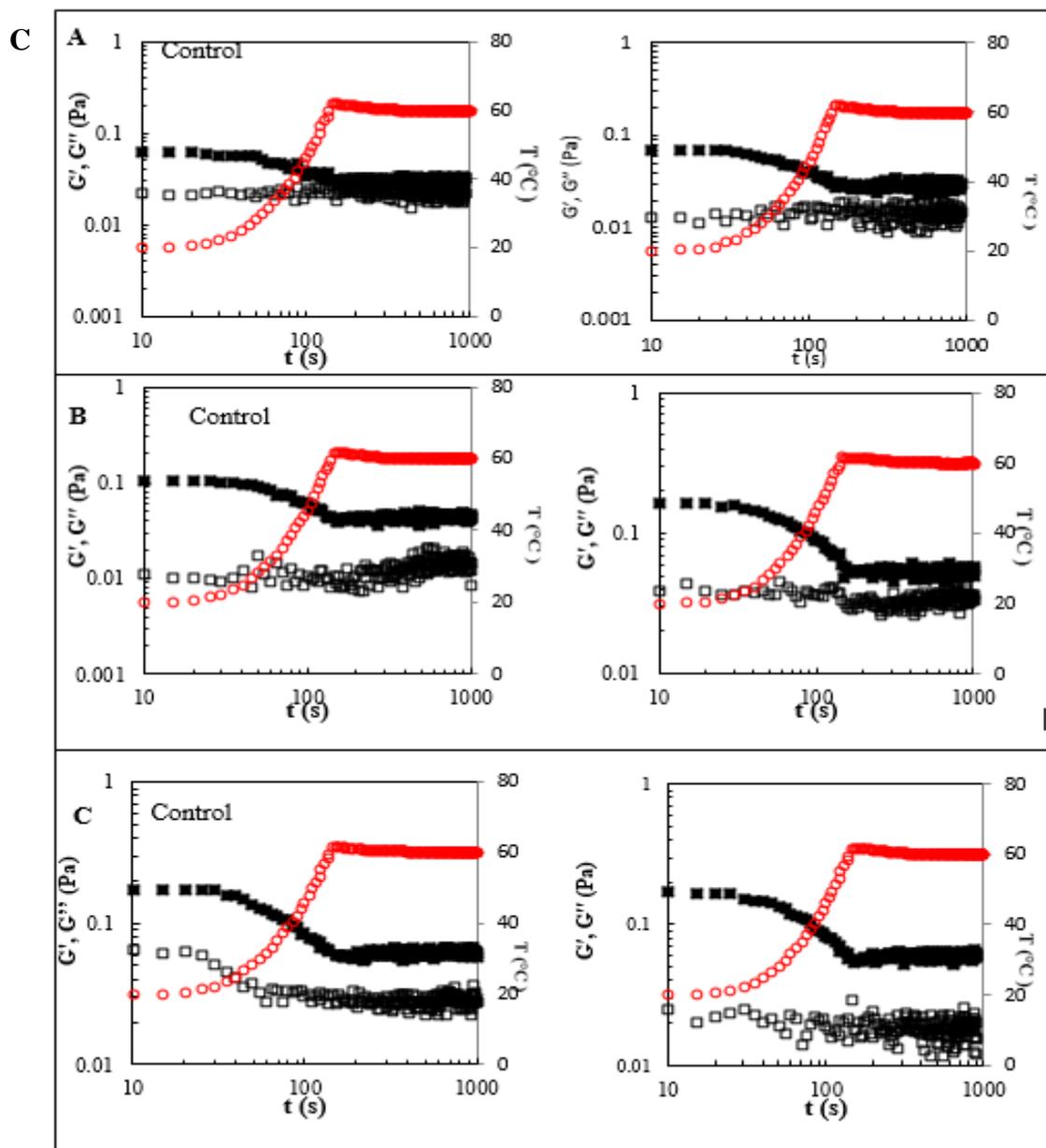
Figure 5.15 The effect of increasing temperature on rheological measurements for (A) HGA - LEM, (B) LGHVA - LEM and (C) LGLVA - LEM. The mechanical spectrum were measured at frequency 10 rad/s, strain 2 %, start temperature 20 °C and final temperature 60 °C showing variation of G' (open square), G" (filled square) *vs* time(s).
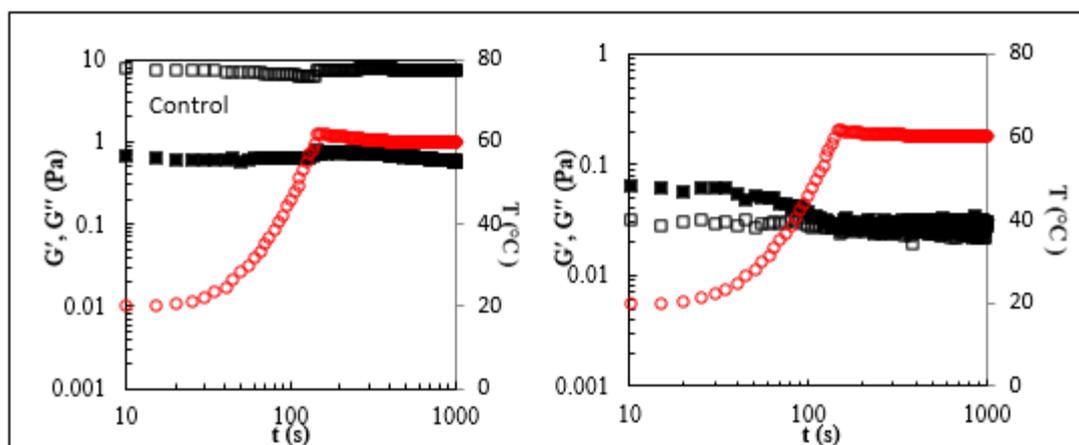
Figure 5.16 The effect of increasing temperature on rheological measurements for Cs - LEM at frequency 10 rad/s, strain 2 %, start temperature 20 °C and final temperature 60 °C showing variation of G' (open square), G" (filled square) against time (s).

5.7. Summary

In summary, in the current study the interaction between polysaccharides and pig gastric mucin were evaluated based on relative viscosity. We suggest that polysaccharide–mucin interactions are not only driven by electrostatic forces, but also the molecular weight, conformation and flexibility of the polymer also played significant roles. In addition, it was found that mixture of mucin and HGA alginate exhibited the greatest positive synergy whereas, the maximum positive synergy appeared less in cases of mucin-LGLVA and mucin-LGHVA. This mean the content G-block in alginate has an effect on interaction degree; increasing the G content of alginate led to increase viscosity. This attributed to that mucin-alginate system is derived by two forces hydrogen bonds (homopolymeric mucin-mucin interactions) and heteropolymeric mucin-alginate interactions (electrostatic repulsion). The presence of G-blocks in the system leads to increase mucin-alginate interactions by promoting mucin-mucin interactions. However, low G-block in the system may lead to the inhibition of homopolymeric mucin-mucin interactions caused by structural composition of M-block thereby the mixture displays less viscosity. Likewise, pectin shows positive synergy; LMP has large deviation from the additive line synergy, whereas HMP displays no appreciable deviation due to lack of negative charge due to the high degree of methylation. As the mucin-HGA system displayed exceptionally high viscosity, the viscoelastic properties of this system were extensively studied. the mechanical spectra of the mucin-HGA blends indicate that with the exception of

the system involving only HGA (0 % mucin) and 60 % mucin, all mixtures including mucin itself displayed typical 'weak gel' rheological behaviour as shown G˙ and G″ gradually increasing with increasing frequency. The bend produced from 90 % w/w mucin exhibits the greatest G' (~10 Pa).

Moreover 80 % of mucin was successfully encapsulated within phospholipids bilayer using liposomal encapsulation technology. The liposomal vesicles with encapsulated mucin display larger sizes than the control vesicles (prepared in DI water) this may be due to the electrostatic interaction between mucin molecules and phospholipid which is the main component the vesicles.

In addition, the potential of interaction between the encapsulated mucin and the polysaccharides was rheologically studied at temperature range 20 °C to 60 °C and there was no evidence indicating the encapsulated mucin interacted with polysaccharides. This is probably due to the concentration of mucin encapsulated in liposome being in sufficient to bind with the polysaccharide to a degree that can be detected rheologically and /or mucin molecules have already electrostatically interacted with the phospholipid which is the main component of liposomal vesicles.

Chapter 6

Characterisation, optimisation polyelectrolyte complexes containing chitosan and naturally occurring polyanions and Study its mucoadhesive properties as pharmaceutical excipient

6. CHARACTERISATION, OPTIMISATION POLYELECTROLYTE OF COMPLEXES CONTAINING CHITOSAN/ POLYANIONS AND THE STUDY OF ITS MUCOADHESIVE PROPERTIES AS PHARMACEUTICAL EXCIPIENT

6.1. Chapter review

6.1.1. Hydrogels

Hydrogels refer to the cross-linked polymeric network which is formed by the interaction of one or more monomers. Hydrogels are not soluble in water because of the chemical or physical links formed between the polymer chains but it has ability to swell and maintain a great fraction of water within its construction utilising the a high amount of hydrophilic groups or domains (Bhattarai *et al.*, 2010, Ahmed, 2015).

Hydrogels can be formed using natural or synthetic polymers. Cs based hydrogels have received a great deal of attention due to their safety, biocompatibility and degradability by human enzymes. Many beneficial characteristics of Cs, such as a net cationic charge, hydrophilicity and functional amino groups, have made Cs an appropriate polymer for the adequate delivery of many macromolecular compounds (Bhattarai *et al.*, 2010). Moreover, hydrogels have important features that make them excellent drug delivery vehicles such as mucoadhesive properties that improve drug residence time and tissue permeability. The mucoadhesive characteristic is attributed to inter-chain bonds between the hydrogel polymer's functional groups and the mucin which support site-specific binding to regions, such as gastrointestinal tract, respiratory system and reproductive system (Bhattarai *et al.*, 2010).

In recent times, the application of complexation between oppositely charged macromolecules (*e.g.* Cs with polyanion) has shown great potential in drug carrier systems such as a drug controlled release formulations (Polk *et al.*, 1994, Fernández-Hervás and Fell, 1998) due to the simplicity of the process and using physical crosslinking by electrostatic interaction can help to avoid possible toxicity of undesirable influences of chemical cross-linker reagents (Shu and Zhu, 2000).

The complexation mechanism of Cs and naturally occurring polyanion (*e.g.* alginate and pectin) have been extensively studied by (Mireles-DeWitt, 1994). Alginate is one of the

main polyanions that have made much interest for pharmaceutical applications either in drug transportation or in controlled drug release (Polk *et al.*, 1994, Liu *et al.*, 1997, Silva *et al.*, 2005).

Recently, Cs /alginate PEC application have been widely applied in pharmaceutical sector. for example, Cs -alginate nanoparticles have been prepared by the ionotropic gelation method to study the possibility to trap hydrophobic nifedipine within the nanoparticles and the drug release has been studied (Li *et al.*, 2008) also alginate coated with Cs have been used in controlled-release matrix tablet formulations for wound dressing (Straccia *et al.*, 2015). Moreover, many formulations of drug transporters prepared from the pectin- Cs polyelectrolyte complexes are used for controlled drug delivery vehicles. Among of these carriers a number of different structures can be prepared including: hydrogels, films, tablets, pellets and beads (Ghaffari *et al.*, 2007, Ghaffari *et al.*, 2006) specially in colonic drug deliveries (Bigucci *et al.*, 2009, Fernandez-Hervas and Fell, 1998, Li *et al.*, 2015, Macleod *et al.*, 1999, Bigucci *et al.*, 2008). The potential of using Cs /pectin PECs in colonic drug deliveries is due to the pH sensitive swelling ability with drug delivery behaviour based on enzyme degradation *e.g*. beta-glucosidase (Hamman, 2010).

6.1.2. Gastrointestinal Tract (GIT)

GIT is a muscular tube expanses from the oral cavity to the anus with a length of 6 m and are lined by mucous membrane that constantly secrete fresh mucus that give the membrane viscoelastic features which derived by mucin (see Chapter three). The GIT has multiple functions which include digesting and absorbing the nutrients and medication, in addition to excretion and protection (Aulton and Taylor, 2013). The average passage time of food through GIT is about 24 h. The four main anatomical areas of GIT are esophagus, stomach, small intestine and the large intestine or colon (**Figure 6.1**).

- **Oesophagus:** it is a thick muscular tube that links between oral cavity the stomach with length of 250 mm and diameter of 20 mm. The normal pH of oesophagus lumen is about 7 (Tutuian and Castell, 2006).
- **Stomach:** it temporarily stores the mixture of food, water and gastric juices then digests food and controls release into the small intestine by the pyloric sphincter (Reed and Wickham, 2009).The capacity of stomach is approximately 1.5 L (Aulton and Taylor, 2013). When food is swallowed the stomach secrets gastric juice comprise of

hydrochloric acid (HCl) (~ 0.1 M), pepsin, gastric lipase, gastrin and mucus (Selinus and Alloway, 2005). The pH of the stomach is acidic which generally range between 1 and 3 depending on the fasted or fed states of the person (Kong and Singh, 2008).

- **Small intestine (small bowel)**: is the part of GIT that locates between the stomach and the large intestine where the most of nutrients and minerals are absorbed. In this part the pancreas, liver secrete digestive juices which normally make the pH of are range from 6 to 7.4 (Fallingborg, 1999). The length of small intestine can be as long as 730 cm which divided to three distinct regions: the duodenum, jejunum, and ileum (Reed and Wickham, 2009).

- **Large intestine (large bowel)**: is the last part of GIT with length is range from 122 to 152 cm (Reed and Wickham, 2009) and pH between pH 6 and pH 6.5 (Fallingborg, 1999). Large intestine is made of the cecum, appendix, colon, rectum, and anal canal. The main function of large intestine absorbing water and any remaining nutrients and converting the waste from liquid state into stool state (Reed and Wickham, 2009).
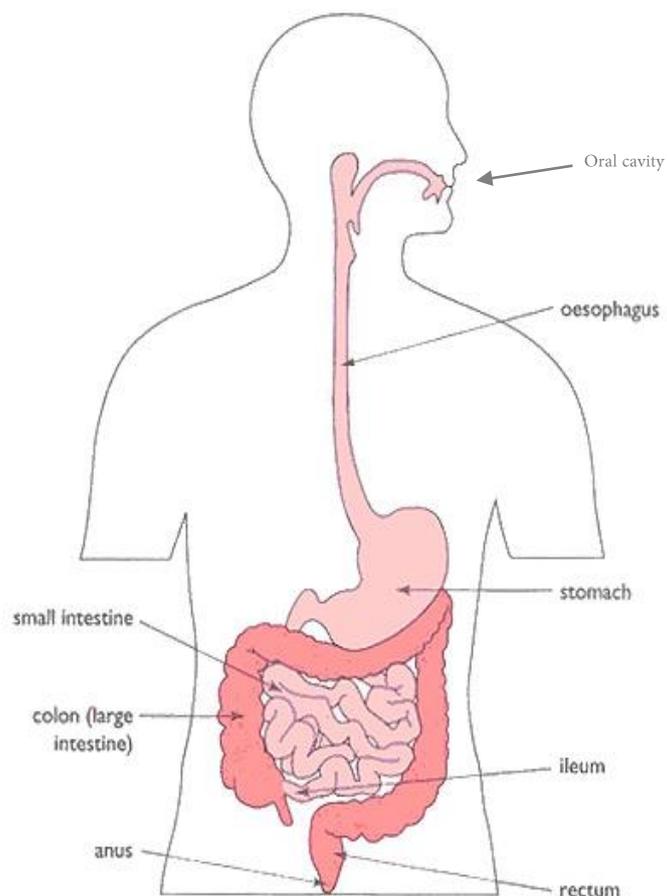
Figure 6.1 Diagram of the human GI tract
(Marieb and Hoehn, 2007)

6.1.3. Ibuprofen

Ibuprofen belongs to the nonsteroidal anti-inflammatory drugs (NSAIDs) and used to treat pain, fever, and inflammation. Chemically, Ibuprofen is (RS)-2-(4-isobutylphenyl) propionic acid with structural formula is $C_{13}H_{18}O_2$ (Rainsford, 2003, Potthast *et al.*, 2005) (**Figure 6.2**). The initial introduction of ibuprofen in the United Kingdom was in 1969 and, in the 1970s it became widely available as a prescription only medication in place of aspirin (Rainsford, 2009, Rainsford, 2003).
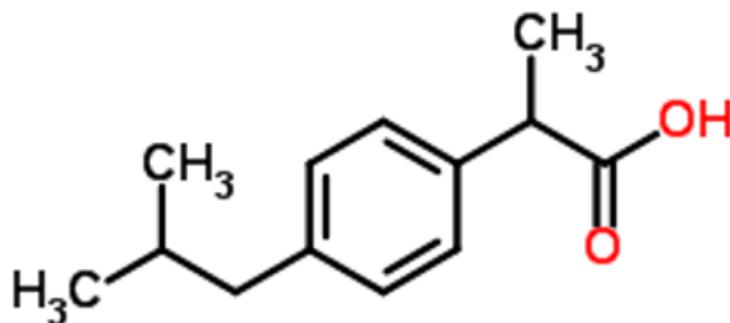
Figure 6.2 Structure of ibuprofen
(Adapted from Rainsford, 2003)

Ibuprofen is white crystalline powder, with a melting point about 74 °C and it dissolves easily in organic solvents such as ethanol and acetone (Potthast *et al.*, 2005). The solubility of ibuprofen increases with increasing pH, the drug readily soluble at alkaline pH and its minimum solubility is at pH 2.0 (Rainsford, 2015, Potthast *et al.*, 2005). Ibuprofen is generally marketed as liquid formulations (*e.g.* Calprofen) or as tablets (Nurofen) with different potencies. In this study ibuprofen is used as a model drug in studying drug release of the formulation due to its hydrophobic properties.

In this chapter, Cs -alginate (including HGA and LGA) and Cs -pectin (including HMP and LMP) hydrogel complexes were prepared using the ionotropic gelation method. Various ratios of Cs and polyanions were used in order to determine the optimum ratio to be used in formulations. The hydrogel samples that formed at the optimum ratio were studied by determining zeta potential, particles size, water uptake, morphology (for both the freeze dried hydrogels and homogenous suspension), gel strength and mucoadhesion. Finally, ibuprofen was encapsulated by the Cs -polyanion hydrogel complexes and the encapsulation efficiency of the formulations was assessed then the drug release from the formulations was evaluated *in vitro* over the time. According to the obtained findings comparison between the two types of pectin (HMP &LMP) and alginate (HGA& LGA) were made to see how the polyanion conformation influences their behaviour in hydrogel formation and drug release.

6.2. Materials

Ibuprofen powder (Ibuprofen 38) was obtained from BASF (Germany), Phosphate buffer saline (PBS) was obtained from Fisher Scientific (Loughborough, UK). Acetonitrile were obtained from Sigma–Aldrich (Gillingham, UK). Porcine mucosal tissue (oesophageal tissue) was kindly donated from a local abattoir. In addition, acetate buffer, Cs, HMP, LMP, HGA and LGA as shown in details in Chapter two, Section 2.2.

6.3. Optimisation polyelectrolyte complexes containing chitosan and naturally occurring polyanions

6.3.1. Methods

6.3.1.1. Preparation PEC of chitosan/ anion at different ratios

Cs, LMP, HMP, LGA and HGA (2 mg / mL of polymer) were separately dissolved in an acetate buffer (0.05 M, 4.3 pH). 5, 15, 25, 35 and 45 mL of Cs solution were then added to 45, 35, 25, 15 and 5 mL of pectin solutions respectively in a conical flask (total volume 50 mL) under stirring at room temperature and then allowed to stand for one hour, thus obtaining different Cs /pectin volume ratios (1:9, 3:7, 1:1, 7:3 and 9:1).due to the fact that charge density of the reactants is one of the main parameters on the PEC formation, the charge ratios between Cs and the polyanions were calculated from molar ratios based on net charge density on the molecular chain as indicated in (Hugerth *et al.*, 1997, de Jong and van de Velde, 2007, Siew *et al.*, 2005). The precipitate was separated by centrifugation (centrifuge 5702) at 4400 rpm for 20 min. The supernatant of each flask was filtered twice under vacuum with a Buchner funnel through filter paper (Whatman No.1) to ensure complete removal of all precipitates formed. The insoluble pellet complex (precipitate) was twice resuspended in deionized water and then centrifuged again. Finally, the washed complex was freeze-dried by using freeze dryer (CHRIST ALPHA 2 - 4 LD plus) and weighed. The homogenous suspensions were obtained by homogenising precipitate and supernatant for 7 minutes.

6.3.1.2. Determination the specific viscosities for supernatant

The specific viscosities of the supernatant solutions were determined from the mean flow times determined by capillary viscometer (Rheotek, Burnham-on-Crouch, UK) at 25 ±

0.1 ℃. Measurements were made at the different concentrations and the Equation 2.6 in Chapter 2 was applied.

6.3.1.3. Determination zeta potential, ζ

Zeta potential of the supernatant solutions and the homogeneous suspensions was determined using Malvern Zetasizer NANO-Z (Malvern Instruments Limited, Malvern, UK). Measurements were performed by using a folded capillary cell at 25.0 ± 0.1 °C. Each data value is an average of three measurements.

6.3.1.4. FTIR analysis of chitosan/pectin at different ionic strengths

The freeze dried PEC samples were performed to FTIR (Thermo electron corporation) in the frequency range of $\nu = 400 - 4000$ cm^{-1}.

6.3.1.5. P-XRD study

The freeze dried PEC samples were performed to P-XRD to study crystallinity using Bruker AXS diffractometer (D2 phasher). The data was recorded at 2θ range of 5º to 100° at a scanning rate of 4º/min.

6.3.1.6. Yield (%) of PECs

The freeze dried PEC samples were weighed on an analytical balance scale at room temperature. The percentage yield was calculated from the weight of dried PEC (W_1) and the initial weigh of the dry starting materials (W_2) as the following formula (Eq.6.1) (Fanun, 2010):

$$Yield\ (\%) = \frac{W_1}{W_2} \times 100 \qquad (6.1)$$

6.3.2. Results and discussions

6.3.2.1. Structure analysis

6.3.2.1.1. FTIR evaluation

FTIR is one of the important techniques that used for studying the structural arrangement of interacted polymers by comparison with the starting materials. Cs -polyanions PECs (Cs:HGA, Cs:LGA, Cs:HMP and Cs:HMP) were characterized through FTIR spectroscopy. By comparing the spectrum of Cs -polyanions complex (**Figures 6.3, 6.4, 6.5 and 6.6**) with the spectra of starting polysaccharides (**Figure 4.1 in Chapter 4**) it is clear that there are a new intense peak was observed at 1613 cm^{-1} in case of Cs – polyanions hydrogels which corresponding to the superposition of the bands assigned to the carboxyl group of polyanion and the amine group of Cs which are consistent with previous studies (Bigucci *et al.*, 2009) (Venkatesan *et al.*, 2014). This confirms the electrostatic interaction between the Cs and polyanions had successfully occurred.
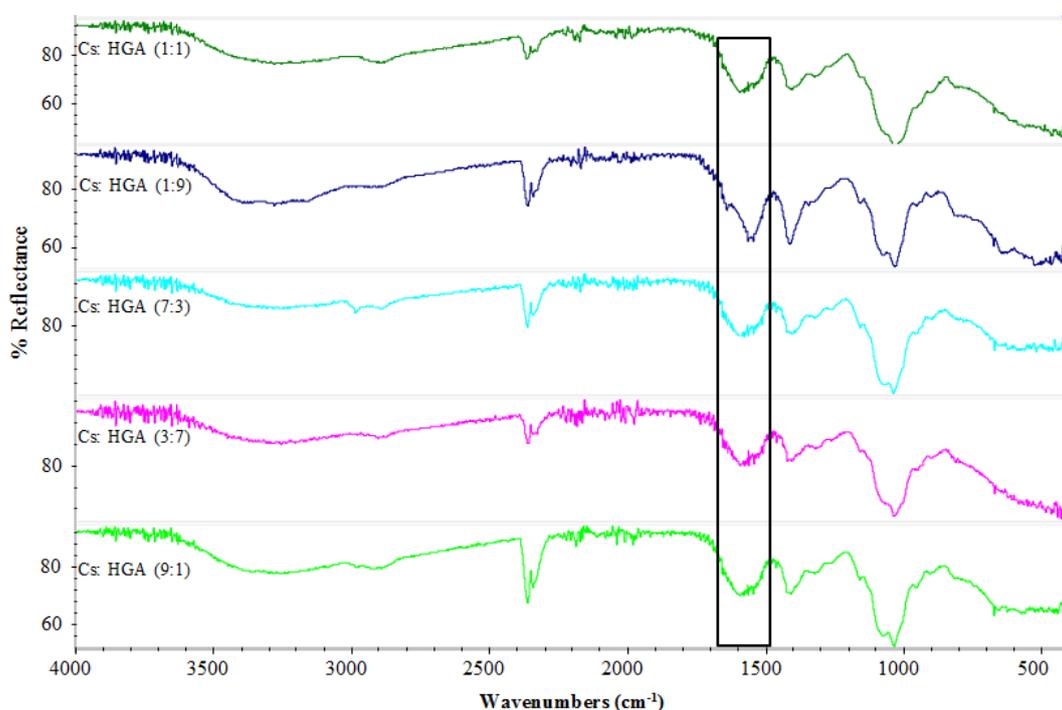
Figure 6.3 Fourier transform infrared spectrum of Cs-HGA hydrogels at various ratios at 25 ºC
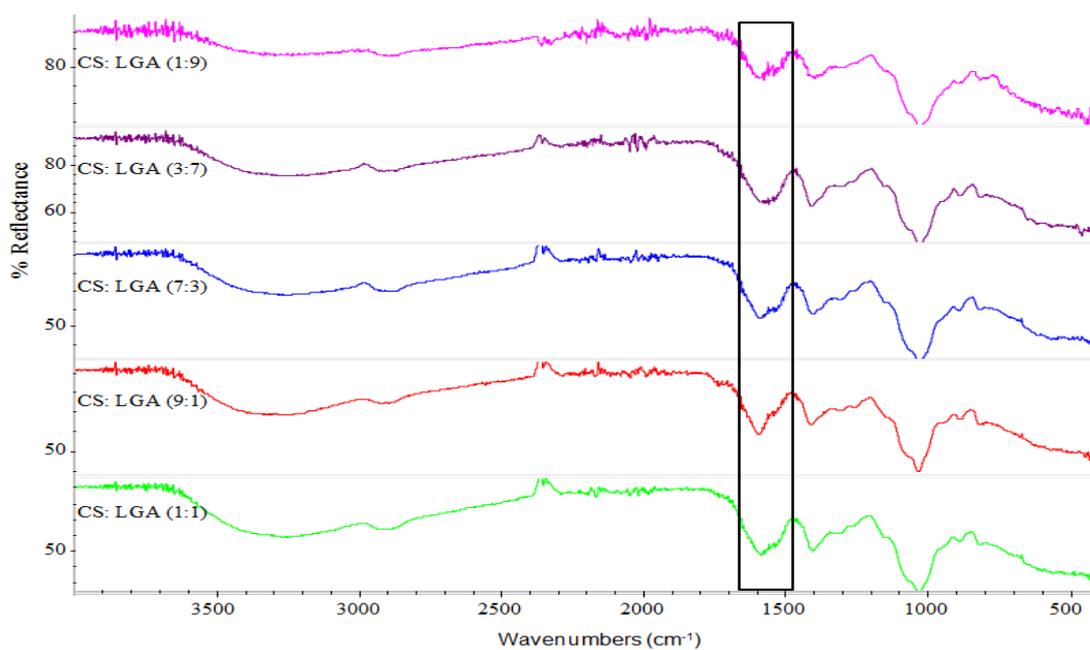
Figure 6.4 Fourier transform infrared spectrum of Cs-LGA hydrogels at various ratios at 25 ℃
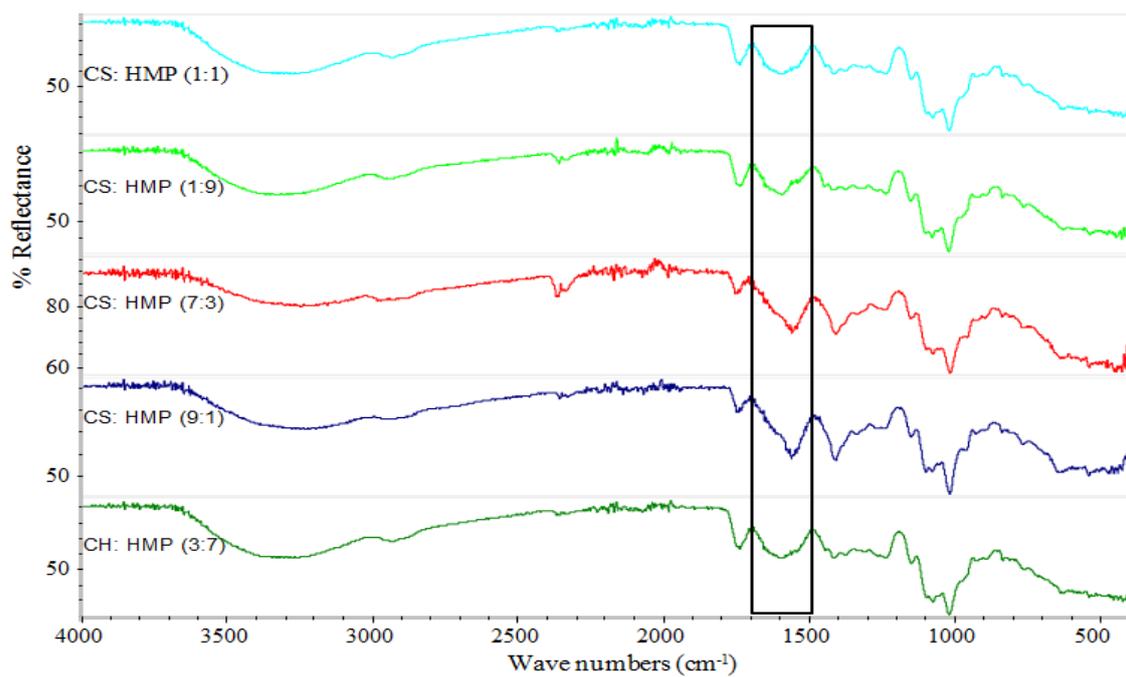
Figure 6.5 Fourier transform infrared spectrum of Cs-HMP hydrogels at various ratios at 25 ℃
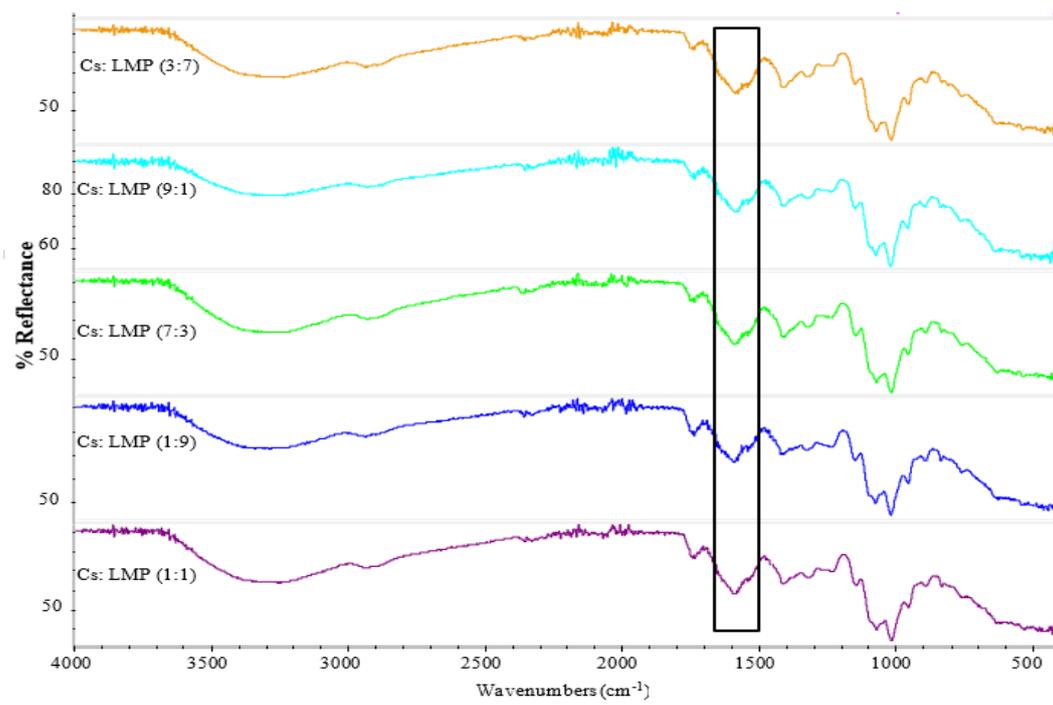
Figure 6.6 Fourier transform infrared spectrum of Cs-LMP hydrogels at various ratios at 25 ℃

6.3.2.1.2. P-XRD analysis

Figure 6.7 demonstrates the Powder XRD patterns of Cs -polyanion hydrogels at different ratios; (A) Cs:HGA,(B) Cs:LGA, (C) Cs:HMP and (D) Cs:LMP. The results indicated that absence of the sharp diffraction peaks comparing with the starting materials which are clarified in Chapter 4 in Section 4.4.1.2. The amorphous nature confirms the interaction between amino groups of Cs and carboxyl group of the polyanions that destroy the crystalline structure of starting materials (Meng *et al.*, 2010).
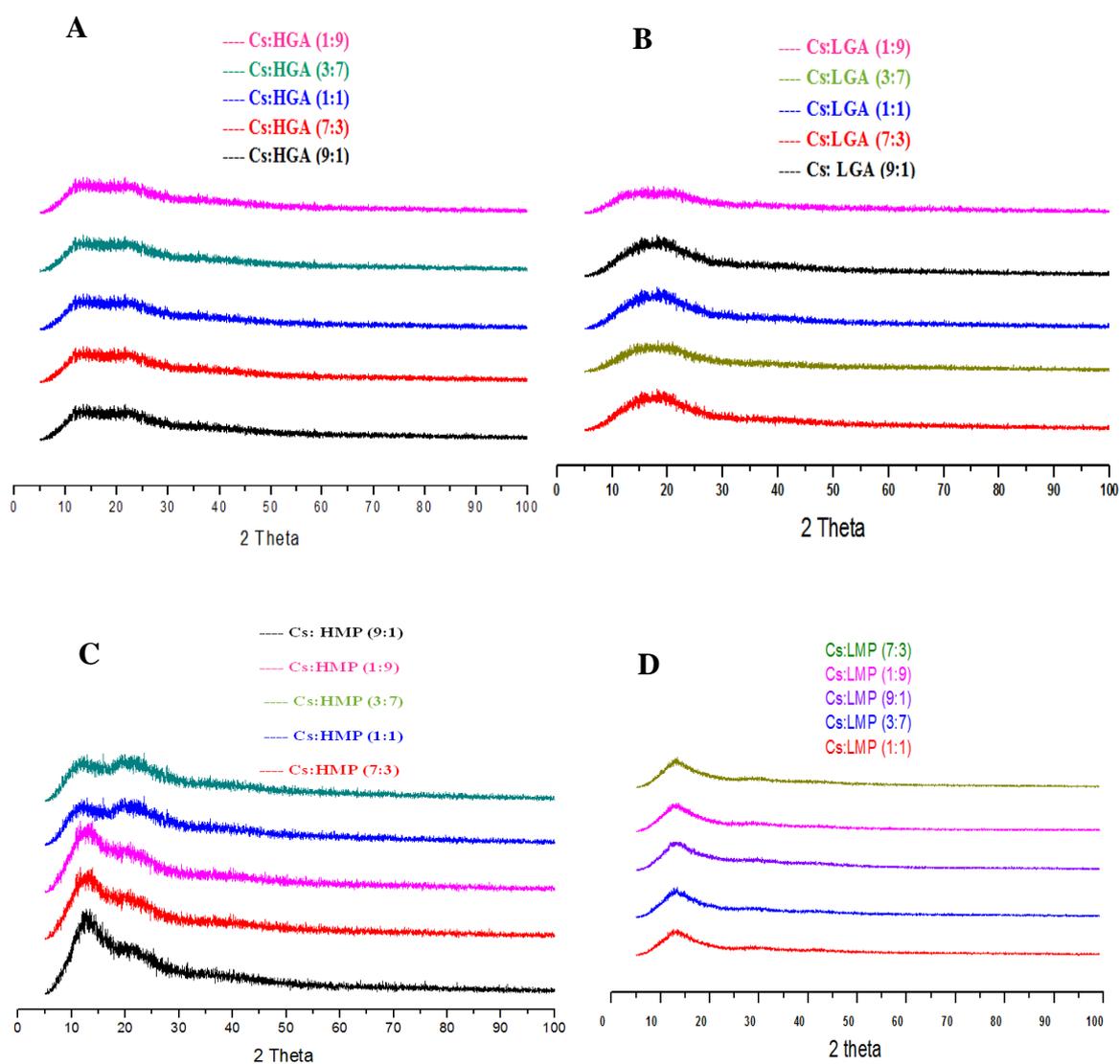
Figure 6.7 PXRD patterns of Cs: HGA (A), Cs:LGA (B), Cs:HMP (C) and Cs:LMP (D) at 25 °C

6.3.2.2. Influence of charge ratio on zeta potential yield of chitosan/polyanions complex formation

In **Figure 6.8** the zeta potential of supernatant was investigated and it was observed that at less than 35 % Cs content the zeta potential of the mixture was negative in all cases and with increasing Cs content the mixture became less negative until the critical ratio was reached which is higher than 40 % for HMP and less than this ratio for the other poly anions. At these points (isoelectric point), where the zeta potential value was nearly zero, equality occurs between the opposed charges and the supernatant contain less amount of the polysaccharides (more material is precipitated).

Moreover, the effect of charge ratio on the yield of Cs -polyanions hydrogel (that obtained after centrifuging) was presented in **Figure 6.9**. The maximum yield of insoluble Cs/pectins complex was formed at 35, 55 % for LMP and HMP respectively while in case of alginates (HGA and LGA) the highest yield was formed at 45 % Cs. This difference is likely to be attributed to polyanion conformation and charge net distributed on the molecular chains because the ionic interactions between COO^- and NH_3^+ is the main driving force behind complex formation; in the case of alginate all units of the chain are fully negatively charged so each negatively charged unit reacts with positively charged unit whereas in pectins due to methylation, the quantity of pectin needed to interact with Cs is greater. Moreover, these results can be observed in the measurements of specific viscosity of the supernatants; **Figure 6.10** indicates that the lowest η_{sp} is at 35 % Cs for LMP, at 55% for HMP and at 45 % Cs for alginates (LGA & HGA) which is ~ zero. This means in these ratios the vast majority of the polysaccharides reacted *i.e.* precipitated as a PEC. For this reason, 1:1 of Cs -alginates and 3:7 of Cs -pectins were chosen as optimum ratios and extensively characterized and the drug release from these formulations was evaluated over the time.
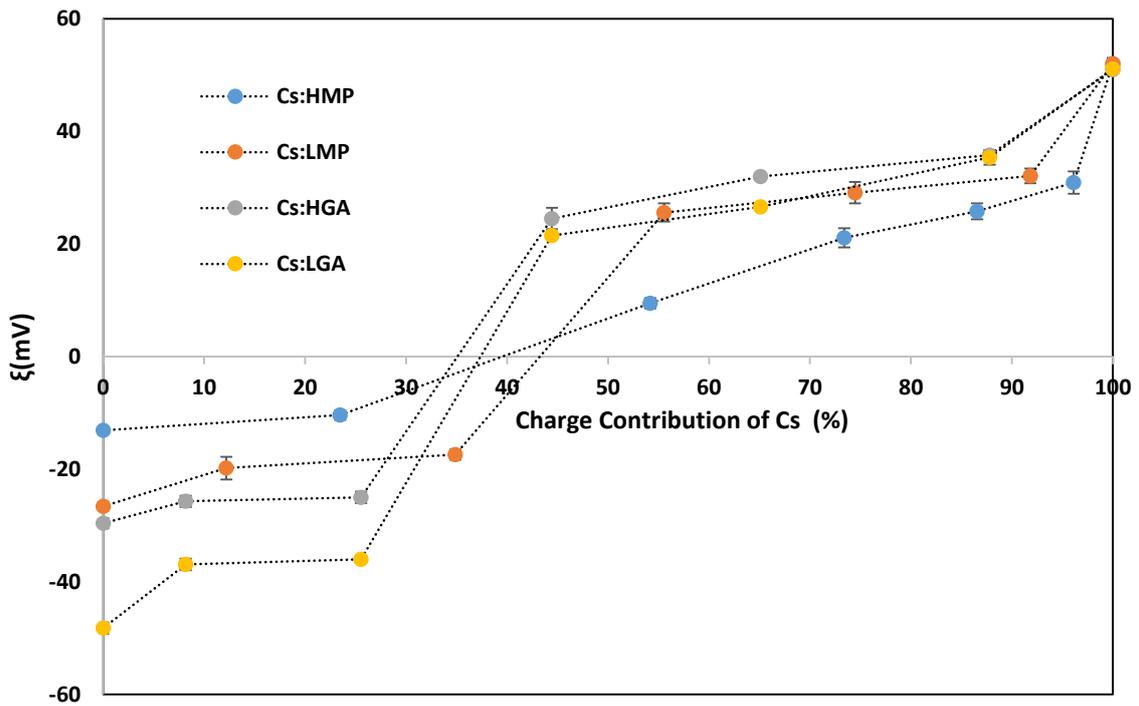
Figure 6.8 Zeta potential of the supernatant of Cs /polyanion (HMP-LMP, HGA and LGA) complexes at various charge ratios at $25\pm0.1\,^{\circ}C$ (mean ± SD, n = 3)
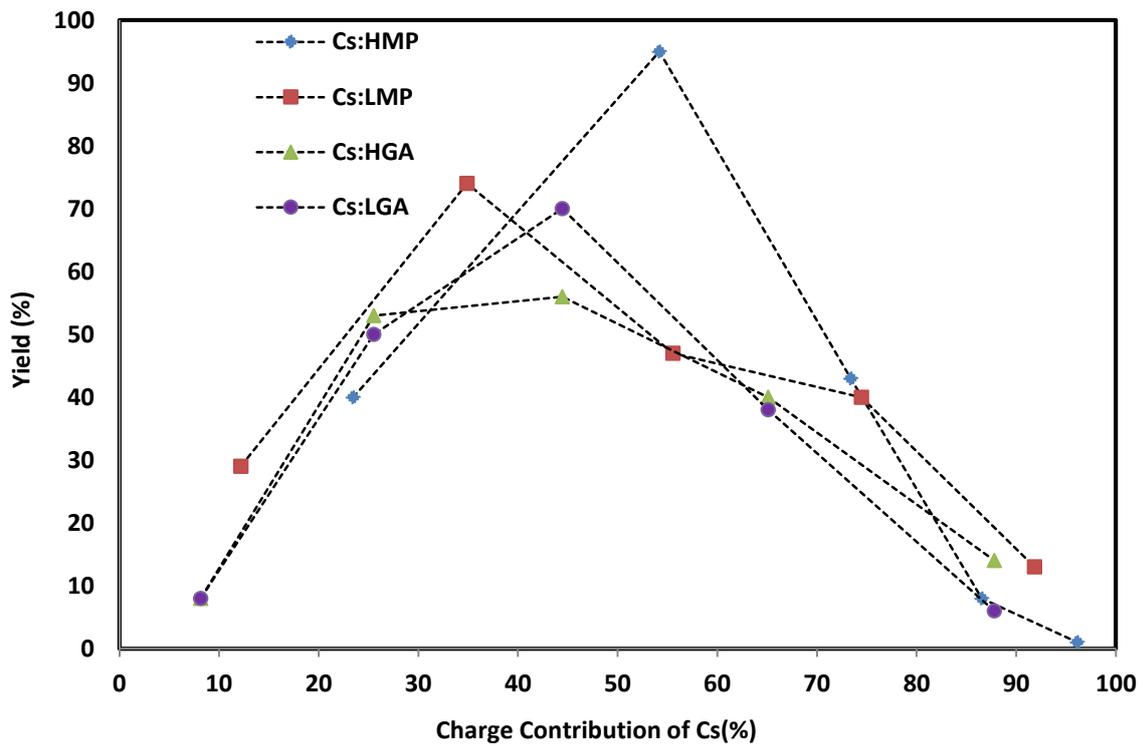
Figure 6.9 : Effect of mixing ratio (charge ratio) on yields percentage of insoluble Cs /polyanion PECs
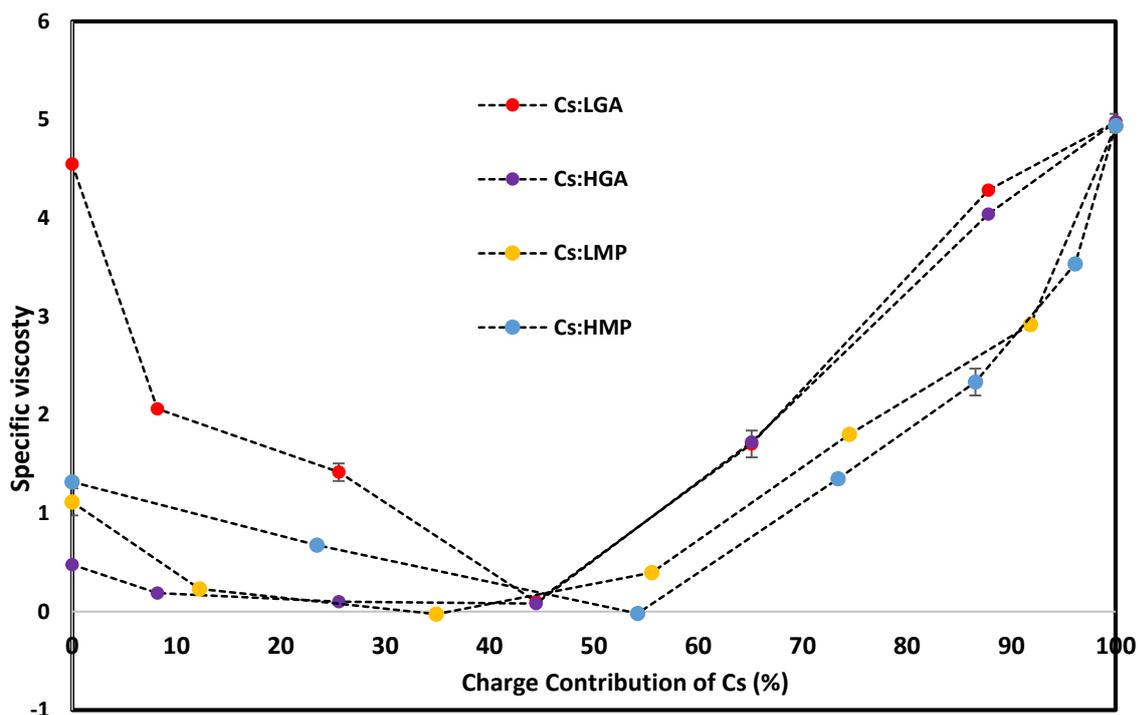
Figure 6.10 Specific viscosity of the supernatant of Cs /polyanion (HMP, LMP, HGA and LGA) complexes at various charge ratio at 25±0.1 ºC (mean ± SD, n = 3)

6.4. Characterisation of pellets

Herein, the hydrogels that prepared in section 6.2.1.1 (at the optimum ratios which are 3:7 for Cs -pectins (HMP and LMP) and 1:1 for Cs -alginates (HGA and LGA) were extensively studied.

6.4.1. Particle size

The particle size distribution of the powder was measured by a Mie scattering using a Malvern Mastersizer 2000 (Malvern Instruments Ltd., Malvern, UK). The dispersion concentration was around 0.1 g/L. The suspension was prepared by dispersing the powder in distilled water. Refractive index of particles and dispersion medium (DI water) was set to 1.8 and 1.33 respectively.

6.4.2. Zeta potential

Zeta potential of 0.5 % w/v of the pellet was determined using Malvern Zetasizer NANO-Z (Malvern Instruments Limited, Malvern, UK). Measurements were performed by using a folded capillary cell at 25.0 ± 0.1 °C.

6.4.3. Microscopy method

Each sample was imaged using an optical microscope (KEYENCE VHX Digital Microscope RZ ×250×1500 real zoom lens, Milton Keynes, UK). Samples were prepared for imaging by applying a drop of the sample on microscope slide and covered by slip slide then scanned under the microscope.

6.4.4. Scanning electron microscopy (SEM)

The samples of freeze dried hydrogels were mounted on a double-sided carbon tape then coated with a thin layer of palladium–gold alloy. The morphological variations of samples were characterised using scanning electron microscopy (SEM) using a JEOL JSM 6060LV (Oxford instruments, model 7582). Images were taken by operating an electron beam accelerating voltage of 20 kV.

6.4.5. Frequency sweep measurement

Frequency sweeps for the prepared the hydrogels were carried out over a frequency range of 0.1 to 10 rad/s strain at 25 °C. The moduli G′ and G″ of the hydrogel were determined within the linear viscoelastic regime at 2 % and plotted as a function of increasing frequency.

6.4.6. Adhesion measurements

The adhesion properties of the PECs were measured using mucoadhesion profile on the rheometer fitted with a CP4/40 SR 2567SS upper plate and PLS 6152174 SS lower plate at gap 0.1mm and 25 °C. The experiment involve putting 1 g of the sample in the centre of the lower plate (with making sure no pressure was applied) then the gap was moved from 0.1 mm to 10 mm and the normal force was recorded as function of time. Negative peaks and negative areas were calculated by Origin v 6.1 (Origin Lab Corp., Northampton, USA).

6.4.7. Water uptake

Specific amounts of each of freeze-dried hydrogels were weighed and placed into a glass vial containing 10 mL of DI water and maintained at 25 ºC in a water bath using a thermostat for 20 hours. Sample were then rapidly blotted to remove free water from the surface using filter paper and weighed using an analytical balance (accuracy = 0.0002 g). The water uptake (WU) was calculated as the following formula (Cooper *et al.*, 2005):

$$WU\ (\%) = ((W_s - W_d)/W_d) \times 100 \qquad (6.2)$$

Where W_s is swollen weight of hydrogel, W_d is dry weight of hydrogel.

6.4.8. *In vitro* release studies for ibuprofen from PEC

6.4.8.1. Preparation polyelectrolyte complex Cs formulation

- **Cs /alginate formulations**

In these experiments ibuprofen was used as a model drug in drug release study. 10 mg of ibuprofen was mixed with 5 mL of Cs (2 mg/ml at acetate buffer 0.05 M, 4.3 pH) to get 2 mg/mL Cs and ibuprofen. 5 mL of each sample of alginates (2 mg/ml LGA or HGA at acetate buffer 0.05 M, 4.3 pH) was added to the 5 mL by drop wise (to get ratio of 1:1). The mixture stand about 1 h then centrifuged for 15 min at 4400 rpm. The precipitate (pellet) was gently washed by 10 mL phosphate buffer (8 pH, 50 mM) to remove the drug on the surface (*i.e.* not encapsulated). The washed pellet was re-suspended in 100 mL phosphate buffer and stirred for 20 h to make sure the drug was completely dissolved in the buffer. The suspension was centrifuged again for 15 min and the supernatant was analysed using a UV spectrophotometer to measure the absorbance at 254 nm to calculate the ibuprofen concentration. **Figure 6.11** elucidates the general procedure for the preparation of Cs hydrogels.

- **Cs /pectin formulations**

6 mg of ibuprofen was mixed with 3 mL of Cs (2 mg/mL at acetate buffer 0.05M, 4.3 pH) to get 2 mg/mL Cs and ibuprofen. 7 mL of each sample of pectins (LMP or HMP) was added the 3 mL by dropwise (to get ratio of Cs to pectins 3:7). The mixture stand about 1h then

centrifuged for 15 min at 4400 rpm. The precipitate (pellet) was gently washed by 10 mL phosphate buffer (8 pH, 50 mM) to remove the drug on the surface (not encapsulated). The washed palate was re-suspended in 100 mL phosphate buffer and shaken by stirrer for 20 h to make sure the drug is completely dissolved in the buffer. The suspension centrifuged again for 15 min then the supernatant was performed to UV spectrophotometer to measure the absorbance at 254 nm.
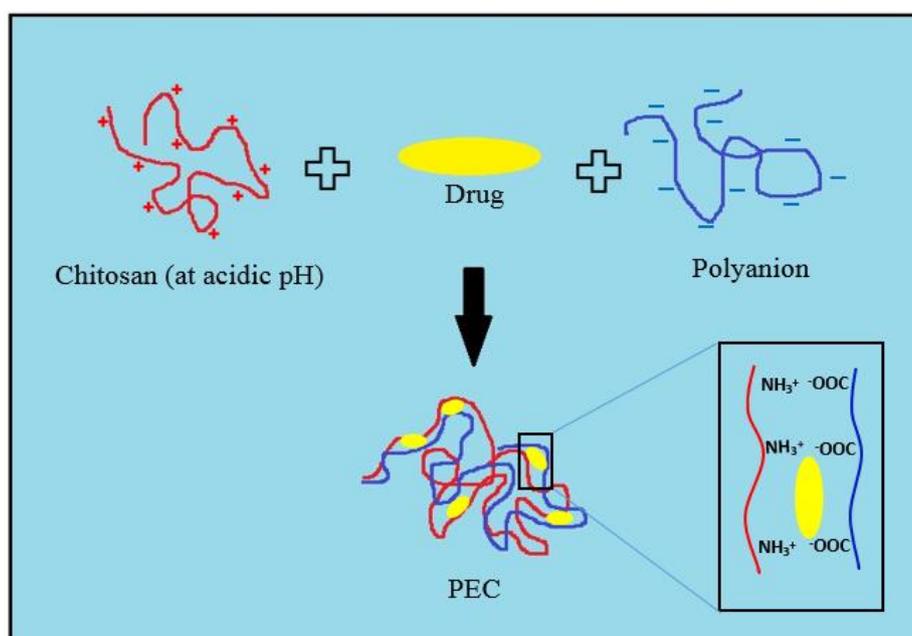
Figure 6.11 Scheme illustration for preparation of Cs - polyanion hydrogel

The formulation formed a cloudy dispersion at pH 4.3 where ibuprofen is poorly soluble and as the experiment was repeated with caffeine which was also unsuccessful due to the solubility of caffeine in acidic pH and therefore the all drug being found in the supernatant.

6.4.8.2. Determination EE of ibuprofen within PEC hydrogel by Ultraviolet (UV) spectroscopy

The concentration of ibuprofen released from the each sample was calculated from the corresponding calibration curve (**Figure 6.12**). EE of ibuprofen was calculated according to the following equation:

EE % = (Weight of ibuprofen entrapped in pellet /total weight of ibuprofen) × 100%   (6.3)
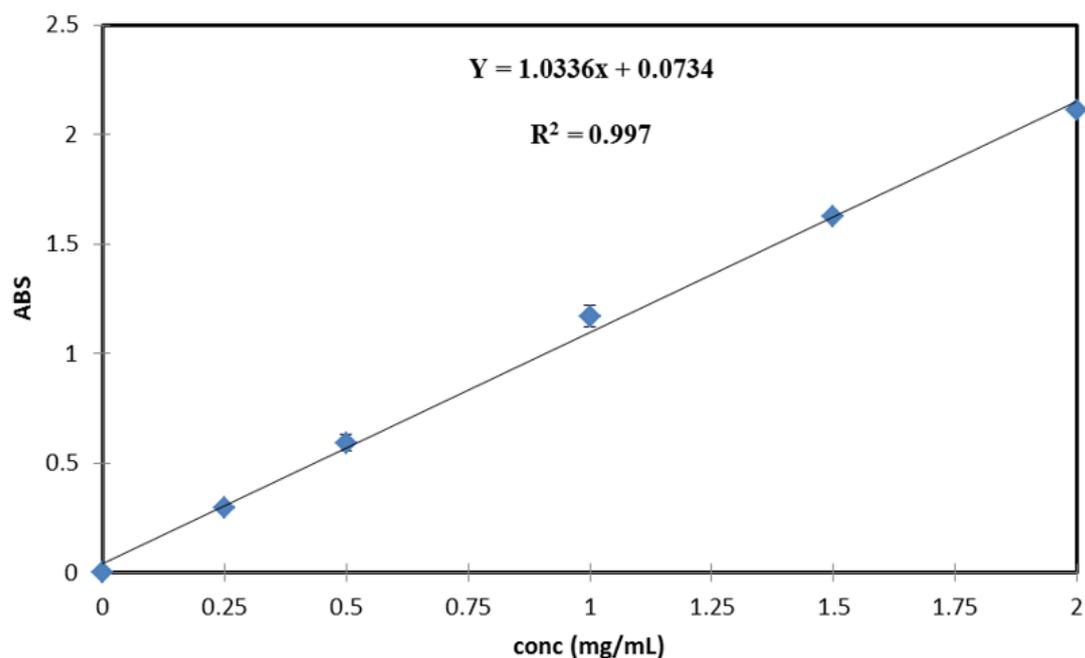
Figure 6.12 A typical calibration curve for ibuprofen prepared in phosphate buffer (8 pH, 50 mM) at concentrations ranging from 0.25 to 2 mg /mL measured at λ 254 nm. Values represent mean ± SD (n=3)

6.4.8.3. Preparation of mucosal membrane for retention studies

The internal tissue of porcine oesophagus was cut into 2×4 cm longitudinal sections after the outer muscle layers were removed and stored at -20 ℃ until ready for use. For retention time measurements, the drug retention time in simulated oesophageal conditions (pH 7.4, 37 ℃) was studied using a bespoke mucoadhesion apparatus as was showed in **Figure 6.13**. A section of defrosted mucosal tissue was securely placed on the apparatus without any prior washing and the ibuprofen-loaded formulations were placed. After that, PBS was perfused over the mucosal membrane at a rate of 1 mL/min. The PBS perfusate was collected at time points up to 60 min and ibuprofen content was measured using a RP-HPLC (as will be explained later in next). Drug retention on the surface was calculated using Eq. (6.4).

$$\frac{[C]-[CP]}{[C]} \times 100 \qquad\qquad (6.4)$$

where [C] is the concentration of ibuprofen that content in in loaded formulations and [CP] is the concentration of ibuprofen detected in the PBS perfusate.
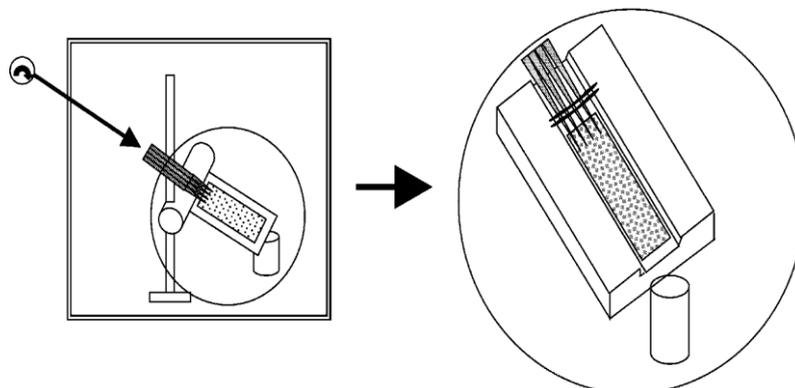
Figure 6.13 Schematic representation of the retention model apparatus
(Adapted from Batchelor et al., 2002)

6.4.8.4. Retention time measurements by HPLC method

Ibuprofen was performed to reverse phase high performance liquid chromatography technique (BECKMAN RP-HPLC) model 127 pump , UV/VIS 190 detector and 32KARAT Software ver.7.0 as the following the method (Alsirawan *et al.*, 2013). Briefly, 100 µL of the prepared samples were injected on to a C18 L1, pH resistant (4.6 mm $\times$250 nm: 5µm) column. The mobile phase consists of water adjusted to pH 2.5 with phosphoric acid and acetonitrile (40/60, v/v), with a flow rate of 1 mL/min. The ibuprofen was detected at a retention time of 6 min using a UV detector at a wavelength of 214 nm.
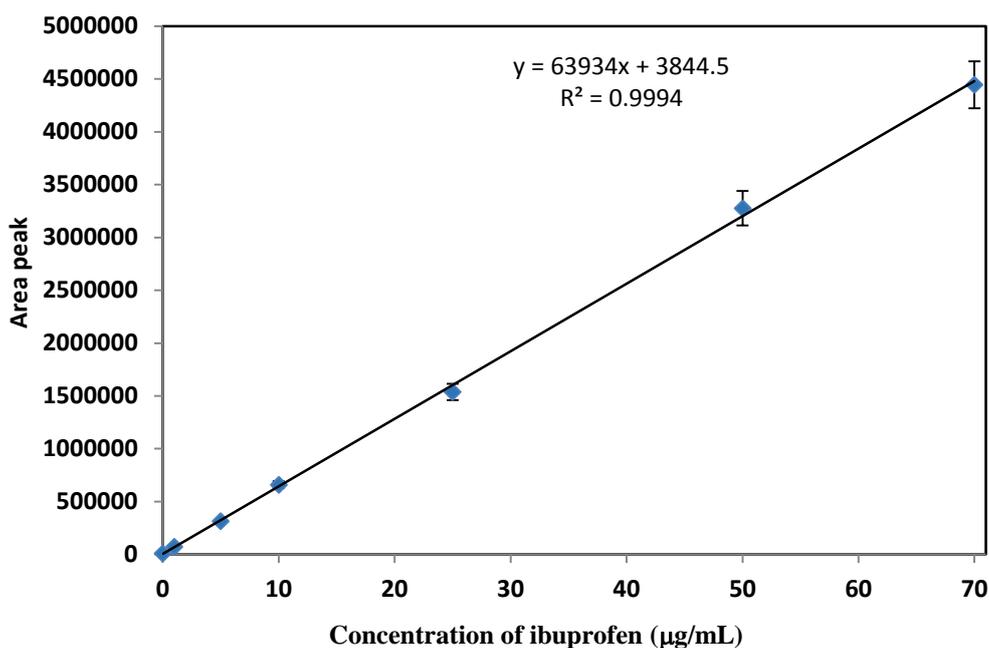
Figure 6.14 Calibration curve for ibuprofen measured at λ= 214nm using (HPLC). Values represent mean ± SD (n=3).

6.4.9. Results and discussion

6.4.9.1. Physiochemical analysis of the pellet

Zeta potential of the homogenous hydrogels was recorded and the findings (**Table 6.1**) were observed that the ζ of the pectins is negative; HMP is -8.6 ± 0.8 and LMP is -30.1 ± 0.6 while HGA and LGA showed positive charges; +2.0 ± 0.3 and +10.0 ± 1.0 respectively. This difference is likely due to degree of esterification in the case of pectin and to structural conformation for alginates; the variation in charge density distributing on the molecular chains of HMP and LMP has an influence on ζ of PECs.

Size distribution of the homogenous hydrogels was measure and as indicated in **Table 6.1** HGA showed the largest size followed by HMP, LMP and LGA. This may be due to the crosslinking density because particle size increases with decreased crosslink density and lower crosslink density (Peppas *et al.*, 2010) such as HGA and LMP demonstrate wider particle size distribution.

Moreover, the EE for all the formulations was evaluated which varies from 36 % to 56 % as presented in **Table 6.1**. The highest entrapment efficiency of exhibited LMP formulation (56.0 ± 0.9 %) followed by the two types of alginate formulations which show no notable difference; HGA = 51.0 ± 1.0 and LGA = 52.0 ± 1.3 while the formulation of HMP has a lower EE. This variation may be related to the strength of crosslinks between the polyelectrolytes (Li *et al.*, 2008); LMP is a tighter network and therefore has a high EE.

The water uptake (WU) ability of the hydrogels was studied by evaluated the swelling behaviour of the hydrogels in ultra-pure water. The findings of WU ability of the Cs: HGA, Cs:LGA, Cs: HMP and Cs:LMP were showed in **Table 6.1**. The results revealed that there was very little variation in the swelling behaviour among the samples, where HMP and LGA displayed the highest ability of WU (97.0 ± 0.7, 96.0 ± 1.4 %) followed by HGA and LMP (92.0 ± 1.0, 90.0 ± 0.5 %) respectively.

Table 6.1 Several characteristics of PECs that prepared includes: ζ, size distribution, water uptake (%) and ibuprofen content (%)

Cs: polyanion	ζ (mV)	Size distribution D[4,3]	(WU) (%)	EE (%)
Cs:HMP	- 8.64 ± 0.8	434 ± 12	97.0 ± 0.7	36.0 ± 0.4
Cs:LMP	- 30.1 ± 0.6	406 ± 44	90.0 ± 0.5	56.0 ± 0.9
Cs:HGA	+ 2.0 ± 0.3	563 ± 35	92.0 ± 1.0	51.0 ± 1.0
Cs:LGA	+10.0 ± 1.0	174 ± 19	96.0 ± 1.4	52.0 ± 1.3

6.4.9.2. Morphological analysis of the pellet

Homogenous hydrogel samples were observed using light microscopy. From **Figure 6.15**, it is evident that the particle sizes of the Cs hydrogels are highly dependent on the polyanions in the complexes. The pectin hydrogels (Cs:HMP & Cs:LMP) have particles in the region of 10 - 25 μm and were generally spherical in shape while in case of the Cs:HGA hydrogel the particles were much larger (≈100 μm) with irregular shape. Cs:LGA case show a high population of particles and the majority of the population in the region of 10 μm .this result is consistent with particles size measurements **Table 6.1**.
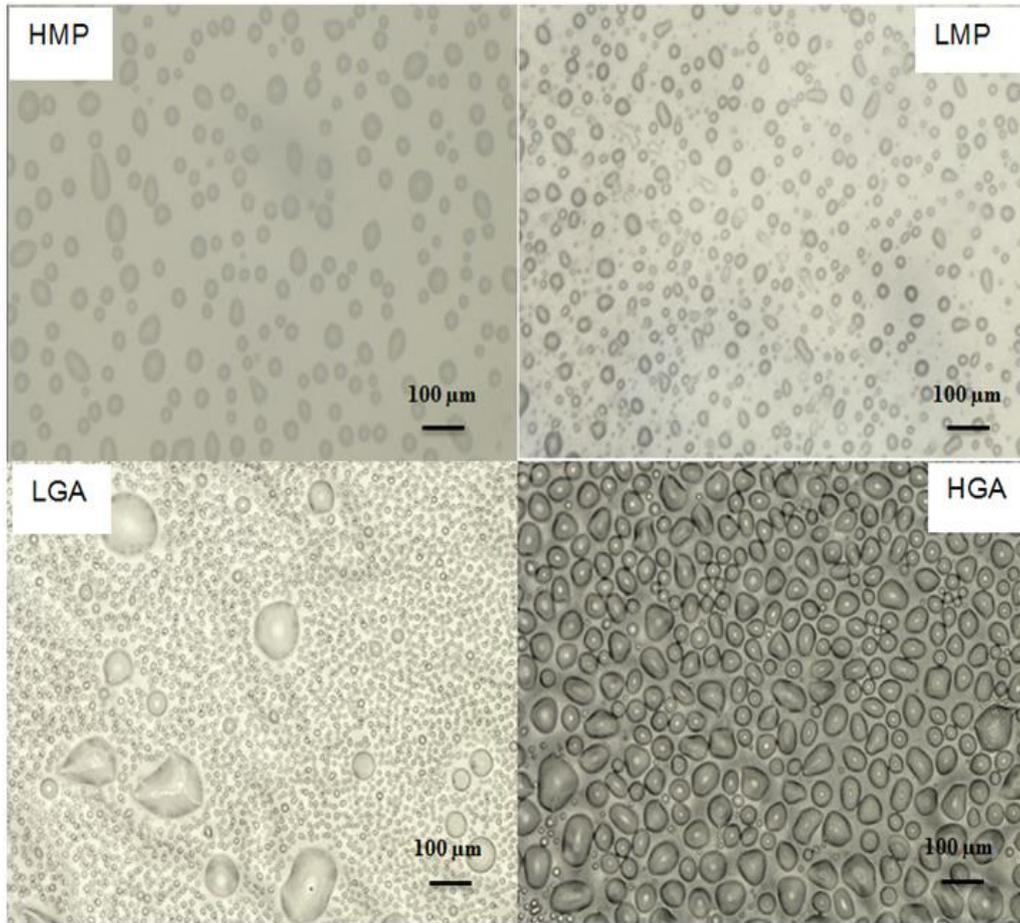
Figure 6.15 The optical microscopic images of PEC of Cs with LMP, HMP, LGA and HGA at 25 ºC

The surface morphology of freeze dried Cs -hydrogels was examined using scanning electron microscopy analysis (**Figure 6.16**). The results indicated that all the samples were found to be highly porous with different pore sizes and distributions; LGA and LMP hydrogels display a smooth and fluffy surface while appearance is rough for HGA hydrogel and highly fibrous HMP hydrogel.
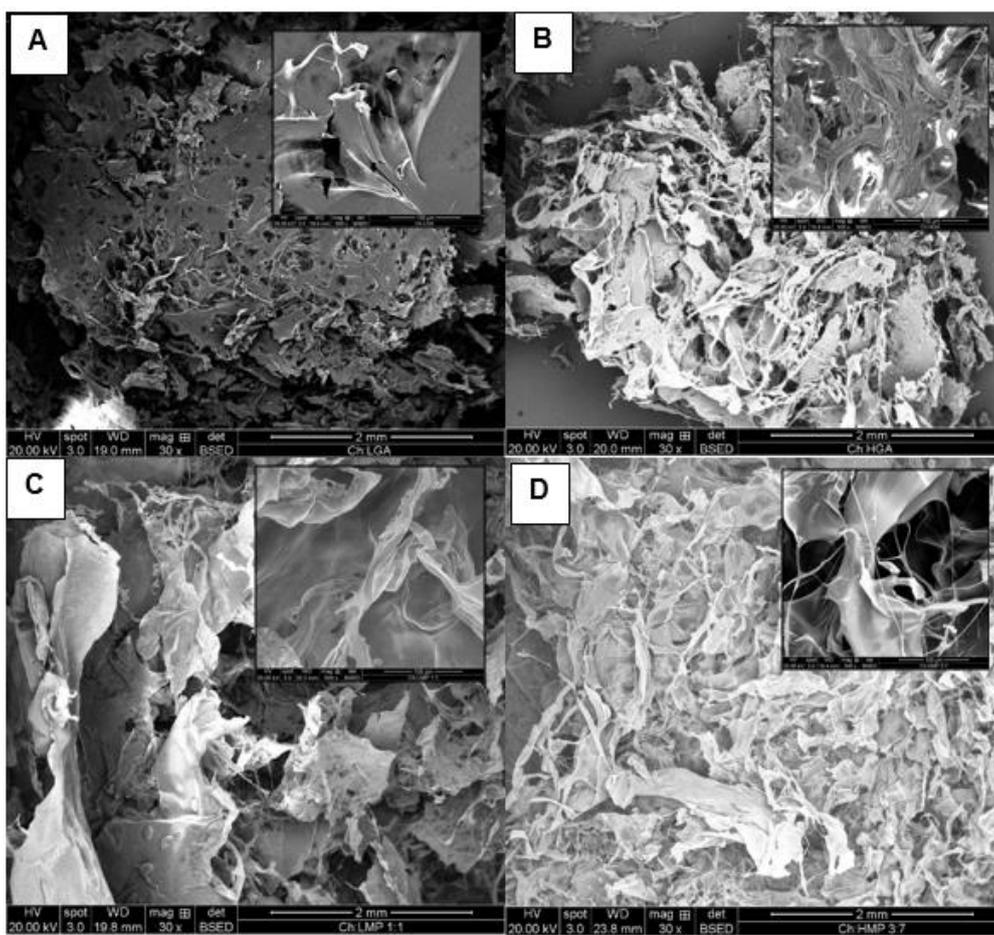
Figure 6.16 SEM micrograph images of freeze dried hydrogel formed from Cs:LGA (A), Cs:HGA (B), Cs:LMP (C) and Cs:HMP (D)

6.4.9.3. Rheological analysis and adhesion study

Dynamic small deformation oscillatory measurements for all samples were performed and the results showed that all the samples exhibited G' greater than G" in frequency range analysed (**Figure 6.17**). These features are characteristic of typical of viscoelastic behaviour (weak gel). The LMP hydrogel shows larger G' when compared with the other samples this likely to be due the highest degree of crosslinking (Li *et al.*, 2009). Furthermore, adhesion evaluation was analysed; **Figure 6.18** indicates the mucoadhesion performance of the Cs hydrogels. The hydrogel prepared with HGA showed the greatest force of adhesion followed by LMP and HMP while LGA had the lowest. This study highlights that HGA and LMP hydrogels display better adhesiveness in comparison with the LGA and HMP and those findings are in agreement with the adhesion results of the individual polymers with mucin (see

section 5.6.1.2.3). This likely to be due to the better rheological gel characteristics as previously shown in **Figure 6.16**; systems with higher elastic component in general exhibit a greater mucoadhesion as reported in (Tamburic and Craig, 1995, Tamburic and Craig, 1997).
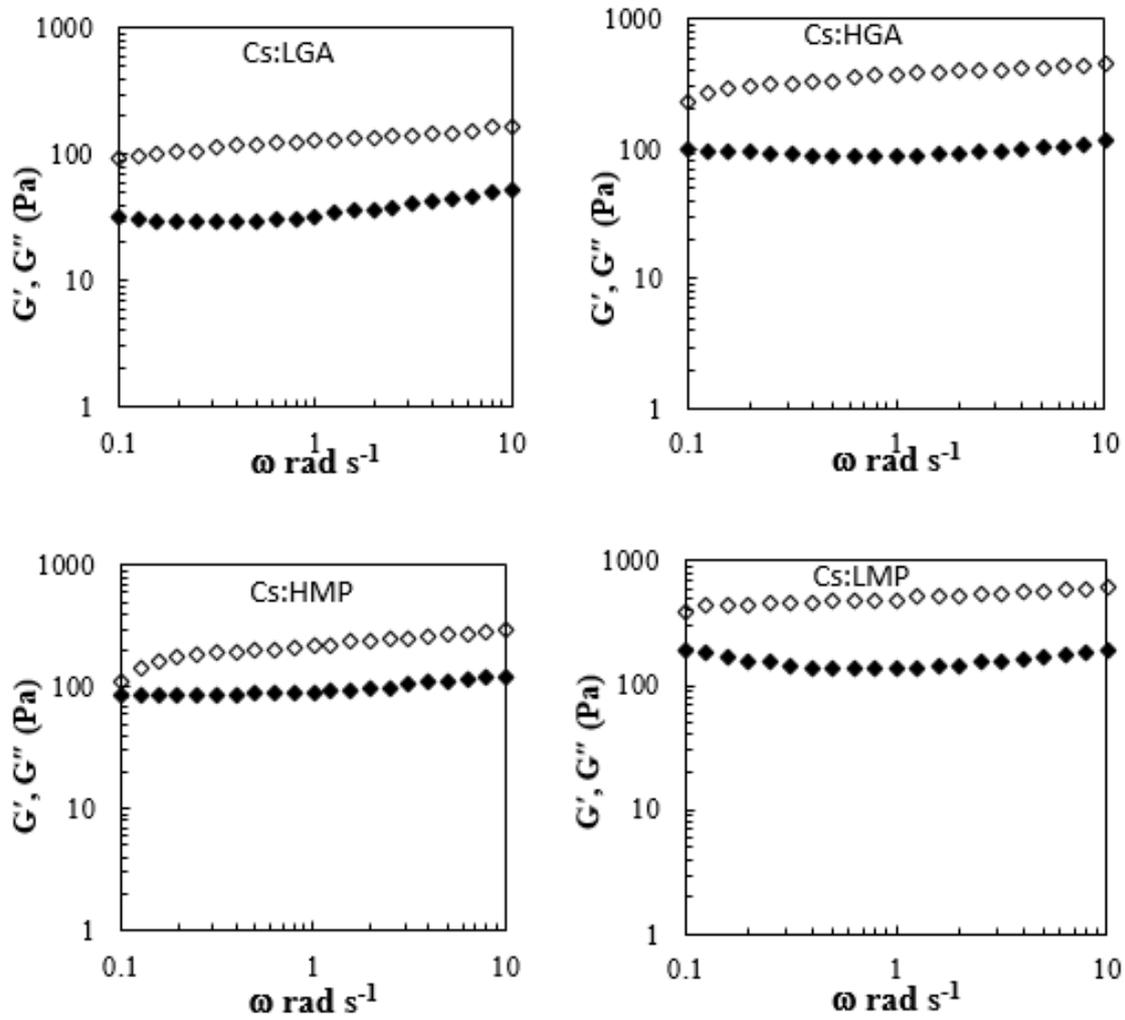
Figure 6.17 Mechanical spectrum of PECs indicating variation of G′ (open squares), G″ (filled squares) at 2 % strain; 25 ℃
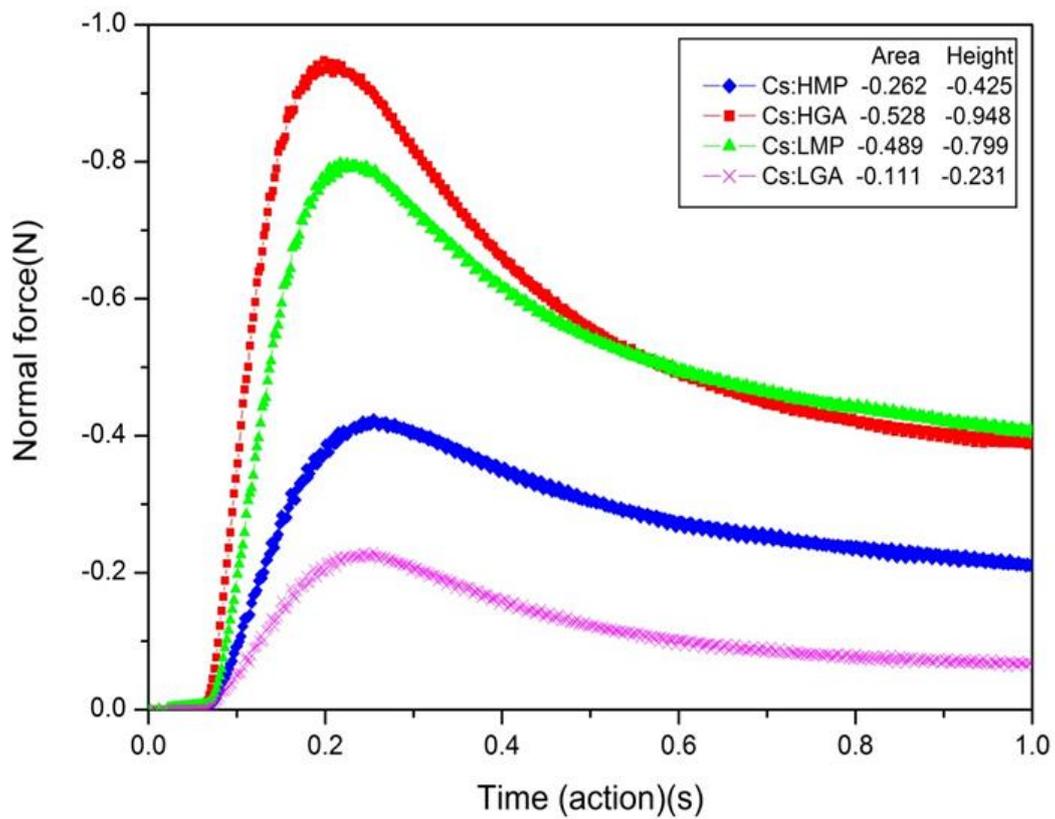
Figure 6.18 Mucoadhesion profiles obtained by rheometer instrument for hydrogel samples at 25 ºC

6.4.9.4. *In vitro* drug release behaviour

In this section ibuprofen was studied *in vitro* as a model drug in drug release study from Cs -polyanion hydrogels using pH 7.4 PBS for 60 min at 37 ℃.

Although drug release behaviours of the prepared hydrogels was not effective because rapid drug release was observed, the study can provide a clear idea about the influences conformation and structure polyanions on the structure of hydrogel formed with Cs and drug release behaviour. This limitation can be attributed to two factors: 1) the preparation method; the prepared hydrogels do not have specific shape such as a tablet, scaffold, particles, bead or matrix, *etc* and a random irregular shape of mucoadhesive may decrease contact area with mucus which has effect on interpenetration and entanglement degree and thereby on inefficiency of mucoadhesion system (Shaikh *et al.*, 2011). 2) The condition of used tissue; the internal porcine oesophagus tissue was frozen more than once this refreezing may have adverse influence on the biomechanical and physiological characterises of the mucus layer (Weist *et al.*, 2010).

Figure.6.19 revealed the percentage of ibuprofen remained in the Cs hydrogel over 60 min. It is observed that HMP and LGA hydrogels displayed the highest percentage of retained ibuprofen following by HGA and LMP. This could be attributed to the fibrous appearance small size of pores, which may impedes movements of entrapped molecules. In addition, these results are in agreement with water uptake, adhesiveness and gel strength this means the samples that display poor swelling behaviour, stronger gel and higher adhesion ability, they have high rate of drug release. Additionally, zero-order, first-order and Higuchi mathematical drug release models were applied to the drug release data **Tables 6.2**.The drug release kinetic parameters indicated best correlation with the first order for all samples **Figure 6.20.** This model is used to describe absorption and drug dissolution. The drug release rate depends on its concentration in the formulation and it is indicative of a porous polymer matrices.
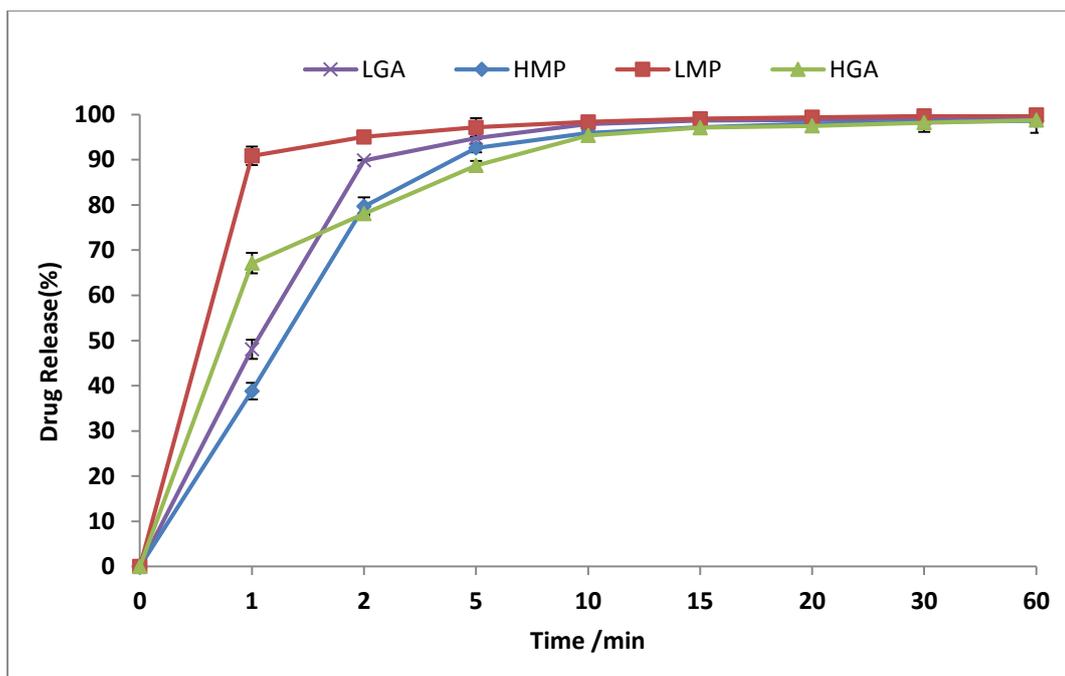
Figure 6.19 Drug release % ibuprofen release on the membrane of oesophagus after 60 min at 37 ℃.
Values are represented as mean ± SD (n=3)

Table 6.2 Release kinetics of the hydrogels (pH 4.3)

Sample	Zero order		1st order		Higuchi	
	K_0(%/min)	R^2	K_1(/min^1)	R^2	K(%/min$^{1/2}$)	R^2
HMP	0.0039	0.309	0.0477	0.581	0.0446	0.51
LMP	0.0008	0.292	0.0760	0.846	0.0094	0.479
LGA	0.0047	0.324	0.0530	0.649	0.0529	0.532
HGA	0.0027	0.365	0.0550	0.771	0.0292	0.576

6.5. Summary

In this chapter Cs -polyanion (HGA, LGA, HMP and LMP) hydrogels complexes were successfully prepared (in acetate buffer 0.05 M, 4.3 pH) at various ratios (10 %, 30 %, 50 %, 70 % and 90 % of Cs) using the ionotropic gelation method. Both supernatant and freeze dried hydrogel were studied. The freeze dried hydrogels were characterized by FT-IR and XRD which confirmed the electrostatic interactions between Cs and polyanions at all ratios also the yield of hydrogel was determined and it was found that the greater amount was obtained from 3:7 and 1:1 of Cs -pectins and Cs -alginates respectively. These findings can be demonstrated by ζ and η_{sp} results of the supernatant which indicate that the lowest values of ζ (close to zero) and η_{sp} were at the above-mentioned ratios (optimum ratios) which may attributed to equivalence between COO^- and NH_3^+ which is the main driving force behind complex formation. The hydrogels of ideal ratios were studied by determining zeta potential, particles size, water uptake, morphology by scanning electron microscopy for freeze dried hydrogels and optical microscopy analysis for homogenous suspension. In addition, dynamic small deformation oscillatory measurements and adhesion property were studied. Finally, ibuprofen was successfully encapsulated by the Cs - polyanion hydrogel complexes and the encapsulation efficiency of the formulations was calculated then the drug release behaviour of the formulations was assessed *in vitro* over the time. The findings demonstrated that HMP and LGA hydrogels displayed the highest percentage of retained ibuprofen following by HGA and LMP. This could be attributed to the fibrous appearance small size of pores which may impedes movements of entrapped molecules. In addition, zero-order, first-order and Higuchi mathematical drug release models were applied to the drug release data. The drug release kinetic parameters indicated best correlation with the first order for all samples. This model is used to describe absorption and drug dissolution. The drug release rate depends on its concentration in the formulation and it is indicative of a porous polymer matrices.

Chapter 7

General Conclusions and Future Recommendations

7. GENERAL CONCLUSIONS AND FUTURE RECOMMENDATIONS

The aim of this research was to investigate the potential applications of polyelectrolyte complexes containing Cs and naturally occurring polyanions (alginate and pectin) as a potential pharmaceutical excipients. To achieve this aim, the physicochemical properties of starting material (including mucin, Cs, pectins and alginates) must be characterized. Moreover, the goals of this thesis, as stated in Chapter 1 (Section 1.5) were successfully achieved and summarised in the following sections.

Chapter 3 discussed the physicochemical properties of extensively degraded mucin and findings revealed that this type of mucin contains: protein, carbohydrate (Fuc, Gal, GalN, GlcN) and sialic acid, which provides the negative charges that becomes progressively stronger with increasing pH. The measurements of viscosity vs. shear rate showed that mucin has a shear thinning behaviour and a relatively low viscosity which is consistent with a high critical overlap concentration (c*), small hydrodynamic size and hence compact structure (high molecular weight coupled with low intrinsic viscosity).

In Chapter 4 the structure of Cs, HMP, LMP, LGA and HGA as powder have been explored; FTIR findings indicate the structure and the functional groups for each polysaccharide whereas powder X-ray (XRD) measurements demonstrated that all the polysaccharides analysed are amorphous in nature except LMP which has number of sharp crystalline peaks which likely is to be due to the low degree of esterification which enables the molecules have long-range interactions. Moreover, solution properties of these polysaccharides were investigated; zeta potential and intrinsic viscosity were investigated at several ionic strengths and pH. Furthermore the molecular weights were evaluated based on intrinsic viscosity and the Smidsrød-Haug stiffness parameter (B) and intrinsic persistence length (L_p) were estimated using the novel ionic strength dependency of zeta potential method and intrinsic viscosity (traditional method). There is further work that could be done to study other polyanions with different conformations such as gellan gum, carrageenan and examine their ability to form polyelectrolyte complexes with Cs.

Chapter 5 focused on evaluating the interaction between polysaccharides and pig gastric mucin based on relative viscosity. We suggest that polysaccharides–mucin interactions are not only driven by electrostatic forces, but also the molecular weight, conformation and flexibility of the polymer also played significant roles. Interestingly, mucin-HGA system displays high

viscosity and the viscoelastic properties of this system were extensively studied therefore more work is needed to investigate the impact of pH temperature on gelation process also the drug delivery behaviour should be studied. Moreover 80 % of mucin was successfully encapsulated within phospholipid bilayers using liposomal encapsulation technology. The liposomal vesicles that encapsulate mucin display larger sizes compared to that the control vesicles (prepared in DI water) this may be due to the electrostatic interaction between mucin molecules and phospholipid which is the main component the vesicles. In addition, the potential of interaction between the encapsulated mucin and the polysaccharides rheologically studied at temperature range 20 °C to 60 °C. In this work, there are many areas of potential opportunities could be expanded, such as preparing liposomal vesicles by different methods and over a range concentrations of mucin and different kind of phospholipids to optimise the particle size and to see how these factors can effect on the physiochemical features. Furthermore the encapsulated mucin can be investigated as new drug delivery vehicle; this formulation could be used in many application such as treatment dry eye syndrome as additive to improve the mucoadhesion of artificial tear drops and vaginal dryness which associated for the menopause.

Chapter 6 highlighted the potential of PECs as pharmaceutical excipients. Firstly Cs - polyanion (including HGA, LGA, HMP and LMP) complex hydrogels were successfully formed at various ratios (10 %, 30 %, 50 %, 70 %, and 90 % of Cs) via ionotropic gelation. The supernatant and freeze dried hydrogels were studied. The freeze dried hydrogels were characterized by FT-IR and XRD which confirmed the electrostatic interactions between Cs and polyanions at all ratios also the yield of hydrogel was determined and it was found that the greater amount was obtained from 3:7 and 1:1 of Cs -pectins and Cs -alginates respectively. Secondly, the hydrogels prepared at optimum ratios were studied by determining zeta potential, particle size, water uptake, morphology by scanning electron microscopy for freeze dried hydrogels and optical microscopy analysis for homogenous suspension, dynamic small deformation oscillatory measurements and adhesion property also were identified. Finally, ibuprofen was successfully encapsulated by the Cs -polyanion hydrogel complexes and the encapsulation efficiency of the formulations was assessed then the drug release from the formulations was in *vitro* evaluated over the time. In addition, zero-order, first-order and Higuchi mathematical drug release models were applied to the drug release data. The drug release kinetic parameters indicated best correlation with the first order for all samples. This model is used to describe absorption and drug dissolution. The drug release rate depends on its

concentration in the formulation and it is indicative of a porous polymer matrices. The obtained results comparison between the two types of pectin (HMP & LMP) and alginate (HGA & LGA) indicate that conformation has an influence on the formation and structure of hydrogel and hence on drug release behaviour. There is further work that can be done to improve these formulations which including controlling the nature of the hydrogel formulation for example in film or tablet form. Moreover, it would be interesting to investigate the hydrogel formulations over a range of pH, temperature and acid exposure times to see how variations in gastric physiology may influence on the mechanical properties and to release behaviour.

Chapter 8

References

8. REFERENCES

Abodinar, A., Smith, A. M. & Morris, G. A. 2014. A novel method to estimate the stiffness of carbohydrate polyelectrolyte polymers based on the ionic strength dependence of zeta potential. *Carbohydrate polymers,* 112**,** 6-9.

Abodinar, A., Tømmeraas, K., Ronander, E., Smith, A. M. & Morris, G. A. 2016. The physicochemical characterisation of pepsin degraded pig gastric mucin. *International Journal of Biological Macromolecules,* 87**,** 281-286.

Adikwu, M. U. 2006. Mucins and their potentials. *Tropical Journal of Pharmaceutical Research,* 5**,** 581-582.

Ahmed, E. M. 2015. Hydrogel: Preparation, characterization, and applications: A review. *Journal of Advanced Research,* 6**,** 105-121.

Akbarzadeh, A., Rezaei-Sadabady, R., Davaran, S., Joo, S. W., Zarghami, N., Hanifehpour, Y., Samiei, M., Kouhi, M. & Nejati-Koshki, K. 2013. Liposome: classification, preparation, and applications. *Nanoscale Research Letters,* 8**,** 1.

Akiyoshi, K., Kang, E.-C., Kurumada, S., Sunamoto, J., Principi, T. & Winnik, F. M. 2000. Controlled association of amphiphilic polymers in water: thermosensitive nanoparticles formed by self-assembly of hydrophobically modified pullulans and poly (N-isopropylacrylamides). *Macromolecules,* 33**,** 3244-3249.

Albalasmeh, A. A., Berhe, A. A. & Ghezzehei, T. A. 2013. A new method for rapid determination of carbohydrate and total carbon concentrations using UV spectrophotometry. *Carbohydrate Polymers,* 97**,** 253-261.

Alexander, A., Sharma, S. & Khan, M. J. 2011. Theories and factors affecting mucoadhesive drug delivery systems: A review. *International Journal of Research in Ayurveda and Pharmacy* 2.

Alsirawan, M. B., Mohammad, M. A., Alkasmi, B., Alhareth, K. & El-Hammadi, M. 2013. Developments and valuation of a simple HPLC method for the determination and of ibuprofen sticking onto punch faces *International Journal of Pharmacy and Pharmaceutical Sciences,* 5.

Anal, A. K. & Stevens, W. F. 2005. Chitosan–alginate multilayer beads for controlled release of ampicillin. *International journal of pharmaceutics,* 290**,** 45-54.

Andrews, G. P., Laverty, T. P. & Jones, D. S. 2009. Mucoadhesive polymeric platforms for controlled drug delivery. *European Journal of Pharmaceutics and Biopharmaceutics,* 71**,** 505-518.

Ankerfors, C. 2008. Polyelectrolyte complexes: their preparation, adsorption behaviour and effect on paper properties.

Aulton, M. E. & Taylor, K. M. 2013. *Aulton's pharmaceutics: the design and manufacture of medicines*, Elsevier Health Sciences.

Bansil, R. & Turner, B. S. 2006. Mucin structure, aggregation, physiological functions and biomedical applications. *Current Opinion in Colloid & Interface Science,* 11**,** 164-170.

Barichello, J. M., Morishita, M., Takayama, K. & Nagai, T. 1999. Encapsulation of hydrophilic and lipophilic drugs in PLGA nanoparticles by the nanoprecipitation method. *Drug development and industrial pharmacy,* 25**,** 471-476.

Barthelmes, J., Dünnhaupt, S., Hombach, J. & Bernkop-Schnürch, A. 2011. Thiomer nanoparticles: stabilization via covalent cross-linking. *Drug delivery,* 18**,** 613-619.

Basbaum, C., Gallup, M., Gum, J., Kim, Y. & Jany, B. 1989. Modification of mucin gene expression in the airways of rats exposed to sulfur dioxide. *Biorheology,* 27**,** 485-489.

Bath, I. 1958. The ultra-violet spectrophotometric determination of sugars and uronic acids. *Analyst,* 83**,** 451-455.

Bernkop-Schnürch, A. 2000. Chitosan and its derivatives: potential excipients for peroral peptide delivery systems. *International journal of pharmaceutics,* 194**,** 1-13.

Bhattarai, N., Gunn, J. & Zhang, M. 2010. Chitosan-based hydrogels for controlled, localized drug delivery. *Advanced Drug Delivery Reviews,* 62**,** 83-99.

Bigucci, F., Luppi, B., Cerchiara, T., Sorrenti, M., Bettinetti, G., Rodriguez, L. & Zecchi, V. 2008. Chitosan/pectin polyelectrolyte complexes: Selection of suitable preparative conditions for colon-specific delivery of vancomycin. *European Journal of Pharmaceutical Sciences,* 35**,** 435-441.

Bigucci, F., Luppi, B., Monaco, L., Cerchiara, T. & Zecchi, V. 2009. Pectin-based microspheres for colon-specific delivery of vancomycin. *Journal of Pharmacy and Pharmacology,* 61**,** 41-46.

Boddupalli, B. M., Mohammed, Z. N., Nath, R. A. & Banji, D. 2010. Mucoadhesive drug delivery system: An overview. *Journal of advanced pharmaceutical technology & research,* 1**,** 381.

Bodmeier, R., Chen, H. & Paeratakul, O. 1989. A novel approach to the oral delivery of micro- or nanoparticles. *Pharmaceutical research,* 6**,** 413-417.

Bowman, K. & Leong, K. W. 2006. Chitosan nanoparticles for oral drug and gene delivery. *International journal of Nanomedicine,* 1**,** 117.

Bozzuto, G. & Molinari, A. 2015. Liposomes as nanomedical devices. *International Journal of Nanomedicine,* 10**,** 975.

Brugnerotto, J., Desbrières, J., Roberts, G. & Rinaudo, M. 2001. Characterization of chitosan by steric exclusion chromatography. *Polymer,* 42**,** 09921-09927.

Byrappa, K., Ohara, S. & Adschiri, T. 2008. Nanoparticles synthesis using supercritical fluid technology–towards biomedical applications. *Advanced Drug Delivery Reviews,* 60**,** 299-327.

Cao, X., Bansil, R., Bhaskar, K. R., Turner, B. S., LaMont, J. T., Niu, N. & Afdhal, N. H. 1999. pH-Dependent Conformational Change of Gastric Mucin Leads to Sol-Gel Transition. *Biophysical Journal,* 76**,** 1250-1258.

Carlstedt, I., Sheehan, J., Corfield, A. & Gallagher, J. T. 1985. Mucous glycoproteins: a gel of a problem. *Essays in biochemistry.*

Carvalho, F. C., Bruschi, M. L., Evangelista, R. C. & Gremião, M. P. D. 2010. Mucoadhesive drug delivery systems. *Brazilian Journal of Pharmaceutical Sciences,* 46**,** 1-17.

Celli, J. P., Turner, B. S., Afdhal, N. H., Ewoldt, R. H., McKinley, G. H., Bansil, R. & Erramilli, S. 2007. Rheology of gastric mucin exhibits a pH-dependent sol-gel transition. *Biomacromolecules,* 8**,** 1580-1586.

Chen, M.-C., Ling, M.-H., Lai, K.-Y. & Pramudityo, E. 2012. Chitosan microneedle patches for sustained transdermal delivery of macromolecules. *Biomacromolecules,* 13**,** 4022-4031.

Chhabra, R. & Richardson, J. 2008. *Non-Newtonian flow and applied Rheology: engineering applications,* GB, Butterworth Heinemann.

Chickering, D. E., Lehr, C.-M. & Mathiowitz, E. 1999. *Bioadhesive Drug Delivery Systems: Fundamentals, Novel Approaches, and Development*, Marcel Dekker.

Cho, J., Heuzey, M.-C., Bégin, A. & Carreau, P. J. 2006. Viscoelastic properties of chitosan solutions: Effect of concentration and ionic strength. *Journal of Food Engineering,* 74**,** 500-515.

Chun, M.-K., Sah, H. & Choi, H.-K. 2005. Preparation of mucoadhesive microspheres containing antimicrobial agents for eradication of H. pylori. *International journal of pharmaceutics,* 297**,** 172-179.

Cooper, S., Horbett, T., Ratner, M. & Stayton, P. 2005. *Gels, genes, grafts and giants: festschrift on the occasion of the 70th birthday of allan S. hoffman*, Taylor & Francis.

Dakhara, S. & Anajwala, C. 2010. Polyelectrolyte complex: A pharmaceutical review. *Systematic Reviews in Pharmacy,* 1**,** 121.

das Neves, J. & Sarmento, B. 2014. *Mucosal Delivery of Biopharmaceuticals*, Springer.

Davidovich-Pinhas, M. & Bianco-Peled, H. 2010. A quantitative analysis of alginate swelling. *Carbohydrate Polymers,* 79**,** 1020-1027.

De Araújo Lopes, S. C., Dos Santos Giuberti, C., Rocha, T. G. R., Dos Santos Ferreira, D., Leite, E. A. & Oliveira, M. C. (eds.) 2013. *Liposomes as carriers of anticancer drugs*.

de Campos, A. M., Diebold, Y., Carvalho, E. L. S., Sánchez, A. & José Alonso, M. 2004. Chitosan nanoparticles as new ocular drug delivery systems: in vitro stability, in vivo fate, and cellular toxicity. *Pharmaceutical Research,* 21**,** 803-810.

de Jong, S. & van de Velde, F. 2007. Charge density of polysaccharide controls microstructure and large deformation properties of mixed gels. *Food Hydrocolloids,* 21**,** 1172-1187.

Deacon, M. P., Davis, S. S., Waite, J. H. & Harding, S. E. 1998. Structure and mucoadhesion of mussel glue protein in dilute solution. *Biochemistry,* 37**,** 14108-14112.

Dekker, J., Rossen, J. W. A., Büller, H. A. & Einerhand, A. W. C. 2002. The MUC family: an obituary. *Trends in Biochemical Sciences,* 27**,** 126-131.

Derjaguin, B., Aleinikova, I. & Toporov, Y. P. 1994. On the role of electrostatic forces in the adhesion of polymer particles to solid surfaces. *Progress in Surface Science,* 45**,** 119-123.

Derjaguin, B. V., Toporov, Y. P., Muller, V. M. & Aleinikova, I. N. 1977. On the relationship between the electrostatic and the molecular component of the adhesion of elastic particles to a solid surface. *Journal of Colloid and Interface Science,* 58**,** 528-533.

Di Cola, E., Yakubov, G. E. & Waigh, T. A. 2008. Double-globular structure of porcine stomach mucin: a small-angle X-ray scattering study. *Biomacromolecules,* 9**,** 3216-3222.

Dodane, V. & Vilivalam, V. D. 1998. Pharmaceutical applications of chitosan. *Pharmaceutical Science & Technology Today,* 1**,** 246-253.

Donald, A. S. R. 1973. The products of pronase digestion of purified blood group-specific glycoproteins. *Biochimica et Biophysica Acta (BBA)-Protein Structure,* 317**,** 420-436.

Draget, K. I., Smidsrød, O. & Skjåk-Bræk, G. 2005. Alginates from algae. *Biopolymers Online*.

Dua, J., Rana, A. & Bhandari, A. 2012. Liposome: methods of preparation and applications. *International Journal of Pharmaceutical Studies and Research,* 3**,** 14-20.

Dubois, M., Gilles, K. A., Hamilton, J. K., Rebers, P. & Smith, F. 1956. Colorimetric method for determination of sugars and related substances. *Analytical Chemistry,* 28**,** 350-356.

Dumitriu, S. 2004. *Polysaccharides: Structural diversity and functional versatility, Second Edition*, CRC Press.

Ebnesajjad, S. 2012. *Handbook of biopolymers and biodegradable plastics: properties, processing and applications*, William Andrew.

Eloy, J. O., de Souza, M. C., Petrilli, R., Barcellos, J. P. A., Lee, R. J. & Marchetti, J. M. 2014. Liposomes as carriers of hydrophilic small molecule drugs: strategies to enhance encapsulation and delivery. *Colloids and Surfaces B: Biointerfaces,* 123**,** 345-363.

Fallingborg, J. 1999. *Intraluminal PH of the human gastrointestinal tract*, Lægeforeningens forlag.

Fanun, M. 2010. *Colloids in biotechnology*, CRC Press.

Farraj, N., Johansen, B., Davis, S. & Illum, L. 1990. Nasal administration of insulin using bioadhesive microspheres as a delivery system. *Journal of Controlled Release,* 13**,** 253-261.

Fernandez-Hervas, M. & Fell, J. 1998. Pectin/chitosan mixtures as coatings for colon-specific drug delivery: an in vitro evaluation. *International journal of pharmaceutics,* 169**,** 115-119.

Fernández-Hervás, M. J. & Fell, J. T. 1998. Pectin/chitosan mixtures as coatings for colon-specific drug delivery: an in vitro evaluation. *International journal of pharmaceutics,* 169**,** 115-119.

Filipe, V., Hawe, A. & Jiskoot, W. 2010. Critical evaluation of Nanoparticle Tracking Analysis (NTA) by NanoSight for the measurement of nanoparticles and protein aggregates. *Pharmaceutical research,* 27**,** 796-810.

Fogg, F., J. J., Hutton, D. A., Jumel, K., Pearson, J. P., Harding, S. E. & Allen, A. 1996. Characterization of pig colonic mucins. *Biochemical Journal,* 316**,** 937-942.

Fukuda, H. 2014. *Plant cell wall patterning and cell shape*, John Wiley & Sons.

Gabizon, A., Isacson, R., Libson, E., Kaufman, B., Uziely, B., Catane, R., Ben-Dor, C. G., Rabello, E., Cass, Y. & Peretz, T. 1994. Clinical studies of liposome-encapsulated doxorubicin. *Acta Oncologica,* 33**,** 779-786.

Gad, S. C. 2008. *Pharmaceutical manufacturing handbook: production and processes*, Wiley.

Gallegos, C. 2010. *Rheology - Volume I*.

Garrec, D. 2013. *Understanding fluid gels and hydrocolloid tribology*, University of Birmingham.

Gåserød, O., Jolliffe, I. G., Hampson, F. C., Dettmar, P. W. & Skjåk-Bræk, G. 1998. The enhancement of the bioadhesive properties of calcium alginate gel beads by coating with chitosan. *International journal of pharmaceutics,* 175**,** 237-246.

Georgiades, P., di Cola, E., Heenan, R. K., Pudney, P. D. A., Thornton, D. J. & Waigh, T. A. 2014. A combined small-angle X-ray and neutron scattering study of the structure of purified soluble gastrointestinal mucins. *Biopolymers,* 101**,** 1154-1164.

Ghaffari, A., Navaee, K., Oskoui, M., Bayati, K. & Rafiee-Tehrani, M. 2007. Preparation and characterization of free mixed-film of pectin/chitosan/Eudragit® RS intended for sigmoidal drug delivery. *European Journal of Pharmaceutics and Biopharmaceutics,* 67**,** 175-186.

Ghaffari, A., Oskoui, M., Helali, K., Bayati, K. & Rafiee-Tehrani, M. 2006. Pectin/chitosan/Eudragit® RS mixed-film coating for bimodal drug delivery from theophylline pellets: Preparation and evaluation. *Acta Pharmaceutica,* 56**,** 299-310.

Gillis, R. B., Adams, G. G., Wolf, B., Berry, M., Besong, T. M. D., Corfield, A., Kök, S. M., Sidebottom, R., Lafond, D., Rowe, A. J. & Harding, S. E. 2013. Molecular weight

distribution analysis by ultracentrifugation: Adaptation of a new approach for mucins. *Carbohydrate Polymers, 93*, 178-183.

Gnanasambandam, R. & Proctor, A. 2000. Determination of pectin degree of esterification by diffuse reflectance Fourier transform infrared spectroscopy. *Food Chemistry, 68*, 327-332.

Gomez-Hens, A. & Fernandez-Romero, J. 2006. Analytical methods for the control of liposomal delivery systems. *TrAC Trends in Analytical Chemistry, 25*, 167-178.

Gotoh, T., Matsushima, K. & Kikuchi, K.-I. 2004. Preparation of alginate–chitosan hybrid gel beads and adsorption of divalent metal ions. *Chemosphere, 55*, 135-140.

Grillet, A. M., Gloe, L. M. & Wyatt, N. B. 2012. *Polymer gel rheology and adhesion*, INTECH Open Access Publisher.

Gu, J., Robinson, J. & Leung, S. 1987. Binding of acrylic polymers to mucin/epithelial surfaces: structure-property relationships. *Critical reviews in therapeutic drug carrier systems, 5*, 21-67.

Gubbala, S. K. 2012. Polyelectrolyte complex : A pharmaceutical review. *International Journal of Pharmacy and Biological Sciences, 2*, 399-407.

Guo, C. 2007. *Chitosan-coated poly (lactide-co-glycolide) nanoparticles for DNA delivery*, ProQuest.

Gurny, R., Meyer, J.-M. & Peppas, N. A. 1984. Bioadhesive intraoral release systems: design, testing and analysis. *Biomaterials, 5*, 336-340.

Halabalova, V., Simek, L. & Mokrejs, P. 2011. Intrinsic viscosity and conformational parameters of chitosan chains. *Rasayan Journal of Chemistry, 4*, 223-241.

Hamman, J. H. 2010. Chitosan based polyelectrolyte complexes as potential carrier materials in drug delivery systems. *Marine Drugs, 8*, 1305-1322.

Harding, S. E. 1997a. Characterisation of chitosan-mucin complexes by sedimentation velocity analytical ultracentrifugation. *Chitin handbook*, 457.

Harding, S. E. 1997b. The intrinsic viscosity of biological macromolecules. Progress in measurement, interpretation and application to structure in dilute solution. *Progress in Biophysics and Molecular Biology, 68*, 207-262.

Harding, S. E., Abdelhameed, A. S. & Morris, G. A. 2011. On the hydrodynamic analysis of conformation in mixed biopolymer systems. *Polymer International, 60*, 2-8.

Harding, S. E., Adams, G. G., Almutairi, F., Alzahrani, Q., Erten, T., Kök, M. S. & Gillis, R. B. 2015. Chapter eighteen-ultracentrifuge methods for the analysis of polysaccharides, glycoconjugates, and lignins. *Methods in Enzymology, 562*, 391-439.

Harding, S. E., Davis, S. S., Deacon, M. P. & Fiebrig, I. 1999. Biopolymer mucoadhesives. *Biotechnology and Genetic Engineering Reviews, 16*, 41-86.

Harding, S. E., Rowe, A. J., Chemistry, R. S. o., Group, B. S. T., Colloid, R. S. o. C. & Group, I. S. 1989. *Dynamic properties of biomolecular assemblies* Royal Society of Chemistry.

Haug, A. 1964. *Composition and properties of alginates*, Norwegian Institute of Seaweed Research.

He, F. 2011. *Bradford protein assay* [Online]. Bio-protocol Bio101. Available: http://www.bio-protocol.org/e45

Heinze, T., Nikolajski, M., Daus, S., Besong, T., Michaelis, N., Berlin, P., Morris, G. A., Rowe, A. J. & Harding, S. E. 2011. Protein-like oligomerization of carbohydrates. *Angewandte Chemie International Edition,* 50**,** 8602-8604.

Hess, M., Jones, R., Kahovec, J., Kitayama, T., Kratochvíl, P., Kubisa, P., Mormann, W., Stepto, R., Tabak, D. & Vohlídal, J. 2006. Terminology of polymers containing ionizable or ionic groups and of polymers containing ions (IUPAC Recommendations 2006). *Pure and Applied Chemistry,* 78**,** 2067-2074.

Hoang, V., Williams, M. & Simpson, H. 2010. Monosaccharide composition of fundic and duodenal mucins in sheep infected with *Haemonchus contortus* or *Teladorsagia circumcincta*. *Veterinary Parasitology,* 170**,** 253-261.

Hugerth, A., Caram-Lelham, N. & Sundelöf, L.-O. 1997. The effect of charge density and conformation on the polyelectrolyte complex formation between carrageenan and chitosan. *Carbohydrate Polymers,* 34**,** 149-156.

Huggins, M. L. 1942. The viscosity of dilute solutions of long-chain molecules. IV. Dependence on concentration. *Journal of the American Chemical Society,* 64**,** 2716-2718.

Hui, Y. H. & Sherkat, F. 2005. *Handbook of food science, technology, and engineering - 4 volume Set*, CRC Press.

Hunter, R. J. 1981. *Zeta potential in colloid science: principles and applications,* London, Academic Press.

Hurd, C. D. 1970. The acidities of ascorbic and sialic acids. *Journal of Chemical Education,* 47**,** 481.

Ibarz, A. & Barbosa-Canovas, G. V. 2014. *Introduction to Food Process Engineering*, CRC Press.

Ichikawa, T. & Ishihara, K. 2011. Protective effects of gastric mucus.

Il Dueik, I. & Morris, G. A. 2013. Latent fingerprint enhancement using tripolyphosphate-chitosan microparticles. *International Journal of Carbohydrate Chemistry,* 2013.

Imura, T., Gotoh, T., Otake, K., Yoda, S., Takebayashi, Y., Yokoyama, S., Takebayashi, H., Sakai, H., Yuasa, M. & Abe, M. 2003. Control of physicochemical properties of liposomes using a supercritical reverse phase evaporation method. *Langmuir,* 19**,** 2021-2025.

Isa, M., Ameh, A., Tijjani, M. & Adama, K. 2012. Extraction and characterization of chitin and chitosan from Nigerian shrimps. *International Journal of Biological and chemical Sciences,* 6**,** 446-453.

Javadi, M.-A. & Feizi, S. 2011. Dry eye syndrome. *Journal of Ophthalmic & Vision research,* 6**,** 192-198.

Jiménez-Castellanos, M. R., Zia, H. & Rhodes, C. T. 1994. Design and testing in vitro of a bioadhesive and floating drug delivery system for oral application. *International Journal of Pharmaceutics,* 105**,** 65-70.

Jones, R. 2002. Soft condensed matter New York Oxford University Press Inc.

Jumel, K., Fogg, F. J., Hutton, D. A., Pearson, J. P., Allen, A. & Harding, S. E. 1997. A polydisperse linear random coil model for the quaternary structure of pig colonic mucin. *European biophysics journal : EBJ,* 25**,** 477-480.

Junker, W. M. 2008. *Molecular and biological studies of MUC17*, ProQuest.

Kasaai, M. R. 2006. Intrinsic viscosity–molecular weight relationship and hydrodynamic volume for pullulan. *Journal of Applied Polymer Science,* 100**,** 4325-4332.

Kim, S. K. 2011. *Marine cosmeceuticals: Trends and prospects*, Taylor & Francis.

Kinloch, A. 1980. The science of adhesion. *Journal of materials science,* 15**,** 2141-2166.

Knuth, K., Amiji, M. & Robinson, J. R. 1993. Hydrogel delivery systems for vaginal and oral applications: Formulation and biological considerations. *Advanced drug delivery reviews,* 11**,** 137-167.

Kong, F. & Singh, R. 2008. Disintegration of solid foods in human stomach. *Journal of Food Science,* 73**,** R67-R80.

Kraemer, E. O. 1938. Molecular weights of celluloses and cellulose derivates. *Industrial & Engineering Chemistry,* 30**,** 1200-1203.

Krauland, A. H., Leitner, V. M., Grabovac, V. & Bernkop-Schnürch, A. 2006. In vivo evaluation of a nasal insulin delivery system based on thiolated chitosan. *Journal of pharmaceutical sciences,* 95**,** 2463-2472.

Kruger, N. J. 1994. The Bradford method for protein quantitation. *Basic protein and peptide protocols***,** 9-15.

Kujawa, P., Schmauch, G., Viitala, T., Badia, A. & Winnik, F. M. 2007. Construction of viscoelastic biocompatible films via the layer-by-layer assembly of hyaluronan and phosphorylcholine-modified chitosan. *Biomacromolecules,* 8**,** 3169-3176.

Kumar, N. & Kumbhat, S. 2016. *Essentials in nanoscience and nanotechnology*, Wiley.

Kumirska, J., Weinhold, M. X., Thöming, J. & Stepnowski, P. 2011. Biomedical activity of chitin/chitosan based materials—influence of physicochemical properties apart from molecular weight and degree of N-acetylation. *Polymers,* 3**,** 1875-1901.

Lakrout, H., Sergot, P. & Creton, C. 1999. Direct observation of cavitation and fibrillation in a probe tack experiment on model acrylic pressure-sensitive-adhesives. *The Journal of Adhesion,* 69**,** 307-359.

Lamarque, G., Lucas, J.-M., Viton, C. & Domard, A. 2005. Physicochemical behavior of homogeneous series of acetylated chitosans in aqueous solution: role of various structural parameters. *Biomacromolecules,* 6**,** 131-142.

Lankalapalli, S. 2009. Polyelectrolyte complexes: A review of their applicability in drug delivery technology. *Indian Journal of Pharmaceutical Sciences,* 71**,** 481.

Laouini, A., Jaafar-Maalej, C., Limayem-Blouza, I., Sfar, S., Charcosset, C. & Fessi, H. 2012. Preparation, characterization and applications of liposomes: state of the art. *Journal of Colloid Science and Biotechnology,* 1**,** 147-168.

Lárez Velásquez, C., Sánchez Albornoz, J. & Millan Barrios, E. 2008. Viscosimetric studies of chitosan nitrate and chitosan chlorhydrate in acid free NaCl aqueous solution. *e-Polymers*.

Larson, R. G. 1999. *The structure and rheology of complex fluids,* New York, Oxford University Press.

Lasic, D. 1997. Recent developments in medical applications of liposomes: sterically stabilized liposomes in cancer therapy and gene delivery in vivo. *Journal of Controlled Release,* 48**,** 203-222.

Laurienzo, P. 2010. Marine polysaccharides in pharmaceutical applications: an overview. *Marine Drugs,* 8**,** 2435-2465.

Lee, B.-J. & Min, G.-H. 1995. Preparation and release characteristics of polymer-reinforced and coated alginate beads. *Archives of Pharmacal Research,* 18**,** 183-188.

Lee, J. W., Park, J. H. & Robinson, J. R. 2000. Bioadhesive-based dosage forms: The next generation. *Journal of Pharmaceutical Sciences,* 89**,** 850-866.

Lehr, C.-M. 1994. Bioadhesion technologies for the delivery of peptide and protein drugs to the gastrointestinal tract. *Critical reviews in therapeutic drug carrier systems,* 11**,** 119-160.

Lehr, C.-M., Boddé, H. E., Bouwstra, J. A. & Junginger, H. E. 1993. A surface energy analysis of mucoadhesion II. Prediction of mucoadhesive performance by spreading coefficients. *European journal of pharmaceutical sciences,* 1**,** 19-30.

Lehr, C.-M., Bouwstra, J. A., Boddé, H. E. & Junginger, H. E. 1992a. A surface energy analysis of mucoadhesion: contact angle measurements on polycarbophil and pig intestinal mucosa in physiologically relevant fluids. *Pharmaceutical research,* 9**,** 70-75.

Lehr, C.-M., Bouwstra, J. A., Schacht, E. H. & Junginger, H. E. 1992b. In vitro evaluation of mucoadhesive properties of chitosan and some other natural polymers. *International journal of Pharmaceutics,* 78**,** 43-48.

Leitner, V. M., Walker, G. F. & Bernkop-Schnürch, A. 2003. Thiolated polymers: evidence for the formation of disulphide bonds with mucus glycoproteins. *European Journal of Pharmaceutics and Biopharmaceutics,* 56**,** 207-214.

Leung, S.-H. S. & Robinson, J. R. 1990. Polymer structure features contributing to mucoadhesion. II. *Journal of controlled release,* 12**,** 187-194.

Li, P., Dai, Y.-N., Zhang, J.-P., Wang, A.-Q. & Wei, Q. 2008. Chitosan-alginate nanoparticles as a novel drug delivery system for nifedipine. *International journal of Biomedical science,* 4**,** 221-228.

Li, R. 2012. *Chitosan particles for the controlled release of proteins.* PhD, Politecnico di Torino.

Li, W., Hao, W., Xiaohua, Z., Yinchen, H., Wangwang, L., Gongming, Y. & Aimin, J. 2015. Pectin-chitosan complex: Preparation and application in colon-specific capsule. *International Journal of Agricultural and Biological Engineering,* 8**,** 151.

Li, Y., Yin, Q., Deng, M.-y., Cui, J.-j. & Jiang, B. 2009. Synthesis and characterization of amphoteric hydrogels based on N-carboxyethylchitosan. *Chinese Journal of Polymer Science,* 27**,** 335-341.

Lin, Y.-H., Liang, H.-F., Chung, C.-K., Chen, M.-C. & Sung, H.-W. 2005. Physically crosslinked alginate/N, O-carboxymethyl chitosan hydrogels with calcium for oral delivery of protein drugs. *Biomaterials,* 26**,** 2105-2113.

Linden, S., Sutton, P., Karlsson, N., Korolik, V. & McGuckin, M. 2008. Mucins in the mucosal barrier to infection. *Mucosal Immunology,* 1**,** 183-197.

Liu, L.-S., Liu, S.-Q., Ng, S. Y., Froix, M., Ohno, T. & Heller, J. 1997. Controlled release of interleukin-2 for tumour immunotherapy using alginate/chitosan porous microspheres. *Journal of Controlled Release,* 43**,** 65-74.

Macleod, G. S., Fell, J. T., Collett, J. H., Sharma, H. L. & Smith, A.-M. 1999. Selective drug delivery to the colon using pectin: chitosan: hydroxypropyl methylcellulose film coated tablets. *International journal of pharmaceutics,* 187**,** 251-257.

Madsen, F., Eberth, K. & Smart, J. D. 1998. A rheological assessment of the nature of interactions between mucoadhesive polymers and a homogenised mucus gel. *Biomaterials,* 19**,** 1083-1092.

Makino, K., Yamada, T., Kimura, M., Oka, T., Ohshima, H. & Kondo, T. 1991. Temperature- and ionic strength-induced conformational changes in the lipid head group region of liposomes as suggested by zeta potential data. *Biophysical Chemistry,* 41**,** 175-183.

Martin, A. N., Sinko, P. J. & Singh, Y. 2011. *Martin's physical pharmacy and pharmaceutical sciences: physical chemical and biopharmaceutical principles in the pharmaceutical sciences*, Lippincott Williams & Wilkins.

Matlack, A. 2010. *Introduction to green chemistry*, CRC Press.

Mazeau, K. & Rinaudo, M. 2004. The prediction of the characteristics of some polysaccharides from molecular modeling. Comparison with effective behavior. *Food Hydrocolloids,* 18**,** 885-898.

McCleary, B. & Prosky, L. 2008. *Advanced Dietary Fibre Technology*, Wiley.

McHugh, D. J. 2003. A guide to the seaweed industry. *FAO Fisheries Technical Paper***,** iii-x, 1-105.

Menchicchi, B., Fuenzalida, J., Bobbili, K. B., Hensel, A., Swamy, M. J. & Goycoolea, F. 2014. Structure of chitosan determines its interactions with mucin. *Biomacromolecules,* 15**,** 3550-3558.

Menchicchi, B., Fuenzalida, J., Hensel, A., Swamy, M., David, L., Rochas, C. & Goycoolea, F. 2015. Biophysical analysis of the molecular interactions between polysaccharides and mucin. *Biomacromolecules,* 16**,** 924-935.

Meng, X., Tian, F., Yang, J., He, C.-N., Xing, N. & Li, F. 2010. Chitosan and alginate polyelectrolyte complex membranes and their properties for wound dressing application. *Journal of Materials Science: Materials in Medicine,* 21**,** 1751-1759.

Mezger, T. G. 2006. *The rheology handbook: for users of rotational and oscillatory rheometers*, Vincentz Network.

Mi, F. L., Shyu, S. S., Kuan, C. Y., Lee, S. T., Lu, K. T. & Jang, S. F. 1999. Chitosan–polyelectrolyte complexation for the preparation of gel beads and controlled release of anticancer drug. I. Effect of phosphorous polyelectrolyte complex and enzymatic hydrolysis of polymer. *Journal of Applied Polymer Science,* 74**,** 1868-1879.

Mireles-DeWitt, C. 1994. *Complex mechanism of chitosan and naturally occurring polyanions.* Masters of Science Oregon State

Mohnen, D. 2008. Pectin structure and biosynthesis. *Current Opinion in Plant Biology,* 11**,** 266-277.

Morris, E. R., Cutler, A. N., Ross-Murphy, S. B., Rees, D. A. & Price, J. 1981. Concentration and shear rate dependence of viscosity in random coil polysaccharide solutions. *Carbohydrate Polymers,* 1**,** 5-21.

Morris, G., Castile, J., Smith, A., Adams, G. & Harding, S. E. 2010. The effect of different storage temperatures on the physical properties of pectin solutions and gels. *Polymer Degradation and Stability,* 95**,** 2670-2673.

Morris, G. A., Adams, G. G. & Harding, S. E. 2014. On hydrodynamic methods for the analysis of the sizes and shapes of polysaccharides in dilute solution: A short review. *Food Hydrocolloids,* 42**,** 318-334.

Morris, G. A., Castile, J., Smith, A., Adams, G. G. & Harding, S. E. 2009. Macromolecular conformation of chitosan in dilute solution: A new global hydrodynamic approach. *Carbohydrate Polymers,* 76**,** 616-621.

Morris, G. A., de al Torre, J. G., Ortega, A., Castile, J., Smith, A. & Harding, S. E. 2008. Molecular flexibility of citrus pectins by combined sedimentation and viscosity analysis. *Food Hydrocolloids,* 22**,** 1435-1442.

Morris, G. A., Foster, T. J. & Harding, S. E. 2002. A hydrodynamic study of the depolymerisation of a high methoxy pectin at elevated temperatures. *Carbohydrate Polymers,* 48**,** 361-367.

Mortazavi, S. & Smart, J. 1993. An in-vitro evaluation of mucosa-adhesion using tensile and shear stresses. *Journal of Pharmacy and Pharmacology,* 45**,** 1108-1108.

Mortazavi, S. A. & Smart, J. D. 1994. Factors Influencing Gel-strengthening at the Mucoadhesive-mucus Interface. *Journal of pharmacy and pharmacology,* 46**,** 86-90.

Mukoma, P., Jooste, B. R. & Vosloo, H. C. M. 2004. A comparison of methanol permeability in Chitosan and Nafion 117 membranes at high to medium methanol concentrations. *Journal of Membrane Science,* 243**,** 293-299.

Murata, H. 2012. Rheology–theory and application to biomaterials. *Janeza Trdine,* 9**,** 403-426.

Mythri, G., Kavitha, K., Rupesh Kumar, M. & Jagadeesh Singh, S. 2011. Novel mucoadhesive polymers –a review. *Journal of Applied Pharmaceutical Science* 1(8)**,** 37-42.

Nii, T. & Ishii, F. 2005. Encapsulation efficiency of water-soluble and insoluble drugs in liposomes prepared by the microencapsulation vesicle method. *International journal of pharmaceutics,* 298**,** 198-205.

Niv, Y. & Boltin, D. 2012. Secreted and membrane-bound mucins and idiopathic peptic ulcer disease. *Digestion,* 86**,** 258-263.

Nordgard, C. T. & Draget, K. I. 2011. Oligosaccharides as modulators of rheology in complex mucous systems. *Biomacromolecules,* 8**,** 3084-3090.

Norton, I. 2010. *Practical food rheology : an interpretive approach,* Hoboken, NJ, USA, Wiley-Blackwell.

Ohara, S., Ishihara, K. & Hotta, K. 1993. Regional differences in pig gastric mucins. *Comparative Biochemistry and Physiology Part B: Comparative Biochemistry,* 106**,** 153-158.

Okano, T. 1998. *Biorelated polymers and gels: controlled release and applications in biomedical engineering*, Academic Press.

Oliveira, G. F., Ferrari, P. C., Carvalho, L. Q. & Evangelista, R. C. 2010. Chitosan–pectin multiparticulate systems associated with enteric polymers for colonic drug delivery. *Carbohydrate Polymers,* 82**,** 1004-1009.

Önal, S. & Zihniğlu, F. 2002. Encapsulation of insulin in chitosan-coated alginate beads: oral therapeutic peptide delivery. *Artificial Cells, Blood Substitutes, and Biotechnology,* 30**,** 229-237.

Park, H. & Robinson, J. R. 1985. Physico-chemical properties of water insoluble polymers important to mucin/epithelial adhesion. *Journal of Controlled Release,* 2**,** 47-57.

Park, K. & Robinson, J. R. 1984. Bioadhesive polymers as platforms for oral-controlled drug delivery: method to study bioadhesion. *International Journal of Pharmaceutics,* 19**,** 107-127.

Partal, P. & Franco, J. M. 2010. Non-Newtonian fluids. *Rheology: encyclopaedia of life support systems (EOLSS), UNESCO. Eolss, Oxford***,** 96-119.

Patel, T. R., Harding, S. E., Ebringerova, A., Deszczynski, M., Hromadkova, Z., Togola, A., Paulsen, B. S., Morris, G. A. & Rowe, A. J. 2007. Weak self-association in a carbohydrate system. *Biophysical Journal,* 93**,** 741-749.

Pawar, S. N. & Edgar, K. J. 2012. Alginate derivatization: a review of chemistry, properties and applications. *Biomaterials,* 33**,** 3279-3305.

Peppas, N. A. & Buri, P. A. 1985. Surface, interfacial and molecular aspects of polymer bioadhesion on soft tissues. *Journal of Controlled Release,* 2**,** 257-275.

Peppas, N. A., Ottenbrite, R. M., Park, K. & Okano, T. 2010. *Biomedical applications of hydrogels handbook*, Springer Science & Business Media.

Phillips, G. O. & Williams, P. A. 2000. Handbook of hydrocolloids. Woodhead Publishing.

Pillai, C., Paul, W. & Sharma, C. P. 2009. Chitin and chitosan polymers: Chemistry, solubility and fiber formation. *Progress in Polymer Science,* 34**,** 641-678.

Pillai, O. & Panchagnula, R. 2001. Polymers in drug delivery. *Current Opinion in Chemical biology,* 5**,** 447-451.

Pinto Reis, C., Neufeld, R. J., Ribeiro, A. J. & Veiga, F. 2006. Nanoencapsulation I. Methods for preparation of drug-loaded polymeric nanoparticles. *Nanomedicine: Nanotechnology, Biology and Medicine,* 2**,** 8-21.

Polk, A., Amsden, B., De Yao, K., Peng, T. & Goosen, M. 1994. Controlled release of albumin from chitosan—alginate microcapsules. *Journal of pharmaceutical Sciences,* 83**,** 178-185.

Ponchel, G., Touchard, F., Duchêne, D. & Peppas, N. A. 1987. Bioadhesive analysis of controlled-release systems. I. Fracture and interpenetration analysis in poly(acrylic acid)-containing systems. *Journal of Controlled Release,* 5**,** 129-141.

Popa, V., Schubert, S. & Schlufter, K. 2011. *Polysaccharides in medicinal and pharmaceutical applications,* GB, Ismithers Rapra.

Potthast, H., Dressman, J., Junginger, H., Midha, K., Oeser, H., Shah, V., Vogelpoel, H. & Barends, D. 2005. Biowaiver monographs for immediate release solid oral dosage forms: Ibuprofen. *Journal of pharmaceutical sciences,* 94**,** 2121-2131.

Rainsford, K. 2009. Ibuprofen: pharmacology, efficacy and safety. *Inflammopharmacology,* 17**,** 275-342.

Rainsford, K. D. 2003. *Ibuprofen: A critical bibliographic review*, CRC Press.

Rainsford, K. D. 2015. *Ibuprofen: Discovery, development and therapeutics*, John Wiley & Sons.

Rajpurohit, H., Sharma, P., Sharma, S. & Bhandari, A. 2010. Polymers for colon targeted drug delivery. *Indian Journal of Pharmaceutical Sciences,* 72**,** 689.

Rao, A. 2010. *Rheology of fluid and semisolid foods: Principles and applications*, Springer US.

Reed, K. K. & Wickham, R. 2009. Review of the gastrointestinal tract: from macro to micro. *Seminars in Oncology Nursing,* 25**,** 3-14.

Reehorst, C. 2014. The mucin-alginate interplay investigating the rheological impact of alginates and their influence on particle mobility.

Rehm, B. H. A. 2009. Alginates: biology and applications. illustrated ed.: Springer Science & Business Media.

Reza, M., Johnson, C., Hatziantoniou, S. & Demetzos, C. 2008. Nanoliposomes and their applications in food nanotechnology. *Journal of Liposome Research,* 18**,** 309-327.

Rinaudo, M. 2008. Main properties and current applications of some polysaccharides as biomaterials. *Polymer International,* 57**,** 397-430.

Rinaudo, M., Milas, M. & Le Dung, P. 1993. Characterization of chitosan. Influence of ionic strength and degree of acetylation on chain expansion. *International Journal of Biological Macromolecules,* 15**,** 281-285.

Sarmento, B., Ribeiro, A., Veiga, F., Sampaio, P., Neufeld, R. & Ferreira, D. 2007. Alginate/chitosan nanoparticles are effective for oral insulin delivery. *Pharmaceutical Research,* 24**,** 2198-2206.

Sartori, C. 1997. *The characterisation of alginate systems for biomedical applications.* Brunel University School of Engineering and Design PhD Theses.

Scawen, M. & Allen, A. 1977. The action of proteolytic enzymes on the glycoprotein from pig gastric mucus. *Biochemical Journal,* 163**,** 363-368.

Schmidt, M., Fehling, E., Glotzbach, C., Here, I. N., Fröhlich, S. & Piotrowski, S. 2012. *Ultra-high performance concrete and nanotechnology in construction. proceedings of hipermat 2012. 3rd international symposium on UHPC and nanotechnology for high performance construction materials*, Kassel University Press.

Schuster, D. 1996. *Encyclopedia of Emulsion Technology*, Taylor & Francis.

Selinus, O. & Alloway, B. J. 2005. *Essentials of medical geology: impacts of the natural environment on public health*, Elsevier Academic Press.

Sellers, L. A., Allen, A., Morris, E. R. & Ross-Murphy, S. B. 1988. Mucus glycoprotein gels. Role of glycoprotein polymeric structure and carbohydrate side-chains in gel-formation. *Carbohydrate Research,* 178**,** 93-110.

Sezer, A. 1999. Release characteristics of chitosan treated alginate beads: I. Sustained release of a macromolecular drug from chitosan treated alginate beads. *Journal of Microencapsulation,* 16**,** 195-203.

Shaikh, R., Singh, T. R. R., Garland, M. J., Woolfson, A. D. & Donnelly, R. F. 2011. Mucoadhesive drug delivery systems. *Journal of Pharmacy and Bioallied Sciences,* 3**,** 89.

Sharma, S. K., Mudhoo, A., Osswald, T. A. & Clark, J. H. 2011. *A Handbook of Applied Biopolymer Technology: Synthesis, Degradation and Applications*, RSC Publishing.

Sheehan, I. C. 1989. Models for the macromolecular structure of mucusglycoproteins,. *In:* S.E. Harding, A. J. R. (ed.) *Dynamic Properties ofBiomolecular Assemblies.* Cambridge, UK,.

Sheehan, J. K. & Carlstedt, I. 1984. Hydrodynamic properties of human cervical-mucus glycoproteins in 6m-guanidinium chloride. *Biochemical Journal,* 217**,** 93-101.

Sheehan, J. K., Kirkham, S., Howard, M., Woodman, P., Kutay, S., Brazeau, C., Buckley, J. & Thornton, D. J. 2004. Identification of molecular intermediates in the assembly pathway of the MUC5AC mucin. *Journal of Biological Chemistry,* 279**,** 15698-15705.

Shu, X. & Zhu, K. 2000. A novel approach to prepare tripolyphosphate/chitosan complex beads for controlled release drug delivery. *International journal of pharmaceutics,* 201**,** 51-58.

Siew, C. K., Williams, P. A. & Young, N. W. 2005. New insights into the mechanism of gelation of alginate and pectin: charge annihilation and reversal mechanism. *Biomacromolecules,* 6**,** 963-969.

Silva, C. M., Ribeiro, A. J., Figueiredo, M., Ferreira, D. & Veiga, F. 2005. Microencapsulation of hemoglobin in chitosan-coated alginate microspheres prepared by emulsification/internal gelation. *The AAPS Journal,* 7**,** E903-E913.

Singh, A. P., Chaturvedi, P. & Batra, S. K. 2007. Emerging roles of MUC4 in cancer: a novel target for diagnosis and therapy. *Cancer Research,* 67**,** 433-436.

Smart, J. D. 2005. The basics and underlying mechanisms of mucoadhesion. *Advanced Drug Delivery Reviews,* 57**,** 1556-1568.

Sriamornsak, P. 2003. Chemistry of pectin and its pharmaceutical uses: A review. *Silpakorn University International Journal,* 3**,** 206-228.

Stephen, A. M., Phillips, G. O. & Williams, P. A. 2006. Food Polysaccharides and Their Applications, Second Edition. CRC PRESS-TAYLOR & FRANCIS GROUP.

Stokke, B. T., Smidsroed, O., Bruheim, P. & Skjaak-Braek, G. 1991. Distribution of uronate residues in alginate chains in relation to alginate gelling properties. *Macromolecules,* 24**,** 4637-4645.

Straccia, M. C., d'Ayala, G. G., Romano, I., Oliva, A. & Laurienzo, P. 2015. Alginate hydrogels coated with chitosan for wound dressing. *Marine Drugs,* 13**,** 2890-2908.

Streng, W. H. 2012. *Characterization of compounds in solution: theory andpractice*, Springer US.

Sudhakar, Y., Kuotsu, K. & Bandyopadhyay, A. 2006. Buccal bioadhesive drug delivery—a promising option for orally less efficient drugs. *Journal of controlled release,* 114**,** 15-40.

Svensson, O. 2008. *Interactions of mucins with biopolymers and drug delivery particles.*

Tamburic, S. & Craig, D. Q. 1995. An investigation into the rheological, dielectric and mucoadhesive properties of poly (acrylic acid) gel systems. *Journal of Controlled Release,* 37**,** 59-68.

Tamburic, S. & Craig, D. Q. 1997. A comparison of different in vitro methods for measuring mucoadhesive performance. *European Journal of Pharmaceutics and Biopharmaceutics,* 44**,** 159-167.

Tanaka, F. 2011. *Polymer physics: applications to molecular association and thermoreversible gelation*, Cambridge University Press.

Taylor, C., Pearson, J. P., Draget, K. I., Dettmar, P. W. & Smidsrød, O. 2005a. Rheological characterisation of mixed gels of mucin and alginate. *Carbohydrate Polymers,* 59**,** 189-195.

Taylor, T. M., Weiss, J., Davidson, P. M. & Bruce, B. D. 2005b. Liposomal nanocapsules in food science and agriculture. *Critical Reviews in Food Science and Nutrition* 45**,** 587-605.

Terbojevich, M., Cosani, A., Conio, G., Marsano, E. & Bianchi, E. 1991. Chitosan: chain rigidity and mesophase formation. *Carbohydrate Research,* 209**,** 251-260.

Tewes, F., Munnier, E., Antoon, B., Okassa, L. N., Cohen-Jonathan, S., Marchais, H., Douziech-Eyrolles, L., Soucé, M., Dubois, P. & Chourpa, I. 2007. Comparative study of doxorubicin-loaded poly (lactide-co-glycolide) nanoparticles prepared by single and

double emulsion methods. *European journal of pharmaceutics and biopharmaceutics,* 66**,** 488-492.

Thakur, B. R., Singh, R. K., Handa, A. K. & Rao, M. A. 1997. Chemistry and uses of pectin — A review. *Critical Reviews in Food Science and Nutrition* 37**,** 47-73.

Tolstoguzov, V. 1991. Functional properties of food proteins and role of protein-polysaccharide interaction. *Food Hydrocolloids,* 4**,** 429-468.

Tømmeraas, K. & Wahlund, P.-O. 2009. Poly-acid properties of biosynthetic hyaluronan studied by titration. *Carbohydrate Polymers,* 77**,** 194-200.

Tsai, R.-Y., Chen, P.-W., Kuo, T.-Y., Lin, C.-M., Wang, D.-M., Hsien, T.-Y. & Hsieh, H.-J. 2014. Chitosan/pectin/gum Arabic polyelectrolyte complex: Process-dependent appearance, microstructure analysis and its application. *Carbohydrate Polymers,* 101**,** 752-759.

Tutuian, R. & Castell, D. O. 2006. Gastroesophageal reflux monitoring: pH and impedance. *GI Motility Online*.

van Hoogmoed, C. G., Busscher, H. J. & de Vos, P. 2003. Fourier transform infrared spectroscopy studies of alginate–PLL capsules with varying compositions. *Journal of Biomedical Materials Research Part A,* 67**,** 172-178.

Vasir, J. K., Tambwekar, K. & Garg, S. 2003. Bioadhesive microspheres as a controlled drug delivery system. *International Journal of Pharmaceutics,* 255**,** 13-32.

Vauthier, C. & Ponchel, G. 2017. *Polymer Nanoparticles for Nanomedicines: A Guide for their Design, Preparation and Development*, Springer.

Venkatesan, J., Bhatnagar, I. & Kim, S.-K. 2014. Chitosan-alginate biocomposite containing fucoidan for bone tissue engineering. *Marine Drugs,* 12**,** 300-316.

Vinod, K., Rohit Reddy, T., Sandhya, S. & David Banji, V. R. B. 2012a. Critical review on mucoadhesive drug delivery systems. *Hygeia JD Med,* 4**,** 1-5.

Vinod, K. R., Reddy, R., Sandhya, Banji, D. & Reddy, V. 2012b. Critical Review on Mucoadhesive Drug Delivery Systems. *Hygeia JD Med,* 4**,** 1-5.

Vold, I. M. N. 2004. Periodate oxidised chitosans: structure and solution properties.

Wagner, A. & Vorauer-Uhl, K. 2010. Liposome technology for industrial purposes. *Journal of Drug Delivery,* 2011.

Walstra, P. 2002. *Physical chemistry of foods*, CRC Press.

Wang, K. & Liu, Q. 2014. Chemical structure analyses of phosphorylated chitosan. *Carbohydrate research,* 386**,** 48-56.

Wang, Y., Dave, R. N. & Pfeffer, R. 2004. Polymer coating/encapsulation of nanoparticles using a supercritical anti-solvent process. *The Journal of supercritical fluids,* 28**,** 85-99.

Weist, S., Brunkau, C., Wittke, J., Eravci, M., Broedel, O., Krause, E., Stephanowitz, H., Eravci, S. & Baumgartner, A. 2010. Effects of thawing, refreezing and storage conditions of tissue samples and protein extracts on 2-DE spot intensity. *Proteomics,* 10**,** 1515-1521.

Weitz, D., Wyss, H. & Larsen, R. 2007. Oscillatory rheology: Measuring the viscoelastic behaviour of soft materials. *GIT laboratory Journal Europe,* 11**,** 68-70.

Wilson, C. G. & Crowley, P. J. 2011. *Controlled Release in Oral Drug Delivery*, Springer US.

Woodley, J. 2012. Bioadhesion. *Clinical Pharmacokinetics,* 40**,** 77-84.

Wyatt, P. J. 1993. Light scattering and the absolute characterization of macromolecules. *Analytica Chimica Acta,* 272**,** 1-40.

Wydro, P., Krajewska, B. & Hąc-Wydro, K. 2007. Chitosan as a lipid binder: A langmuir monolayer study of chitosan-lipid interactions. *Biomacromolecules,* 8**,** 2611–2617.

Xu, R. 2006. *Particle characterization: light scattering methods*, Springer Netherlands.

Xu, X., Costa, A. & Burgess, D. J. 2012. Protein encapsulation in unilamellar liposomes: high encapsulation efficiency and a novel technique to assess lipid-protein interaction. *Pharmaceutical Research,* 29**,** 1919-1931.

Yakubov, G. E., Papagiannopoulos, A., Rat, E., Easton, R. L. & Waigh, T. A. 2007. Molecular structure and rheological properties of short-side-chain heavily glycosylated porcine stomach mucin. *Biomacromolecules,* 8**,** 3467-3477.

Yan, N. & Chen, X. 2015. Don't waste seafood waste: Turning cast-off shells into nitrogen-rich chemicals would benefit economies and the environment. *Nature (London),* 524**,** 155.

Yang, J., Han, S., Zheng, H., Dong, H. & Liu, J. 2015. Preparation and application of micro/nanoparticles based on natural polysaccharides. *Carbohydrate Polymers,* 123**,** 53-66.

Yang, X., Forier, K., Steukers, L., Van Vlierberghe, S., Dubruel, P., Braeckmans, K., Glorieux, S. & Nauwynck, H. J. 2012. Immobilization of pseudorabies virus in porcine tracheal respiratory mucus revealed by single particle tracking. *PloS one,* 7**,** e51054.

Yitbarek, E. 2010. *Characterization and Analytical Applications of Dye-encapsulated Zwitterionic Liposomes.* Doctor of Philosophy, North Carolina State University.

Yu, T., Andrews, G. P. & Jones, D. S. 2014. Mucoadhesion and characterization of mucoadhesive properties. *In:* das Neves, J. & Sarmento, B. (eds.) *Mucosal Delivery of Biopharmaceuticals.* Springer US.

Zimmer, A. & Kreuter, J. 1995. Microspheres and nanoparticles used in ocular delivery systems. *Advanced Drug Delivery Reviews,* 16**,** 61-73.

Zosel, A. 1985. Adhesion and tack of polymers: Influence of mechanical properties and surface tensions. *Colloid and Polymer Science,* 263**,** 541-553.

Zosel, A. 1989. Adhesive failure and deformation behaviour of polymers. *The Journal of Adhesion,* 30**,** 135-149.